Assessment of Oxygenated Fuels for Lowering NO_x Emissions of a Diesel Engine

Mohammad Anwar

A thesis by publication submitted in fulfilment of the requirements for the

Degree of Doctor of Philosophy (PhD)

School of Engineering and Technology (SET)
CQUniversity Australia
Rockhampton, QLD, Australia

December 2019

To my mom for her strong wishes

Keywords

Biofuel, Biodiesel, Optimization, diesel engine, *Carica papaya*, stone fruit biodiesel, apricot biodiesel, multiple criteria decision analysis (MCDA), Bio-oil transesterification, Fatty acid methyl ester (FAME), binary and ternary biodiesel, engine performance, emission and combustion characteristics.

Abstract

The supply of petroleum sources is finite, non-renewable and, at the current rate of consumption, it will become severely depleted by 2050. Furthermore, the use of petroleum fuel increases greenhouse gas (GHG) emissions, leading to global warming which is harmful. Thus, there is an urgent need to find alternative sources of energy that are renewable, cost effective and can be produced in a sustainable manner. Non-edible feedstock biodiesels are a promising alternative fuel for reducing most petroleum fuel related environmental problems. They are attracting increasing attention due to their abundant availability and similar physicochemical properties as petroleum-derived diesel. This study carefully investigated six major non-edible vegetable oils (papaya seed oil, stone fruit kernel oil, jatropha oil, rapeseed oil, beauty leaf tree oil and waste cooking oil), that are locally available, out of 350 oil-bearing crops that could be potentially used to produce biodiesel. Four multiple criteria decision analysis (MCDA) methods with twelve physicochemical properties of biodiesel feedstocks and three different weightage (%) determination methods were used to rank these six feedstocks, with the view to find the best performing biodiesel feedstocks. The overall results show that the stone fruit kernel oil (SFO) was ranked as the best performing feedstock on the basis of engine performance amongst the six locally available feedstocks examined, papaya seed oil (PSO) came out as the second best, and the waste cooking oil was the worst performing biodiesel.

Alkali catalysed transesterification reaction is the most widely used method for producing biodiesel from oil/animal fats due to its higher conversion efficiency in a short reaction time (30-60 min). The current study was undertaken to optimise the transesterification process for PSO and SFO with the view to increasing the efficiency of biodiesel conversion. A response surface method (RSM) based Box-Behnken design was employed to optimise biodiesel conversion processes for both PSO and SFO. Biodiesel conversion efficiencies of 96.5% and 95.8% were found for PSO and SFO at their respective optimum operating conditions.

These PSO and SFO biodiesels were evaluated using a 4-cylinder, 4-stroke Kubota diesel engine. In general, both PSO and SFO blends decreased engine performance slightly compared to diesel as expected, however, SFO biodiesel blends gave about 3% better performance compared to PSO blends. On the other hand, PSO blends (20%) decreased most of the engine emissions by up to 34% except for an increase of about 5% in nitrogen oxide (NO_x) compared to diesel. These emission performances are up to 14% better than the corresponding SFO

emissions. Although the SFO biodiesel blends have slightly better engine performance than PSO biodiesel blends, the PSO biodiesel blends proved to be a better overall choice due to their excellent environmentally friendly attributes as they can reduce exhaust emissions to a great extent. Therefore, PSO was chosen subsequently to develop interactive relationships between three operating parameters of PSO, namely biodiesel blends, engine load, and engine speed and four responses of brake power (BP), torque, brake specific fuels consumption (BSFC), and brake thermal efficiency (BTE) for engine testing and emissions behaviour.

Analysis of variance (ANOVA) and a statistical regression model show that load and speed were the two most important parameters that affect all four responses. The biodiesel blends parameter had a significant effect on BSFC. The engine load and engine speed were the two most important parameters that affect four of the responses (NO_x, hydrocarbon (HC), particulate matter (PM) and carbon monoxide (CO)). In-cylinder peak pressures for PSO biodiesel blends were higher than for diesel irrespective of engine speed. Heat release rates of PSO biodiesel blends were found to be lower than for diesel due to lower ignition delays and lower caloric values of biodiesel. The maximum cylinder temperatures of PSO biodiesel blends were higher (3.73%) than that of diesel. To minimise the exhaust emissions, PSO biodiesel blends were mixed with two oxygenated additives, namely diethylene glycol dimethyl ether (diglyme) and n-butanol, to make ternary blends. These blends were tested for both engine performance and emissions. The addition of oxygenated additives increased the BP, torque and BTE values of PSO biodiesel ternary blends and it lowered the average BSFC by 0.5% and 17.7% compared with diesel and PSO blends (20%), respectively. PSO-diglyme-diesel ternary blend performed better than all other binary blends as well as the PSO-n-butanol-diesel ternary blend. The average reductions of HC, CO, NO_x and PM of PSO-diglyme-diesel ternary blends compared with diesel were 32.4%, 61%, 0.64% and 47.4% respectively, whereas a 2.8% increase in carbon dioxide (CO_2) emission was observed. The average increase of NO_x, and CO_2 for PSO blends (20%) compared with diesel were 4.1% and 4.5%, respectively.

In conclusion, this study provided a solid base of new knowledge regarding biodiesel feedstock selection and optimisation techniques for PSO and SFO, assessed the suitability of PSO and SFO as alternatives to petroleum diesel and analysed how the emissions from these biodiesels could be reduced. These are very useful information for engine manufacturers, Government, stakeholders and policy makers to eliminate the lack of awareness of using second-generation biodiesel in Australia.

Table of contents

List of figures

Chapter 1 Introduction

Chapter 2 The potential of utilising papaya seed oil and stone fruit kernel oil as non-edible feedstock for biodiesel production in Australia- A review

Chapter 3 The efficacy of multiple-criteria design matrix for biodiesel feedstock selection

List of tables

List of symbols

D	Engine displacement volume (m^3)
DU	Degree of unsaturation
$\frac{dQ}{\mathrm{d}\theta}$	Heat release rate (J/°CA)
f	Fuel consumption rate (g/hour)
KOH	Potassium Hydroxide
L	Litre
ML	Million litres
MJ	Megajoule
NaOH	Sodium Hydroxide
P	Instantaneous cylinder pressure (Pa)
PJ	Petajoule
V	Instantaneous cylinder volume (m^3)
γ	Specific heat ratio
θ	Crank angle (°CA)
η	Efficiency
wt	Weight

List of acronyms

ANOVA	Analysis of variance
AV	Acid value
B5	5% biodiesel and 95% diesel
B10	10% biodiesel and 90% diesel
B20	20% biodiesel and 80% diesel
BP	Brake power
BMEP	Brake mean effective pressure
BSFC	Brake specific fuel consumption
BTE	Brake thermal efficiency
CA	Crank angle
CI	Compression ignition
CN	Cetane number
CO	Carbon monoxide
CO_2	Carbon dioxide
CP	Cylinder pressure
CV	Calorific value
Diglyme	Bis (2-methoxyethyl) ether, i.e., Diethylene glycol dimethyl ether
EGT	Exhaust gas temperature
FAME	Fatty acid methyl ester
FFA	Free fatty acid
FP	Flash point
FTIR	Fourier Transform Infrared
GAIA	Graphical analysis for interactive assistance
GC	Gas Chromatography
HC	Hydrocarbon
HHV	Higher heating value
HRR	Heat release rate
ID	Ignition delay
IP	Indicated power
IV	Iodine value
KV	Kinematic viscosity

LCSF	Long chain saturated factor
LHV	Lower heating value
MCDA	Multi-criteria decision analysis
MFB	Mass fraction burned
MUFA	Monounsaturated fatty acid
NO_x	Nitrogen oxides
OS	Oxidation stability
P20	20% PSO biodiesel and 80% diesel
P20DG5	20% PSO biodiesel, 75% diesel and 5% diglyme
P20BT5	20% PSO biodiesel, 75% diesel and 5% n-butanol
PM	Particulate matter
PPM	Parts per million
PROMETHEE	Preference ranking organization method for enrichment evaluation
PSO	Papaya seed oil
PSFO20	10% PSO biodiesel, 10% SFO biodiesel and 80% diesel
PUFA	Polyunsaturated fatty acid
RPM	Revolution per minute
RSM	Response surface methodology
SFA	Saturated fatty acid
SFO	Strone fruit kernel oil
SV	Saponification value
TOPSIS	Technique for order preference by similarity to ideal solution
WCB	Waste cooking oil biodiesel
WSM	Weighted sum method
WPM	Weighted product method

Candidate's Statement

By submitting this thesis for formal examination at CQUniversity Australia, I declare that it meets all requirements as outlined in the Research Higher Degree Theses Policy and Procedure.

Mohammad Anwar

Statement Authorship and Originality

By submitting this thesis for formal examination at CQUniversity Australia, I declare that all of the research and discussion presented in this thesis is original work performed by the author. No content of this thesis has been submitted or considered either in whole or in part, at any tertiary institute or university for a degree or any other category of award. I also declare that any material presented in this thesis performed by another person or institute has been referenced and listed in the reference section.

Mohammad Anwar

Copyright Statement

Acknowledgements

First and foremost, I would like to thank Almighty for giving me an opportunity to finish my study in due time. My special thanks go to my supervisors, Prof. Mohammad Golam Rasul and A/Prof. Nanjappa Ashwath for their continuous support, guidance, motivation and encouragement throughout the journey. Without their support and guidance, this thesis would have been a challenging task to complete.

I would like to express my thanks to all teaching and technical staff in Central Queensland University for providing me excellent support during my full-time work and study. I would like to express appreciation to laboratory manager Mr. Ian Tomlinson for his endless support and encouragement. I am grateful to my research authors and colleagues Mr. Patrick O'Grady and Mrs. Heather Smyth for helping me in different stages and situations of my study. Special thanks to Dr. Mofijur Rahman, Dr. Muhammad Mostafa Kamal Bhuiya and Mr. Hazrat Ali for their continuous support in my study. The services from the School of Graduate Research were excellent throughout my candidature and I would like to thank all their staff. A very special acknowledgement to Prof. Steve Hall, Prof. Susan Kinnear, Prof. Steven Moore and Dr. Jo Luck for their professional support.

I would like to acknowledge the support, encouragement and motivation given by my parents, Mohammad Abdur Rabb and Jahanara Begum. I wish my mom could be here to celebrate this completion of my journey. Finally, my whole-hearted appreciation goes to my family. I am grateful to my loving wife Dr Tanzina Afrin and my young kids Ariq Anwar and Ariba Anwar for their tremendous support, countless sacrifice and patience. Without their true love and continuous encouragement, this thesis could not have been successfully completed.

This RHD candidature was supported under the Commonwealth Government's Research Training Program/Research Training Scheme. I gratefully acknowledge the financial support provided by the Australian Government.

Professional editor, Mr. Tim Mcsweeney, provided copyediting and proof-reading services, according to the guidelines laid out in the University-endorsed national guidelines, 'The editing of research theses by professional editors'.

List of Publications

Articles directly related to this thesis are numbered below:

PEER-REVIEWED JOURNALS

[1] **Anwar, M**., M.G. Rasul, N. Ashwath, and M.D.N. Nabi, 2019, *The potential of utilising papaya seed oil and stone fruit kernel oil as non-edible feedstock for biodiesel production in Australia—A review*. **Energy Reports**, **5**, p. 280-297 [Q1].

[2] **Anwar, M**., M.G. Rasul, and N. Ashwath, 2019, *The efficacy of multiple-criteria design matrix for biodiesel feedstock selection*. **Energy Conversion and Management**, **198**, p. 111790 [Q1].

[3] **Anwar, M**., M.G. Rasul, and N. Ashwath, 2018, *Production optimization and quality assessment of papaya (Carica papaya) biodiesel with response surface methodology*. **Energy Conversion and Management**, **156**, p. 103-112 [Q1].

[4] **Anwar, M**., M. Rasul, N. Ashwath, and M. Rahman, 2018, *Optimisation of Second-Generation Biodiesel Production from Australian Native Stone Fruit Oil Using Response Surface Method*. **Energies**, **11(10)**, p. 2566 [Q2].

[5] **Anwar, M**., M. Rasul, and N. Ashwath, 2018, *A Systematic Multivariate Analysis of Carica papaya Biodiesel Blends and Their Interactive Effect on Performance*. **Energies**, **11(11)**, p. 2931 [Q2].

[6] **Anwar, M**., M. Rasul, and N. Ashwath, 2020, *A pragmatic and critical analysis of engine emissions for biodiesel blended fuels*. **Fuel, 270,** p. 117513 [Q1].

[7] **Anwar, M**., M.G. Rasul, and N. Ashwath, 2019, *The synergistic effects of oxygenated additives on papaya biodiesel binary and ternary blends*. **Fuel**, **256**, p. 115980 [Q1].

PEER-REVIEWED CONFERENCES

[1] **Anwar, M**., M.G. Rasul, and N. Ashwath, 2017, *Optimization of biodiesel production process from papaya (Carica papaya) seed oil.* in 2017 IEEE 7th International Conference on Power and Energy Systems (ICPES).

[2] **Anwar, M**., M. Rasul, and N. Ashwath, 2019, *Optimization of biodiesel production from stone fruit kernel oil*. Energy Procedia, **160**, p. 268-276.

[3] **Anwar, M**., M. Rasul, and N. Ashwath. *A comparative study of engine performance and emission characteristics of biodiesels produced from the waste seeds of papaya and stone fruit, IEEE 2nd International Conference on Renewable Energy and Power Engineering*. 2019. Toronto, Canada, Nov 2-4, 2019, Paper ID PE042.

[4] **Anwar, M**., M. Rasul, and N. Ashwath. *Combustion characteristics of an agricultural diesel engine fuelled with papaya and stone fruit biodiesel: A comparison, IEEE 2nd*

International Conference on Renewable Energy and Power Engineering. 2019. Toronto, Canada, Nov. 2-4, 2019, Paper ID PE043.

[5] **Anwar, M**., M. Rasul, and N. Ashwath, *Investigation on the impact of papaya biodiesel-diesel blends on combustion of an agricultural CI engine*, International Conference on Sustainable Energy and Green Technology 2019, Bangkok, Thailand (submitted), Paper ID 55.

[6] **Anwar, M**., M. Rasul, N. Ashwath and M. M. K. Bhuiya, *Ternary or binary blend? A case study using papaya seed oil biodiesel*, 13th International Conference on Mechanical Engineering (ICME2019), Dhaka, Bangladesh (submitted), Paper ID 78.

[7] **Anwar, M**., M. Rasul, and N. Ashwath, *Use of waste papaya seed as an alternative fuel source* (ready to submit).

{this page is intentionally left blank}

Chapter 1: Introduction

1.1 Background

The developing energy calamity and growing environmental pollutions are the most resounding issues that the world is facing today. The total energy consumption is growing more rapidly than the population growth [1]. The International Energy Agency (IEA) estimates that there will be about a 53% increase in global energy consumption by 2050 [2, 3]. Global primary energy consumption had increased by 2.9% in 2018, as compared to 2.2% in 2017, 1% in 2016, 0.9% in 2015 and 1% in 2014 [4]. This energy consumption grew in 2018 and it almost doubled at an average annual rate of 1.5% since 2010. Globally, the industrial sector (e.g. manufacturing, mining, construction, agriculture) is the largest energy consumer followed by the building and transportation sectors, while the transportation sector is growing faster than all the others. The transportation sector is mostly dependent on petroleum fuels (crude oil derived gasoline and diesel). This sector currently consumes nearly 30% of crude oil globally and this will increase by 59% by 2050 [5]. It is projected that, from 2010-40, the transportation sector will be consuming about 37,982 PJ or 36 Quadrillion BTU, accounting for 63% of global consumption of petroleum and liquid fuels [6].

After Switzerland, Australia is the 2nd wealthiest nation in terms of wealth per adult. Australia is estimated to have the world's 13th highest Gross domestic product (GDP) and 11th highest GDP per capita [7]. Australia is the 6th largest developed country. Like all other countries, Australia's economy totally depends on the energy use at the present time and this will continue in the future. Australia exports energy that includes coal, natural gas and uranium oxide. About 94% of Australia's total energy consumption is primarily through non-renewable energy resources, mainly coal, oil and gas, whereas renewable energy accounts for only 6.2% and the source of the majority of renewable energy came from biomass [8].

Most prominent primary energy resources in Australia are black coal, brown coal, natural gas, oil, LPG, uranium oxide and renewables. In 2017-18, black coal production grew by 2%, whereas brown coal production fell by 19% [8]. Black coal production increased by about 5% in Queensland and fell by 2% in New South Wales. Brown coal was affected by the closure of power stations. In 2017-18, natural gas production rose by 15% to 4,731 PJ or 121 billion cubic metres [8]. Western Australia is the largest gas producer, as half of total gas production comes

from this state. Queensland's gas production was 31% of the total production, nearly five times what it was in 2013-14. In 2017-18, Australia produced less crude oil and liquid natural gas (about 4% less than previous year), accounting for 572 PJ (15.5 billion litres) [8]. Renewable energy is getting popular and its production increased by 1% in 2017-18 to reach 382 PJ compared to 2016-17. Renewable energy, mainly wind and solar, accounted for 2% of the total energy production in 2017-18. Uranium production decreased by 9% to 6,654 tonnes, i.e., 3,127 PJ. It can be seen from Figure 1 that there is a huge gap between oil production and consumption. Day by day, this difference is getting larger. Therefore, Australia is heavily reliant on imported petroleum fuels (85% and costing about $18 billion per year) to meet this ongoing demand.

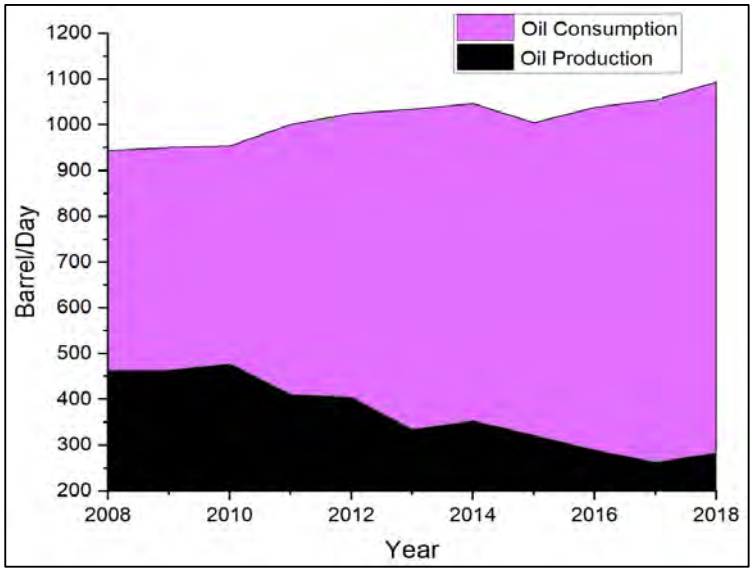

Figure 1: Australian oil production and consumption, 2008-2018 [9].

Australian energy consumption increased by 0.9% in 2017-18 to 6,172 petajoules, which is the highest ever recorded level. In the last 10 years, Australia's energy consumption has increased by 0.6% a year [8] on an average. The most significant energy consumption sectors in 2017-18 were mining, electricity generation and transportation. Energy usage (both natural gas and electricity) in the mining sector increased by 9% in 2017-18 than in the previous year to support liquefied natural gas (LNG) exports. However, energy usage for electricity generation decreased by 4% in 2017-18 despite a slight increase in electricity output reflecting less use of brown coal and increased use of renewable energy. The transport sector is the largest energy consumer in Australia, which grew steadily by 2.4% in 2017-18. The largest primary energy source in Australia was petroleum oil and it accounted for 38.7% in 2017-18, followed by coal (29.9%), natural gas (25.2%) and renewables (6.2%) [8]. Figure 2(a) shows leading primary

energy sources in Australia and their consumption in percentage (%). Coal consumption decreased by 4% in 2017-18 and brown coal dropped significantly due to closure of power plants. Natural gas consumption increased by 4% in 2015-16 to support LNG exports and electricity generation, although gas consumption in the manufacturing sector dropped. Renewable energy consumption, mainly solar and wind energy, increased by 1% in 2017-18. This renewable energy is used for various purposes such as electricity generation, residential heating using firewood, bagasse use in manufacturing and solar hot water. Both solar and wind energy continued to be substantial factors of the growth in renewables, increasing by 23% and 20% respectively in 2017-18 (Figure 2(b)).

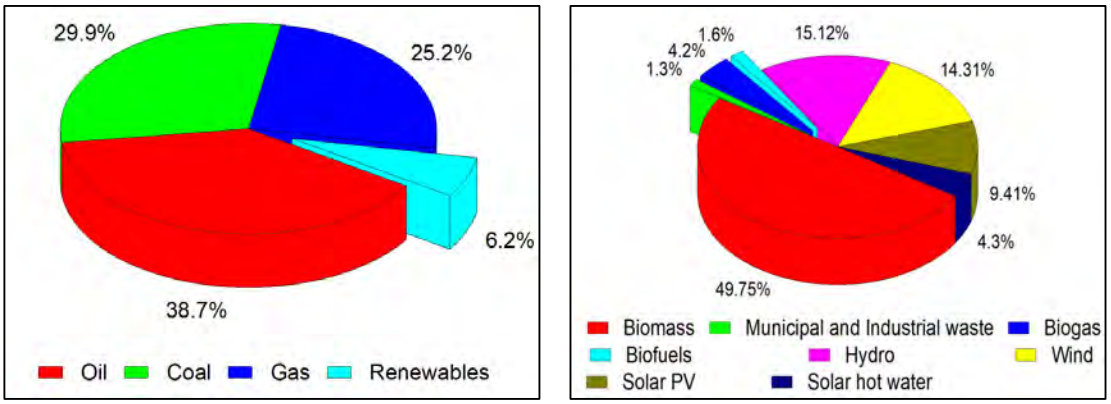

(a) (b)

Figure 2: Australian energy consumption (%) in 2017-2018 (a) Fuel type, (b) Renewable energy consumption by source [8].

The largest Australian primary energy-consuming sector was transportation, accounting for about 28.1% in 2017-18. The average annual growth rate for the transport sector is 2% a year, which increases to 1731.8 PJ in 2017-18. Annual growth for road and air transport sectors increased by about 1.7% and 4.5% respectively and these are likely to continue to grow rapidly. The overall consumption in the transport sector is projected to increase slightly from 29% to 32% over the period to 2019-50 [5, 9]. The second largest energy-consuming sector was electricity supply which accounted for 26.3% as shown in 2017-18 (Table 1).

Table 1: Australian primary energy consumption by sector [8].

Sector	**2017-18 (PJ)**	**Share (%)**	**Average annual growth 2017-18 (%)**	**Average annual growth 10 years (%)**
Transport	1731.8	28.1	2.4	1.9
Electricity generation	1621.5	26.3	-3.6	-1.9
Manufacturing	1076.2	17.4	-0.4	-0.9
Mining	729.7	11.8	9.1	7.9

Residential	458.8	7.4	0.1	0.5
Commercial	336.2	5.4	1.6	2.1
Agriculture	117.6	1.9	1.1	2.5
Construction	25.9	0.4	6.9	0.1
Water and waste	17.9	0.3	12.1	3.1
Others	56.2	0.9	9.8	-2.9
Total	6171.7	100.0	0.9	0.6

The manufacturing sector was the third largest energy consumer in 2017-18 and accounted for 17.4%, followed by mining (11.8%), residential (7.4%), commercial (5.4%), agriculture (1.9%), construction (0.4%), water and waste (0.3%) and others (0.9%). Energy consumption in the manufacturing sector was relatively flat in 2017-18. The average annual growth of energy consumption of the mining sector was 9.1% in 2017-18. Therefore, the primary energy sectors were transportation, electricity generation and manufacturing which together accounted for about 71.8% of Australia's total energy consumption. However, the Australian transportation sector remains the principal end use consumption source.

The Australian transportation sector is mostly dependent on petroleum fuels, such as petrol and diesel. Generally, the light vehicle sector uses petrol as a dominant fuel, whereas diesel is used in the heavy vehicle sector. The share of diesel is increasing day-by-day due to better fuel efficiency and performance in modern automobile engines. Nowadays automobile manufacturers are focusing more on diesel-based vehicles. Diesel vehicle numbers have doubled since 2010 to 4.8 million vehicles in 2019 [8]. The share of petrol is declining whereas diesel and aviation fuels have grown due to mining activities and increased air transport activities. However, due to severe political unrest in some crude oil producing countries and prolonged economic embargoes on certain counties, the world is facing extreme challenges to keep the fuel supply chain economically sustainable. World leaders, politicians and policy makers are giving emphasis not only to solving these geopolitical situations, but also pushing hard for research and development for finding alternative fuel sources that are locally available, cost-effective and sustainable.

Biofuel, and particularly the biodiesel, is drawing more attention due to its environmentally friendly nature (minimise environmental pollution and global warming) and its potential to serve as an alternative energy source [10, 11]. It is a sulphur free, non-toxic, renewable, biodegradable clean burning ester based oxygenated fuel [12-15] and is a mixture of alkyl esters of long chain fatty acids. Through esterification and/or transesterification of free fatty acids and

triglycerides, those long chain fatty acids are synthesised [6, 11, 16]. Hence, biodiesel is also known as fatty acid methyl ester (FAME) and are derived from vegetable oils either edible or non-edible and animal fats [17-19]. Biodiesel can be used directly in diesel engines as an alternative fuel source with no or minimum modification of the engine. It may even provide better engine performance and lubrication [20]. It is a globally accepted fuel to reduce exhaust gas emissions and environmental issues. Finally, it meets the international standards and is compatible with petroleum diesel. It can be blended with petroleum diesel at various proportions (5, 10, 15 or 20%) and modern engines can cope with these blended biodiesel-diesel fuels without any major modifications [21].

1.2 Significance of the study

This study was carried out with the aim of investigating the prospect of using Australian non-edible second-generation biodiesels as a sustainable source of transport fuel. Australia is largely dependent on imported transport fuel. However, the petroleum source is finite, non-renewable and, at the current rate of consumption, it will be depleted within 2062-2094 [22]. The cost of this fuel fluctuates almost every day, and this affects the total economies of the country. The uncertainty and political imbalance situation in major fuel producing countries also make sustainable supply difficult. In addition, increased use of petroleum fuel results in the release of greenhouse gases such as nitrogen oxides, unburned hydrocarbons, carbon dioxide, carbon monoxide and particulate matter into the atmosphere, causing severe health issues. The use of petroleum fuel increases global warming, greenhouse gas (GHG) emissions, acid rain formation and unseasonable rains, which all contribute to climate change [23]. The study has shown that, by 2030, greenhouse gas (GHG) emissions would increase by 39% if no actions are taken now [24]. Norhasyima et al. [25] predict that the average global temperature would increase by 2 °C by 2050 if the current rate of CO_2 emission is not reduced by 50%. Thus, there is an urgent need to identify alternative sources of renewable energy that are sustainable, reliable and cost effective. Biofuel is the promising alternative fuel for solving most petroleum fuel related environmental problems. Federal government regulations are applied to ensure that the quality of petrol and diesel fuel in Australia maintained. The Fuel Quality Standards Act 2000 ensures a legislative framework for setting national fuel quality and fuel quality information standards for petrol, diesel, biodiesel, auto gas and ethanol E85 [26]. The objective of the New South Wales (NSW) Biofuels Act 2007 is not only to support the development of sustainable biofuels industry in NSW, but also to contribute to (i)

improving air quality, (ii) addressing climate change through reducing greenhouse gas emissions, (iii) providing cheaper fuel, (iv) reducing the reliance on imported fossil fuels and (v) supporting regional development. As per the NSW mandate, both ethanol and biodiesel must represent 6% (E6) and 2% (B2) of the total volume of petrol and diesel sold in NSW, respectively. According to the Department of Energy and Water Supply [27], the Queensland's biofuel mandate that commenced on 1st January 2017 set the minimum requirements for selling bio-based diesel (E4 and B0.5). Both the Queensland and Federal Governments of Australia are actively encouraging development of the biofuel industry to achieve a cleaner and greener future for Australia. Australian Government organisations such as Australian Renewable Energy Agency (ARENA) and Australian Competition and Consumer Commission (ACCC) are also promoting the biodiesel industry by satisfying all stakeholders. This study investigates the prospect of two potential 2nd generation biofuel feedstocks, namely papaya seed oil (PSO) and stone fruit kernel seed oil (SFO) chosen amongst six biodiesel feedstocks based on their physicochemical properties. Optimisation of their biodiesel production process increases the productivity and saves time, cost and effort. These biodiesels reduce the GHG emissions and play an important role in the economy by creating new opportunities to the biofuel industry. In addition, it enhances the stability of the Australian fuel market as well as creating new jobs and development, especially in the regional areas. Finally, this research will provide a strong base of new knowledge and promote biodiesel usage in Australia.

1.3 Research problems and gaps

The usage of first-generation biodiesel has raised many concerns due to the food versus fuel debate as well as major environmental problems such as deforestation and destruction of vital soil resources. The focus has now shifted to second generation non-edible vegetable oils for biodiesel production due to their availability and low cost [28]. Although more than 350 oil-bearing crops have been identified for biodiesel production, an ideal biodiesel feedstock should be easily available locally, and its use be technically and economically feasible [29, 30]. Again, there is an ongoing debate on the ideal or the best possible biodiesel feedstocks in terms of their technical, environmental, economic and social aspects. Technical aspects of the biodiesel selection process include assessing physico-chemical properties, fatty acid composition, safety, and availability criteria. Environment-related criteria such as land usage, irrigation and cultivation methods, are considered under the environmental aspect. All costs that are associated with the issues such as cultivation, harvesting, labour and transportation, are listed

under the criteria of economic aspects. The social aspects include activities such as job creation, social acceptance and community benefits. Different multiple criteria decision analysis (MCDA) methods such as PROMETHEE GAIA, weighted sum method (WSM), weighted product method (WPM), Technique for Order Preference by Similarity to Ideal Solution (TOPSIS), Fuzzy analytic hierarchy process (AHP)-TOPSIS, and Operational competitiveness rating analysis (OCRA) can be used to screen biodiesel feedstocks [31-34].

The use of crude vegetable oil straight in the engine causes significant engine problems due to high viscosity (about 10 to 17 times higher than petroleum diesel fuel). Besides, a lower cetane number and lower calorific values restrict the use of crude vegetable oil as an effective fuel for compression ignition (CI) engines. Again, most non-edible vegetable oils have high free fatty acid contents (FFA). Thus, the use of crude vegetable oil, would end up producing high smoke, unburnt-hydrocarbons (HC), and carbon monoxide (CO) emissions, lower brake thermal efficiency and poor engine performance [35]. Additionally, higher viscosity and lower volatility of crude vegetable oil can result in poor fuel flow, incomplete combustion, severe carbon deposits, injector coking and piston ring sticking [36-38]. There are many techniques, methods and processes to overcome these problems. These include pyrolysis, micro emulsification, dilution and transesterification [39-44]. Among them, transesterification is the most popular technique used to reduce the viscosity and oxygen content of crude vegetable oil. The transesterification process converts triglycerides into alkyl esters using an alcohol. Researchers have used both methanol and ethanol as alcohol in the transesterification process [45]. However, methanol is less costly and has better reactivity, and the fatty acid methyl esters (FAME) produced are more susceptible to evaporate easily than corresponding ethyl esters. On the other hand, ethanol is derived from renewable feedstocks and it is also less toxic [32]. Several process parameters such as reaction temperature, catalyst type, catalyst concentration, type of alcohol and their oil to molar ratio, reaction time and agitation speed affect biodiesel yield production and biodiesel quality. Therefore, the transesterification optimisation process is very vital for better quality and higher yield of biodiesel fuel.

Biodiesel can be used as alternatives to fossil fuel in CI engines to reduce their HC, smoke and CO emissions. As biodiesels are considered to be oxygenated fuels, the excess oxygen content in biodiesel ensures better combustion, resulting in higher exhaust gas temperature as well as higher NO_x formation. Nabi et al. [46] reported that particulate matter (PM) generation from biodiesel combustion is significantly reduced due to higher oxygen content and absence of

aromatics in the fuel. Sathiyamoorthi et al. [47] investigated palmarosa oil biodiesel at different blends with diesel, and found lower CO, HC, smoke emissions and slightly higher NO_x emission generation in all biodiesel blends compared with pure diesel. Castor biodiesel (B20) can reduce CO and HC by 8.2% and 8.9% respectively. In addition, a considerable reduction in oxides of nitrogen was claimed by Arunkumar et al. [48]. Roy et al. [49] used canola oil biodiesel at different blends and found there was no increase in NO_x emission as well as lower CO and HC emissions at 5% biodiesel blend. Uyumaz [50] investigated mustard seed oil biodiesel and found remarkable reductions in CO and smoke emissions at 30% biodiesel blend, whereas NO_x emission was increased by 22.1%. Sanjid et al. [51] mixed two non-edible feedstocks, kapok and moringa, and found average NO_x and CO_2 emissions for those mixed blends were 14-17% and 1-3% higher respectively than for diesel. Again, the lower calorific value, higher viscosity, density and pour point, poor cold flow property, lower volatility, higher brake specific fuel consumption (BSFC), lower brake thermal efficiency (BTE), and the generation of higher NO_x and CO_2 emissions and EGT limit the use of biodiesel over diesel fuel [52-55]. Beauty leaf tree biodiesel reduced CO by 6%, and HC by 8% at B20 [56].

Research shows that incorporation of various additives and alcohols in the biodiesel blend can reduce engine exhaust emissions as well as overcome some of the above-mentioned limitations [57-60]. Therefore, this study focuses on the multiple criteria decision making for biodiesel feedstock selection, and to optimise the biodiesel production process to achieve a sustainable production at cheaper cost. This study undertakes an engine testing programme using papaya seed oil (PSO) and stone fruit kernel seed oil (SFO) biodiesels to determine engine performance, emission levels as well as combustion characteristics. Since there was no literature found on engine performance, emissions analysis and combustion characteristics of ternary blends of PSO biodiesel using any alcohol or additive, the effects of papaya seed oil (PSO) biodiesel binary blends and ternary blends on a diesel engine are critically evaluated experimentally in this study.

1.4 Research questions

The fundamental research questions that are addresses in the thesis are based on the above research problems and gaps. This study addressed the following research questions:

[Q1] Are PSO and SFO biodiesels able to meet biodiesel quality standards?

[Q2] What are the optimum production process parameters for biodiesel production from PSO and SFO?

[Q3] What are the effects of PSO and SFO biodiesel on engine performance, exhaust emission behaviour and combustion characteristics? How do they compare with each other and standard diesel?

[Q4] What are the impacts of operating parameters of biodiesel-diesel blends to enhance engine performance, exhaust emissions and combustion behaviour?

[Q5] What are the optimum binary (diesel-biodiesel) and ternary (diesel-biodiesel-additive) blends of biodiesel-diesel and their quality assessment in engine performance, emission behaviour and combustion characteristics?

1.5 Research objectives

The main aim of this study is to optimise the production process parameters for biodiesel production from PSO and SFO and investigate the performance, emission behaviour and combustion characteristics of a diesel engine fuelled with diesel-biodiesel (binary) blends as well as diesel-biodiesel-additives (ternary) blends. This study identified the best operational conditions for improving the engine performance and reducing emissions. The above-mentioned research questions and the main aims are addressed through experimental measurements and numerical analysis. The specific objectives are to:

[1] Determine the physicochemical properties of 2nd generation biodiesel produced from Australian native PSO and SFO.

[2] Identify the prospective 2nd generation biodiesel feedstocks using the multiple criteria decision-making process.

[3] Optimise the biodiesel production process using a mathematical and statistical model.

[4] Investigate the impact of operating conditions of PSO biodiesel on engine performance.

[5] Optimise the impact of operating conditions of PSO biodiesel on engine emission behaviour.

[6] Compare PSO and SFO biodiesel in terms of engine performance, and combustion characteristics

[7] Analyse the impact of binary and ternary blends of PSO biodiesel on diesel engine performance, emission behaviour and combustion characteristics.

1.6 Research approach

This thesis is prepared as a thesis by publication format with a total of nine chapters. A conceptual flow chart of this research is presented in Figure 3.

Chapter 2 is based on the comprehensive literature review of the current biodiesel situation in Australia. This chapter discusses the potential of papaya seed and stone fruit kernel biodiesels - the two sources of 2nd generation transportation biodiesels in Australia. The challenges associated with biodiesel production and their possible solutions, particularly on feedstock selection, oil extraction, conversion of oil into biodiesel, biodiesel storage and transport, costs of production and the information needs for commercialising these sources of biodiesels are discussed, along with the eco-friendly attributes of these biodiesels with regard to the Australian transport sector.

This chapter has been published in "Energy Reports" journal. The full reference is Anwar, M., M.G. Rasul, N. Ashwath, and M.D.N. Nabi, 2019, *The potential of utilising papaya seed oil and stone fruit kernel oil as non-edible feedstock for biodiesel production in Australia—A review*. **Energy Reports**, **5,** p. 280-297, **Elsevier BV**, The Netherlands [Q1].

Chapter 3: The selection of the appropriate biodiesel feedstock was the most important step in this research. In Chapter 3, six biodiesels, namely papaya seed oil biodiesel (PSO), stone fruit kernel oil biodiesel (SFO), jatropha oil biodiesel (JBD), rapeseed oil biodiesel (RBD), beauty leaf tree biodiesel (BLT), and waste cooking oil biodiesel (WCB) were analysed. Twelve physico-chemical properties, namely kinematic viscosity (KV), density, higher heating value (HHV), oxidation stability (OS), acid value (AV), flash point (FP), cold filter plug point (CFPP), cetane number (CN), iodine value (IV), monounsaturated fatty acid (MUFA), polyunsaturated fatty acid (PUFA) and long chain saturated factor (LCSF) were used as criteria for ranking the above biodiesels. Three weightage (%) methods of EQUAL, CRITIC and ENTROPY were used for weight determination of criteria. Four different multiple-criteria decision analysis (MCDA) methods, namely PROMETHEE Graphical Analysis for Interactive Assistance (GAIA), Weighted sum method (WSM), Weighted product method (WPM), and

Technique for order preference by similarity to ideal solution (TOPSIS) were used for the analysis.

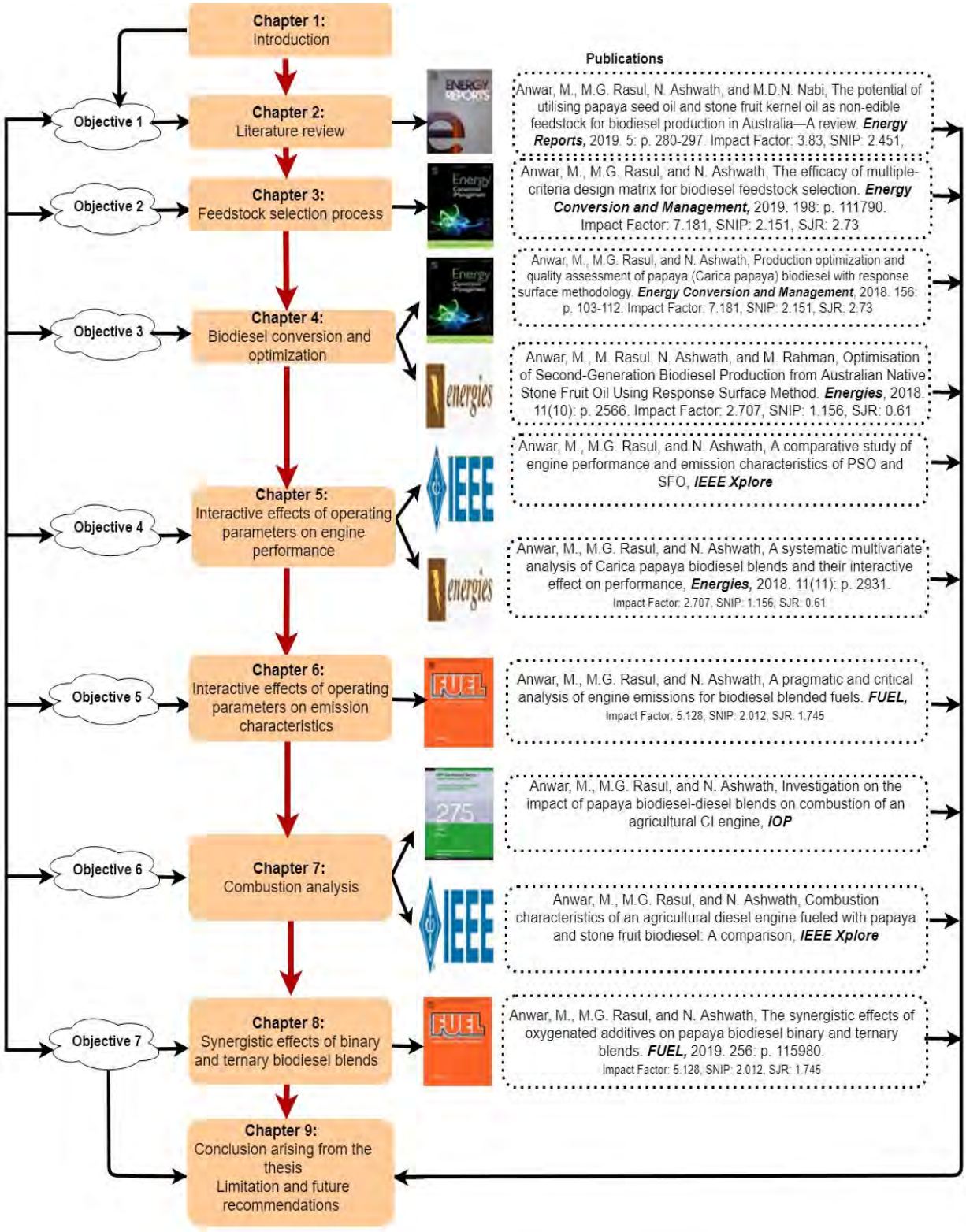

Figure 3: Outline of the thesis.

Chapter 3 has been published in ***"Energy Conversion and Management"*** journal. The full reference is Anwar, Rasul, and Ashwath, 2019, *The efficacy of multiple-criteria design matrix for biodiesel feedstock selection.* **Energy Conversion and Management**, **198**, p. 111790, **Elsevier BV**, The Netherlands [Q1].

Chapter 4 is based on the biodiesel production process optimisation. This chapter has two parts. Part A investigated the optimisation of the papaya seed oil biodiesel production process, whereas the optimisation of stone fruit kernel biodiesel production process was focused on in part B. Biodiesel production process parameters such as catalyst concentration, methanol: oil molar ratio and reaction temperature were optimised by using the Response Surface Methodology based on the Box-Behnken experimental design. The statistical tool MINITAB 17 was used to draw both 3D surface plots and 2D contour plots to predict the optimum biodiesel yield.

Part A and Part B have been published in ***"Energy Conversion and Management"*** journal and ***'Energies'*** journal respectively. Chapter 4, Part A was referenced as Anwar,. Rasul, and Ashwath, 2018, *Production optimization and quality assessment of papaya (Carica papaya) biodiesel with response surface methodology*. **Energy Conversion and Management**, **156**, p. 103-112, **Elsevier BV**, The Netherlands [Q1] and Part B was referenced as Anwar, Rasul, Ashwath, and Rahman, 2018, *Optimisation of Second-Generation Biodiesel Production from Australian Native Stone Fruit Oil Using Response Surface Method.* **Energies**, **11(10)**, p. 2566, **MDPI**, Switzerland [Q2].

Chapter 5 is about the interactive effects of operating parameters on engine performance. This chapter has two parts as well. Part A investigates the engine performance and emission characteristics of the biodiesels synthesised from papaya seed oil (PSO) and stone fruit kernel oil (SFO) blends using a diesel engine. All experiments were carried out at full load condition with different engine speeds ranging from 1200 rpm to 2400 rpm at intervals of 200 rpm. Diesel (100%) and its four blends of 10% biodiesel with 90% diesel (PSO10, SFO10), and 20% biodiesel with 80% diesel (PSO20, SFO20) were considered for comparative analysis. The results show that SFO biodiesel blends have better engine performance than PSO biodiesel blends. However, the PSO biodiesel blends prove to be a better overall choice due to their excellent environmentally friendly attributes that can reduce the exhaust emissions to a greater extent.

Chapter 5, Part A has been published in ***IEEE Xplore*** journal and referenced as Anwar, Rasul and Ashwath, *A comparative study of engine performance and emission characteristics of biodiesels produced from the waste seeds of papaya and stone fruit.* **IEEE** 2nd International Conference on Renewable Energy and Power Engineering, Toronto, Canada, Nov. 2-4, 2019, Paper PE042.

Chapter 5, Part B investigates the interactive relationship between three operating parameters (papaya seed oil (PSO) biodiesel blends, engine load, and engine speed) and four responses (brake power, BP; torque; brake specific fuel consumption, BSFC; and, brake thermal efficiency, BTE) for engine testing. A fully instrumented four cylinder four-stroke, naturally aspirated agricultural diesel engine was used for all experiments. Three different blends: B5 (5% PSO biodiesel +95% diesel), B10 (10% PSO biodiesel + 90% diesel), and B20 (20% PSO biodiesel + 80% diesel) were tested. Physicochemical properties of these blends and pure PSO biodiesel were characterised, and the engine's performance characteristics were analysed. The analysis of variance and quadratic regression modelling showed that both load and speed were the most important parameters that affect engine performance, while PSO biodiesel blends had a significant effect on BSFC.

Chapter 5, Part B has been published in ***Energies*** journal and referenced as Anwar, Rasul, and Ashwath, 2018, *A Systematic Multivariate Analysis of* Carica papaya *Biodiesel Blends and Their Interactive Effect on Performance*. **Energies**, **11(11)**, p. 2931, **MDPI**, Switzerland [Q2].

Chapter 6 investigates the effects of non-edible biodiesel blends on the exhaust emission characteristics of a naturally aspirated four stroke multi-cylinder diesel engine under different loading conditions. A comparative analysis of the emission characteristics of four non-edible biodiesel blends (20% vol. = B20) and petroleum diesel was performed by varying engine loads and speeds. The aim was to optimise operating parameters such as biodiesel blends, engine loads and speed on engine emissions of nitrogen oxide (NO_x), carbon dioxide (CO_2), hydrocarbon (HC), particulate matter (PM), carbon monoxide (CO) and exhaust gas temperature (EGT). A statistical model and analysis of variance (ANOVA) were used to optimise various parameters. The results revealed that the engine load and speed were the two most imperative parameters that affected emissions (NO_x, HC, PM and CO). Both biodiesel blend and the load were responsible for changing the EGT and NO_x emission. While NO_x emission was unaffected by variations in biodiesel blends, load or speed, the CO_2 emission was not influenced by the biodiesel blends at various operating parameters.

Revised version of Chapter 6 has been submitted in ***Fuel*** journal and is entitled, *"A pragmatic and critical analysis of engine emissions for biodiesel blended fuels"*.

Chapter 7 investigates the impact of papaya biodiesel blends on combustion characteristics of a diesel engine. In Part A, various PSO blends (5%, 10%, and 20%) were tested and compared with diesel at speeds of 1400 rpm and 2400 rpm at full load condition. The combustion characteristics of in-cylinder pressure, heat release rate, ignition delay, mass fraction burned, ignition duration and cylinder temperature were tested. The results show that PSO blends have some excellent attributes as fuel regarding combustion characteristics. Part B shows the comparative analysis of combustion characteristics of a diesel engine fuelled with PSO and SFO biodiesel blends. Amongst the two biodiesels tested, the PSO blends performed better than those of SFO blends in all combustion characteristics.

Chapter 7, Part A has been published in ***Earth and Environmental Science*** journal and entitled, *"Investigation on the impact of papaya biodiesel-diesel blends on combustion of an agricultural CI engine"*. Again, Part B has been published in ***IEEE Xplore*** journal and referenced as Anwar, Rasul and Ashwath, *Combustion characteristics of an agricultural diesel engine fuelled with papaya and stone fruit biodiesel: A comparison*, **IEEE** 2nd International Conference on Renewable Energy and Power Engineering, Toronto, Canada, Nov. 2-4, 2019, Paper PE043.

Chapter 8 explores PSO binary and ternary blends in a diesel engine which are compared with diesel fuel in terms of engine performance, exhaust emissions and combustion behaviour. The PSO biodiesel of 20% v/v with 80% v/v diesel was considered as the binary blend (P20). Two ternary fuel blends of 5% v/v of oxygenated additives (diglyme and n-butanol) with P20 biodiesel and 75% v/v of diesel which are referred to as P20DG5 (diglyme) and P20BT5 (n-butanol). Another ternary blend of 10% v/v of PSO biodiesel with 80% v/v diesel and 10% v/v stone fruit oil (SFO) biodiesel referred to as PSFO20 was used to compare the overall results. P20DG5 proved to be an excellent choice for mitigating the environmental problems without compromising the engine performance and enhanced better combustion.

Chapter 8 has been published in ***Fuel*** journal and referenced as Anwar, Rasul, and Ashwath, 2019, *The synergistic effects of oxygenated additives on papaya biodiesel binary and ternary blends*. **Fuel**, **256**, p. 115980, **Elsevier BV**, The Netherlands [Q1].

Chapter 9 summarises the key findings of this research and proposes some recommendations for future work.

References

1. Ong, H.C., T.M.I. Mahlia, and H.H. Masjuki, *A review on energy scenario and sustainable energy in Malaysia.* Renewable and Sustainable Energy Reviews, 2011. **15**(1): p. 639-647.
2. Bilen, K., O. Ozyurt, K. Bakırcı, S. Karslı, S. Erdogan, M. Yılmaz, and O. Comaklı, *Energy production, consumption, and environmental pollution for sustainable development: A case study in Turkey.* Renewable and Sustainable Energy Reviews, 2008. **12**(6): p. 1529-1561.
3. *IEA, International Energy Agency; 2017, [cited 8 December 2018] Available from:* <http://www.iea.org/>.
4. *BP Statistical Review of World Energy June 2017.*
5. *EIA's International Energy Outlook 2019 (IEO2019).*
6. *EIA's International Energy Outlook 2017* (IEO2017).
7. Trading economics, *Australia GDP, 2019, [cited 20 November 2019] Available from:* <https://tradingeconomics.com/australia/gdp>.
8. *Department of the Environment and Energy (2019), Australian Energy Update 2019, Canberra, August.*
9. CEIC Data, *Australia oil consumption, 2019, [cited 15 November 2019] Available from:* <https://www.ceicdata.com/en/indicator/australia/oil-consumption>.
10. Mofijur, M., M.A. Hazrat, M.G. Rasul, and H.M. Mahmudul, *Comparative Evaluation of Edible and Non-edible Oil Methyl Ester Performance in a Vehicular Engine.* Energy Procedia, 2015. **75**: p. 37-43.
11. Bhuiya, M.M.K., M.G. Rasul, M.M.K. Khan, N. Ashwath, and A.K. Azad, *Prospects of 2nd generation biodiesel as a sustainable fuel—Part: 1 selection of feedstocks, oil extraction techniques and conversion technologies.* Renewable and Sustainable Energy Reviews, 2016. **55**: p. 1109-1128.
12. Dincer, K., *Lower Emissions from Biodiesel Combustion.* Energy Sources, Part A: Recovery, Utilization, and Environmental Effects, 2008. **30**(10): p. 963-968.
13. Mosarof, M.H., M.A. Kalam, H.H. Masjuki, A. Alabdulkarem, A.M. Ashraful, A. Arslan, H.K. Rashedul, and I.M. Monirul, *Optimization of performance, emission,*

friction and wear characteristics of palm and Calophyllum inophyllum *biodiesel blends.* Energy Conversion and Management, 2016. **118**: p. 119-134.

14. Ganjehkaviri, A., M. Mohd Jaafar, S. Hosseini, and A. Musthafa, *Performance Evaluation of Palm Oil-Based Biodiesel Combustion in an Oil Burner.* Energies, 2016. **9**(2): p. 97.
15. Rahman, S.M.A., H.H. Masjuki, M.A. Kalam, M.J. Abedin, A. Sanjid, and M.M. Rahman, *Assessing idling effects on a compression ignition engine fueled with Jatropha and Palm biodiesel blends.* Renewable Energy, 2014. **68**: p. 644-650.
16. Atabani, A.E., A.S. Silitonga, H.C. Ong, T.M.I. Mahlia, H.H. Masjuki, I.A. Badruddin, and H. Fayaz, *Non-edible vegetable oils: A critical evaluation of oil extraction, fatty acid compositions, biodiesel production, characteristics, engine performance and emissions production.* Renewable and Sustainable Energy Reviews, 2013. **18** (Supplement C): p. 211-245.
17. Azad, A.K., M.G. Rasul, M.M.K. Khan, S.C. Sharma, and M.A. Hazrat, *Prospect of biofuels as an alternative transport fuel in Australia.* Renewable and Sustainable Energy Reviews, 2015. **43**(Supplement C): p. 331-351.
18. Md Mofijur Rahman, M.R., Nur Md Sayeed Hassan and Justin Hyde, *Prospects of Biodiesel Production from Macadamia Oil as an Alternative Fuel for Diesel Engines.* Energies, 2016. **9**(403).
19. Lin, L., Z. Cunshan, S. Vittayapadung, S. Xiangqian, and D. Mingdong, *Opportunities and challenges for biodiesel fuel.* Applied Energy, 2011. **88**(4): p. 1020-1031.
20. Cornejo, A., I. Barrio, M. Campoy, J. Lázaro, and B. Navarrete, *Oxygenated fuel additives from glycerol valorization. Main production pathways and effects on fuel properties and engine performance: A critical review.* Renewable and Sustainable Energy Reviews, 2017. **79**: p. 1400-1413.
21. Mofijur, M., H.H. Masjuki, M.A. Kalam, M.A. Hazrat, A.M. Liaquat, M. Shahabuddin, and M. Varman, *Prospects of biodiesel from Jatropha in Malaysia.* Renewable and Sustainable Energy Reviews, 2012. **16**(7): p. 5007-5020.
22. ZME Science, How long before the world runs out of fossil fuels? 2018, [cited 25 November 2019] Available from: <https://www.zmescience.com/other/feature-post/how-long-fossil-fuels-last-43432/>.
23. Math, M.C. and K.N. Chandrashekhara, *Optimization of Alkali Catalyzed Transesterification of Safflower Oil for Production of Biodiesel.* Journal of Engineering, 2016. **2016**: p. 7

24. Sims R., R. Schaeffer, F. Creutzig, X. Cruz-Núñez, M. D'Agosto, D. Dimitriu, M.J. Figueroa Meza, L. Fulton, S. Kobayashi, O. Lah, A. McKinnon, P. Newman, M. Ouyang, J.J. Schauer, D. Sperling, and G. Tiwari, 2014*: Transport. In: Climate Change 2014: Mitigation of Climate Change*. Contribution of Working Group III to the Fifth Assessment Report of the Intergovernmental Panel on Climate Change *[Edenhofer, O., R. Pichs-Madruga, Y. Sokona, E. Farahani, S. Kadner, K. Seyboth, A. Adler, I. Baum, S. Brunner, P. Eickemeier, B. Kriemann, J. Savolainen, S. Schlömer, C. von Stechow, T. Zwickel and J.C. Minx (eds.)]. Cambridge University Press, Cambridge, United Kingdom and New York, NY, USA.*

25. Norhasyima, R.S. and T.M.I. Mahlia, *Advances in CO_2 utilization technology: A patent landscape review.* Journal of CO_2 Utilization, 2018. **26**: p. 323-335.

26. *USDA Foreign Agricultural service: Australia Biofuels Annual 2017, Canberra.*

27. Department of Energy and Water Supply, *Towards a clean energy economy: achieving a biofuel mandate for Queensland.* 2015.

28. Jamil, F., A.H. Al-Muhtaseb, L. Al-Haj, M.A. Al-Hinai, P. Hellier, and U. Rashid, *Optimization of oil extraction from waste "Date pits" for biodiesel production.* Energy Conversion and Management, 2016. **117** (Supplement C): p. 264-272.

29. Mofijur, M., H.H. Masjuki, M.A. Kalam, and A.E. Atabani, *Evaluation of biodiesel blending, engine performance and emissions characteristics of Jatropha curcas methyl ester: Malaysian perspective.* Energy, 2013. **55**: p. 879-887.

30. Mofijur, M., H.H. Masjuki, M.A. Kalam, A.E. Atabani, I.M.R. Fattah, and H.M. Mobarak, *Comparative evaluation of performance and emission characteristics of Moringa oleifera and Palm oil based biodiesel in a diesel engine.* Industrial Crops and Products, 2014. **53**: p. 78-84.

31. Ahmad, F.B., Z. Zhang, W.O.S. Doherty, and I.M. O'Hara, *A multi-criteria analysis approach for ranking and selection of microorganisms for the production of oils for biodiesel production.* Bioresource Technology, 2015. **190**: p. 264-273.

32. Nwokoagbara, E., A.K. Olaleye, and M. Wang, *Biodiesel from microalgae: The use of multi-criteria decision analysis for strain selection.* Fuel, 2015. **159**: p. 241-249.

33. Samanlioglu, F., *A Multi-Criteria Decision Making Approach to Feedstock Selection.* 2018, 2018. **49**(1): p. 15.

34. Javier Martínez and Ricardo A.N.C., *Use of Multicriteria Decision Making (MCDM) Methods for Biomass Selection Aimed to Fischer Tropsch Processes.* International Journal of Engineering Trends and Technology (IJETT), 2016. **V34(6)**: p. 266-272.

35. Mosarof, M.H., M.A. Kalam, H.H. Masjuki, A. Alabdulkarem, A.M. Ashraful, A. Arslan, H.K. Rashedul, and I.M. Monirul, *Optimization of performance, emission, friction and wear characteristics of palm and* Calophyllum inophyllum *biodiesel blends.* Energy Conversion and Management, 2016. **118**(Supplement C): p. 119-134.
36. Pramanik, K., *Properties and use of* Jatropha curcas *oil and diesel fuel blends in compression ignition engine.* Renewable Energy, 2003. **28**(2): p. 239-248.
37. Ramadhas, A.S., S. Jayaraj, and C. Muraleedharan, *Characterization and effect of using rubber seed oil as fuel in the compression ignition engines.* Renewable Energy, 2005. **30**(5): p. 795-803.
38. Anwar, M., M.G. Rasul, and N. Ashwath, *Production optimization and quality assessment of papaya (*Carica papaya*) biodiesel with response surface methodology.* Energy Conversion and Management, 2018. **156**: p. 103-112.
39. Lin, L., Z. Cunshan, S. Vittayapadung, S. Xiangqian, and D. Mingdong, *Opportunities and challenges for biodiesel fuel.* Applied Energy, 2011. **88**(4): p. 1020-1031.
40. Atabani, A.E., A.S. Silitonga, H.C. Ong, T.M.I. Mahlia, H.H. Masjuki, I.A. Badruddin, and H. Fayaz, *Non-edible vegetable oils: A critical evaluation of oil extraction, fatty acid compositions, biodiesel production, characteristics, engine performance and emissions production.* Renewable and Sustainable Energy Reviews, 2013. **18** (Supplement C): p. 211-245.
41. Demirbas, A., *Biodiesel production from vegetable oils via catalytic and non-catalytic supercritical methanol transesterification methods.* Progress in Energy and Combustion Science, 2005. **31**(5): p. 466-487.
42. Agarwal, A.K., *Biofuels (alcohols and biodiesel) applications as fuels for internal combustion engines.* Progress in Energy and Combustion Science, 2007. **33**(3): p. 233-271.
43. Singh, S.P. and D. Singh, *Biodiesel production through the use of different sources and characterization of oils and their esters as the substitute of diesel: A review.* Renewable and Sustainable Energy Reviews, 2010. **14**(1): p. 200-216.
44. Yusuf, N.N.A.N., S.K. Kamarudin, and Z. Yaakub, *Overview on the current trends in biodiesel production.* Energy Conversion and Management, 2011. **52**(7): p. 2741-2751.
45. Alptekin, E. and M. Canakci, *Optimization of transesterification for methyl ester production from chicken fat.* Fuel, 2011. **90**(8): p. 2630-2638.
46. Nabi, M.N., A. Zare, F.M. Hossain, M.M. Rahman, T.A. Bodisco, Z.D. Ristovski, and R.J. Brown, *Influence of fuel-borne oxygen on European Stationary Cycle: Diesel*

engine performance and emissions with a special emphasis on particulate and NO emissions. Energy Conversion and Management, 2016. **127**: p. 187-198.

47. Sathiyamoorthi, R., G. Sankaranarayanan, S.B. Adhith kumaar, T. Chiranjeevi, and D. Dilip Kumar, *Experimental investigation on performance, combustion and emission characteristics of a single cylinder diesel engine fuelled by biodiesel derived from* Cymbopogon Martinii. Renewable Energy, 2019. **132**: p. 394-415.
48. Arunkumar, M., M. Kannan, and G. Murali, *Experimental studies on engine performance and emission characteristics using castor biodiesel as fuel in CI engine.* Renewable Energy, 2019. **131**: p. 737-744.
49. Roy, M.M., W. Wang, and J. Bujold, *Biodiesel production and comparison of emissions of a DI diesel engine fueled by biodiesel–diesel and canola oil–diesel blends at high idling operations.* Applied Energy, 2013. **106**: p. 198-208.
50. Uyumaz, A., *Combustion, performance and emission characteristics of a DI diesel engine fueled with mustard oil biodiesel fuel blends at different engine loads.* Fuel, 2018. **212**: p. 256-267.
51. Sanjid, A., M.A. Kalam, H.H. Masjuki, M. Varman, N.W.B.M. Zulkifli, and M.J. Abedin, *Performance and emission of multi-cylinder diesel engine using biodiesel blends obtained from mixed inedible feedstocks.* Journal of Cleaner Production, 2016. **112**: p. 4114-4122.
52. Örs, I., S. Sarıkoç, A.E. Atabani, S. Ünalan, and S.O. Akansu, *The effects on performance, combustion and emission characteristics of DICI engine fuelled with TiO2 nanoparticles addition in diesel/biodiesel/n-butanol blends.* Fuel, 2018. **234**: p. 177-188.
53. Sivalakshmi, S. and T. Balusamy, *Performance and emission characteristics of a diesel engine fuelled by neem oil blended with alcohols.* International Journal of Ambient Energy, 2011. **32**(4): p. 170-178.
54. Murugesan, A., C. Umarani, T.R. Chinnusamy, M. Krishnan, R. Subramanian, and N. Neduzchezhain, *Production and analysis of bio-diesel from non-edible oils—A review.* Renewable and Sustainable Energy Reviews, 2009. **13**(4): p. 825-834.
55. Comin, M., A.C.D. de Souza, A.C. Roveda, S.S. Yahagi, L.H. de Oliveira, M.S. Amaral, C.A.A. Silva, A.R. Fiorucci, R.S. Gomes, A.R.L. Caires, and M.A.G. Trindade, *Alternatives binary and ternary blends and its effects on stability of soybean biodiesel contaminated with metals.* Fuel, 2017. **191**: p. 275-282.

56. Bhuiya, M., M. Rasul, M. Khan, and N. Ashwath, Performance and emission characteristics of a compression ignition (CI) engine operated with beauty leaf biodiesel. Energy Procedia, 2019. 160: p. 641-647.

57. Misra, R.D. and M.S. Murthy, *Blending of additives with biodiesels to improve the cold flow properties, combustion and emission performance in a compression ignition engine—A review*. Renewable and Sustainable Energy Reviews, 2011. **15(**5): p. 2413-2422

58. Rashedul, H.K., H.H. Masjuki, M.A. Kalam, A.M. Ashraful, S.M. Ashrafur Rahman, and S.A. Shahir, *The effect of additives on properties, performance and emission of biodiesel fuelled compression ignition engine.* Energy Conversion and Management, 2014. **88**: p. 348-364.

59. Nabi, M.N., *Theoretical investigation of engine thermal efficiency, adiabatic flame temperature, NOx emission and combustion-related parameters for different oxygenated fuels.* Applied Thermal Engineering, 2010. **30**(8): p. 839-844.

60. Wang, X., C.S. Cheung, Y. Di, and Z. Huang, *Diesel engine gaseous and particle emissions fueled with diesel–oxygenate blends.* Fuel, 2012. **94**: p. 317-323.

{this page is intentionally left blank}

Declaration of Co-authorship and Contribution

Research Division

CHAPTER 2: Literature Review

Title of the paper	The potential of utilising papaya seed oil and stone fruit kernel oil as non-edible feedstock for biodiesel production in Australia—A review
Full bibliographic reference	Anwar, M., M.G. Rasul, N. Ashwath, and M.D.N. Nabi, The potential of utilising papaya seed oil and stone fruit kernel oil as non-edible feedstock for biodiesel production in Australia—A review. Energy Reports, 2019. 5: p. 280-297. https://www.sciencedirect.com/science/article/pii/S2352484718303640
Status	Published

Nature of Candidate's Contribution, including percentage of total
I was responsible for Design concept of the article, analysed the literature, drafted the manuscript and acted as the corresponding author. [80%]

Nature of all Co-Authors' Contributions, including percentage of total
My co-authors, Prof Mohammad Rasul, A/Professor Nanjappa Ashwath and Dr Md Nurun Nabi, were designed concept and reviewed the literature related to biodiesel in Australian context. [20%]

Has this paper been submitted for an award by another research degree candidate (Co- Author), either at CQUniversity or elsewhere? (if yes, give full details)
No

Candidate's Declaration

I declare that the publication above meets the requirements to be included in the thesis as outlined in the Research Higher Degree Theses Policy and Procedure.

Mohammad Anwar

Energy Reports 5 (2019) 280–297

Contents lists available at ScienceDirect

Energy Reports

journal homepage: www.elsevier.com/locate/egyr

Review article

The potential of utilising papaya seed oil and stone fruit kernel oil as non-edible feedstock for biodiesel production in Australia—A review

Mohammad Anwar [a,*], Mohammad G. Rasul [a], Nanjappa Ashwath [b], M.D. Nurun Nabi [c]

[a] Central Queensland University, School of Engineering and Technology, Queensland 4702, Australia
[b] Central Queensland University, School of Health, Medical and Applied Sciences, Queensland 4702, Australia
[c] Central Queensland University, School of Engineering and Technology, Perth, WA 6000, Australia

ARTICLE INFO

Article history:
Received 2 November 2018
Received in revised form 14 February 2019
Accepted 15 February 2019
Available online xxxx

Keywords:
Papaya seed
Stone fruit kernel
Apricot
RSM
Biodiesel
Renewable energy
Australia
Optimisation
Challenges
Engine performance
Emission
Second generation

ABSTRACT

This paper reviews and discusses the potential of papaya seed and stone fruit kernel biodiesels — the two sources of 2nd generation transport biodiesels in Australia. The challenges associated with biodiesel production and their possible solutions, particularly on feedstock selection, oil extraction, conversion of oil into biodiesel, biodiesel storage and transport, costs of production and the information needs for commercialising these sources of biodiesels are discussed, along with the eco-friendly attributes of these biodiesels to Australian transport sector. Some researchers report that the use of papaya seed and stone fruit kernel biodiesels reduce engine power only 2 to 5%), however significantly reduce harmful engine emission such as HC reductions of 9 to 19%, PM reductions of 19.5 to 35% and CO reductions of 11 to 29%.

Contents

https://doi.org/10.1016/j.egyr.2019.02.007

1. Introduction

Australia's economy heavily depends on energy use, and this dependence will continue to grow into the future. At present, 94% of Australia's total energy consumption is catered by non-renewable sources of energy which includes coal, oil and gas. Fig. 1(a) shows leading primary energy sources in 2015–16, and their consumption by fuel type. As can be seen that oil was the primary source of energy and accounted for 37%, whereas coal was 32.2% followed by gas 24.8%. Over the last 10 years, Australia's energy consumption has increased by 0.6% a year (Department of the Environment and Energy, 2017). The renewable energy accounts for only 6% and the majority of bioenergy is sourced from biomass. Fig. 1(b) shows the percentage usage of renewable energy by various sources in 2015–16, of which biomass accounts for 55% whereas biofuel only 12%. Both biomass and biofuels are drawing larger attention in Australia as an alternative renewable source of energy.

The most significant primary energy-consuming sector in Australia in 2015–16 was electricity generation which accounted for 1755.7 PJ or 29% of the total national consumption, and had an annual growth of 3.4% in that year. The second large energy-consuming sector was the transport sector which accounted for 27%. Yearly growth for road and air transport sectors have increased by 1.7% in 2015–2016, and this trend is likely to continue. The share of energy consumption by the transport sector is projected to increase slightly from 29% to 32% over the period to 2049–50 (Australian Energy Projections, 2014). Table 1 shows the 2015–16 energy consumption details for Australia by sector.

Australian liquid fuel consumption has been static over the last 15 years, and the local refineries have produced 26 billion litres of fuels that include both petrol and diesel (80% together in 2016). Australia is heavily reliant on imported refined crude oil to meet its demand. Nearly 80% of the crude oil and other feedstocks were imported in 2016. The Australian production of crude oil has been declining, and about 76% of it was exported, as these oils are mostly unsuitable for local refineries. Furthermore, the number of Australian oil refineries has declined from seven to five since 2010, indicating limited scope for local supply fuel in Australia. The projection of diesel fuel usage by different sectors is shown in Table 2.

The Australian transportation sector is mostly reliant on petroleum fuels such as petrol and diesel. Generally, the light vehicle sector uses petrol as its dominant fuel, whereas the heavy vehicles use diesel. The share of diesel usage is increasing day-by-day even though the fuel efficiency and vehicle performance have improved. Nowadays, automobile manufacturers are focusing more on diesel-based vehicles than on petrol-based vehicles. Petrol, diesel and aviation fuel accounted for 90% energy usage in the transport sector in 2015. The share of petrol is declining, whereas the use of diesel and aviation fuels are continuing to increase due to mining and increased air transport activities, respectively. Biodiesel is attracting large attention throughout the world due to its similarity with diesel and its environmentally-friendly nature. As biodiesel production in Australia from its native plants has not yet fully exploited, a detailed review on biodiesel production from Australian native 2nd generation feedstocks and its potential as an alternative fuel for transport sector is therefore needed, and is presented in this paper.

* Corresponding author.
E-mail address: m.anwar@cqu.edu.au (M. Anwar).

2. Biodiesel—an alternative source of energy in Australia

Biodiesel is becoming popular due to its environmentally-friendly nature, including its reduced environmental pollution and its potential to serve as an alternative source of energy (Rahman et al., 2015; Bhuiya et al., 2016). It is sulphur-free, non-toxic, renewable, biodegradable, clean burning, ester-based, and it is an oxygenated fuel (Dincer, 2008; Mosarof et al., 2016; Ganjehkaviri et al., 2016; Rahman et al., 2014). It is a mixture of alkyl esters of long chain fatty acids which are synthesised via esterification and transesterification of free fatty acids and triglycerides, respectively (Bhuiya et al., 2016; Atabani et al., 2013; Luque et al., 2008). Biodiesel is also known as fatty acid methyl ester (FAME), and is derived from vegetable oils (edible or non-edible) and animal fats (Azad et al., 2015; Rahman et al., 2016; Lin et al., 2011). The biodiesel fuel can be added directly into diesel engines, with no or minimal modification of the engine. Often biodiesel has proven to provide better engine performance and lubrication (Cornejo et al., 2017). It is a globally accepted fuel to reduce exhaust gas emissions and environmental issues. When synthesised appropriately, biodiesel will meet international fuel standards and is highly compatible for mixing with diesel. Biodiesel can be blended with diesel at any proportion, and the modern diesel engines can cope with this blended biodiesel–diesel fuel without any issues (Rahman et al., 2012). The USA, European Union, and Australia have set their own specifications and technical regulations for biodiesel. These include ASTM 6751—02, EN14214 and the Australian Fuel Standard (biodiesel), respectively (Table 3).

Potential biodiesel sources can be categorised into three major divisions, namely (i) first-generation biodiesel feedstocks, i.e., edible vegetable oil sources, (ii) second-generation biodiesel feedstocks, i.e., non-edible vegetable oil and animal fat sources, and (iii) third-generation biodiesel feedstocks, i.e., microalgae, algae, fungi, latexes, bacteria and terpenes (Atabani et al., 2013). While significant advances have been made for producing the first-generation biodiesel, the research on second and third-generation biodiesels is limited, particularly from the point of view of commercialisation. Furthermore, the usage of first-generation biodiesel has raised many concerns, for example, the food versus fuel debate, as well as severe environmental problems such as deforestation and vital soil loss due to land clearing for biodiesel production. The focus now has shifted to second-generation biodiesel production from non-edible vegetable oils due to their accessibility and low cost (Bhuiya et al., 2016; Jamil et al., 2016).

Some popular second-generation feedstocks include *Calophyllum inophyllum*, *Eruca sativa*, *Jatropha curcas*, papaya seed oil, *Pongamia pinnata (or glabra)* (karanja), *Madhuca indica*, *Salvadora oleoides*, cottonseed, tobacco, rubber seed, desert date, fish oil, jojoba, neem, apricot seed, *Moringa oleifera*, sal, chicken fat, pork lard, beef tallow and waste cooking oil (Rahman et al., 2012; Avinash et al., 2014; Baiju et al., 2009; Godiganur et al., 2009; Kaul et al., 2007; Aydin and Bayindir, 2010; Usta, 2005; Li et al., 2009; Özcanlımath et al., 2011; Atabani et al., 2012). Table 4 shows popular biodiesel feedstocks used in various countries around the world.

The biodiesel industry of Australia has significantly reduced its production in recent years due to lower crude oil prices, high feedstock prices and a changing policy framework (USDA, 2017). It is predicted that total production in 2018 will be 290 ML (250 ML of ethanol and 40 ML of biodiesel). This estimated production would be unchanged from 2017. However, biodiesel production had peaked at 400 ML in 2014 when the consumption had approached 800 ML that also included imported biodiesel. This biodiesel production has collapsed due to high costs of feedstocks and the low world crude oil price. Some of the Australian biodiesel processing facilities were closed in early 2016

Table 1
Australian primary energy consumption by sector (Department of the Environment and Energy, 2017).

Sector	2015–16 (PJ)	Share (%)	Average annual growth 2015–16 (%)	Average annual growth 10 years (%)
Electricity generation	1755.7	28.5	3.4	−0.5
Transport	1642.8	27.1	1.7	1.6
Manufacturing	1144.4	18.4	−1.8	−1.3
Mining	610.0	10.1	14.2	7.2
Residential	457.4	7.5	0.3	0.8
Commercial	321.5	5.6	1.0	2.0
Agriculture	110.3	1.8	5.6	1.8
Construction	23.4	0.4	−8.6	−1.3
Others	30.5	0.7	−18.4	−6.3
Total	6065.9	100.0	2.3	0.6

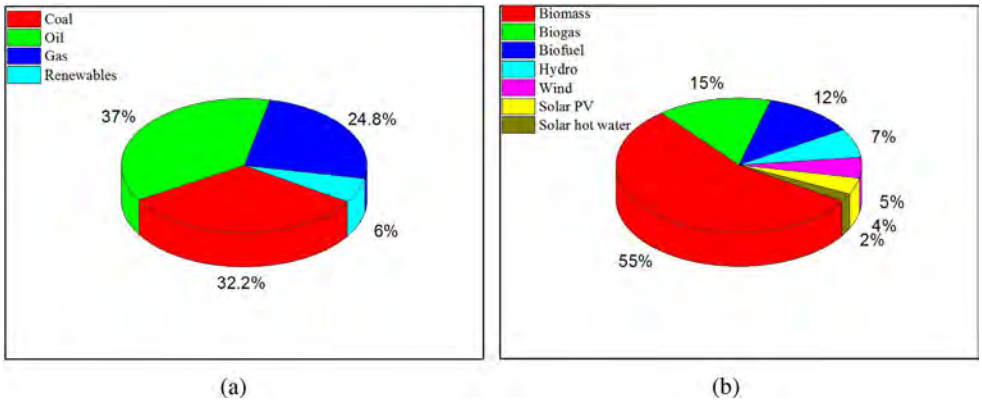

Fig. 1. Australian energy consumption (%) in 2015–2016 by: (a) Fuel type, and (b) Renewable energy type (Department of the Environment and Energy, 2017).

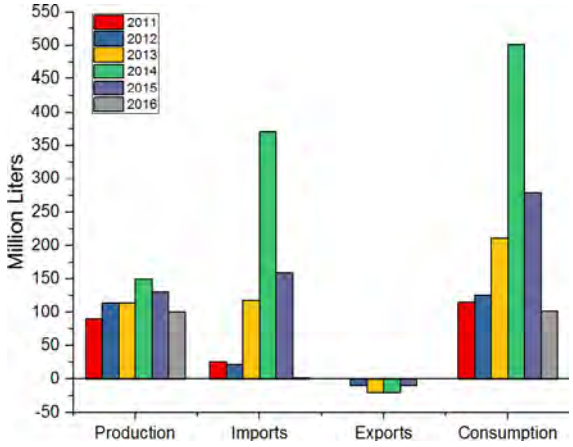

Fig. 2. Australian biodiesel scenario.
Source: Redrawn from USDA (2017).

due to uncompetitive prices with standard diesel. No commercial production of second and third-generation biodiesel occurs in Australia, and no subsidy scheme is being offered for commercial sales. Recently, the Queensland (Australia) Government has announced some programs aimed at making the state a centre of bio-manufacturing and biodiesel production. It is also expected that the commercial production of biodiesel will be used in the military, maritime and aviation sectors. Fig. 2 shows the Australian scenario of biodiesel production, imports, exports and consumption from 2011 to 2016. It can be seen that biodiesel consumption is much higher than production, therefore a significant amount import was needed.

Table 2
Australian fuel consumption projections — 2017 to 2024 (Million litres, ML) (USDA, 2017; Department of Industry, 2016).

Year	2017	2018	2019	2020	2021	2022	2023	2024
Diesel	24.0	24.0	24.2	24.4	24.6	24.8	25	25.2
On-road	7.7	7.9	8.1	8.3	8.6	8.8	9.0	9.2
Agriculture	3.5	3.6	3.7	3.8	3.9	4.0	4.1	4.2
Construction/mining	7.9	8.1	8.3	8.6	8.8	9.0	9.3	9.5
Shipping/rail	0.9	0.9	0.9	0.9	1.0	1.0	1.0	1.0
Industry	1.3	1.4	1.4	1.4	1.5	1.5	1.5	1.6
Jet fuel	0.4	0.4	0.5	0.5	0.5	0.5	0.5	0.5

The feedstocks used for producing second-generation biodiesel in Australia are primarily animal fats (tallow) and waste cooking oil (recycled yellow grease). Using these same feedstocks, renewable diesel can be produced. The difference between renewable diesel and biodiesel is noticeable. The renewable diesel is chemically balanced and fully compatible with diesel, whereas the biodiesel needs to meet range requirements specified in the ASTM and EU standards. Hydrogenated or hydrotreated vegetable oil (HVO) is the only type of renewable diesel that is available at a large commercial scale. So far, there is no commercial production of HVO biodiesel in Australia. Since 2012, Australia has imported and consumed small volumes of biodiesels. The first known shipment was 21.4 ML in 2013 from Singapore. Australia regularly exports tallow to Singapore which used to produce HVO. Table 5 shows the total biodiesel imports from various countries. The largest imports of biodiesels was from Singapore and Indonesia until 2015. Only 769 thousand litres of biodiesel was imported in 2016 and Indonesia supplied 89.2% (686 thousand litres) of it.

Australia has considered the addition of 5% biodiesel into diesel (B5) as a common blend due to its similar fuel properties with diesel. According to Australian Fuel Standard (biodiesel) Determination 2003, B5 is sold unlabelled whereas a 20% biodiesel

Table 3
ASTM D6751-2, EN 14214 and Australian fuel standard (biodiesel) determination 2003 specifications for biodiesel without blend (Rahman et al., 2012; Jayed et al., 2009; Singh and Singh, 2010; Atadashi et al., 2010; Murugesan et al., 2009).

Properties	Unit	ASTM D6751-2		EN 14214		Australian fuel standard (biodiesel) determination 2003	
		Limit	Method	Limit	Method	Limit	Method
Density at 15 °C	kg/m^3	870–890	ASTM D4052–91	860–900	EN ISO 3675, EN ISO12185	860–890	ASTM D1298
Viscosity @ 40 °C	mm^2/s	1.9–6.0	ASTM D445	3.5–5.0	EN ISO 3140	3.5–5.0	ASTM D445
Flash point	°C	Min 130	ASTM D93	Min 101	EN ISO 3679	Min 120	ASTM D93
Cloud point	°C	–	ASTM D2500	–	EN ISO 23015	–	EN ISO 23015
Cetane number	–	Min 47	ASTM D613	Min 51	EN ISO 5165	Min 51	ASTM D613
Acid number	mg KOH/g	Max 0.5	ASTM D664	Max 0.5	EN 14104	Max 0.8	ASTM D664
Oxidation stability	Hour	Min 3	ASTM D6751/ D7467	Min 6	EN ISO 14112	Min 6	EN ISO 14112
Iodine number	g I/100 g	–	–	Max 120	EN 14111	Max 120	EN 14111
Water content and sediment	mg/kg	Max 0.05 (%v)	ASTM D2709	Max 0.05	EN ISO 12937	Max 0.05 (%v)	ASTM D2709
Free glycerine	% m/m	Max 0.02	ASTM D6584	Max 0.02	EN 14105/ 14016	Max 0.02	ASTM D6584
Total glycerol	% m/m	Max 0.24	ASTM D6548	0.25	EN 14105	Max 0.25	ASTM D6584
Methanol content	% m/m	Max 0.2	EN 14110	Max 0.2	EN 14110	Max 0.2	EN 14110
Sulfated ash	% m/m	Max 0.02	ASTM D874	Max 0.02	EN ISO 3987	Max 0.02	ASTM D874
Phosphorus	mg/kg	Max 10	ASTM D4951	Max 10	EN 14107	Max 10	EN 14107
Carbon residue	% wt	Max 0.05	ASTM D4530	Max 0.3	EN ISO 10370	Max 0.3	ASTM D4530
Calcium and Magnesium	ppm	Max 5	EN 14538	Max 5	EN 14538	Max 5	EN 14538

Table 4
Popular biodiesel feedstocks around the world (Azad et al., 2015; Avinash et al., 2014; Rahman et al., 2013; Damanik et al., 2018; Milano et al., 2018).

Country	Popular feedstocks	
	Edible feedstocks	*Non-edible feedstocks*
Argentina	Soybeans, corn, wheat, sugarcane	–
Australia	Canola oil	Beauty leaf, *Jatropha curcas*, pongamia, waste cooking oil, tallow
Bangladesh	–	Rubber seed, *pongamia pinnata*
Brazil	Soybeans, palm, corn, sugarcane	Castor, cotton oil
Canada	soybeans, mustard, flax	Rapeseed, animal fat, yellow grease, and tallow
China	Corn, soybeans, wheat, sugarcane	*Jatropha curcas*, waste cooking oil, rapeseed
Colombia	Sugarcane, palm	–
Cuba	Sugarcane	*Jatropha curcas*, moringa, neem,
France	Sunflower	Rapeseed
Germany	–	Rapeseed
Ghana	Palm	
Greece	–	Cottonseed
India	Soybean, sunflower, sugarcane	*Jatropha curcas, Pongamia glabra* (karanja), rapeseed
Indonesia	Palm, coconut	*Jatropha curcas*
Iran	Palm	*Jatropha curcas*, castor, algae
Ireland	–	Waste cooking oil, animal fats
Italy	Sunflower	Rapeseed
Japan	–	Waste cooking oil
Kenya	–	Castor
Malaysia	Palm	–
Mali	–	*Jatropha curcas*
Mexico	Sugarcane and corn	Animal fat, waste oil
New Zealand	–	Waste cooking oil, tallow
Norway	–	Animal fats
Pakistan	–	*Jatropha curcas*
Peru	Palm	*Jatropha curcas*
Philippines	Coconut	*Jatropha curcas*
Singapore	Palm	–
Spain	Soybeans, olive oil, palm, Linseed oil, sunflower	–
Sweden	–	Rapeseed
Thailand	Palm, coconut	*Jatropha curcas*
Turkey	Sunflower	Rapeseed
UK	–	Rapeseed, waste cooking oil
USA	Soybeans, peanut, corn	Poultry fat, animal fat, tallow, waste oil
Zimbabwe	–	*Jatropha curcas*

blend (B20) is labelled and sold for commercial operations. Most diesel fuel in Australia is sold in bulk on long-term contracts to commercial/industrial customers such as mining and transport companies, whereas only a quarter is sold through retail outlets.

Table 5
Australian imports of biodiesel by country, 2012–2016 ('000 litres) (USDA, 2017).

Country	2012	2013	2014	2015	2016
Singapore	858	39,741	209,583	139,355	0
Argentina	0	28,604	32,189	4,748	0
Indonesia	15,488	28,339	116,956	6,084	686
United States	0	11,352	0	1,105	1
Canada	5,018	5,482	1,057	0	0
Other	46	4,185	10,980	8,128	82
Total	21,410	117,703	370,765	159,420	769

Again, about 80% of this retail sale is bought by the long-haul trucking industry. Most diesel engine manufacturers limit the usage of biodiesel with conventional diesel to a maximum of 5% (B5 biodiesel blends), considering that this blend meets the Australian fuel standard. A limited number of engine manufactures encourage the use of higher than 5% blends in Australia. However, some local council trucks, i.e., fleet operations, are using biodiesel blends up to 99.9%.

Compared to other developed countries, Australian biodiesel production is very low (only 40 ML in 2017 and 2018). Several factors that have led to this low biodiesel production, include the closure of local biodiesel production facilities, continued unfavourable conditions of limited mandate support, higher feedstock prices, and lower international fuel prices. Although the current capacity of biodiesel production is 400 ML, only 10% of the capacity was utilised in both 2017 and 2018. Table 6 shows the total picture of Australian biodiesel use from 2009.

From 2016, biodiesel production declined significantly leading to insignificant export and import of biodiesels. Under new Australian excise and import duty arrangements, imported biodiesel became uncompetitive with diesel. Australia had imposed anti-dumping and countervailing duties on imported biodiesel from the United States in 2011. These duties were imposed due to a United States federal tax credit of US $1/gallon. Although the Australian government terminated the anti-dumping measure to imported biodiesel from the United States in 2016, no records were found of the imports of biodiesel from the USA.

In comparison with other developing countries, Australian biodiesel production facilities are growing slower than expected. Although some biofuel production companies were closed in 2016, three major biofuel facilities are still in operation, one 'Manildra facility' in Nowra (New South Wales), the other 'Sarina Distillery and the third 'Dalby Bio-Refinery' in Queensland (Puri et al., 2012). Among these, the Manildra group is the largest commercial biofuel producer in Australia. Biofuel mandates in different states encourage all companies to increase their production capacity to meet their state government's demand. Table 7 summarises the biodiesel production capacity scenario in Australia.

3. Australian native papaya and stone fruit-Sources of second-generation biodiesel

Biodiesel production from various feedstocks has been a popular area of research in recent times. Researchers have explored many types of feedstocks representing a variety of sources. These species are generally selected based on some key parameters such as reasonable plant yield, higher oil content, high conversion rate to biodiesel, local availability and cost-effectiveness. The plants that consume less water, require less maintenance, can grow in marginal soils, can grow in diverse climatic conditions, and are unsuitable for human consumption are ideal for biodiesel feedstocks. Again, physical and chemical properties such as density, kinematic viscosity, higher heating value, cetane number, iodine value, cold filter plugging point and the like can indicate

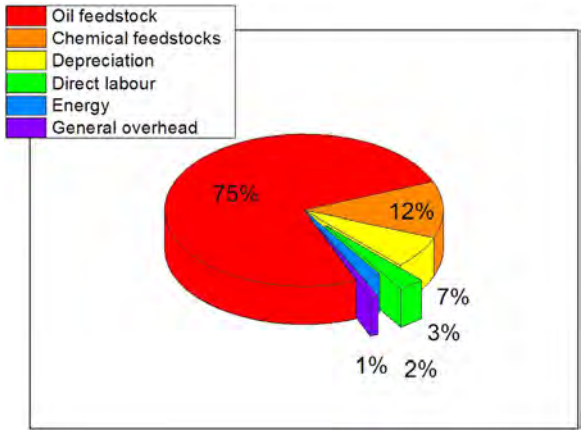

Fig. 3. Overall cost breakdown for biodiesel production (Lim and Teong, 2010).

a suitable biodiesel feedstock. Furthermore, a suitable biodiesel feedstock must be amenable for its production at the lowest possible price and in abundance, in comparison with the prices of diesel in the competitive market. A few researchers (Rahman et al., 2012; Lim and Teong, 2010) mention that the price and supply of feedstock will cost more than 75% of biodiesel production cost. Fig. 3 shows the overall cost breakdown for biodiesel production.

Table 8 shows the Australian research that has examined optimised biodiesel production from specific feedstocks with regard to engine performance, emissions studies and combustion characteristics.

Some researchers have aimed to explore the potential of Australian native plants as a source of second-generation biodiesel. Ashwath (2010) evaluated more than 200 species and provenances and found that only four of the tested species were meeting the biodiesel production criteria. Amongst these, he found the beauty leaf tree (BLT; *Calophyllum inophyllum* L.) showing greater promise than other species (candlenut tree, pongamia, and coconut). Bhuiya et al. (2015) have investigated biodiesel from BLT, refined poppy oil, crude jojoba oil and waste cooking oil, comparing their results for biodiesel yield and physicochemical properties. Highest biodiesel conversion efficiency was achieved with poppy oil (93.4%) followed by BLT oil (92.3%). Bhuiya et al. (2015) concluded that both BLT and poppy biodiesels have the potential to become suitable second-generation biodiesels. Jahirul et al. (2014) investigated 11 Australian native and naturally-grown non-edible biodiesel feedstocks, namely Beauty leaf (BLT) (*Calophyllum inophyllum*), Candlenut (*Aleurites moluccana*), Blueberry lily (*Dianella caerulea*), Queen Palm (*Syagrus romanzoffiana*), Castor (*Ricinus communis*), bottle tree (*Brachychiton bidwillii*), Karanja (*Pongamia pinnata*), Whitewood (*Atalaya hemiglauca*), Cordyline (*Cordyline manners — suttoniae*), Flame tree (*Brachychiton acerifolius*) and Chinese rain tree (*Koelreuteria formosana*). They suggested that BLT biodiesel was the top-ranked candidate for second-generation biodiesel followed by Queen palm, Castor, and Karanja. Islam et al. (2015) investigated fatty acid profiles of nine microalgae species and examined their fuel properties to identify suitable microalgae for biodiesel production. They recommended that a blend of 10% to 20% marine microalgae biodiesel with diesel could achieve similar power and brake specific fuel consumption as pure diesel. Rahman et al. (2016) researched *Macadamia integrifolia* oil as a native plant source of biodiesel feedstock in Australia and suggested up to 20% macadamia biodiesel blends with diesel in a diesel engine were suitable without further engine modification.

Table 6
Summary of Australian biodiesel scenario (USDA, 2017).

Year	2009	2010	2011	2012	2013	2014	2015	2016	2017	2018
Production (ML)	85	85	90	114	114	150	130	100	40	40
Imports (ML)	11	9	25	21	118	371	159	1	0	0
Exports (ML)	0	0	0	10	20	20	10	0	0	0
Consumption (ML)	96	94	115	125	212	501	279	101	40	40
Number of bio-refineries	8	6	6	7	7	8	8	5	3	3
Production capacity (ML)	380	380	380	400	400	400	400	400	400	400
Capacity utilised (%)	22.4	22.4	23.7	28.5	28.5	37.5	32.5	25.0	10.0	10.0

Table 7
Biodiesel production capacity scenario in Australia, 2017 (USDA, 2017).

Biodiesel plant	Location	Capacity (ML)	Feedstock	Production start
Australian Renewable Fuels (ARF) largs bay	South Australia	45	Tallow, used cooking oil	2006 (closed 2016)
Australian Renewable Fuels (ARF) picton	Western Australia	45	Tallow, used cooking oil	2006 (closed 2016)
Biodiesel Industries Australia (BIA)	New South Wales	20	Used cooking oil, vegetable oil	2003
Australian Renewable Fuels (ARF) barnawartha	Victoria	60	Tallow, used cooking oil	2006 (closed 2016)
Ecotech biodiesel	Queensland	30	Tallow, used cooking oil	2006
Smorgon fuels biomax plant	Victoria	100	Tallow, Canola oil and Juncea oil	2005 (closed 2016)
Macquarie Oil	Tasmania	15	Poppy oil, waste vegetable oil	2008
Territory biofuels	Northern Territory	140	Palm oil, Tallow, used cooking oil	closed in 2009

Table 8
Summary of Australian biodiesel researches until 2018.

Biodiesel feedstocks used	Biodiesel production and optimisation	Engine performance	Emission studies	Combustion characteristics	Research conducted	Ref.
Evening-primroses (*Oenothera lamarckiana*)	√	√	√	X	2018	Hoseini et al. (2019)
Waste cooking oil	√	X	X	X	2018	Mowla et al. (2018), Gardy et al. (2018), Nabi and Rasul (2018), Zare et al. (2018) and Ming et al. (2018)
Waste cooking oil with additives	√	√	√	√	2018	Rahman et al. (2018a)
Grease trap waste	√	X	X	X	2018	Tran et al. (2018)
Microalgae	√	√	√	√	2018, 2017	Rahman et al. (2018a), Xie et al. (2018) and Sitepu et al. (2018)
Macadamia (*Macadamia integrifolia)*	√	√	√	√	2018, 2016,	Rahman et al. (2016) and Nabi and Rasul (2018)
Tree of heaven *(Ailanthus altissima)*	√	√	√	X	2018	Hoseini et al. (2018)
Canola oil	√	√	√	√	2018	Ming et al. (2018)
Rice bran biodiesel	√	√	√	X	2017	Rahman et al. (2018b)
Beauty leaf	√	√	√	√	2016	Azad et al. (2016), Bhuiya et al. (2015), Jahirul et al. (2014) and Jahirul et al. (2015)
Licella biofuel (*Pinus radiata)*	√	√	√	√	2015	Nabi et al. (2015)
Waste tyres	√	√	√	X	2018	Verma et al. (2018)
Essential oil (orange oil)	√	√	√	X	2017	Rahman et al. (2017a)
Palm oil	√	√	√	X	2011	Yusaf et al. (2011)
Diesel with additives	√	√	√	√	2018	Algayyim et al. (2018)
Poppy seed oil	√	√	√	X	2017	Bhuiya et al. (2017)

Azad et al. (2017) found a 5% macadamia biodiesel blend with diesel performed better compared to a 20% biodiesel blend. They revealed that the 5% biodiesel blend slightly increased BSFC and decreased BTE while reducing emissions (CO, HC, and PM) significantly. Azad (2017) also studied Mandarin peel waste, cramble, tamanu, borage, waste avocado flesh and bush nut for biodiesel production and found that mandarin biodiesel showed higher calorific value (44.66 MJ/kg) and higher flash point (52 °C), which closely matched with commercial jet fuel. Zare et al. (2017) used waste cooking biodiesel and triacetin (highly oxygenated additive) to analyse cold-start and hot-start operations. They found the use of oxygenated fuel during cold-starts increased harmful nucleation mode particles significantly. Rahman et al. (2018b) used a 20% blend of rice bran biodiesel with diesel to lower air pollution without affecting engine power significantly. In another

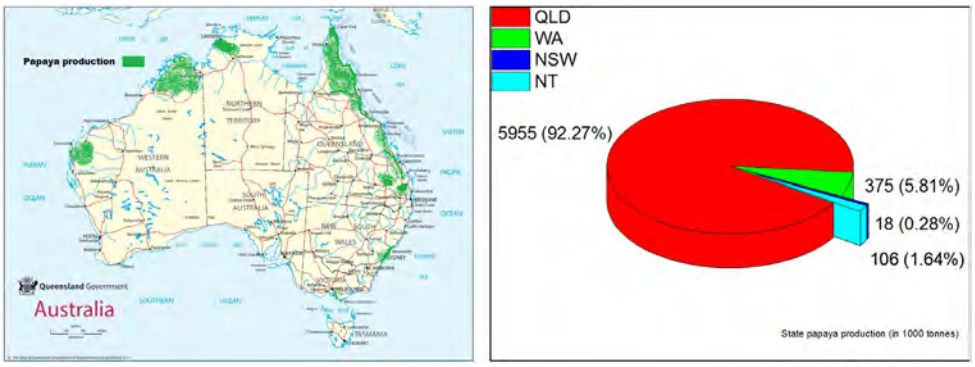

Fig. 4. Papaya production in Australia: Regional distribution (left) and State & Territory outputs in 2009 ('000 tonnes) (right). *Source:* This figure has been modified from the Queensland Government Department of Natural Resources, Mines and Energy website (Department of Natural Resources, 2018).

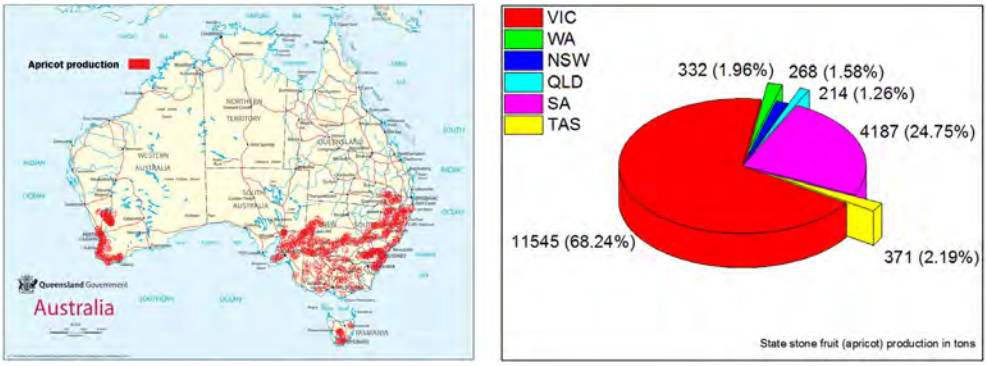

Fig. 5. Stone fruit (apricot) production in Australia: Regional distribution (left) and state outputs in 2008 (tons) (right). *Source:* This figure has been modified from the Queensland Government Department of Natural Resources, Mines and Energy website (Department of Natural Resources, 2018).

study of fuel properties (physical, chemical and tribological), Rahman et al. (2017b) showed that palm biodiesel was the most suitable blending alternative followed by macadamia, moringa, jatropha and beauty leaf biodiesel. Rahman et al. (2018a) suggested that 10% blends of essential oils (orange, eucalyptus and tea tree) with diesel can be used in diesel engines.

The potentiality of waste papaya seed oil and stone fruit oil as second-generation biodiesel feedstocks have never been investigated in Australia. However, a very few researchers from other parts of the world have researched second-generation papaya seed oil (PSO) and stone fruit kernel oil (SFO) biodiesels (Gumus and Kasifoglu, 2010; Wang and Yu, 2012; Fadhil, 2017; Fan et al., 2016; Wang, 2013; Ullah et al., 2009; Jannatizadeh et al., 2008; Yadav et al., 2017; Wong and Othman, 2014; Agunbiade and Adewole, 2014; Mohan and Sen, 2015). The current study has reviewed the details of papaya and stone fruit biodiesel, and identified some challenges and solutions to use papaya and stone fruit as alternative sources of biodiesel for Australian transport sector.

3.1. Papaya seed oil

The papaya (*Carica papaya*) originates from the tropics of the Americas and is mainly cultivated in tropical climates of Asia, South America, Africa and Polynesia. Fig. 4 shows details of papaya production in Australia. Papaya being a tropical fruit, it grows well in sub-tropical regions. Papaya fruit can weigh from 200 g to more than 3000 g, and its seed content can be approximately 15%–20% of the wet weight of the fruit (Salunkhe and Kadam, 1995; Chan et al., 1978; Samaram et al., 2013; Hameed, 2009). Since the seeds are not consumed, 15%–20% of the biomass (i.e., the amount of seeds) is discarded (Chan et al., 1978; Daryono and Sinaga, 2017). These seeds contain 30%–34% oil with nutritional and functional properties similar to that of olive oil (Chielle et al., 2016; Puangsri et al., 2004; Lee et al., 2011). These seed oils can be utilised as the feedstocks for biodiesel synthesis.

3.2. Stone fruit oil

The stone fruit, particularly apricot (*Prunus armeniaca* L.), originates from India and Armenia, and is mainly cultivated in cool frost-free sites due to its early blooming properties (Salunkhe and Kadam, 1995). Its commercial cultivation is limited to humid climates due to fungal disease. This crop is now widely cultivated in Australia, especially in Victoria and South Australia. Australia produces about 100,000 tons of summer stone-fruits from October to April each year and, in 2008, about 16,917 tons of apricot were produced in all six mainland states in Australia. The apricot (*Prunus armeniaca*) belongs to the Rosaceae family and it is native to western Asia and possibly China. Two other species that are related to apricot are also cultivated, and they are *Prunus mandshurica* (from Manchuria, Korea) and *P. siberica* (from Siberia, Manchuria, and northern China). Another species that bears purple fruits (*P. dasycarpa*) and a Japanese apricot (*P. mume*) are also cultivated. The fruits are green and turn to orange or yellow–orange on maturity. The fruits contain soft flesh and hard seed (stone/kernel).

Fig. 5 shows apricot production and its growing regions in Australia (Salunkhe and Kadam, 1995). Stone fruit is similar to a small peach, generally 1.5–2.5 cm diameter, with its colour varying from yellow to orange or red. Its single seed is enclosed in a hard stony shell. The fruits yield 22 to 38% of kernels and 54.2%

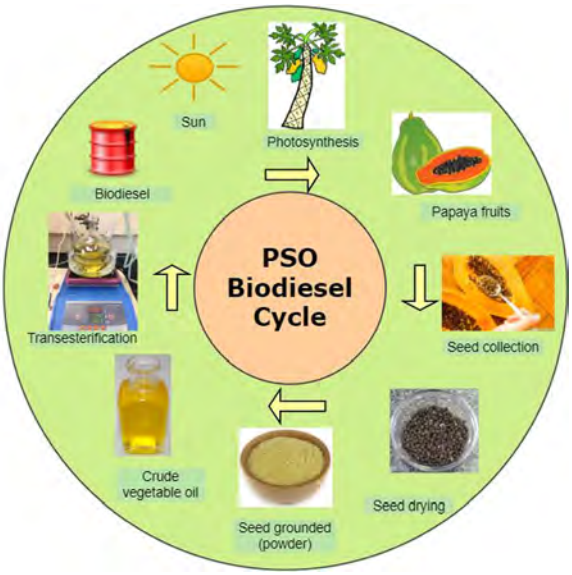

Fig. 6. Life cycle steps for biodiesel production from Papaya seed oil (Anwar et al., 2018a).

oil (Yadav et al., 2017; Kate et al., 2014). During fruit processing, for a variety of uses, the seeds are discarded as they are not edible due to the presence of hydro-cyanic acid (Sharma et al., 2012). The potentiality of this biomass as a biodiesel feedstock thus deserves investigation.

4. Life cycle steps for papaya and stone fruit biodiesel production

4.1. Cultivation

Fig. 6 shows various steps involved in biodiesel production from PSO. The details of the optimisation and conversion of PSO biodiesel was discussed in Anwar et al. (2018c). Papaya (*Carica papaya*; Caricaceae) is a giant herbaceous tree that originated in Central America and is cultivated in many parts of the tropics. The common name "papaya" or pawpaw also refers to the fruit of other *Carica* species (*C. pubescens* and *C. stipulata*) and the varieties derived from these species. The fruit shape varies from oval to round, and the size differs considerably amongst the cultivars, ranging from 0.5 kg to 9 kg. Fruit shape also differs from oval to cylindrical, and the length varies from 10 cm to 50 cm with a diameter of 5 cm to 20 cm. Green fruits produce copious amounts of white latex, and the mature fruits lack this latex. The flesh of the fruit varies from yellow to orange to red, and is thick and juicy. The central cavity of the fruit is filled with brown to black coloured seeds. Fruits differ in the seed content, and the seed content ranges from seedless to heavily seeded, depending on the way the cultivar has been bred (pure line or hybrid). The seed content of the fruit varies from nil (seedless) to 20% of the wet weight.

The apricot kernel is rich in protein and oil. The steps involved in producing biodiesel from apricot kernels are shown in Fig. 7. The details of optimisation and conversion of apricot kernels biodiesel was discussed in Anwar et al. (2018c).

4.2. Oil extraction system

Oil extraction is the first stage in biodiesel production. There are many methods of oil extraction from the original sources such as seeds, fruits, and other oil bearing materials. A simple mechanical press can be used for extracting the oil without further processing. This process is also known as cold pressing. Not all seeds are suitable for extraction using mechanical press; some of them involve a complex process such as a combination of pressing, cooking and solvent extraction. The oil extraction methods are described below for both papaya seed and apricot kernel.

4.2.1. Mechanical extraction

The mechanical extraction method is the conventional method of extracting oil from seeds. An expeller or ram press or engine driven screw press is used for expelling or pressing seeds. The oil extraction rate depends on the type of seeds and type of press. However, oil extracted by mechanical extraction needs further treatment of filtration and degumming.

4.2.2. Chemical extraction

Removing one constituent from a solid by means of a liquid solvent is known as chemical extraction. It is also known as solvent extraction process. The rate of extraction of oil depends on the type of liquid chosen, particle sizes, temperature and agitation of the solvent. The most common solvent used in the chemical extraction process is hexane due to its low cost and low toxicity (Mahanta, 2004).

4.2.3. Enzymatic extraction

Oil extraction through an enzymatic extraction method, using suitable enzymes while crushing, is gaining popularity due to its excellent environmental attributes and for not producing volatile organic compounds (Rosenthal et al., 2001; Shah et al., 2005; Vasco-Correa and Zapata Zapata, 2017). However, the main barrier of this method is enzyme cost and the need for a long processing time to liberate oil bodies (Mahanta, 2004).

Table 9 shows a summary of research undertaken into oil extraction from papaya seed and apricot kernel. It can be seen that most researchers have found the chemical extraction process was convenient to extract oil from both papaya seed and stone fruit seed.

5. PSO and SFO analysis

Both Papaya seed oil (PSO) and Apricot kernel oil (SFO) are characterised for viscosity, density, specific gravity, acid value, refractive index, angular rotation, stability oxidative, iodine value, calorific value and saponification number. PSO is reddish yellow in colour. Generally, solvent extracted oil tends to have more yellow and red colour than enzyme extracted oil (Puangsri et al., 2004). SFO is generally light yellow in colour. Depending on the variety and extraction process, its colour can change to slightly darker yellow, and there is a nutty aroma in this oil. Table 10 shows the properties of PSO and SFO along with diesel. These properties are compared with both measured value and reviewed value.

The fatty acid compositions were analysed by a gas chromatograph using the EN14103 standard. The compositional analysis set out in Table 11 shows that the PSO contains high proportion of unsaturated fatty acids (87.5%). Amongst these, the oleic acid (C18:1) was found to be the dominant fatty acid (47.7%). Linoleic acid (C18:2) was found at 37.3% and the saturated fatty acids, palmitic acid (C16:0), was found at 6.1%. SFO has a high level (89.7%) of unsaturated fatty acids such as polyunsaturated and monounsaturated fatty acids. Saturated fatty acids such as palmitic acid, stearic acid, and behenic acid were found at 5.9%, 2.51% and 0.66% respectively.

The fatty acid profiles of both PSO and SFO are compared in Fig. 8. Both PSO and SFO have higher oleic acid and linoleic acid as well as similar level of unsaturated fatty acids 87.5% and 89.7% for PSO and SFO respectively.

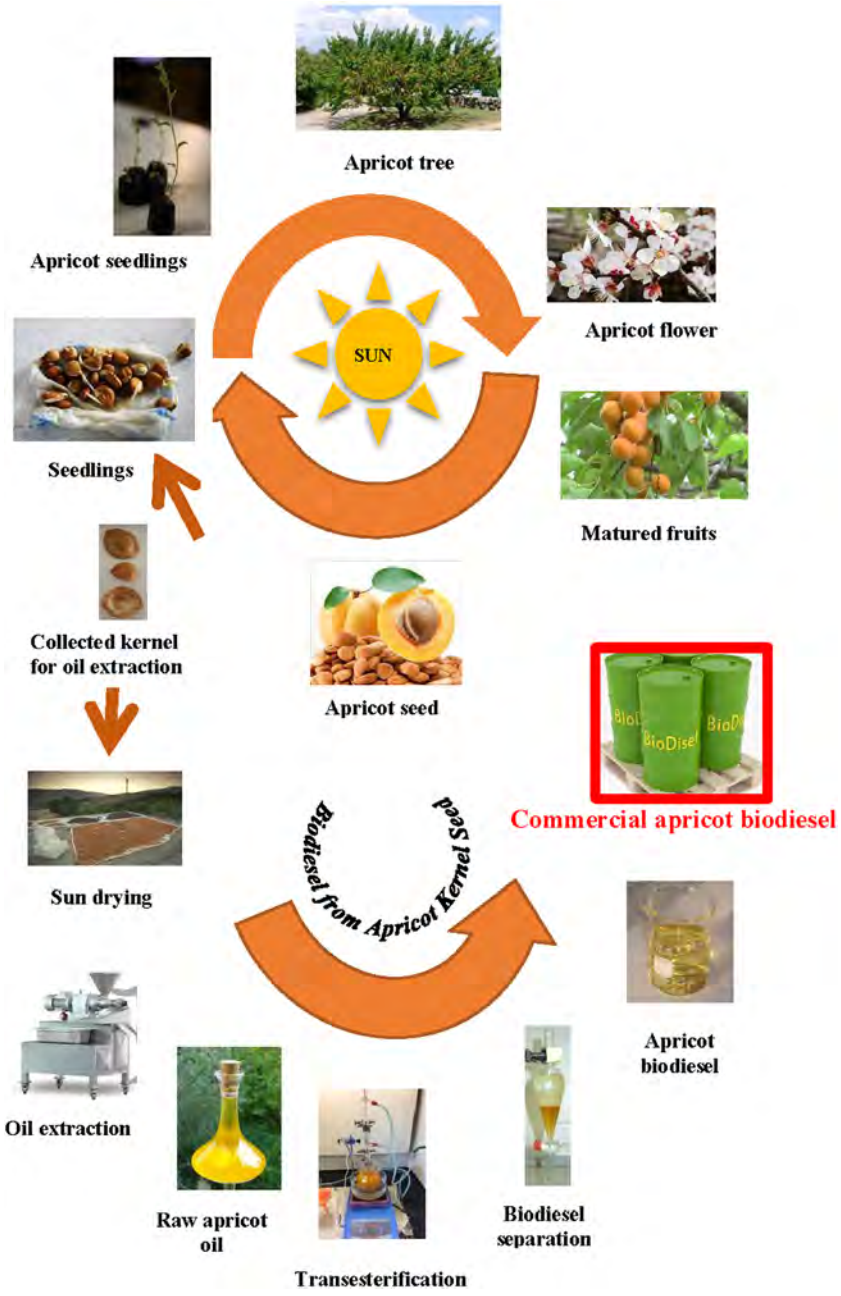

Fig. 7. Life cycle steps for biodiesel production from Apricot kernel oil (Anwar et al., 2018c).

6. PSO and SFO biodiesel production

Alkali catalysed transesterification reaction is the most widely used method for producing biodiesel due to its higher conversion efficiency in a short time (30–60 min), as compared to an acid catalysed process. Researchers have used both methanol and ethanol as alcohol in the transesterification process (Kaul et al., 2007). However, methanol is less costly and has better reactivity. Furthermore, the fatty acid methyl esters (FAMEs) produced from methanol are more susceptible to evaporation than those generated from ethanol (ethyl esters). On the other hand, ethanol is derived from renewable feedstocks and it is less toxic to humans than methanol (Kaul et al., 2007). De Melo et al. (2011) used alkaline transesterification with 0.5% sodium methoxide with a methanol:oil molar ratio of 8:1. Several process parameters such as reaction temperature, catalyst type, catalyst concentration, type of alcohol and their oil to molar ratio, reaction time and agitation speed, all affect biodiesel yield and quality. Therefore, the transesterification optimisation process is critical to produce high quality biodiesel at a low cost.

Papaya seed oil (PSO): A number of researchers have studied biodiesel production from various feedstocks, but very few researchers (Wong and Othman, 2014; Agunbiade and Adewole, 2014; Mohan and Sen, 2015; Daryono and Sinaga, 2017; Anwar et al., 2018a; Patel and Nayak, 2017; Sivasubramanian, 2017) have looked into papaya biodiesel production. Wong and Othman (2014) produced papaya biodiesel via enzymatic transesterification using lipase at a methanol:oil molar ratio of 6:1. Agunbiade and Adewole (2014) have shown that the crude papaya seed oil can be transesterified by two-stage catalysis using a methanol:oil molar ratio of 9:1. Mohan and Sen (2015) used CaO as the catalyst to produce 20% papaya biodiesel and 80% chicken biodiesel blend. Daryono and Sinaga (2017) used sodium hydroxide as an alkaline

Table 9
Research summary of oil extraction process of papaya seed and stone fruit seed (apricot kernel).

Source	Oil extraction	Method	Temperature	Process time	Results	Ref.
Papaya seed	Mechanical extraction	Heat generated by friction	–	–	Oil yield 142 g/kg.	Lee et al. (2011)
		Screw pressing	85–90 °C	–	Oil yield 152 g/kg	
		Roasting papaya seed at 160 °C, then screw pressing	100–105 °C	–	Oil yield 139 g/kg	
	Chemical extraction	– Solvent (n-hexane) extraction	– 25–50 °C	– 3, 6, 9 and 12 h	UAE was quicker procedure resulting in higher extraction yield than conventional methods.	Samaram et al. (2013)
		– Ultrasound-assisted extraction (UAE) method	– 50 °C	– 30 min		
		Percolation method	70 °C	4 h	Oil yield 265 g/kg	Chielle et al. (2016)
		Four solvents (ethanol, acetone, ethyl acetate and n-hexane) extraction	–	–	Oil yield 151–300 g/kg	Lee et al. (2011)
		Solvent n-hexane	–	–	Oil yield 31.2%	Agunbiade and Adewole (2014)
		Solvent n- hexane	–	8 h	Oil yield 34.3%	Wong and Othman (2014)
		Solvent n- hexane	110 °C	2 h	Converted oil was collected by separating from benzene solution	Mohan and Sen (2015)
		Solvent n- hexane	40–60 °C	8 h	Oil yield 30.7%	Puangsri et al. (2004)
		Solvent n- hexane	27 °C	33 min	Oil yield 225.9 g/kg	Daryono and Sinaga (2017)
		Solvent n- hexane	40–60 °C	6 h	Oil yield 29.16%	Malacrida et al. (2011)
		Solvent n- hexane	–	–	Oil yield 280 ± 20 g/kg	De Melo et al. (2011)
		Solvent n- hexane	60 °C	8 h	Oil yield 30.1%	Syed et al. (2011)
	Enzymatic extraction	Protease, pectinase, α-amylase and cellulose enzymatic extraction			Enzymatic method produced less amount of oil than solvent extraction (30.7%).	Puangsri et al. (2004)
Apricot Kernel	Mechanical extraction	–	-	–	–	–
	Chemical extraction	Soxhlet extractor (using petroleum ether)	45–50 °C	6–8 h	Oil extracted 50.2%	Wang and Yu (2012)
		Soxhlet extractor (using petroleum ether)	–	–	Oil extracted 48.7%	Ullah et al. (2009)
		Solvent n- hexane	25 °C	–	Oil extracted 51.6%	Fan et al. (2016)
		Pyrolysis in a fixed bed reactor	450 °C	60 min	Oil extracted 43.7%	Fadhil (2017)
		Supercritical fluid extraction system	110 °C	25–90 min	Oil extracted 48%	Özkal et al. (2005)
	Enzymatic extraction	–	–	–	–	–

catalyst for the transesterification process to produce biodiesel from papaya seed. Anwar et al. (2018a) have shown that PSO can be transesterified by single-stage method using KOH catalyst and with a methanol:oil molar ratio of 10:1. Patel and Nayak (2017) have used 0.5% NaOH catalyst with methanol:oil molar ratio of 9:1 to obtain 96.7% biodiesel yield. Sivasubramanian (2017) used NaOH catalyst with methanol:oil molar ratio of 5:1 in a single-stage transesterification reaction for PSO biodiesel production. They have all claimed that the physicochemical properties of papaya seed oil biodiesel were very close to those of diesel.

Apricot kernel oil (SFO): Very few researchers (Gumus and Kasifoglu, 2010; Wang and Yu, 2012; Fadhil, 2017; Fan et al., 2016; Wang, 2013; Ullah et al., 2009; Jannatizadeh et al., 2008; Yadav et al., 2017; Anwar et al., 2018c) have investigated of SFO biodiesel. Among all the SFO biodiesel researchers, a handful of them (Gumus and Kasifoglu, 2010; Fadhil, 2017; Ullah et al., 2009; Yadav et al., 2017) focused their research on apricot (*Prunus armeniaca* L.). Other researchers have used either Siberian apricot kernel oil (*Prunus sibirica* L.) or Manchurian apricot kernel oil (Prunus mandshurica Skv.). Gumus and Kasifoglu (2010) and Anwar et al. (2018c) used alkali transesterification with methanol and potassium hydroxide catalyst for producing SFO methyl ester. Fadhil (2017) produced SFO biodiesel via alkali transesterification with 0.75% potassium hydroxide catalyst and at a methanol:oil molar ratio of 6:1. Ullah et al. (2009) have shown that the wild apricot kernel oil (*Prunus armeniaca* L.) can be transesterified by a single step via the use of sodium hydroxide catalyst and a methanol:oil molar ratio of 6:1, and reported a biodiesel yield of 93%. Yadav et al. (2017) performed single step alkali transesterification using 1% potassium hydroxide as a catalyst at 55 °C and 60 min reaction time with a constant stirring speed of 400 rpm and obtained a biodiesel yield of 96.5%. The above researchers have claimed that their SFO biodiesel quality and physicochemical properties had matched with ASTM and EN standards and were found to be very close to those of the diesel. Thus, several process parameters, including reaction temperature, catalyst type and catalyst concentration, type of alcohol used

Table 10
Comparison of the properties of PSO and SFO with diesel.

Sl. No.	Properties	PSO		SFO		Diesel
		Measured	Reviewed (Agunbiade and Adewole, 2014; Malacrida et al., 2011; Marfo et al., 1986)	Measured	Reviewed (Gumus and Kasifoglu, 2010; Fadhil, 2017; Yadav et al., 2017)	
1	Kinematic viscosity (mm^2/s) @ 40 °C	27.3	8.3–27.4	34.54	20.53–34.82	3.23
2	Density (kg/m^3)	885	890–926	910	913–919.9	830
3	Specific gravity @ 15 °C	0.885	0.89–0.926	0.91	0.91	0.83
4	Acid value (mg KOH/g)	0.98	2.91	1.65	0.68–2.60	0.05
5	Refractive Index @ 25 °C	1.457	1.45–1.4678	–	–	–
6	Angular rotation (°) @ 20 °C	−8.75	–	–	–	–
7	Stability oxidative (h)	77.97	77.97–78.86	–	–	–
8	Iodine value (g I 100 g^{-1})	79.95	74.8–86.7	103	90.3–101.32	–
9	Calorific value (MJ/kg)	–	40.23	38.45	31.47–39.64	45.3
10	Saponification number (mg KOH/g)	–	97.77–197	173	187.22–188.56	–

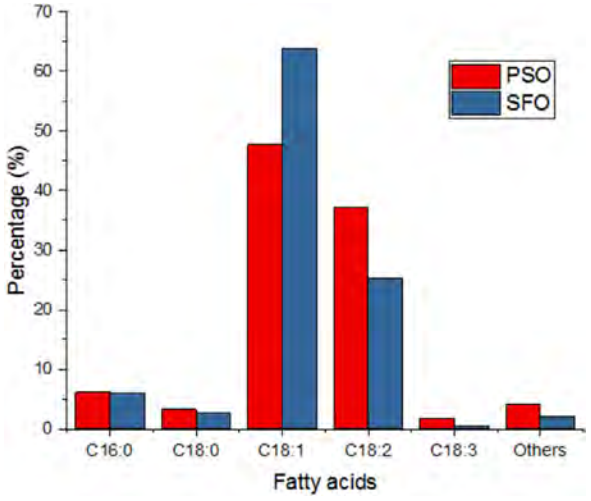

Fig. 8. Fatty acid profile of PSO and SFO.

Table 11
Fatty acid composition of PSO and SFO.

Oil	Fatty acids (% w/w)						Ref.
	C16:0	C18:0	C18:1	C18:2	C18:3	Others	
PSO	6.07	3.13	47.73	37.25	1.78	4.04	
PSO[a]	16.16	4.73	71.30	6.06	–	1.75	Malacrida et al. (2011)
PSO[b]	16.6	1.90	79.10	2.57	–	–	Marfo et al. (1986)
PSO[c]	18.9	5.20	69.80	4.80	–	1.3	De Melo et al. (2011)
PSO[d]	16.2	5.0	74.3	0.4	–	4.1	Agunbiade and Adewole (2014)
PSOe	13.4	4.6	76.9	3.2	–	1.9	Puangsri et al. (2004)
SFO	5.85	2.51	63.84	25.34	0.51	1.95	
SFO[a]	5.62	1.27	67.31	24.68	0.08	1.04	Gumus and Kasifoglu (2010)
SFO[b]	4.20	2.32	71.00	20.15	1.20	1.13	Yadav et al. (2017)
SFO[c]	3.87	0.92	67.21	27.12	0.11	0.77	Wang (2013)
SFO[d]	3.79	1.01	65.23	28.92	0.14	0.91	Wang and Yu (2012)
SFO[e]	–	–	66.20	28.20	–	5.60	Kate et al. (2014)

Note: The superscripts a, b, c, d and e refer to other researchers' work as per the last column.

and the oil to methanol molar ratio, reaction time and agitation speed have been found to influence the optimum transesterification process (Atabani et al., 2012; Hamze et al., 2015; Atadashi et al., 2012; Banerjee and Chakraborty, 2009; Yaakob et al., 2013). However, the potential of both PSO and SFO biodiesel as source of future second-generation biodiesels are yet to be established due to limited knowledge on its consistent optimum production processes.

Biodiesel process optimisation: Traditional experimental methods of any process optimisation are time-consuming and labour intensive. Moreover, they cannot explain the actual interaction effects of variables of the experimental data which lead to misinterpretation of results. There are a few statistical approaches that can be used in experimental design to overcome the limitations of traditional methods. Both Taguchi methods and Response surface methodology (RSM) are very popular methods for biodiesel process optimisation. However, there was no literature on Taguchi methods for optimising biodiesel production process from PSO or SFO.

RSM is a set of mathematical and statistical methods used for modelling and problem solving, wherein the response is influenced by several operating or process parameters (Hamze et al., 2015). RSM is very effective when designing the experiments for maximising yield and minimising production cost. RSM not only simplifies the complex nature of many experimental runs but also studies the interactive effect of several operating parameters and the effects on the response (target). Many researchers have successfully worked with RSM methods and were able to optimise their production process parameters with both central composite design (CCD) and Box–Behnken design models. Researchers investigating optimisation of biodiesel production processes mainly used the RSM approach and their process parameters were: (1) methanol: oil molar ratio, (2) catalyst concentration, (3) reaction temperature, (4) reaction time, and (5) agitation speed. Bello et al. (2016) used a RSM approach with a central composite experimental design (CCD) model for optimising waste frying biodiesel production by varying five process parameters. A CCD method for optimising safflower biodiesel production process parameters and their combined effects were investigated using RSM by Math and Chandrashekhara (Math and Chandrashekhara, 2016). A *Madhuca indica* oil to biodiesel conversion process was

optimised using a RSM approach with a CCD model by Muthukumaran et al. (2017). The RSM approach with a CCD model was used for the biodiesel conversion process from various feedstocks or oils such as camelina oil (Yang et al., 2015), sunflower oil (Mansourpoor, 2012), a mixture of edible and nonedible vegetable oils (thumba oil, karanja oil, linseed oil and palm oil) (Gupta et al., 2016), refined cottonseed (Onukwuli et al., 2017), waste cooking oil (Babaki et al., 2017), lard oil (Ezekannagha et al., 2017), soybean oil (Rahimi et al., 2014), date pits (Jamil et al., 2016), *Thevetia peruviana* seed oil (Ogaga et al., 2017) and crambe oil (Vieira Silveira et al., 2017). The optimisation of biodiesel production from other bio-oils or feedstocks, namely microalgae (Makareviciene et al., 2014), waste cooking oil (Hamze et al., 2015), karanja oil (Verma et al., 2016), mixed nonedible oils (*Jatropha curcas* and *Ceiba pentandra* oil) (Dharma et al., 2016), *Brucea javanica* seed oil (Hasni et al., 2017), were investigated using the RSM approach with Box–Behnken design and fractional factorial design. Anwar et al. (2018a) used RSM approach with Box–Behnken design to optimise PSO biodiesel production process and they demonstrated that 96.5% biodiesel was obtained with the reaction conditions to be a methanol:oil molar ratio 10:1, KOH catalyst concentration of 1 wt% and reaction temperature of 45 °C. In another study by Anwar et al. (2018c) showed that maximum SFO biodiesel yield of 95.8% was obtained at a methanol: oil molar ratio of 6:1, KOH catalyst concentration of 0.5 wt% and a reaction temperature of 55 °C.

7. PSO and SFO biodiesel properties- a comparison with selected second-generation biodiesels

The converted biodiesel properties are characterised by major physicochemical properties such as density, viscosity, calorific value, flash point, cetane number, iodine value, and oxidation stability. A selection of properties for various nonedible biodiesel are shown in Table 12.

Silitonga et al. (2014) mentioned that the density of a fuel influences the fuel atomisation efficiency in airless combustion system. The density of biodiesel should be 860–900 kg/m^3 as per both ASTM and EU standard. The density of diesel was measured as 827.2 kg/m^3, whereas PSO and SFO densities were recorded as 840 kg/m^3 and 855 kg/m^3 respectively. The density of karanja biodiesel was found to be the highest (931 kg/m^3). The viscosity of PSO and SFO ranged from 1.9 to 6 mm^2/s. Higher acid value of biodiesel can cause corrosion of engine and other metal parts. Both ASTM and EU standard limits the maximum acid value of 0.5 mg KOH/g. Calorific value is another important property and all biodiesels have slightly less calorific values than diesel, as expected. Cetane number, flashpoint, iodine value and oxidation stability of both PSO and SFO are found to be within the range of ASTM/EU standard.

8. Engine performance and emission studies of PSO and SFO biodiesel

Most biodiesels have lower calorific values than diesel which narrows their usage in compression ignition (CI) i.e. diesel engines. Some challenges include higher brake specific fuel consumption (BSFC), lower brake thermal efficiency (BTE), and higher particulate matter (PM) and nitrogen oxides (NOx) emissions. Very limited literature has been found regarding the use of PSO and SFO biodiesel to examine engine performance and emission studies. Prabhakaran et al. (2016) have done engine performance analysis of a single cylinder Kirlosar-TV1 diesel engine with PSO biodiesel blends of B25, B50, B75 and B100. They also studied the emissions of biodiesel blends. They concluded that the BTE of PSO blends was lower than that of diesel at all load conditions. They also found that the BSFC of B25 was lower than that for all other blends. They recommended B25 blend as a suitable biodiesel blend due to lower carbon monoxide (CO) and NOx emissions. Raj and Karthikayan (2016) have undertaken diesel engine (single cylinder) performance analysis with papaya diesel blends of B25 and B25 with additives (B25A), B100 and B100 with additives (B100A). They found that the PSO diesel blends with additives have better combustion and emission characteristics with reductions in the NOx emissions compared with PSO diesel blends as well as lower smoke density compared with the diesel. Prabakaran et al. (2015) have done the engine performance analysis of a single cylinder diesel engine with papaya diesel blends such as B25, B50, B75 and B100. They found that the PSO biodiesel B50 with standard injection timing showed slight improvement (3%) in BTE compared to diesel. Anwar et al. (2018b) have done the engine performance analysis of a four cylinder diesel engine with papaya diesel blends B5, B10 and B20 and found average BP value reduction of 2.88%, 3.87% and 5.13% respectively. Furthermore, they reported that reduction in HC emissions of 9 to 19%, PM it emissions of 19.5 to 35% and CO emissions of 11 to 29%can be achieved. They suggested that B5 and B10 biodiesel–diesel blends can be used to diesel engine without further engine modification. Mohan and Sen (2015) used CaO as the catalyst and analysed the emissions of a single cylinder diesel engine using 20% papaya biodiesel and 80% chicken biodiesel blend. Although the NOx emissions showed a marginal increase, other emission characteristics such as CO, hydrocarbon (HC) and smoke were reduced compared with diesel.

Gumus and Kasifoglu (2010) have used SFO biodiesel–diesel blends of B5, B20, B50 and B100 in a Lombardini 6LD400 single cylinder diesel engine and found that B5 and B20 gave better engine power and lower BSFC. The B50 and B100 blends produced less CO, HC and smoke density; however they produced higher NOx emissions and lower engine performance characteristics than diesel. Kumar et al. (2018) have conducted engine performance and emission studies of SFO biodiesel with B20 and B20, with BHA and PG antioxidants. They found that B20 has lower CO, HC emissions than diesel. With B20/BHA4000, both HC and CO emissions were recorded at their lowest at full load. CO emission with the B20/PG4000 blend was found to be similar to that of diesel at full load conditions. NOx emissions were also found to be lower at low load for B20 blend, but these were raised when the load was increased. Table 13 shows the summary of engine performance and emissions studies for PSO and SFO biodiesels.

9. Combustion characteristics of PSO and SFO biodiesel

Prabhakaran et al. (2016) investigated the combustion characteristics of PSO biodiesel and reported that the addition of PSO biodiesel to diesel fuel considerably decreased the ignition delay period and resulted in maximum in-cylinder pressure due to higher cetane number and oxygen contents of biodiesel. It was reported that the peak pressure of the biodiesel blend B25 was higher than those of all other blends. Again, the heat release rate of B25 blend was found to be higher than those of other blends due to reduced viscosity and improved spray formation. The higher viscous biodiesel leads to a reduction in air fuel mixing rates which end up producing a lower heat release rate compared to diesel. Raj and Karthikayan (2016) reported that PSO biodiesel blends ignited earlier and finished combustion earlier than diesel. It was also reported that PSO biodiesel with Di-tert butyl peroxide (DTBP) additive produced higher peak pressure due to oxygen buffer character of the additive which enhanced complete combustion process. The heat release rate was also improved with the use of DTBP additive by 13.7% and 39% respectively, on biodiesel

Table 12
Some non-edible biodiesels and their properties.

Non-edible biodiesels	Density (kg/m^3)	Viscosity at 40 °C (mm^2/s)	Acid value (mg KOH/g)	Cetane number (CN)	Calorific value (MJ/kg)	Flash point (°C)	Iodine value (IV) (mg I_2/100 g)	Oxidation stability (OS) (h)
Diesel	827.2	3.23	0.05	48.00	45.30	68.5	38.3	39.0
PSO (Anwar et al., 2018a)	840.0	3.53	0.42	48.29	38.49	112	115.89	5.61
SFO (Anwar et al., 2018c)	855.0	4.26	0.25	50.45	39.64	105	104.70	7.15
Tobacco (Atabani et al., 2012; Hasni et al., 2017)	888.5	4.23	–	51.60	–	165.4	136	0.80
Jatropha (Hasni et al., 2017)	879.5	4.80	0.40	51.60	39.23	135	104	2.30
Rapeseed (Atabani et al., 2012)	882.0	4.43	–	54.40	37.00	170	–	7.60
Cotton-seed (Atabani et al., 2012)	875.0	4.07	0.16	54.13	40.43	150	–	1.83
Neem (Atabani et al., 2012; Hasni et al., 2017)	868.0	5.21	0.65	–	39.81	76	–	7.10
Karanja (Hasni et al., 2017)	931.0	6.13	0.42	55.00	43.42	95	–	–
Moringa (Atabani et al., 2012)	883.0	5.00	0.18	67.1	–	160	74	2.3
ASTM D6751	880.0	1.9–6.0	max 0.5	min. 47	–	100–170	–	min. 3
EN14214	860–900	3.5–5.0	max 0.5	min. 51	35	>120	max 120	min. 6

blends B25 and B100 respectively, compared to diesel. Prabakaran et al. (2015) have shown that the peak cylinder pressure was slightly higher for B50 blend. They also reported that the heat release rate of diesel is slightly lower than that of PSO biodiesel B50 blend. To the best of our knowledge, there is no substantial work previously undertaken on an engine combustion using SFO biodiesel.

10. Discussion

Biodiesel is drawing vast attention as an alternative fuel source, but in reality, it is facing some challenges not only in Australia but also in many parts of the world. This study has identified some specific challenges for PSO and SFO biodiesels. Some challenges are associated with biodiesel feedstock selection, optimisation and production processes, the oil extraction and conversion process, fuel characterisation and property analysis, storage and transport. The study also identified some ways to overcome these challenges.

Research shows that correct feedstocks selection and their ongoing availability are the major challenges for biodiesel production (Biswas et al., 2011). Biodiesel feedstocks are generally selected based on some key parameters such as higher oil content, high conversion rate to biodiesel, local availability and cost-effectiveness. Again, availability of feedstocks depends on different climatic conditions and growing seasons. Thus supplying continuous feedstock may be difficult (Zhu and Ketola, 2012). As Australia is a huge size country with several different climate zones, right feedstocks selections for its different climate zones are big challenges. Again, some parts of Australia is quite warm and dry in winter whereas some parts are hot and humid in the summer, prolonged drought is also a common phenomenon in some part of Australia. Therefore, the plants that consume less water, require less maintenance, less fertile soil, can grow in diverse climatic conditions and are unsuitable for human consumption are ideal for biodiesel feedstock.

One of the most challenging issues is to identify a cost-effective and higher biodiesel yielding strategy that can be used on a commercial scale (Puri et al., 2012). Extensive research and knowledge is required to optimise any biodiesel production process. Oil extraction and conversion processes may cause environmental pollution hazards, e.g., chemical oil extraction processes may involve chemical contamination of water source while washing and drying processes take place (Jayed et al., 2009; Hoekman, 2009). Sustainable and environmentally-friendly chemicals and technologies are a focus globally to mitigate these oil extraction challenges. Combined and collaborative research projects are ongoing with different Universities in Australia focusing on sustainable biodiesels and their production.

Storage of feedstocks can be challenging as they are biodegradable and can produce gum (Mukherjee et al., 2011). Biodiesel is non-flammable and is safe to store. However, prolonged storage can result in acidity problems due to easy oxidisation with oxygen at ambient temperature. Odour can occur due to prolonged storage of biodiesel. Strong Government policy is needed to ensure continuous consumption of biodiesel and their blends to minimise storage and transportation issues. State Government of Australia such as Queensland and New South Wales have introduced biofuel mandates to promote biodiesel consumption.

There is no generalised technique that can be applied to all feedstocks for converting to biodiesel. This is a major technical challenge (Greenwell et al., 2010; Santacesaria et al., 2012). For instance, different equipment and testing facilities are required in the biodiesel production processes and some of that equipment may not be needed for all feedstocks; thus, production cost per unit of biodiesel can be higher than for ordinary techniques (Vasudevan and Briggs, 2008; Mettler et al., 2012; Goldemberg, 2008). Some feedstocks, i.e. bio-oils, may have toxic acids that require advanced techniques and longer processing times, and this would lead to higher costs for fuel processing (Liu et al., 2012). To overcome technical challenges, advanced and organised research and development efforts are required among various universities, biodiesel producing companies and the state

Table 13
Summary of engine performance and emission studies for PSO and SFO biodiesels.

Parameters	Papaya seed oil (PSO) biodiesel	Apricot kernel oil (SFO) biodiesel
Engine performance		
BSFC increase	Blend B50, B75 and B100 (Prabhakaran et al., 2016); B5, B10, B20 (Anwar et al., 2018b)	Blend B100 (Gumus and Kasifoglu, 2010)
BSFC decrease	Blend B25 (Prabhakaran et al., 2016); B25 (Raj and Karthikayan, 2016)	Blend B5 and B20 (Gumus and Kasifoglu, 2010); Blend B20, B20/BHA4000, B20/PG4000 (Kumar et al., 2018)
BTE increase	Blend B25 (Prabhakaran et al., 2016); Mixed B25 and B25A (Raj and Karthikayan, 2016); B25, B50 (Prabakaran et al., 2015); B5, B10, B15 (Sivasubramanian, 2017)	–
BTE decrease	Blend B50, B75 and B100 (Prabhakaran et al., 2016); B5, B10, B20 (Anwar et al., 2018b)	Blend B20, B20/BHA4000, B20/PG4000 (Kumar et al., 2018)
Brake power increase	–	–
Brake power decrease	B5, B10, B20 (Anwar et al., 2018b)	–
Emission parameters		
CO increased	Blend B50, B75 and B100 (Prabhakaran et al., 2016); B75, B100 (Prabakaran et al., 2015)	Blend B20, B20/PG4000 (Kumar et al., 2018)
CO decreased	Blend B25 (Prabhakaran et al., 2016); B25, B50 (Prabakaran et al., 2015)	Blend B5, B20, B50 and B100 (Gumus and Kasifoglu, 2010); B20/BHA4000 (Kumar et al., 2018)
CO_2 increased	–	Blend B5, B20, B50 (Gumus and Kasifoglu, 2010)
CO_2 decreased	–	B100 (Gumus and Kasifoglu, 2010)
NO_x increased	Blend B25 (Prabhakaran et al., 2016); B25, B50 (Prabakaran et al., 2015)	Blend B5, B20, B50 and B100 (Gumus and Kasifoglu, 2010)
NO_x decreased	Blend B50, B75 and B100 (Prabhakaran et al., 2016); mixed B25 and B25A (Raj and Karthikayan, 2016); B75. B100 (Prabakaran et al., 2015)	Blend B20/BHA4000, B20/PG4000 (Kumar et al., 2018)
HC increased	Blend B25, B50, B75 and B100 (Raj and Karthikayan, 2016); B75, B100 (Prabakaran et al., 2015)	Blend B20, B50 and B100 (Gumus and Kasifoglu, 2010); B20/PG4000 (Kumar et al., 2018)
HC decreased	Blend B25 (Prabhakaran et al., 2016); B25, B50 (Prabakaran et al., 2015); B5, B10, B15 (Sivasubramanian, 2017)	Blend B5 (Gumus and Kasifoglu, 2010); B20/BHA4000 (Kumar et al., 2018)
EGT increased	B5, B10, B15 (Sivasubramanian, 2017)	–
EGT decreased	–	–
Smoke opacity increased	Blend B50, B75 and B100 (Prabhakaran et al., 2016); B25 and B100A (Raj and Karthikayan, 2016); B75, B100 (Prabakaran et al., 2015)	–
Smoke opacity decreased	Blend B25 (Prabhakaran et al., 2016); B25 and B100 (Raj and Karthikayan, 2016); B25, B50 (Prabakaran et al., 2015)	Blend B5, B20, B50 and B100 (Gumus and Kasifoglu, 2010)

Note: EGT refers to exhaust gas temperature; B25A and B100A refer to additives added to B25, and B100; B20/BHA4000 refers to B20 blend with butylated hydroxyl anisole (BHA) antioxidants at 4000 ppm; B20/PG4000 refers to B20 blend with propyl gallate (PG) antioxidants at 4000 ppm.

governments. Strong and favourable government policy and end user (public) support can help produce and maintain production efficiencies (Azad et al., 2015).

Most people are not aware of the benefits of biodiesel usage in their vehicles (Santacesaria et al., 2012). Lack of knowledge about the benefits of biodiesel prevents the public from using more biodiesel in their vehicles to enhance engine life as well as save the environment (Lin et al., 2011; Hannon et al., 2010). Increased publicity and attractive incentives to use biodiesel eliminate lack of awareness problem (McKone et al., 2011; Wang et al., 2009). Australian Government has initiated public awareness programs including advertisement on daily news, bill board poster, social media, radio, and television commercials to promote biofuel usage.

Generally, the production cost of biodiesel is higher than that of diesel. This is the biggest challenge, as the customers are not willing to pay extra for biodiesel. Customers are not focusing on long-term benefits of biodiesel usage in their vehicles such as increasing engine life. They are more inclined to take some savings at present (Lim and Teong, 2010; Santacesaria et al., 2012; Daniel et al., 2012; Ajanovic and Haas, 2010). Mass scale production and strong Government support, price compensation, i.e., incentives, can encourage customers to use biodiesel (Sulaiman, 2007; Li et al., 2011). Strong positive renewable energy policy is vital to promote biodiesel usage and mitigate increasing energy demands as well as decrease environmental emissions (Lin et al., 2011; Chu and Majumdar, 2012). Australian Government organisations such as Australian Renewable Energy Agency (ARENA) and Australian Competition and Consumer Commission (ACCC) are promoting biodiesel industry by satisfying all stakeholders.

11. Conclusions

This study reviewed both papaya and stone fruits as biodiesel feedstocks, and their biological life cycles. The study covers oil extraction methods, oil properties, biodiesel conversion process, biodiesel properties and their compliance to international standards, engine performance and emission studies, and combustion characteristics. Biodiesels from newer sources cannot be verified easily due to a lack of confidence, i.e., hesitation of users and engine manufacturers to accept unproven products. Since biodiesel production in Australia is not extensive, the potential of second-generation biodiesel from Australian native plants, in particular from PSO and SFO, is not fully exploited. An extensive literature review has been conducted to identify research problems and challenges in using PSO and SFO. Salient fuel properties of both PSO and SFO biodiesels have been investigated and compared with other popular non-edible biodiesels and diesel. While engine performance and emission analysis of both PSO and SFO biodiesels have been reported, there is insufficient research conducted on combustion analysis of SFO biodiesel. Further research on combustion, corrosion, tribo-corrosion, long-term engine durability testing and tribological performance analysis of PSO and SFO would be required before recommending them as future alternative energy sources in Australia.

Acknowledgement

The authors would like to acknowledge Central Queensland University for providing financial support for this publication.

References

Agunbiade, F.O., Adewole, T.A., 2014. Methanolysis of carica papaya seed oil for production of biodiesel. J. Fuels 2014, 6.
Ajanovic, A., Haas, R., 2010. Economic challenges for the future relevance of biofuels in transport in EU countries. Energy 35 (8), 3340–3348.
Algayyim, S.J.M., Wandel, A.P., Yusaf, T., Al-Lwayzy, S., Hamawand, I., 2018. Impact of butanol-acetone mixture as a fuel additive on diesel engine performance and emissions. Fuel 227, 118–126.
Anwar, M., Rasul, M.G., Ashwath, N., 2018a. Production optimization and quality assessment of papaya (Carica papaya) biodiesel with response surface methodology. Energy Convers. Manage. 156, 103–112.
Anwar, M., Rasul, M., Ashwath, N., 2018b. A systematic multivariate analysis of carica papaya biodiesel blends and their interactive effect on performance. Energies 11 (11), 2931.
Anwar, M., Rasul, M., Ashwath, N., Rahman, M., 2018c. Optimisation of second-generation biodiesel production from Australian native stone fruit oil using response surface method. Energies 11 (10), 2566.
Ashwath, N., 2010. Evaluating biodiesel potential of australian native and naturalised plant species. In: Rural Industries Research and Development Corporation, (Canberra). p. 96.
Atabani, A.E., Silitonga, A.S., Badruddin, I.A., Mahlia, T.M.I., Masjuki, H.H., Mekhilef, S., 2012. A comprehensive review on biodiesel as an alternative energy resource and its characteristics. Renew. Sustain. Energy Rev. 16 (4), 2070–2093.
Atabani, A.E., Silitonga, A.S., Ong, H.C., Mahlia, T.M.I., Masjuki, H.H., Badruddin, I.A., Fayaz, H., 2013. Non-edible vegetable oils: a critical evaluation of oil extraction, fatty acid compositions, biodiesel production, characteristics, engine performance and emissions production. Renew. Sustainable Energy Rev. 18 (Supplement C), 211–245.
Atadashi, I.M., Aroua, M.K., Abdul Aziz, A.R., Sulaiman, N.M.N., 2012. The effects of water on biodiesel production and refining technologies: a review. Renew. Sustain. Energy Rev. 16 (5), 3456–3470.
Atadashi, I.M., Aroua, M.K., Aziz, A.A., 2010. High quality biodiesel and its diesel engine application: A review. Renew. Sustain. Energy Rev. 14 (7), 1999–2008.
Australian Energy Projections to 2049-50, BREE, Canberra, 2014.
Avinash, A., Subramaniam, D., Murugesan, A., 2014. Bio-diesel—A global scenario. Renew. Sustain. Energy Rev. 29, 517–527.
Aydin, H., Bayindir, H., 2010. Performance and emission analysis of cottonseed oil methyl ester in a diesel engine. Renew. Energy 35 (3), 588–592.
Azad, A., 2017. Biodiesel from mandarin seed oil: a surprising source of alternative fuel. Energies 10 (11), 1689.
Azad, A.K., Rasul, M., Khan, M.M., Sharma, S., 2017. Macadamia biodiesel as a sustainable and alternative transport fuel in australia. Energy Procedia 110, 543–548.
Azad, A.K., Rasul, M.G., Khan, M.M.K., Sharma, S.C., Hazrat, M.A., 2015. Prospect of biofuels as an alternative transport fuel in Australia. Renew. Sustain. Energy Rev. 43 (Supplement C), 331–351.
Azad, A.M., Rasul, M.G., Khan, M.M.K., Sharma, S.C., Mofijur, M., Bhuiya, M.M.K., 2016. Prospects, feedstocks and challenges of biodiesel production from beauty leaf oil and castor oil: A nonedible oil sources in Australia. Renew. Sustain. Energy Rev. 61, 302–318.
Babaki, M., Yousefi, M., Habibi, Z., Mohammadi, M., 2017. Process optimization for biodiesel production from waste cooking oil using multi-enzyme systems through response surface methodology. Renew. Energy 105 (Supplement C), 465–472.
Baiju, B., Naik, M.K., Das, L.M., 2009. A comparative evaluation of compression ignition engine characteristics using methyl and ethyl esters of Karanja oil. Renew. Energy 34 (6), 1616–1621.
Banerjee, A., Chakraborty, R., 2009. Parametric sensitivity in transesterification of waste cooking oil for biodiesel production—A review. Resour. Conserv. Recycl. 53 (9), 490–497.
Bello, Emmanuel I., Labunmi Lajide, I.T.I.O., Daniyan, Ilesanmi A., 2016. Daniyan optimization of process parameters for biodiesel production using response surface methodology. Amer. J. Energy Eng. 4 (2), 8–16.
Bhuiya, M., Rasul, M., Khan, M., Ashwath, N., 2017. Performance and emission characteristics of binary mixture of poppy and waste cooking biodiesel. Energy Procedia 110, 523–528.
Bhuiya, K.M.M., Rasul, M.G., Khan, M.M.K., Ashwath, N., Azad, A.K., 2016. Prospects of generation biodiesel as a sustainable fuel—Part: 1 selection of feedstocks, oil extraction techniques and conversion technologies. Renew. Sustain. Energy Rev. 55, 1109–1128.
Bhuiya, K.M.M., Rasul, M.G., Khan, M.M.K., Ashwath, N., Azad, A.K., Mofijur, M., 2015. Optimisation of oil extraction process from australian native beauty leaf seed (Calophyllum Inophyllum). Energy Procedia 75, 56–61.
Biswas, B., Scott, P.T., Gresshoff, P.M., 2011. Tree legumes as feedstock for sustainable biofuel production: opportunities and challenges. J. Plant Physiol. 168 (16), 1877–1884.
Chan, H.T., Heu, R.A., Tang, C.S., Okazaki, E.N., Ishizaki, S.M., 1978. Composition of papaya SEEDs. J. Food Sci. 43 (1), 255–256.
Chielle, D.P., Bertuol, D.A., Meili, L., Tanabe, E.H., Dotto, G.L., 2016. Convective drying of papaya seeds (Carica papaya L.) and optimization of oil extraction. Ind. Crops Prod. 85 (Supplement C), 221–228.
Chu, S., Majumdar, A., 2012. Opportunities and challenges for a sustainable energy future. Nature 488, 294.

Cornejo, A., Barrio, I., Campoy, M., Lázaro, J., Navarrete, B., 2017. Oxygenated fuel additives from glycerol valorization. main production pathways and effects on fuel properties and engine performance: a critical review. Renew. Sustain. Energy Rev. 79, 1400–1413.

Damanik, N., Ong, H.C., Tong, C.W., Mahlia, T.M.I., Silitonga, A.S., 2018. A review on the engine performance and exhaust emission characteristics of diesel engines fueled with biodiesel blends. Environ. Sci. Pollut. Res. 25 (16), 15307–15325.

Daniel, K.-M., Piotr, O.-P., A, S.B., W, B.H., 2012. The challenge of enzyme cost in the production of lignocellulosic biofuels. Biotechnol. Bioeng. 109 (4), 1083–1087.

Daryono, E.D., Sinaga, E.J., 2017. Rapid in situ transesterification of papaya seeds to biodiesel with the aid of co-solvent. Int. J. Renewable Energy Res. 7 (1), 379–385.

De Melo, L.M.S., Santos, N.A., Rosenhaim, R., Souza, A.G., Athayde Filho, P.F., 2011. Use of thermal analysis techniques for evaluation of the stability and chemical properties of papaya biodiesel (Carica Papaya L.) at low temperatures. J. Thermal Anal. Calorimetry 106 (3), 831–836.

Department of Industry, Innovation and Sceience (2016), Australian energy update 2016, Canberra, September.

Department of Natural Resources, Mines and Energy, 2018 [cited 16 2018]; available from https://www.dnrm.qld.gov.au/mapping-data/maps.

Department of the Environment and Energy (2017), Australian Energy Update 2017, Canberra, August.

Dharma, S., Masjuki, H.H., Ong, H.C., Sebayang, A.H., Silitonga, A.S., Kusumo, F., Mahlia, T.M.I., 2016. Optimization of biodiesel production process for mixed Jatropha curcas–Ceiba pentandra biodiesel using response surface methodology. Energy Convers. Manage. 115, 178–190.

Dincer, K., 2008. Lower emissions from biodiesel combustion. Energy Sour. A 30 (10), 963–968.

Ezekannagha, C.B., Ude, C.N., Onukwuli, O.D., 2017. Optimization of the methanolysis of lard oil in the production of biodiesel with response surface methodology. Egyptian J. Petroleum.

Fadhil, A.B., 2017. Evaluation of apricot (Prunus armeniaca L.) seed kernel as a potential feedstock for the production of liquid bio-fuels and activated carbons. Energy Convers. Manage. 133, 307–317.

Fan, S., Liang, T., Yu, H., Bi, Q., Li, G., Wang, L., 2016. Kernel characteristics, oil contents fatty acid compositions and biodiesel properties in developing siberian apricot (Prunus sibirica L.) seeds. Ind. Crops Prod. 89, 195–199.

Ganjehkaviri, A., Mohd Jaafar, M., Hosseini, S., Musthafa, A., 2016. Performance evaluation of palm oil-based biodiesel combustion in an oil burner. Energies 9 (2), 97.

Gardy, J., Osatiashtiani, A., Céspedes, O., Hassanpour, A., Lai, X., Lee, A.F., Wilson, K., Rehan, M., 2018. A magnetically separable SO4/Fe-Al-TiO2 solid acid catalyst for biodiesel production from waste cooking oil. Appl. Catal. B 234, 268–278.

Godiganur, S., Suryanarayana Murthy, C.H., Reddy, R.P., 2009. 6BTA 5.9 G2-1 Cummins engine performance and emission tests using methyl ester mahua (Madhuca indica) oil/diesel blends. Renew. Energy 34 (10), 2172–2177.

Goldemberg, J., 2008. The challenge of biofuels. Energy Environ. Sci. 1 (5), 523–525.

Greenwell, H.C., Laurens, L.M.L., Shields, R.J., Lovitt, R.W., Flynn, K.J., 2010. Placing microalgae on the biofuels priority list: a review of the technological challenges. J. R. Soc. Interface 7 (46), 703–726.

Gumus, M., Kasifoglu, S., 2010. Performance and emission evaluation of a compression ignition engine using a biodiesel (apricot seed kernel oil methyl ester) and its blends with diesel fuel. Biomass Bioenergy 34 (1), 134–139.

Gupta, J., Agarwal, M., Dalai, A.K., 2016. Optimization of biodiesel production from mixture of edible and nonedible vegetable oils. Biocatal. Agric. Biotechnol. 8 (Supplement C), 112–120.

Hameed, B.H., 2009. Evaluation of papaya seeds as a novel non-conventional low-cost adsorbent for removal of methylene blue. J. Hazardous Mater. 162 (2), 939–944.

Hamze, H., Akia, M., Yazdani, F., 2015. Optimization of biodiesel production from the waste cooking oil using response surface methodology. Process Safety Environ. Protection 94, 1–10.

Hannon, M., Gimpel, J., Tran, M., Rasala, B., Mayfield, S., 2010. Biofuels from algae: challenges and potential. Biofuels 1 (5), 763–784.

Hasni, K., Ilham, Z., Dharma, S., Varman, M., 2017. Optimization of biodiesel production from Brucea javanica seeds oil as novel non-edible feedstock using response surface methodology. Energy Convers. Manage. 149 (Supplement C), 392–400.

Hoekman, S.K., 2009. Biofuels in the U.S. – challenges and opportunities. Renew. Energy 34 (1), 14–22.

Hoseini, S.S., Najafi, G., Ghobadian, B., Mamat, R., Ebadi, M.T., Yusaf, T., 2018. Novel environmentally friendly fuel: The effects of nanographene oxide additives on the performance and emission characteristics of diesel engines fuelled with Ailanthus altissima biodiesel. Renew. Energy 125, 283–294.

Hoseini, S.S., Najafi, G., Ghobadian, B., Mamat, R., Ebadi, M.T., Yusaf, T., 2019. Characterization of biodiesel production (ultrasonic-assisted) from evening-primroses (Oenothera lamarckiana) as novel feedstock and its effect on CI engine parameters. Renew. Energy 130, 50–60.

Islam, M.A., Brown, R.J., Brooks, P.R., Jahirul, M.I., Bockhorn, H., Heimann, K., 2015. Investigation of the effects of the fatty acid profile on fuel properties using a multi-criteria decision analysis. Energy Convers. Manage. 98, 340–347.

Jahirul, M.I., Brown, R.J., Senadeera, W., Ashwath, N., Rasul, M.G., Rahman, M.M., Hossain, F.M., Moghaddam, L., Islam, M.A., O'Hara, I.M., 2015. Physio-chemical assessment of beauty leaf (Calophyllum inophyllum) as second-generation biodiesel feedstock. Energy Rep. 1, 204–215.

Jahirul, M., Koh, W., Brown, R., Senadeera, W., Hara, I., Moghaddam, L., 2014. Biodiesel production from non-edible beauty leaf (Calophyllum inophyllum) oil: process optimization using response surface methodology (RSM). Energies 7 (8), 5317.

Jamil, F., Al-Muhtaseb, A.A.H., Al-Haj, L., Al-Hinai, M.A., Hellier, P., Rashid, U., 2016. Optimization of oil extraction from waste date pits for biodiesel production. Energy Convers. Manage. 117 (Supplement C), 264–272.

Jannatizadeh, A., Naderi-Boldaji, M., Ghasemi Varnamkhasti, F.R.M., Tabatabaeefar, A., 2008. Some postharvest physical properties of Iranian apricot (Prunus armeniaca L.) fruit. Vol. 22.

Jayed, M.H., Masjuki, H.H., Saidur, R., Kalam, M.A., Jahirul, M.I., 2009. Environmental aspects and challenges of oilseed produced biodiesel in southeast asia. Renew. Sustain. Energy Rev. 13 (9), 2452–2462.

Kate, A.E., Lohani, U.C., Pandey, J.P., Shahi, N.C., Sarkar, A., 2014. Traditional and mechanical method of the oil extraction from wild apricot kernel: a comparative study. Res. J. Chem. Environ. Sci 2, 54–60.

Kaul, S., Saxena, R.C., Kumar, A., Negi, M.S., Bhatnagar, A.K., Goyal, H.B., Gupta, A.K., 2007. Corrosion behavior of biodiesel from seed oils of indian origin on diesel engine parts. Fuel Process. Technol. 88 (3), 303–307.

Kumar, S., Kumar, R., Kumar, M., 2018. Experimental investigations of oxidation stability of biodiesel produced from prunus armeniaca oil (apricot oil) and effect of various antioxidants on stability, engine performance and emissions. Fuel 216 (Supplement C), 861–869.

Lee, W.-J., Lee, M.-H., Su, N.-W., 2011. Characteristics of papaya seed oils obtained by extrusion–expelling processes. J. Sci. Food Agric. 91 (13), 2348–2354.

Li, S., Wang, Y., Dong, S., Chen, Y., Cao, F., Chai, F., Wang, X., 2009. Biodiesel production from Eruca sativa gars vegetable oil and motor, emissions properties. Renew. Energy 34 (7), 1871–1876.

Li, Y.-G., Xu, L., Huang, Y.-M., Wang, F., Guo, C., Liu, C.-Z., 2011. Microalgal biodiesel in China: Opportunities and challenges. Appl. Energy 88 (10), 3432–3437.

Lim, S., Teong, L.K., 2010. Recent trends, opportunities and challenges of biodiesel in Malaysia: An overview. Renew. Sustain. Energy Rev. 14 (3), 938–954.

Lin, L., Cunshan, Z., Vittayapadung, S., Xiangqian, S., Mingdong, D., 2011. Opportunities and challenges for biodiesel fuel. Appl. Energy 88 (4), 1020–1031.

Liu, C.-Z., Wang, A.R., Guo, C., 2012. Ionic liquids for biofuel production: opportunities and challenges. Appl. Energy 92, 406–414.

Luque, R., Herrero-Davila, L., Campelo, J.M., Clark, J.H., Hidalgo, J.M., Luna, D., Marinas, J.M., Romero, A.A., 2008. Biofuels: a technological perspective. Energy Environ. Sci. 1 (5), 542–564.

Mahanta, P.S.A., 2004. Technology development of bio-diesel as an energy alternative. pp. 1–19.

Makareviciene, V., Skorupskaite, V., Levisauskas, D., Andruleviciute, V., Kazancev, K., 2014. The optimization of biodiesel fuel production from microalgae oil using response surface methodology. Int. J. Green Energy 11 (5), 527–541.

Malacrida, C.R., Kimura, M., Jorge, N., 2011. Characterization of a high oleic oil extracted from papaya (Carica papaya L.) seeds. Food Sci. Technol. 31, 929–934.

Mansourpoor, M.S.A., 2012. Optimization of biodiesel production from sunflower oil using response surface methodology. J. Chem. Eng. Process. Technol. 3 (141).

Marfo, E.K., Oke, O.L., Afolabi, O.A., 1986. Chemical composition of papaya (Carica papaya) seeds. Food Chem 22, 259–266.

Math, M.C., Chandrashekhara, K.N., 2016. 2016 optimization of alkali catalyzed transesterification of safflower oil for production of biodiesel. J. Eng. 7.

McKone, T.E., Nazaroff, W.W., Berck, P., Auffhammer, M., Lipman, T., Torn, M.S., Masanet, E., Lobscheid, A., Santero, N., Mishra, U., Barrett, A., Bomberg, M., Fingerman, K., Scown, C., Strogen, B., Horvath, A., 2011. Grand challenges for life-cycle assessment of biofuels. Environ. Sci. Technol. 45 (5), 1751–1756.

Mettler, M.S., Vlachos, D.G., Dauenhauer, P.J., 2012. Top ten fundamental challenges of biomass pyrolysis for biofuels. Energy Environ. Sci. 5 (7), 7797–7809.

Milano, J., Ong, H.C., Masjuki, H.H., Silitonga, A.S., Chen, W.-H., Kusumo, F., Dharma, S., Sebayang, A.H., 2018. Optimization of biodiesel production by microwave irradiation-assisted transesterification for waste cooking oil-Calophyllum inophyllum oil via response surface methodology. Energy Convers. Manage. 158, 400–415.

Ming, C., Rizwanul Fattah, I.M., Chan, Q.N., Pham, P.X., Medwell, P.R., Kook, S., Yeoh, G.H., Hawkes, E.R., Masri, A.R., 2018. Combustion characterization of waste cooking oil and canola oil based biodiesels under simulated engine conditions. Fuel 224, 167–177.

Mohan, A., Sen, S., 2015. Emission analysis of the biodiesel from papaya and chicken blends. Int. J. Informative Futuristic Res. 2 (7), 2258–2264.

Mosarof, M.H., Kalam, M.A., Masjuki, H.H., Alabdulkarem, A., Ashraful, A.M., Arslan, A., Rashedul, H.K., Monirul, I.M., 2016. Optimization of performance, emission, friction and wear characteristics of palm and Calophyllum inophyllum biodiesel blends. Energy Convers. Manage. 118, 119–134.

Mowla, O., Kennedy, E., Stockenhuber, M., 2018. In-situ FTIR study on the mechanism of both steps of zeolite-catalysed hydroesterification reaction in the context of biodiesel manufacturing. Fuel 232, 12–26.

Mukherjee, P., Varshney, A., Johnson, T.S., Jha, T.B., 2011. Jatropha curcas: a review on biotechnological status and challenges. Plant Biotechnol. Rep. 5 (3), 197–215.

Murugesan, A., Umarani, C., Chinnusamy, T.R., Krishnan, M., Subramanian, R., Neduzchezhain, N., 2009. Production and analysis of bio-diesel from non-edible oils—A review. Renew. Sustain. Energy Rev. 13 (4), 825–834.

Muthukumaran, C., Praniesh, R., Navamani, P., Swathi, R., Sharmila, G., Manoj Kumar, N., 2017. Process optimization and kinetic modeling of biodiesel production using non-edible madhuca indica oil. Fuel 195, 217–225.

Nabi, M.N., Rahman, M.M., Islam, M.A., Hossain, F.M., Brooks, P., Rowlands, W.N., Tulloch, J., Ristovski, Z.D., Brown, R.J., 2015. Fuel characterisation, engine performance, combustion and exhaust emissions with a new renewable Licella biofuel. Energy Convers. Manage. 96, 588–598.

Nabi, M.N., Rasul, M.G., 2018. Influence of second generation biodiesel on engine performance, emissions, energy and exergy parameters. Energy Convers. Manage. 169, 326–333.

Ogaga, I.B., Adeleke, I.A., Damus, M., Adeola, H.J., Ernest, K.O., Betiku, E., 2017. Optimization of biodiesel production from thevetia peruviana seed oil by adaptive neuro-fuzzy inference system coupled with genetic algorithm and response surface methodology. Energy Convers. Manage. 132 (Supplement C), 231–240.

Onukwuli, D.O., Emembolu, L.N., Ude, C.N., Aliozo, S.O., Menkiti, M.C., 2017. Optimization of biodiesel production from refined cotton seed oil and its characterization. Egyptian J. Petroleum 26 (1), 103–110.

Özcanlımath, M., Keskin, A., Aydın, K., 2011. Biodiesel production from terebinth (Pistacia Terebinthus) oil and its usage in diesel engine. Int. J. Green Energy 8 (5), 518–528.

Özkal, S.G., Yener, M.E., Bayındırlı, L., 2005. Mass transfer modeling of apricot kernel oil extraction with supercritical carbon dioxide. J. Supercrit. Fluids 35 (2), 119–127.

Patel, K.A., Nayak, M.G., 2017. Production of FAME using waste papaya seeds by different experimental conditions in a batch system. Int. J. Adv. Eng. Res. Dev. (IJAERD) 4 (1), 244–248.

Prabakaran, P., Saravanan, C.G., Yadav, S.P.R., Aalam, C.S., 2015. Experimental investigation of papaya methyl ester on performance, combustion and emission characteristics of DI diesel engine. Int. J. Innovative Res. Creative Technol. 1 (4).

Prabhakaran, P., Saravanan, C.G., Aalam, C.S., 2016. Effects of papaya methyl ester on DI diesel engine combustion, emission and performance characteristics. Int. Res. J. Eng. Technol. (IRJET) 3 (2).

Puangsri, T., Abdulkarim, S.M., Ghazali, H.M., 2004. Properties of Carica papaya L. (papaya) seed oil following extractions using solvent and aqueous enzymatic methods. J. Food Lipids 12, 62–76.

Puri, M., Abraham, R.E., Barrow, C.J., 2012. Biofuel production: Prospects, challenges and feedstock in Australia. Renew. Sustain. Energy Rev. 16 (8), 6022–6031.

Rahimi, M., Aghel, B., Alitabar, M., Sepahvand, A., Ghasempour, H.R., 2014. Optimization of biodiesel production from soybean oil in a microreactor. Energy Convers. Manage. 79, 599–605.

Rahman, M.M., Hassan, N.M.S., Hyde, J., 2016. Prospects of biodiesel production from macadamia oil as an alternative fuel for diesel engines. Energies 9 (403).

Rahman, M.M., Hazrat, M.A., Rasul, M.G., Mahmudul, H.M., 2015. Comparative evaluation of edible and non-edible oil methyl ester performance in a vehicular engine. Energy Procedia 75, 37–43.

Rahman, A.M.S., Hossain, F.M., Van, T.C., Dowell, A., Islam, M.A, Rainey, T.J., Ristovski, Z.D., Brown, R.J., 2017a. Comparative evaluation of the effect of sweet orange oil-diesel blend on performance and emissions of a multi-cylinder compression ignition engine. AIP Conf. Proc. 1851 (1), 020007.

Rahman, S.M.A., Masjuki, H.H., Kalam, M.A., Abedin, M.J., Sanjid, A., Rahman, M.M., 2014. Assessing idling effects on a compression ignition engine fueled with Jatropha and Palm biodiesel blends. Renew. Energy 68, 644–650.

Rahman, M.M., Masjuki, H.H., Kalam, M.A., Atabani, A.E., Shahabuddin, M., Palash, S.M., Hazrat, M.A., 2013. Effect of biodiesel from various feedstocks on combustion characteristics, engine durability and materials compatibility: A review. Renew. Sustain. Energy Rev. 28, 441–455.

Rahman, M.M., Masjuki, H.H., Kalam, M.A., Hazrat, M.A., Liaquat, A.M., Shahabuddin, M., Varman, M., 2012. Prospects of biodiesel from Jatropha in malaysia. Renew. Sustain. Energy Rev. 16 (7), 5007–5020.

Rahman, S.M.A., Nabi, M., Van, T.C., Suara, K., Jafari, M., Dowell, A., Islam, M.A., Marchese, A.J., Tryner, J., Hossain, M.F., Rainey, T.J., Ristovski, Z.D., Brown, R.J., 2018a. Performance and combustion characteristics analysis of multi-cylinder ci engine using essential oil blends. Energies 11 (4), 738.

Rahman, M.M., Rasul, M.G., Hassan, N.M.S., Khan, M.M.K., Rashedul, H.K., 2018b. Gaseous and particle emissions from a compression ignition engine fueled with biodiesel–diesel blends. In: Khan, A.A., Hassan, N.M.S. (Eds.), Application of Thermo-fluid Processes in Energy Systems: Key Issues and Recent Developments for a Sustainable Future. Springer Singapore, Singapore, pp. 35–56.

Rahman, M.M., Rasul, M.G., Hassan, N.M.S., Masjuki, H.H., Kalam, M.A., Mahmudul, H.M., 2017b. Chapter fourteen - assessment of physical, chemical, and tribological properties of different biodiesel fuels. In: Rasul, M.G., Azad, A.k., Sharma, S.C. (Eds.), Clean Energy for Sustainable Development. Academic Press, pp. 441–463.

Raj, C.S., Karthikayan, M., 2016. Effect of additive on the performance, emission and combustion characteristics of a diesel engine run by diesel-papaya methyl ester blends. Int. J. Chem. Sci 14 (4), 2823–2834.

Rosenthal, A., Pyle, D.L., Niranjan, K., Gilmour, S., Trinca, L., 2001. Combined effect of operational variables and enzyme activity on aqueous enzymatic extraction of oil and protein from soybean. Enzyme Microb. Technol. 28 (6), 499–509.

Salunkhe, D.K., Kadam, S.S., 1995. Handbook of Fruit Science and Technology: Production, Composition, Storage, and Processing. Taylor & Francis.

Samaram, S., Mirhosseini, H., Tan, C., Ghazali, H., 2013. Ultrasound-assisted extraction (Uae) and solvent extraction of papaya seed oil: yield, fatty acid composition and triacylglycerol profile. Molecules 18 (10), 12474.

Santacesaria, E., Vicente, G.M., Di Serio, M., Tesser, R., 2012. Main technologies in biodiesel production: state of the art and future challenges. Catalysis Today 195 (1), 2–13.

Shah, S., Sharma, A., Gupta, M.N., 2005. Extraction of oil from jatropha curcas l. seed kernels by combination of ultrasonication and aqueous enzymatic oil extraction. Bioresour. Technol. 96 (1), 121–123.

Sharma, R., Gupta, A., Abrol, G.S., Joshi, V.K., 2012. Value addition of wild apricot fruits grown in north-west himalayan regions: a review. J. Food Sci. Technol.

Silitonga, A.S., Ong, H.C., Mahlia, T.M.I., Masjuki, H.H., Chong, W.T., 2014. Biodiesel conversion from high FFA crude jatropha curcas, calophyllum inophyllum and ceiba pentandra oil. Energy Procedia 61 (Supplement C), 480–483.

Singh, S.P., Singh, D., 2010. Biodiesel production through the use of different sources and characterization of oils and their esters as the substitute of diesel: a review. Renew. Sustain. Energy Rev. 14 (1), 200–216.

Sitepu, E.K., Corbin, K., Luo, X., Pye, S.J., Tang, Y., Leterme, S.C., Heimann, K., Raston, C.L., Zhang, W., 2018. Vortex fluidic mediated direct transesterification of wet microalgae biomass to biodiesel. Bioresour. Technol. 266, 488–497.

Sivasubramanian, H., 2017. Performance and emission characteristics of papaya seed oil methyl ester–n-butanol–diesel blends on a stationary direct-injection Ci engine. Biofuels 1–10.

Sulaiman, A.-Z., 2007. Production of biodiesel: possibilities and challenges. Biofuels, Bioprod. Biorefin. 1 (1), 57–66.

Syed, H.M., P, K.S., Jadhav, B.A., Salve, R.V., 2011. Extraction and characterization of papaya seed oil Elixir Agriculture, 37A: 4102-4105.

Tran, N.N., Tišma, M., Budžaki, S., McMurchie, E.J., Gonzalez, O.M.M., Hessel, V., Ngothai, Y., 2018. Scale-up and economic analysis of biodiesel production from recycled grease trap waste. Appl. Energy 229, 142–150.

Ullah, F., Nosheen, A., Hussain, I., Bano, A., 2009. Base catalyzed transesterification of wild apricot kernel oil for biodiesel production. Afr. J. Biotechnol. 8 (14), 3289–3293.

USDA Foreign Agricultural service: Australia Biofuels Annual 2017, Canberra.

Usta, N., 2005. Use of tobacco seed oil methyl ester in a turbocharged indirect injection diesel engine. Biomass Bioenergy 28 (1), 77–86.

Vasco-Correa, J., Zapata Zapata, A.D., 2017. Enzymatic extraction of pectin from passion fruit peel (Passiflora edulis f. flavicarpa) at laboratory and bench scale. LWT - Food Sci. Technol. 80, 280–285.

Vasudevan, P.T., Briggs, M., 2008. Biodiesel production—current state of the art and challenges. J. Ind. Microbiol. Biotechnol. 35 (5), 421.

Verma, P., Sharma, M.P., Dwivedi, G., 2016. Prospects of bio-based alcohols for karanja biodiesel production: an optimisation study by response surface methodology. Fuel 183 (Supplement C), 185–194.

Verma, P., Zare, A., Jafari, M., Bodisco, T.A., Rainey, T., Ristovski, Z.D., Brown, R.J., 2018. Diesel engine performance and emissions with fuels derived from waste tyres. Sci. Rep. 8 (1), 2457.

Vieira Silveira, E., Santos Vilela, L., de Souza Castro, C.F., Morais Lião, L., Fernandes Gambarra Neto, F., Santos Mello de Oliveira, P., 2017. Chromatographic characterization of the crambe (Crambe abyssinica Hochst) oil and modeling of some parameters for its conversion in biodiesel. Ind. Crops Prod. 97 (Supplement C), 545–551.

Wang, L., 2013. Properties of manchurian apricot (Prunus mandshurica Skv.) and siberian apricot (Prunus sibirica L.) seed kernel oils and evaluation as biodiesel feedstocks. Ind. Crops Prod. 50 (Supplement C), 838–843.
Wang, F., Xiong, X.-R., Liu, C.-Z., 2009. Biofuels in china: opportunities and challenges. Vitro Cellular Dev. Biology - Plant 45 (3), 342–349.
Wang, L., Yu, H., 2012. Biodiesel from siberian apricot (Prunus sibirica L.) seed kernel oil. Bioresour. Technol. 112 (Supplement C), 355–358.
Wong, C.S., Othman, R., 2014. Biodiesel production by enzymatic transesterification of papaya seed oil and rambutan seed oil. Int. J. Eng. Technol. (IJET) 6 (6), 2773–2777.
Xie, B., Gong, W., Tian, Y., Qu, F., Luo, Y., Du, X., Tang, X., Xu, D., Lin, D., Li, G., Liang, H., 2018. Biodiesel production with the simultaneous removal of nitrogen, phosphorus and COD in microalgal–bacterial communities for the treatment of anaerobic digestion effluent in photobioreactors. Chem. Eng. J. 350, 1092–1102.
Yaakob, Z., Mohammad, M., Alherbawi, M., Alam, Z., Sopian, K., 2013. Overview of the production of biodiesel from waste cooking oil. Renew. Sustainable Energy Rev. 18 (Supplement C), 184–193.
Yadav, A.K., Pal, A., Dubey, A.M., 2017. Experimental studies on utilization of Prunus armeniaca L. (wild apricot) biodiesel as an alternative fuel for CI engine. Waste Biomass Valorization.
Yang, J.C.K., He, QS., Caldwell, C., 2015. The optimization of alkali-catalyzed biodiesel production from camelina sativa oil using a response surface methodology. Bioprocess Biotech 5 (235).
Yusaf, T.F., Yousif, B.F., Elawad, M.M., 2011. Crude palm oil fuel for diesel-engines: Experimental and ANN simulation approaches. Energy 36 (8), 4871–4878.
Zare, A., Bodisco, T.A., Nabi, M.N., Hossain, F.M., Ristovski, Z.D., Brown, R.J., 2018. A comparative investigation into cold-start and hot-start operation of diesel engine performance with oxygenated fuels during transient and steady-state operation. Fuel 228, 390–404.
Zare, A., Nabi, M.N., Bodisco, T.A., Hossain, F.M., Rahman, M.M., Chu Van, T., Ristovski, Z.D., Brown, R.J., 2017. Diesel engine emissions with oxygenated fuels: A comparative study into cold-start and hot-start operation. J. Cleaner Prod. 162, 997–1008.
Zhu, L., Ketola, T., 2012. Microalgae production as a biofuel feedstock: risks and challenges. Int. J. Sustainable Dev. World Ecol. 19 (3), 268–274.

{this page is intentionally left blank}

Declaration of Co-authorship and Contribution

Research Division

CHAPTER 3: Feedstock Selection

Title of the paper	The efficacy of multiple-criteria design matrix for biodiesel feedstock selection
Full bibliographic reference	Anwar, M., M.G. Rasul, and N. Ashwath, The efficacy of multiple-criteria design matrix for biodiesel feedstock selection. Energy Conversion and Management, 2019. 198: p. 111790. https://www.sciencedirect.com/science/article/pii/S0196890419307721
Status	Published

Nature of Candidate's Contribution, including percentage of total
I was responsible for Design concept of the article, analysed the literature, drafted the manuscript. [80%]

Nature of all Co-Authors' Contributions, including percentage of total
My co-authors, Prof Mohammad Rasul and A/Professor Nanjappa Ashwath, were supervised the project and reviewed the manuscript. [20%]

Has this paper been submitted for an award by another research degree candidate (Co- Author), either at CQUniversity or elsewhere? (if yes, give full details)
No

Candidate's Declaration

I declare that the publication above meets the requirements to be included in the thesis as outlined in the Research Higher Degree Theses Policy and Procedure.

Mohammad Anwar

Energy Conversion and Management 198 (2019) 111790

Contents lists available at ScienceDirect

Energy Conversion and Management

journal homepage: www.elsevier.com/locate/enconman

The efficacy of multiple-criteria design matrix for biodiesel feedstock selection

Mohammad Anwar[a], Mohammad G. Rasul[a,*], Nanjappa Ashwath[b]

[a] Central Queensland University, School of Engineering and Technology, Queensland 4701, Australia
[b] Central Queensland University, School of Health, Medical and Applied Sciences, Queensland 4701, Australia

ARTICLE INFO

Keywords:
PROMETHEE GAIA
Multiple criteria decision analysis
Papaya
Stone fruit
Biodiesel
TOPSIS
WSM
WPM
MCDM
Critic
Entropy

ABSTRACT

The increasing demand for energy and depletion of fossil fuels are drawing attention to biofuel as a replacement for petroleum diesel. Hundreds of non-edible biodiesel feedstocks are available and are derived from seeds and animal fat or tallow. However, the selection of appropriate feedstock is fraught with difficulty, as these feedstocks have not been fully evaluated for various parameters that impact upon the performance and cost of the biofuel. Various technical, environmental, economic and social factors influence biodiesel feedstocks selection process. This paper focuses on technical aspects such as physico-chemical properties and fatty acid compositions of biodiesels in the screening process. Six biodiesels, namely papaya seed oil biodiesel (PSO), stone fruit kernel oil biodiesel (SFO), jatropha oil biodiesel (JBD), rapeseed oil biodiesel (RBD), beauty leaf tree biodiesel (BLT), and waste cooking oil biodiesel (WCB) were analysed in this study. Twelve physico-chemical properties of kinematic viscosity (KV), density, higher heating value (HHV), oxidation stability (OS), acid value (AV), flash point (FP), cold filter plug point (CFPP), cetane number (CN), iodine value (IV), monounsaturated fatty acid (MUFA), polyunsaturated fatty acid (PUFA) and long chain saturated factor (LCSF) were selected as criteria for ranking the above biodiesels. Three weightage (%) methods of EQUAL, CRITIC and ENTROPY were used for weight determination of criteria. Four different multiple-criteria decision analysis (MCDA) methods, namely PROMETHEE Graphical Analysis for Interactive Assistance (GAIA), Weighted sum method (WSM), Weighted product method (WPM), and Technique for order preference by similarity to ideal solution (TOPSIS) were used for the analysis. Properties of these biodiesels were found to be within the limits of ASTM D6751-2, EN 14214 and the Australian standard. Finally, the results show that SFO was ranked as the best performer amongst the six biodiesel feedstocks examined in this study, PSO came out as the second best, and the WCB biodiesel feedstock was identified as the worst performer.

1. Introduction

Energy consumption has increased over the last few decades due to the expansion of human population and industrialisation, leading to depletion of fossil fuel reserves and increasing petroleum price [1]. The emissions from burning of fossil fuel are a major cause for environmental pollution. The greenhouse gas emissions from fossil fuels will increase by 39% by 2030 if no precautions are taken [2].The readily available conventional fossil fuels increase the emissions of combustion generated pollutants and greenhouse gases, resulting in atmospheric pollution and global warming. Researchers are working tirelessly to find alternative fuels that can replace fossil fuels to minimise environmental pollution and to find sustainable sources of fuel. Some alternative options can be renewable energy sources, natural gas, ethanol, electricity and methanol that can reduce global warming, fossil fuels consumption and exhaust emissions. Biodiesel is a renewable energy source that has received widespread acceptance due to its excellent environment-friendly attributes. Researchers conclude that using biodiesels in an internal combustion engine can reduce ongoing fossil fuel demand as well as minimise adverse environmental effects on the planet [3,4].

Biodiesels can be produced from renewable sources such as vegetable oil, waste cooking oil and animal fats. Biodiesel is non-explosive, biodegradable, non-flammable, renewable, and non-toxic. Some feedstocks of biodiesels are called 1st generation feedstocks as they are currently being used as food items. Some 1st generation biodiesel feedstocks are soybean oil, palm oil, corn oil, sunflower oil, castor oil, olive oil, mustard oil, and linseed oil. The option of increasing their use

* Corresponding author.
E-mail address: m.rasul@cqu.edu.au (M.G. Rasul).

https://doi.org/10.1016/j.enconman.2019.111790
Received 18 April 2019; Received in revised form 4 July 2019; Accepted 5 July 2019

Table 1
Properties of non-edible biodiesel feedstocks.

	Papaya oil [22]	Apricot oil [23]	Jatropha oil [24,25]	BLT oil [26,27]	Rapeseed oil [28]	Waste cooking oil [29]
Oil content (%)	30–34	54.2	50–60	46–65	38–46	–
Kinematic viscosity at 40 °C (mm^2/s)	27.3	34.54	24.5	56.74	36.3	45.34
Density at 15 °C (kg/m^3)	885	910	940	964	906.2	918.4
Higher heating value (MJ/kg)	–	38.4	38.65	38.10	–	35.82
Oxidation stability (h)	77.97	–	–	–	–	–
Acid value (mg KOH/g)	0.98	1.65	28	36.26	2.7	2.896
Cetane number	–	–	38	–		30
Iodine value (g I/100 g)	79.95	103	94	–	113.5	92.5
Saponification value	–	173	198	–	194.7	195.48

in the production for biodiesel will put strains on food security. Furthermore, extensive cultivation of such crops for biofuel production can also result in a decline in soil fertility. The research, therefore, has shifted from 1st generation feedstocks to non-edible vegetable oil and animal fat as sources of biodiesel feedstock and these feedstocks are referred to as 2nd generation biodiesel feedstocks. Due to the non-edible nature of vegetable oil and waste fat from animals, the 2nd generation biodiesel feedstocks are much cheaper and more sustainable than 1st generation biodiesel feedstocks.

More than 350 oil-bearing crops can be used as feedstocks in biodiesel production [5]. Again, there is an ongoing debate on the ideal or best possible biodiesel feedstocks in terms of their technical, environmental, economic and social aspects. Technical aspects of the biodiesel selection process include assessing physico-chemical properties, fatty acid composition, safety, and availability criteria. Environment-related criteria such as land usage, irrigation, cultivation methods, etc., are considered under the environmental aspect. All costs that are associated with issues such as cultivation, harvesting, labour, transportation, etc., are under the criteria of economic aspects. The social aspects include activities such as job creation, social acceptance and community benefits. Different multiple criteria decision analysis (MCDA) methods such as PROMETHEE GAIA, weighted sum method (WSM), weighted product method (WPM), Technique for Order Preference by Similarity to Ideal Solution (TOPSIS), Fuzzy analytic hierarchy process (AHP)-TOPSIS, and Operational competitiveness rating analysis (OCRA) can be used for screening biodiesel feedstocks [6–9]. The current study only focused on the technical aspects of choosing biodiesel feedstocks from a selection of six non-edible biodiesel feedstocks. The screening process was based on four different MCDA methods, namely PROMETHEE GAIA, WSM, WPM and TOPSIS due to their user-friendliness and strong ability to solve single dimensional problems. Twelve physico-chemical properties of kinematic viscosity (KV), density, higher heating value (HHV), oxidation stability (OS), acid value (AV), flash point (FP), cold filter plug point (CFPP), cetane number (CN), iodine value (IV), monounsaturated fatty acid (MUFA), polyunsaturated fatty acid (PUFA), and long chain saturated factor (LCSF) were selected as the parameters for ranking those biodiesels. Three weightage (%) methods of EQUAL, CRITIC and ENTROPY were also used for weight determination criteria.

2. Biodiesel feedstocks

Selection of biodiesel feedstocks is a significant matter, as the correct decision may allow a commercial scale operation to either “make it or break it”. Amongst the many sources of non-edible biodiesel feedstocks, papaya seed oil, stone fruit seed oil, *Jatropha curcas* seed oil, Beauty leaf tree kernel oil, rapeseed oil and waste cooking oil were used as prospective biodiesel feedstocks in the present study.

Papaya (Carica papaya) is a tropical crop and is cultivated in Asia, South America, Africa and Polynesia. Although it originates from the tropics of the Americas, India is the largest papaya fruit producer in the world. India contributes to 42% of the world’s production, which equates to 3 million tonnes per year [10,11]. Papaya also grows well in the sub-tropical regions. Papaya fruits vary in size from 200 g to 3000 g. The seed content also vary from one cultivar to the other, and there are cultivars that do not set seeds. However, most papaya cultivars contain seeds, and the seeds make up 15% of the wet weight of the fruit [12,13]. Seeds are not consumed so that they will be discarded along with the peeled skin [13,14]. These seeds are rich in oil and they may be used in biodiesel production and cattle feed formulations. PSO is high in oleic acid and linoleic acid, these being 47.7% and 37.2% respectively of the total fatty acid composition.

Stone fruit, also known as prune (*Prunus armeniaca* L.), originates from India and Armenia, but it is widely cultivated in Turkey followed by Iran and Uzbekistan. Stone fruit prefers cool, frost-free sites due to its early blooming properties [12]. Its fruits are 1.5–2.5 cm in diameter and they vary in colour from yellow to orange or red. The fruit is made up of a soft outer layer and a stony seed. While the outer soft layer is consumed, the stony portion is generally discarded. These stones have high oil content and hence they can be used in biodiesel production. The fruits yield is 22–38% of kernels which contain up to 54.2% oil [15]. SFO is high in oleic acid that is about 63.8% of the total fatty acid composition. During fruit processing, the seeds are discarded due to the presence of hydro-cyanic acid [16].

Jatropha curcas is a drought-resistant small tree or large shrub (5–7 m tall) and belongs to the Euphorbiaceae family which includes eight hundred species [5]. It is well capable of surviving in abandoned and degraded land. This plant is native to Central America, Africa, and Southeast India, and has recently spread to the entire pantropical region. It bears fruits from the second year of planting and can continue to bear fruits for 30–50 years [17,18]. It can produce seeds from 0.1-8 tonnes per hectare in a year. The oil content of *Jatropha curcas* seed is 50–60% (Table 1) and the yield of fruit is about 1590 kg/hectare [19,20]. Jatropha oil is high in oleic acid (44.6%) and linoleic acids (31.9%).

Beauty leaf tree (*Calophyllum inophyllum*) seed is one of the most popular biodiesel feedstocks around the world due to its high oil content. Its oil content is found to be relatively high (65%) amongst the various species of this study (Table 1). It has high palmitic acid (14.9%), stearic acid (17.2%), oleic acid (38.2%) and linoleic acid (27.6%) content of the total fatty acid composition. It has a higher heating value, lower feedstock cost and can grow in degraded lands in different climatic conditions. These features make the beauty leaf tree an excellent source of feedstock for biodiesel production. Beauty leaf tree grows mainly in Australia, Pacific islands, Papua New Guinea, India and Sri Lanka. It attains reproductive maturity in 5–7 years and continues to yield fruits for more than 200 years [21]. Fruits are spherical drupes and arranged in clusters. The oil yield ranges from 2000 kg to 4000 kg/ha/yr [17,21].

Rapeseed (*Brassica napus*) is an annual plant belonging to the mustard family (Brassicaceae). It grows up to 60 cm and its seeds are used in extracting edible oil. There are many species of rapeseeds. The presence of erucic acid (about 50%) in natural rapeseed makes it a non-edible oil. However, one cultivar of rapeseed is used to produce canola oil. Rapeseed grows mainly in cool weather and in wide ranges of well-

drained soils. It grows well in the European Union, Canada, China, India and Australia. It contains about 38–46% of oil (Table 1). Like beauty leaf oil, rapeseed oil has high concentrations of palmitic acid (20.3%), oleic acid (43.5%) and linoleic acid (31%).

Waste cooking oil (WCO) is available from restaurants and household kitchens and is drawing more attention as an alternative feedstock for biodiesel production. Conversion of waste cooking oil to biodiesel can solve the problem of dumping huge amounts of waste oil into landfills, which will eventually contaminate watercourses or groundwater. The biodiesel generated from such waste oil can be cost effective as the waste cooking oil does not hold any monetary value. Increasing food consumption in countries with large populations and has a great impact on waste cooking oil production. Generally, physico-chemical properties of waste oils mostly depend on the type of vegetable oil used in the cooking. In most cases, waste cooking oil is a burnt oil which contains a mixture of several types of vegetable oils like soybean, palm, sunflower and canola oil. This WCO has high contents of free fatty acids (FFAs) and water molecules. A high FFA content can lead to saponification during biodiesel conversion, and a high water content can result in hydrolysis. Waste cooking oil is also high in oleic acid (66.3%).

The oil content (%), oil yield per hectare and the conversion of oil to biodiesel are the most important parameters to be considered for any feedstock as a source of biodiesel. Table 1 shows various properties of the six biodiesel feedstocks in this study, including their oil content yield as a percentage of the weight of seeds or cooking oil.

3. Biodiesel production process

As seen from Table 1, all the studied biodiesel feedstock non-edible vegetable oils have high viscosity and low volatility. The large amounts of polyunsaturated fatty acid (PUFA) present in the vegetable oils can cause undesired soap formation leading to lower biodiesel conversion yield. A chemical reaction is required to lower the viscosity and acid value of the vegetable oils. A single stage chemical reaction, i.e., transesterification using an alkaline catalyst, is sufficient for the oils with low FFA content. However, oils with high FFA content and high viscosities require a two stage reaction. This two stage reaction includes treatment of the oil with an acid and then normal alkali-mediated transesterification. Prior to these treatments, the oil should be pretreated by refining. The refining process involves removal of waxes/resins, neutralisation and decolourisation. This process can also reduce the FFA content of the oil to less than 1% [30,31]. Once the acid value of the oil is reduced to 2 mg KOH/g through esterification, an alkali catalyst transesterification reaction is carried out [32]. The alkali catalyst transesterification reaction removes the glycerides and produced fatty acid methyl or ethyl esters. Fig. 1 shows the biodiesel production process.

In the two stage biodiesel production process, the crude oil was initially filtered through a Whatman® 541-grade filter paper (pore size 22 μm) to remove any solid particles from the oil. The oil was refined and it was then poured into a three-neck laboratory reactor (2 L capacity) along with defined amounts of methanol (methanol to oil molar ratio) and sulphuric acid. The mixture was heated to a defined temperature for a set time. The mixture was stirred at 600 rpm using a magnetic stirrer. After completion of the chemical reaction, the product was transferred into a separating funnel for separating excess alcohol with FFA, sulphuric acid and impurities that were contained in the top layer of the mixture. The bottom layer (lower FFA containing esterified oil) was separated and heated at 95 °C for 1 h to remove alcohol and water. Then the esterified oil was processed in an alkali-catalysed transesterification.

The single stage (transesterification reaction) process was carried out in the same reactor equipped with a reflux condenser, thermocouple and a magnetic stirrer. The oil was preheated to 40 °C and potassium methoxide was poured into the reactor. After completion of the transesterification reaction at set times and agitation speeds, the mixture was transferred into a separating funnel for phase separation. The upper part contained the methyl ester, i.e., biodiesel, and the lower part contained glycerol with unreacted methanol and impurities. The biodiesel was collected after the lower part was drained off. The biodiesel was heated at 65–70 °C to remove traces of methanol. Then it was washed with warm distilled water to remove any dissolved impurities of KOH, soap or glycerol. The washed biodiesel was heated again at 95 °C for 1 h to remove water and then dried using sodium sulphate (Na_2SO_4). Finally, the biodiesel was filtered through Whatman® qualitative grade 1 filter paper and stored at room temperature for characterization.

There are many ways of optimizing the biodiesel production process to obtain the highest yield. Biodiesel yield can be calculated using Eq. (1), and its composition can be determined via gas chromatography (GC) [33]. Table 2 shows the optimization of the biodiesel production process from the studied non-edible feedstocks.

$$Biodiesel\ \ Yield = FAME\ \ percent\ \ from\ \ GC\ \ analysis \times \frac{Weight\ \ of\ \ biodiesel}{Weight\ \ of\ \ refined\ \ oil} \quad (1)$$

4. Physico-chemical properties of biodiesel

4.1. Determination of fatty acid composition

The first step of selecting a biodiesel for use in a diesel engine is validating its chemical composition. All biodiesels are mono alkyl esters of fatty acids, i.e., fatty acid methyl or ethyl esters. The fatty acids present in the studied biodiesels that are shown in Table 3 are different due to their varying sources or feedstocks and variations in the biodiesel conversion processes. All fatty acids are different in their chain length, degree of unsaturation and presence of other chemical components. However, every biodiesel generally contains both saturated and unsaturated (poly and mono) fatty acids. The structures of fatty acids are mainly indicated by two numbers shown in the second column of Table 3: the first number represents the carbon atoms and the second number is the number of double bonds. The prominent fatty acids are found to be palmitic acid (16:0), stearic acid (18:0), oleic acid (18:1), and linoleic acid (18:2). The highest saturated fatty acid (SFA) was recorded in BLT (33.4%) and the lowest was in SFO (9.0%). SFA plays an important role in the fuel properties, as the cetane number (CN) increases with an increase in SFA. BLT has a higher long chain saturated factor of 10.96, whereas SFO was found lowest (2.83). A balance of both saturated and unsaturated fatty acid composition is a requirement for a high-quality biodiesel.

4.2. Physico-chemical properties of biodiesel

Properties of biodiesel need to meet the minimum requirements as per relevant quality standards before being considered for use as a commercial fuel. Due to the differences in the compositional profile of each feedstock, every feedstock's biodiesel properties are different as discussed in Section 4.1. Biodiesels from the same type of feedstock can be obtained with different chemical properties due to different origins of the feedstock, different climatic conditions during growing and variations in the working environment. In order to mitigate these problems, international standards such as ASTM D6751-2 and EN14214 and an Australian Standard are employed. Table 4 shows the summary of important physico-chemical properties of the studied non-edible biodiesel feedstocks in comparison with the international standards.

4.2.1. Kinematic viscosity

Kinematic viscosity (KV) is one of the most important fuel properties of biodiesels. Researchers [26,37] state that KV affects the quality of

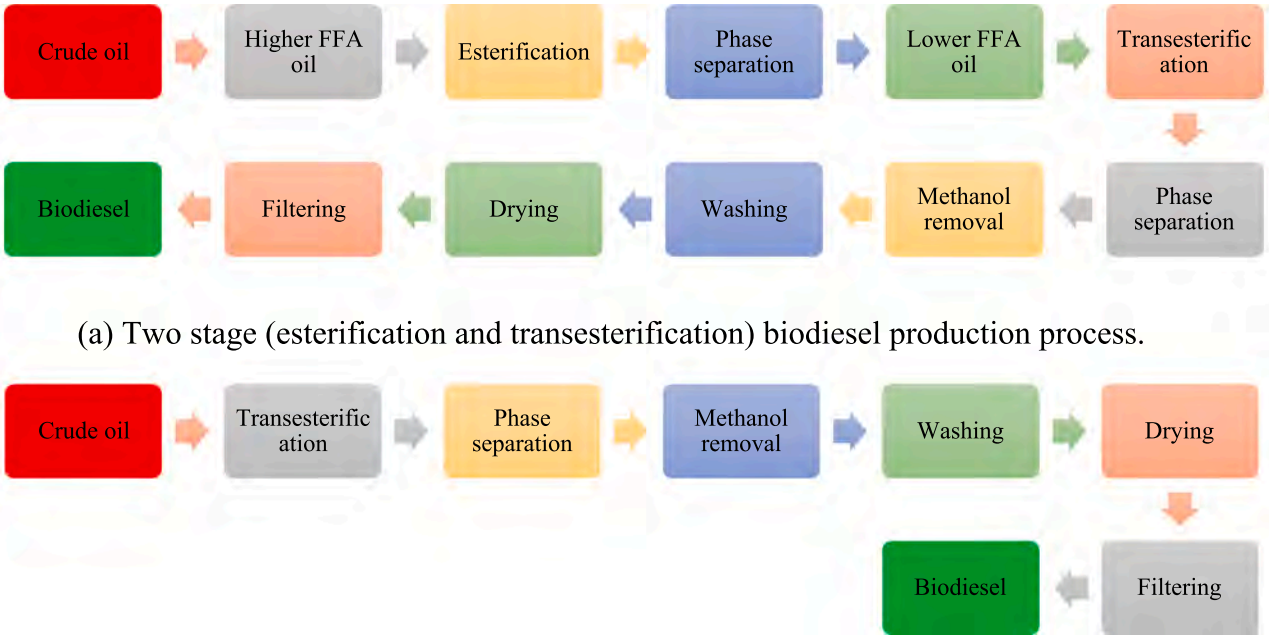

Fig. 1. Biodiesel production processes.

Table 2
Optimization of the biodiesel production process.

Biodiesel	Reaction type	Methanol: oil molar ratio	Catalyst type and concentration (wt%)	Reaction temperature (°C)	Reaction time (min)	Biodiesel yield (%)	Refs.
PSO	Single stage, (transesterification)	10:1	KOH (1 wt%)	45	60	96.48	[22]
SFO	Single stage (transesterification)	6:1	KOH (0.5 wt%)	55	60	95.8	[23]
JBD	Single stage (transesterification)	6:1	NaOH (1 wt%)	60	90	99.87	[34]
BLT	Two stages (pre-esterification and transesterification)	30:1 7.5:1	H_2SO_4 (10 wt%) NaOH (1 wt%)	75 55	120 90	93	[35]
RSB	Two stages (pre-esterification and transesterification)	– 6.5:1	NaCl (0.7 wt%) NaOH (1 wt%)	70–75 48.2	120 65.4	83.34	[36]
WCB	Single stage (transesterification)	7.5:1	KOH (1.4 wt%)	65	60	99.38	[33]

fuel atomization, fuel-air mixture formation, drop size, jet penetration, spray characteristics and combustion quality. Fuel KV quality can severely affect engine performance. A low KV of any fuel can increase engine wear and leakage due to lower lubrication. A high KV fuel will form larger droplets during injection, thus affecting the combustion quality which leads to higher exhaust emissions [26]. Furthermore, high KV may lead to soot formation and engine deposits due to poor fuel atomisation [5]. Therefore, the upper and lower limits of the biodiesel KV are defined in all standards presented in Table 4. BLT has the highest KV (5.68 mm^2/s), followed by JBD (5.2 mm^2/s), WCB (5.04 mm^2/s), RSB (4.6 mm^2/s), SFO (4.26 mm^2/s) and PSO (3.53 mm^2/s). Kinematic viscosities of all tested fuels are within the range of the international standards.

4.2.2. Density

Density is an important fuel property that affects engine performance characteristics significantly. Researchers [5,37,39] found that the density also influences the fuel atomisation efficiency and combustion characteristics. The energy content of the air-fuel mixture inside the combustion chamber is largely dependent upon fuel density. Improper density can lead to engine oil sludge problems. Generally, biodiesels have higher density than a conventional diesel fuel, which means that a volumetrically operated fuel pump will handle the greater mass of biodiesel than diesel at any given time. Some researchers [40,41] also noted that higher NO_x emissions were correlated with a higher density of biodiesel. The upper and lower limits of biodiesel density are presented in Table 4. The range of standard limits as per ASTM D6751-2 is 870–890 kg/m^3, whereas it is 860–900 kg/m^3 for EN 14214, and 860–890 kg/m^3 for the Australian standard. Most of the tested biodiesels were found to be within the above limits; however, both PSO (840 kg/m^3) and SFO (855 kg/m^3) were recorded close to the specified range.

4.2.3. Higher heating value

Higher heating value (HHV) is the measure of the energy content of the fuel per unit mass. A high value of HHV is desired for diesel engines to ensure better combustion, i.e., better power output. There are no specific limits of HHV in ASTM, EN or the Australian standard. However, HHV of all the studied biodiesels was found to be close to each other in this study. As per Table 4, SFO had the highest HHV of

Table 3
Fatty acid compositions of the studied biodiesels derived from non-edible oils [23,37,38].

Fatty acids	Structure	PSO	SFO	JBD	BLT	RSB	WCB
		wt%					
Lauric	12:0			0.1		0.1	
Myristic acid	14:0			0.1		0.3	0.2
Palmitic	16:0	6.07	5.85	14.6	14.9	20.3	8.0
Palmitoleic	16:1			0.6		0.2	0.2
Stearic	18:0	3.13	2.51	7.6	17.2	2.0	2.9
Oleic	18:1	47.73	63.8	44.6	38.2	43.5	66.3
Linoleic	18:2	37.25	25.3	31.9	27.6	31.0	17.5
Linolenic	18:3	1.78	0.51	0.3	0.3	0.6	0.5
Arachidic	20:0			0.3	0.9	0.8	0.3
Eicosenoic	20:1	0.76				0.5	0.4
Behenic	22:0	0.68	0.66			0.3	0.7
Erucic	22:1	1.51					0.1
Lignoceric	24:0					0.4	0.4
Others		1.09	1.29		0.9		2.3
Total saturated fatty acid (SFA)		9.88	9.02	22.6	33.4	24.2	12.5
Total monounsaturated fatty acid (MUFA)		48.49	63.84	45.2	38.7	44.2	67.2
Total polyunsaturated fatty acid (PUFA)		39.03	25.85	32.2	27.9	31.6	18.0
Long chain saturated factor (LCSF)		3.19	2.83	5.26	10.96	5.08	4.40

39.64 MJ/kg and JBD was found to have the lowest at 34.50 MJ/kg.

4.2.4. Oxidation stability

Oxidation stability (OS) is one of the major fuel properties that can influence the use of biodiesel commercially. Researchers [42] found that the biodiesels that have high polyunsaturated fatty acid content resulted in low OS. Another study [37] shows that biodiesels produced from vegetable oil were more vulnerable to oxidation at higher temperatures and air contact due to their double bond molecular structure. Biodiesels show less OS compared to conventional diesel due to their chemical composition. As per ASTM, EN and Australian standards, the minimum OS period should be 3 h, 6 h and 6 h respectively. It is very difficult to meet EN and Australian standards unless antioxidants are added to the biodiesel. All the biodiesels listed in Table 4 met the ASTM standard, but failed both the EN and Australian standards except SFO biodiesel (7.15 h). The other biodiesels of PSO, JBD, BLT, RSB and WCB recorded OS values of 5.61 h, 3.02 h, 4.45 h, 3.58 h, 2 h, and 0.47 h, respectively.

4.2.5. Acid value

Acid value (AV) indicates the amount of the carboxylic acid present in the fatty acid of any fuel. It also indicates the level of lubricant degradation of a fuel in service [17,43]. The fuel with a higher acid value can have a higher level of lubricant degradation and severe corrosion in the engine fuel system [26]. Acid value is expressed as the amount of KOH (mg) required to neutralise 1 gram of fatty acid methyl ester or biodiesel. AV is set to a maximum value of 0.5 mg KOH/g in the ASTM and EU standards, whereas the Australian standard sets it at 0.8 mg KOH/g. Table 4 shows that all the studied biodiesels met all the standards, except that WCB (0.59 mg KOH/g) was found to exceed the ASTM and EU standards, but was within the range of the Australian standard.

4.2.6. Flash point

Flash point (FP) is an important property of a fuel in terms of a safety measure for its storage. Fuel will ignite if exposed to a flame or a spark at or above a certain temperature. Biodiesel has a higher FP than the conventional diesel, thus making the biodiesel very safe for storage. FP varies inversely with the volatility of a fuel [40]. As per the ASTM, EU and Australian standards, the minimum FP temperature is 130 °C, 101 °C and 120 °C, respectively. Low FPs were found for both PSO and SFO (Table 4), although they are within the range of the EU standard. However, the highest FP value was recorded as 180 °C for WCB.

4.2.7. Cold filter plugging point

One of the most important fuel properties is its ability to flow in cold weather. Cold filter plugging point (CFPP) indicates the temperature at which a test filter is plugged due to the start of crystallisation or gel formation by fuel components. CFPP is an indicator of cold weather performance and operability of any fuel. In frosty weather, the fuel line, fuel pump and the injector could be jammed or clogged due to the lower operating temperature leading to thickening of fuel [17]. There are no specific CFPP limits in any international standards; however, the lower CFPP for biodiesel is considered better for diesel engine running in cold climates. In this study, PSO is found to have the lowest CFPP of −17 °C and SFO of −15 °C.

4.2.8. Cetane number

Cetane number (CN) is widely used as the dimensionless parameter for ignition delay time and combustion quality at a fixed condition. The higher the CN of a fuel, the better is its ignition qualities. Researchers [37,48] show that fuels with a high CN will have a quick engine start and smooth combustion. Ramos et al. [42] mentioned that a higher CN helps good cold start properties and minimises white smoke formation. A lower CN fuel can affect the combustion system, leading to the production of more hydrocarbon (HC) and particulate matter (PM), and higher combustion noise. The minimum CN as per the EU and Australian standards is 51, whereas it is 47 for the ASTM standard. CNs of biodiesels are dependent on the chemical compositions of their feedstocks used in biodiesel production. The longer the fatty acid carbon chain and saturated components, the higher the CN [49]. Table 4 shows that RSB has the highest CN, followed by BLT, WCB, JBD, SFO and PSO.

4.2.9. Iodine value

Iodine value (IV) is a parameter used for measuring the degree of unsaturation of vegetable oil. It indicates the mass of iodine (I_2) in grams that is necessary to completely saturate 100 grams of oil in a stoichiometric reaction. The biodiesels with higher concentrations of saturated fatty acids such as palmitic acid and stearic acid, lower will be the IV. The higher heating of unsaturated fatty acid can result in the

Table 4
Summary of the biodiesel properties of the studied feedstocks in comparison with the ASTM, EN and Australian standards [3,23,37,44–47].

Properties	PSO	SFO	JBD	BLT	RSB	WCB	ASTM D6751-2	EN 14214	Australian Standards
Kinematic viscosity at 40 °C (mm^2/s)	3.53	4.26	5.20	5.68	4.60	5.04	1.9–6	3.5–5	3.5–5
Density at 15 °C (kg/m^3)	840	855	865.7	868.7	882	879.7	870–890	860–900	860–890
Higher heating value (MJ/kg)	38.49	39.64	34.50	39.38	37.50	38.66			
Oxidation stability (h)	5.61	7.15	3.02	3.58	2.0	0.47	Min. 3	Min. 6	Min. 6
Acid value (mg KOH/g)	0.42	0.25	0.5	0.34	0.3	0.59	Max. 0.5	Max. 0.5	Max. 0.8
Flash point (°C)	112	105	175	141.5	145	180	Min. 130	Min. 101	Min. 120
CFPP (°C)	−17	−15	10.0	8.0	−4.0	−3.0			
Cetane number	48.29	50.45	51.0	54.0	55.0	53.0	Min. 47	Min. 51	Min. 51
Iodine value (g I/100 g)	115.89	104.7	99.0	86.0	109.0	93.42		Max. 120	Max. 120

formation of polymerisation of glycerides which imposes the limitation of unsaturated fatty acid. Researchers show that high IV can lead to the formation of deposits or to the deterioration of lubrication properties of the biodiesel [42]. Table 4 shows that the IV of the six biodiesels ranges from 86 g I/100 g (BLT) to 115.89 g I/100 g (PSO). There is no ASTM standard for IV; however, both the EU and Australian standards show the maximum level of IV at 120 g I/100 g. All the studied biodiesels have an IV within the range as per the EN and the Australian standards.

5. Multiple-criteria decision analysis (MCDA) method

In this study, six 2nd generation biodiesel feedstocks were considered for identifying the best feedstock. Twelve technical criteria covering physico-chemical properties of feedstocks and their fatty acid compositions have been used as a measurement of the ranking. To identify the best feedstocks, four different methods of multiple criteria decision analysis (MCDA) have been used. MCDAs are chosen from both value-based methods and outranking based methods. PROMETHEE is an example of the outranking method that uses an individual's preferences on criteria and alternatives. Value-based methods use a rating scale, such as higher and lower values to represent the highest desire or the lowest desire qualities. WSM, WPM and TOPSIS are examples of the value based method. Three weightage (%) methods, namely EQUAL, CRITIC and ENTROPY method were used for determining the weighting of the various criteria. In this study, a complete ranking of biodiesel feedstocks was performed using PROMETHEE, WSM, WPM and TOPSIS methods by varying the weightage criteria.

5.1. Weight determination

The weighting of criteria is the heart of any MCDA method. All criteria are not evenly significant; some are considered more important than others. For example, CFPP will be the least significant criterion in a MCDA method if the diesel engine test is considered for a tropical climatic zone. Weighting involves assigning numerical values to each criterion according to their relative importance [7]. It is important to assign weights reasonably so as to obtain meaningful results. In this study, three weightage methods were used, namely equal, critic and entropy methods.

An equal weightage method is the simplest form of assigning weights to each criterion, irrespective of its relative importance. This method can be used where all criteria are assumed equally important. The percentage is commonly used as weights out of a total of 100. The total weight is divided by the number of criteria to obtain equal weightage. Eq. (2) shows the formula used in this study for finding the equal weightage percentage.

$$Equal\ \ weightage(\%),\quad W_j = \frac{Total\ \ weight}{Total\ \ criteria} = \frac{100}{12} = 8.333\% \tag{2}$$

The CRITIC (Criteria Importance through Intercriteria Correlation) method belongs to the class of correlation methods [50]. Usually, the critic method generates uniformed weight values that are close to the equal weightage methods. The following steps are used in this study to determine the weights for the criteria using the critic method:

- Step 1 is to normalize the decision matrix using Eq. (3):

$$\bar{X}_{ij} = \frac{X_{ij} - X_j^{worst}}{X_j^{best} - X_j^{worst}} \tag{3}$$

- Step 2 is to calculate the standard σ_j deviation for each criterion.
- Step 3 is to determine the symmetric matrix of n × n with element r_{ij}, which is the linear correlation coefficient between the vectors X_i and X_j.
- Step 4 is to calculate the measure of the conflict created by criterion j with respect to the decision situation defined by the rest of the criteria in Eq. (4):

$$\sum_{i=1}^{m} (1 - r_{ij}) \tag{4}$$

- Step 5 is to determine the quantity of the information in relation to each criterion using Eq. (5):

$$C_j = \sigma_j \times \sum_{i=1}^{m} (1 - r_{ij}) \tag{5}$$

- Step 6 is to determine the objective weights using Eq. (6):

$$W_j = \frac{C_j}{\sum_{i=1}^{m} C_j} \tag{6}$$

The Entropy method is based on the measurement of uncertain information contained in the decision matrix. Srđević et al. [51] reported that the entropy method generates a set of weights for a given criteria based on mutual contrast of individual criteria values of alternatives for each criterion and then for all the criteria at the same time. The entropy method for determination of objective criteria weights can be carried out in three steps:

- Step 1 is to normalize the decision matrix using Eq. (7):

$$r_{ij} = \frac{X_{ij}}{\sum_{i=1}^{m} X_{ij}} \tag{7}$$

- Step 2 is to compute entropy using Eq. (8):

$$e_j = -h \sum_{i=1}^{m} r_{ij} \ln r_{ij} \tag{8}$$

where $j = 1, 2, 3, \ldots, n$; $h = \frac{1}{\ln(m)} = \frac{1}{\ln(6)} = 0.55811$; m is the number of alternatives;

- Step 3 is to compute the weight vector using Eq. (9):

$$W_j = \frac{1 - e_j}{\sum_{j=1}^{n} (1 - e_j)}, j = 1, 2, \cdots, n \tag{9}$$

The entropy method generates weighted criteria values directly from the criteria value variations and eliminates the problem of subjectivity, incompetence or absence of decision makers.

5.2. Preference ranking organization method for enrichment evaluation (PROMETHEE)

PROMETHEE is an MCDA method that has six different extensions, PROMETHEE I to VI. Those extensions are based on the raking requirement where PROMETHEE I is used for partial ranking, II uses complete ranking and so on. PROMETHEE II complete ranking (Phi) is the measure of net preference flow that showed the balance between the positive and negative outranked by others. PROMETHEE I partial ranking consists of positive preference flows that measures the extent to which an alternative outranks all others, whereas negative preference flows measure the extent to which an alternative is outranked by others [52]. In this study, both PROMETHEE I and II will be used along with Graphical Analysis for Interactive Assistance (GAIA). PROMETHEE-GAIA has significant advantages over other MCDA methods as its decision vector stretches towards the best alternatives [52]. GAIA was used to further analyse and visualize the outcomes of the analysis. This study applied the PROMETHEE GAIA algorithm to rank the best possible biodiesel feedstocks suitable for biodiesel production. Fig. 2 shows the working process of PROMETHEE [53].

PROMETHEE works in five steps, as follows:

I. The preference function converts the deviations between the evaluations of two alternatives for each criterion into a preference

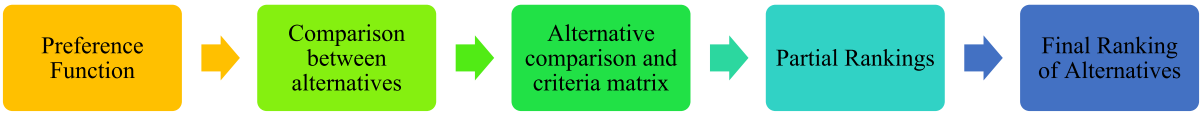

Fig. 2. PROMETHEE method flow chart.

Fig. 3. TOPSIS method flow chart.

degree ranging from 0 to 1.

II. The proposed set of alternatives are compared within the preference function.
III. The alternative comparison results and criteria of each alternative are presented in a matrix.
IV. PROMETHEE I is used in the fourth step to provide the partial ranking.
V. The PROMETHEE II process completes the final ranking of the alternatives.

5.3. Weighted sum method

The weighted sum method (WSM) is the simplest and widely used available method that applies to single-dimensional problems. It is often called the "Simple Additive Weighting" or "Weighted Scoring" method [53,54]. WSM is easily applicable when the criteria range is the same; however, when both qualitative and quantitative attributes are employed, it becomes hard to manage WSM. A normalization scheme is used to make all criteria on the same scale. In the WSM method, all criteria are weighted according to their priority or importance. The alternatives are selected based on the summation of specific criterion and weighted product values. The higher weighted product sum in the list is chosen as the best alternative that closely matches the criteria. The WSM is described by:

$$A_i^{WSM} = \sum_{i=1}^{n} W_j X_{ij} \tag{10}$$

where $i = 1, 2, 3....n$; A_i is the preferential score or best score of alternative at i; X_{ij} is the performance value, i.e., score, of alternative i using criteria j; W_j is the weight of each criterion. All criteria (different units) need to be normalized and compared within the same scale. The linear normalizing Eqs. (11) and (12) are as follows [55]:

Beneficial/positive/maximizing criteria are given by:

$$\bar{X}_{ij} = \frac{X_{ij}}{X_{ij}^{Max}} \tag{11}$$

Non-beneficial/cost/negative/minimum criteria are given by:

$$\bar{X}_{ij} = \frac{X_{ij}^{Min}}{X_{ij}} \tag{12}$$

where X_{ij}^{Max} is the maximum value of criteria j with alternative i; X_{ij}^{Min} is the minimum value of criteria j with alternative i.

5.4. Weighted product method

The weighted product method (WPM) is an alternative to WSM. The basic difference between WSM and WPM is that a product instead of the sum is used in WPM. In this method, the weights become exponents associated with each criterion value and a product of those of each rows are compared with the others. The higher the preferential score, the better is the alternative that meets all criteria. These criteria do not need to be transformed into dimensionless values by normalisation as they are suitable for both single and multi-dimensional cases. The equation for the WPM is:

$$A_i^{WPM} = \prod_{i=1}^{n} X_{ij}^{W_i} \tag{13}$$

where A_i is the preferential score or best score of the alternative at i; X_{ij} is the performance value, i.e., score, of alternative i using criteria j; W_i is the weight of each criterion.

5.5. Technique for order preference by similarity to ideal solution (TOPSIS)

Hwang et al. [56] originally developed the TOPSIS method and it selects the best alternatives at the closest possible distance from the positive (best) ideal solution and the farthest from the negative (worst) ideal solution at the same time. The process of the TOPSIS method is presented in Fig. 3.

At the first step, all criteria (j) and alternatives (i) in normalised decision matrix is developed. The normalised value is X_{ij} and is shown by:

$$\bar{X}_{ij} = \frac{X_{ij}}{\sqrt{\sum_{i=1}^{n} X_{ij}^2}} \tag{14}$$

The normalized weighted values v_{ij} are calculated in the second step, as shown by:

$$v_{ij} = W_i \times X_{ij} \tag{15}$$

where X_{ij} is the performance value, i.e., score, of alternative i using criteria j; W_i is the weight of each criterion and v_{ij} is the weighted normalized ratings.

The Euclidean distance from the ideal best and worst solutions are measured in Eqs. (16) and (17), respectively.

$$S_i^{+} = \left[\sum_{i=1}^{n} (v_{ij} - v_j^{+})^2\right]^{0.5} \tag{16}$$

$$S_i^{-} = \left[\sum_{i=1}^{n} (v_{ij} - v_j^{-})^2\right]^{0.5} \tag{17}$$

where S_i^{+} and S_i^{-} are the positive and negative ideal solutions.

The performance score or similarity index (P_i) is calculated from Eq. (18). This indicates the relative closeness to the ideal solution for all the alternatives with the highest P_i value being selected as the best.

$$P_i = \frac{S_i^{-}}{S_i^{+} + S_i^{-}} \tag{18}$$

6. Process and assumptions of MCDA method

Multiple-criteria decision analysis (MCDA) methods can be implemented in the selection of biodiesel feedstocks. The working

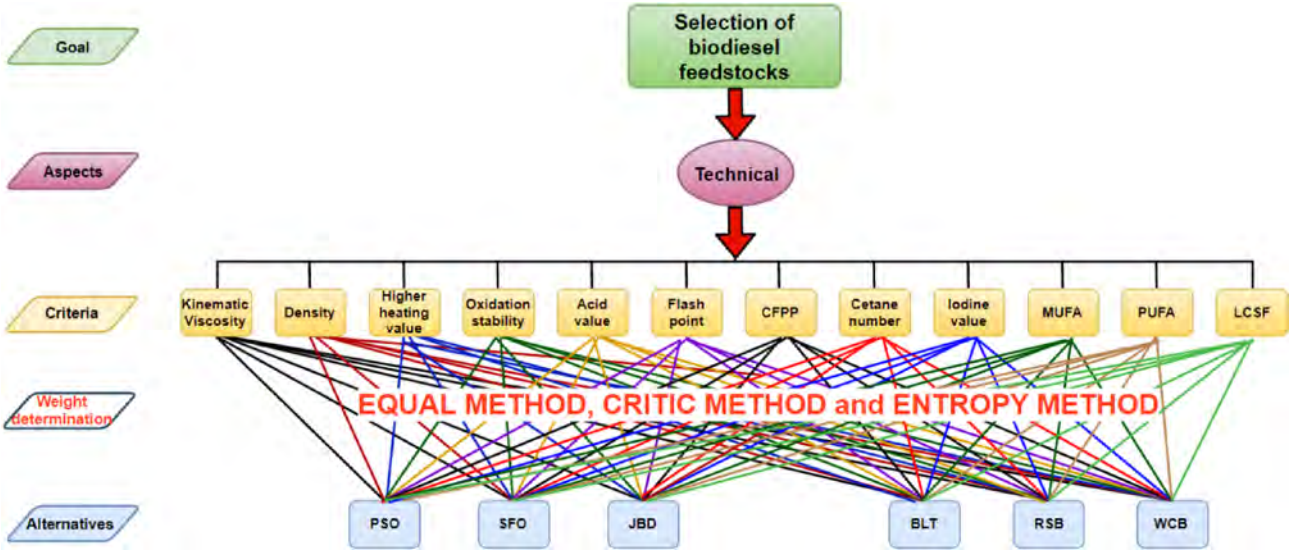

Fig. 4. MCDA process hierarchy for biodiesel feedstock selection.

principle of a MCDA method is shown in Fig. 4. Six biodiesel feedstocks are evaluated using twelve technical criteria with three different weightage determination methods for each criterion to identify the best feedstocks for commercial application.

The following assumptions are used in this study:

- All biodiesel feedstocks are characterised; conversion of biodiesel and testing are performed under international standards
- All biodiesel feedstocks are tested under similar climatic conditions.
- All criteria are given the same importance, i.e., weightage, in the equal method irrespective of their relative information contents.

The criteria, alternatives, preferences, and the weightages are presented in Table 5.

7. Biodiesel feedstock selection process (MCDA)

7.1. PROMETHEE GAIA method

Fig. 5(a) shows three different weightage methods of the PROMETHEE I partial ranking of six biodiesel feedstocks (alternatives) which were calculated using positive and negative preference flow values. The presence of the crossed tie lines shows the indicator of non-comparative attributes of alternatives. The ranking order of biodiesel feedstocks is PSO-SFO-RSB-BLT-WCB-JBD in the positive preference flow for the Equal weight method. The negative preference flow is different as expected, being PSO-SFO-RSB-WCB-BLT-JBD. For the critic weight method, the ranking order of biodiesels in the positive preference flow is PSO-SFO-RSB-BLT-WCB-JBD and, for the negative flow, is PSO-SFO-RSB-WCB-BLT-JBD. Both equal and critic weightage methods generate the same partial ranking. However, the entropy weight method produces a twist in the ranking. The positive preference flow for the entropy method is PSO-SFO-BLT-JBD-RSB-WCB, and, for the negative preference flow, is PSO-SFO-JBD-BLT-RSB-WCB. Although both PSO and SFO rankings are the same for all weightage methods, it is not sufficient just to rank the best alternatives; PROMETHEE II can provide a complete ranking. Fig. 5(b) shows the complete ranking of the studied biodiesel feedstocks. The net preference flow is considered to get the best performance. The ranking order of biodiesel feedstocks is PSO-SFO-RSB-WCB-BLT-JBD for both equal and critic methods. However, the entropy method generates the complete ranking somewhat differently than the others, and this is PSO-SFO-BLT-JBD-RSB-BLT. It can be seen that only two feedstocks (PSO and SFO) obtained positive Phi scores irrespective of any of the weightage methods.

Table 6 shows the overall ranking of the feedstocks using all weighting methods. The Phi score is the net flow score that could be negative or positive depending on the angular distance from the decision vector and the distance from the centre [57]. JBD is found the worst biodiesel feedstock in both the equal and critic methods. However, WCB is ranked the last in the entropy method. Both PSO and SFO are ranked as first and second irrespective of any of the weightage methods.

The performance evaluation of the six biodiesel feedstocks can be analysed in a GAIA plane plot as shown in Fig. 6. Feedstocks are lying far away from each other which represents their different fuel properties. It has a quality significance level of 76.9% (> 70% significance level). The PI decision axis is aligned in the direction of PSO feedstocks. This agrees with the results from both the PROMETHEE I and II

Table 5
Criteria, alternatives and weightage (%).

Criteria (*j*) Preferences		KV (1) min	D (2) min	HHV (3) max	OS (4) max	AV (5) min	FP (6) max	CFPP (7) min	CN (8) max	IV (9) max	MUFA (10) min	PUFA (11) min	LCSF (12) max
Weightage (%)	Equal method (1)	8.333	8.333	8.333	8.333	8.333	8.333	8.333	8.333	8.333	8.333	8.333	8.333
	Critic method (2)	7.132	7.456	8.040	9.711	6.944	9.370	8.713	7.331	9.592	9.930	8.582	7.198
	Entropy method (3)	2.126	0.027	0.200	39.213	8.144	3.779	12.527	0.185	0.913	3.930	4.881	24.074
Alternatives (*i*)	PSO (1)	3.53	840	38.49	5.61	0.42	112	−17	48.29	115.89	48.49	39.03	3.19
	SFO (2)	4.26	855	39.64	7.15	0.25	105	−15	50.45	104.7	63.84	25.85	2.83
	JBD (3)	5.2	865.7	34.5	3.02	0.5	175	10	51	99	45.2	32.2	5.26
	BLT (4)	5.68	868.7	39.38	3.58	0.34	141.5	8	54	86	38.7	27.9	11.64
	RSB (5)	4.6	882	37.5	2	0.3	145	−4	55	109	44.2	31.6	5.08
	WCB (6)	5.04	879.7	38.66	0.47	0.59	180	−3	53	93.42	67.2	18	4.4

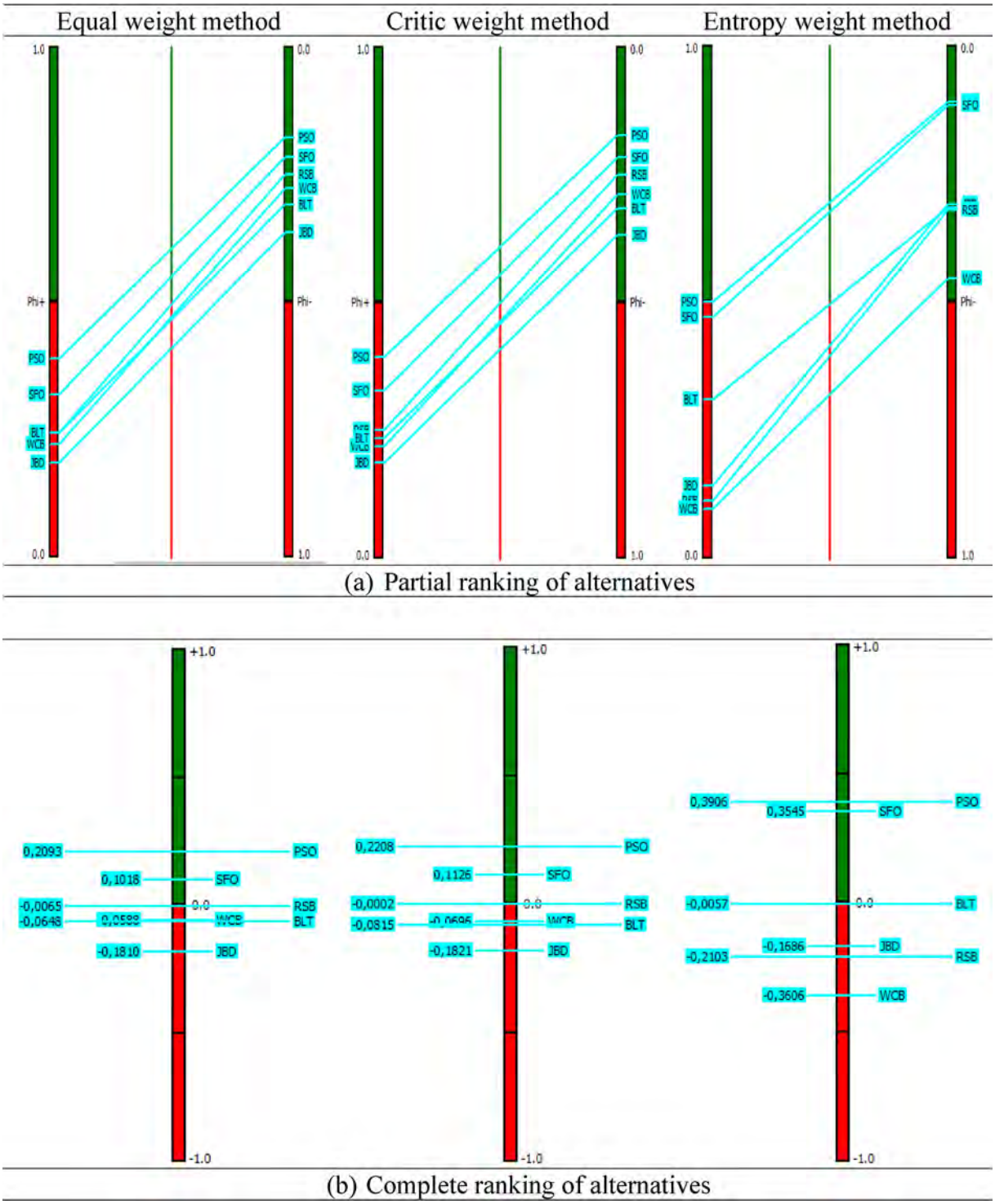

Fig. 5. (a) PROMETHEE I partial ranking of alternatives, and (b) PROMETHEE II complete ranking of alternatives.

rankings. The criteria vectors that lie in the same direction as the decision vector (the red line) represents an influence that these criteria have on the decision. Fuel properties such as KV, IV and CFPP have a positive influence on the decision for both equal and critic methods. Instead, HHV, OS and density have a positive preference for the decision for the entropy method. The higher weightage of OS in the entropy method affects the decision vector marginally towards the SFO biodiesel feedstock. However, the overall Phi ranking in Table 6 confirms the close relationship between PSO and SFO in all the methods. In the GAIA plane, the criteria that lie close to (± 45°) are positively related while others that lie in a reverse bearing (135–225°) are negatively related, and those that lie in the orthogonal direction have no or minimal influence [26]. The direction and length of the criteria are indicative of their influence on the decision vector. Criteria such as KV, HHV, FP, PUFA and LCSF have short lengths of their criteria vectors, which indicates a little effect on the decision vector.

GAIA Web was used to further analyse the impact of individual criteria on the preference of biodiesel feedstocks (Fig. 7). It was found that biodiesels with similar preferences are located close to each other in both GAIA Web and GAIA plane. The radial distance of key criteria in

Table 6
Corresponding ranking and Phi value of biodiesels.

Biodiesel	Phi Value			Rank		
	Equal weight method	Critic weight method	Entropy weight method	Equal weight method	Critic weight method	Entropy weight method
PSO	0.2093	0.2208	0.3906	1	1	1
SFO	0.1018	0.1126	0.3545	2	2	2
JBD	−0.1810	−0.1821	−0.1686	6	6	4
BLT	−0.0648	−0.0815	−0.0057	5	5	3
RSB	−0.0065	−0.0002	−0.2103	3	3	5
WCB	−0.0588	−0.0696	−0.3606	4	4	6

GAIA Web indicates unicriterion net flows with −1 value at the centre of the web and +1 on the outer circle [6] of the web. Both Fig. 7(a) and (b) show the differences of criteria, however they both showed very good preferences.

7.2. WSM

It can be seen from Table 5 that the beneficial criteria are HHV, OS, FP, CN, IV, and LCSF; the non-beneficial criteria are KV, Density, AV, CFPP, MUFA, and PUFA. At first, the beneficial criteria and non-beneficial criteria values are calculated from Eqs. (11) and (12). The rankings are calculated based on those derived values and the weightage of individual criteria by applying Eq. (10). Table 7 shows the weighted sum design matrix using the three weighting methods along with rankings of the alternatives. Both equal and critic methods generate the

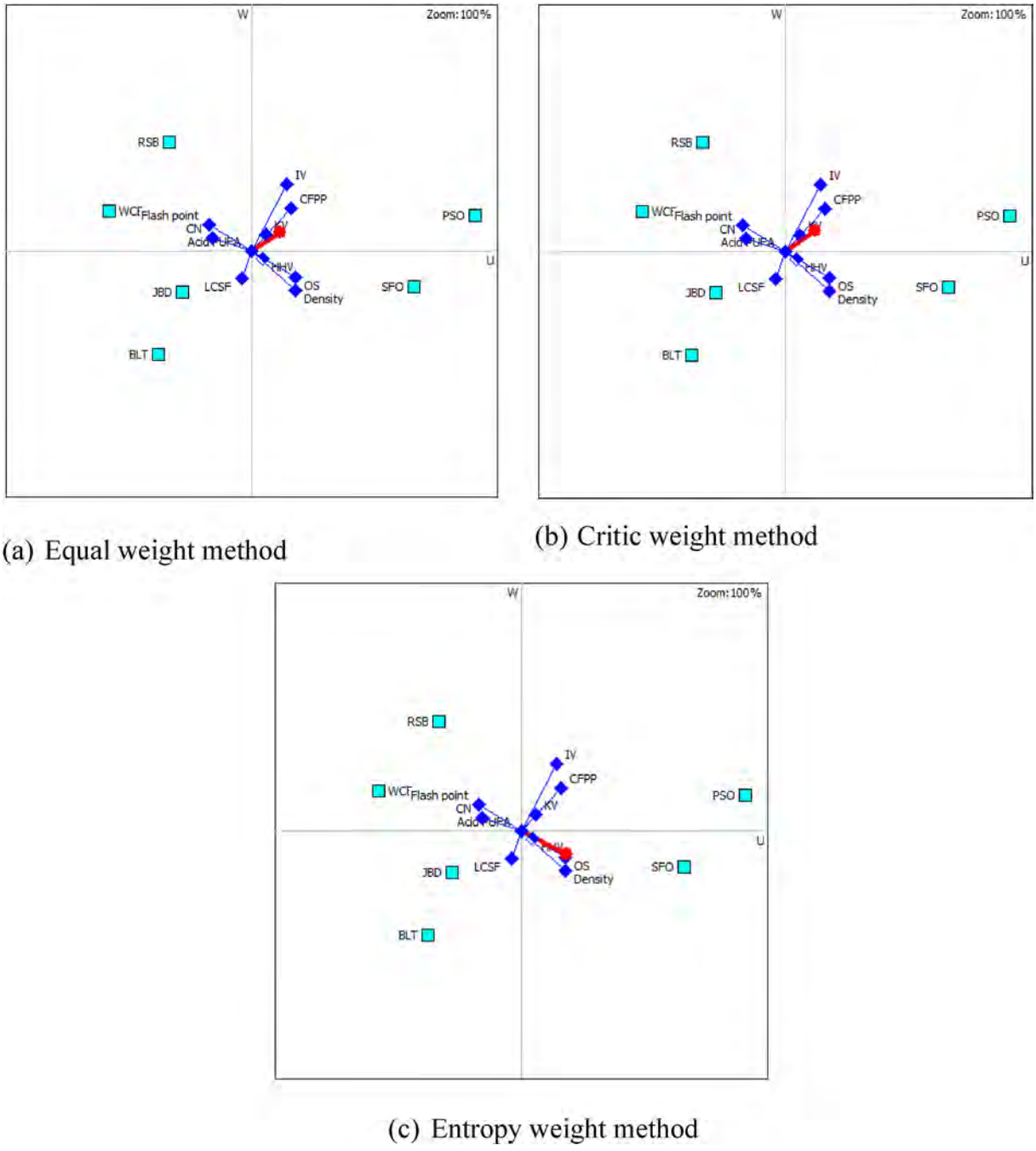

Fig. 6. GAIA plane at 100% zoom for six biodiesels showing twelve criteria and the decision vector (76.9%).

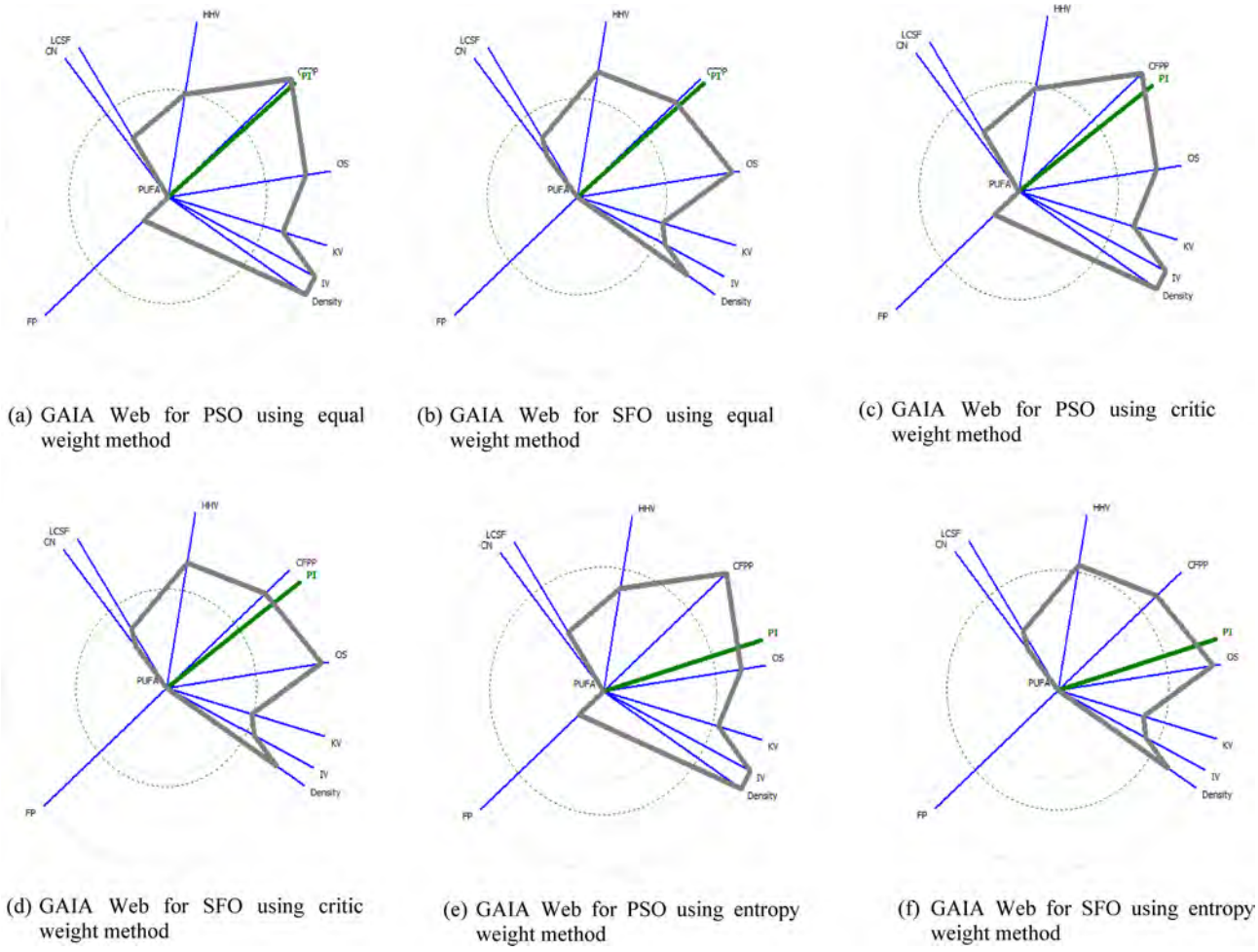

(a) GAIA Web for PSO using equal weight method

(b) GAIA Web for SFO using equal weight method

(c) GAIA Web for PSO using critic weight method

(d) GAIA Web for SFO using critic weight method

(e) GAIA Web for PSO using entropy weight method

(f) GAIA Web for SFO using entropy weight method

Fig. 7. GAIA Webs for the top two biodiesels of PSO and SFO.

Table 7
Weighted sum normalized decision matrix (WSM).

(a) Equal weightage method:															
Alternative	Criteria	KV	Density	HHV	OS	AV	FP	CFPP	CN	IV	MUFA	PUFA	LCSF	Preference Score	Rank
(6 biodiesels)	Weightage (%)	8.333	8.333	8.333	8.333	8.333	8.333	8.333	8.333	8.333	8.333	8.333	8.333		
	PSO	0.0833	0.0833	0.0809	0.0654	0.0496	0.0518	0.0833	0.0731	0.0833	0.0665	0.0384	0.0228	0.7817	2
	SFO	0.0690	0.0818	0.0833	0.0833	0.0833	0.0486	0.0735	0.0764	0.0753	0.0505	0.0580	0.0203	0.8033	1
	JBD	0.0565	0.0808	0.0725	0.0352	0.0417	0.0810	−0.0490	0.0772	0.0712	0.0713	0.0466	0.0376	0.6226	6
	BLT	0.0518	0.0805	0.0828	0.0417	0.0613	0.0655	−0.0392	0.0818	0.0618	0.0833	0.0537	0.0833	0.7083	4
	RSB	0.0639	0.0793	0.0788	0.0233	0.0694	0.0671	0.0196	0.0833	0.0783	0.0729	0.0474	0.0364	0.7199	3
	WCB	0.0583	0.0795	0.0812	0.0055	0.0353	0.0833	0.0147	0.0803	0.0671	0.0480	0.0833	0.0315	0.6681	5
(b) Critic weightage method:															
Alternative	Criteria	KV	Density	HHV	OS	AV	FP	CFPP	CN	IV	MUFA	PUFA	LCSF	Preference Score	Rank
(6 biodiesels)	Weightage (%)	6.788	7.316	8.687	9.810	7.996	8.635	8.057	7.614	9.604	9.958	8.389	7.147		
	PSO	0.0679	0.0732	0.0843	0.0770	0.0476	0.0537	0.0806	0.0669	0.0960	0.0795	0.0387	0.0196	0.7849	2
	SFO	0.0562	0.0719	0.0869	0.0981	0.0800	0.0504	0.0711	0.0698	0.0868	0.0604	0.0584	0.0174	0.8073	1
	JBD	0.0461	0.0710	0.0756	0.0414	0.0400	0.0839	−0.0474	0.0706	0.0820	0.0853	0.0469	0.0323	0.6277	6
	BLT	0.0422	0.0707	0.0863	0.0491	0.0588	0.0679	−0.0379	0.0748	0.0713	0.0996	0.0541	0.0715	0.7083	4
	RSB	0.0521	0.0697	0.0822	0.0274	0.0666	0.0696	0.0190	0.0761	0.0903	0.0872	0.0478	0.0312	0.7192	3
	WCB	0.0475	0.0699	0.0847	0.0064	0.0339	0.0863	0.0142	0.0734	0.0774	0.0573	0.0839	0.0270	0.6621	5
(c) Entropy weightage method:															
Alternative	Criteria	KV	Density	HHV	OS	AV	FP	CFPP	CN	IV	MUFA	PUFA	LCSF	Preference Score	Rank
(6 biodiesels)	Weightage (%)	2.126	0.027	0.200	39.213	8.144	3.779	12.527	0.185	0.913	3.930	4.881	24.074		
	PSO	0.0213	0.0003	0.0019	0.3077	0.0485	0.0235	0.1253	0.0016	0.0091	0.0314	0.0225	0.0660	0.6590	2
	SFO	0.0176	0.0003	0.0020	0.3921	0.0814	0.0220	0.1105	0.0017	0.0082	0.0238	0.0340	0.0585	0.7523	1
	JBD	0.0144	0.0003	0.0017	0.1656	0.0407	0.0367	−0.0737	0.0017	0.0078	0.0337	0.0273	0.1088	0.3651	5
	BLT	0.0132	0.0003	0.0020	0.1963	0.0599	0.0297	−0.0589	0.0018	0.0068	0.0393	0.0315	0.2407	0.5626	3
	RSB	0.0163	0.0003	0.0019	0.1097	0.0679	0.0304	0.0295	0.0018	0.0086	0.0344	0.0278	0.1051	0.4337	4
	WCB	0.0149	0.0003	0.0019	0.0258	0.0345	0.0378	0.0221	0.0018	0.0074	0.0226	0.0488	0.0910	0.3089	6

Table 8
Weighted product normalized decision matrix (WPM).

(a) Equal weightage method:														
Alternative	Criteria	KV	Density	HHV	OS	AV	FP	CFPP	CN	IV	MUFA	PUFA	LCSF	Preference Score	Rank
(6 biodiesels)	Weightage (%)	8.333	8.333	8.333	8.333	8.333	8.333	8.333	8.333	8.333	8.333	8.333	8.333		
	PSO	1.0000	1.0000	0.9976	0.9800	0.9577	0.9612	1.0000	0.9892	1.0000	0.9814	0.9376	0.8978	0.7354	3
	SFO	0.9845	0.9985	1.0000	1.0000	1.0000	0.9561	0.9896	0.9928	0.9916	0.9592	0.9703	0.8889	0.7575	2
	JBD	0.9682	0.9975	0.9885	0.9307	0.9439	0.9977	0.9568	0.9937	0.9870	0.9872	0.9527	0.9360	0.6912	4
	BLT	0.9612	0.9972	0.9995	0.9440	0.9747	0.9802	0.9391	0.9985	0.9755	1.0000	0.9642	1.0000	0.7619	1
	RSB	0.9782	0.9959	0.9954	0.8993	0.9849	0.9821	0.8865	1.0000	0.9949	0.9890	0.9542	0.9333	0.6553	5
	WCB	0.9708	0.9962	0.9979	0.7971	0.9310	1.0000	0.8655	0.9969	0.9822	0.9551	1.0000	0.9222	0.5345	6
(b) Critic weightage method:														
Alternative	Criteria	KV	Density	HHV	OS	AV	FP	CFPP	CN	IV	MUFA	PUFA	LCSF	Preference Score	Rank
(6 biodiesels)	Weightage (%)	6.788	7.316	8.687	9.810	7.996	8.635	8.057	7.614	9.604	9.958	8.389	7.147		
	PSO	1.0000	1.0000	0.9974	0.9765	0.9594	0.9599	1.0000	0.9901	1.0000	0.9778	0.9371	0.9116	0.7419	3
	SFO	0.9873	0.9987	1.0000	1.0000	1.0000	0.9545	0.9900	0.9934	0.9903	0.9514	0.9701	0.9039	0.7647	1
	JBD	0.9740	0.9978	0.9880	0.9189	0.9461	0.9976	0.9581	0.9943	0.9850	0.9847	0.9524	0.9448	0.6924	4
	BLT	0.9682	0.9975	0.9994	0.9344	0.9757	0.9794	0.9411	0.9986	0.9718	1.0000	0.9639	1.0000	0.7588	2
	RSB	0.9822	0.9964	0.9952	0.8825	0.9855	0.9815	0.8900	1.0000	0.9941	0.9869	0.9539	0.9425	0.6526	5
	WCB	0.9761	0.9966	0.9978	0.7656	0.9336	1.0000	0.8696	0.9972	0.9795	0.9465	1.0000	0.9328	0.5204	6
(c) Entropy weightage method:														
Alternative	Criteria	KV	Density	HHV	OS	AV	FP	CFPP	CN	IV	MUFA	PUFA	LCSF	Preference Score	Rank
(6 biodiesels)	Weightage (%)	2.126	0.027	0.200	39.213	8.144	3.779	12.527	0.185	0.913	3.930	4.881	24.074		
	PSO	1.0000	1.0000	0.9999	0.9093	0.9586	0.9822	1.0000	0.9998	1.0000	0.9912	0.9629	0.7323	0.5982	3
	SFO	0.9960	1.0000	1.0000	1.0000	1.0000	0.9798	0.9844	0.9998	0.9991	0.9805	0.9825	0.7114	0.6577	1
	JBD	0.9918	1.0000	0.9997	0.7132	0.9451	0.9989	0.9357	0.9999	0.9986	0.9939	0.9720	0.8259	0.4977	4
	BLT	0.9899	1.0000	1.0000	0.7624	0.9753	0.9909	0.9099	1.0000	0.9973	1.0000	0.9788	1.0000	0.6478	2
	RSB	0.9944	1.0000	0.9999	0.6068	0.9853	0.9919	0.8342	1.0000	0.9994	0.9948	0.9729	0.8191	0.3897	5
	WCB	0.9925	1.0000	0.9999	0.3439	0.9325	1.0000	0.8047	0.9999	0.9980	0.9785	1.0000	0.7912	0.1979	6

same biodiesel feedstock ranking of SFO-PSO-RSB-BLT-WCB-JBD. However, the entropy method generates a slightly different order in the lower rankings, giving SFO-PSO-BLT-RSB-JBD-WCB. Both JBD and WCB were found to be the least preferred choice of biodiesel feedstocks using this design matrix.

7.3. WPM

The rankings of the alternatives are calculated by applying Eq. (13) to the data in Table 5. The weighted product design matrix with rankings of the alternatives are presented in Table 8. Interestingly, both critic and entropy methods generate the same ranking of SFO-BLT-PSO-JBD-RSB-WCB. However, using the equal weighting method, the rank of biodiesel feedstocks is slightly changed to BLT-SFO-PSO-JBD-RSB-WCB. In all cases, both RSB and WCB were found to be the least preferred choice biodiesel feedstocks.

7.4. TOPSIS

From Table 5, the normalised criteria values ($\bar{X}_{ij}$)can be obtained by applying Eq. (14). The normalised criteria is shown in Table 9. The $\bar{X}_{ij}$ values are then multiplied with the weightage of each criterion (Eq. (15)) to get the weighted normalised design matrix (Table 10). Ideal best (S_i^+) and worst (S_i^-) solutions can be obtained from Eqs. (16) and (17). Finally, the performance score (Pi) is calculated using Eq. (18). Both equal and critic methods generate the exact same biodiesel feedstock ranking of SFO-PSO-RSB-BLT-WCB-JBD. However, the entropy method generates a slightly different order of SFO-PSO-BLT-JBD-RSB-WCB. Table 10 shows the weighted normalized criteria along with the rankings.

8. Discussion

As discussed in the fuel properties Section 4.2 that higher KV may lead to soot formation, higher density may produce higher NO_x emissions, higher acid value can have a higher level of lubricant degradation and severe corrosion in the engine fuel system, and a lower cetane number of fuel can affect the combustion system, leading to the production of more hydrocarbon (HC) and particulate matter (PM), and higher combustion noise. Out of several factors, those are prominent for the screening process. The preferences (min and max) of criteria (fuel properties) presented in Table 5 influence the results.

The results from the four multiple-criteria decision methods using three different weightage methods for the selection of the best biodiesel feedstocks are summarised in Table 11. Eight out of twelve results agree that SFO is the best feedstock, while PSO is found to be the second best. However, the results are not uniform for all feedstocks, as most of the MCDM methods have produced slightly diverse results. An averaging of the results from the different methods has been performed. It can be seen that the SFO is placed first in the average score ranking, while WCB is placed last in the list. In the mode ranking, SFO and PSO were found to be the first and second best feedstocks in the list, whereas both

Table 9
TOPSIS: Normalized criteria ($\bar{X}_{ij}$).

	Criteria $\sqrt{\sum_{i=1}^{n} X_{ij}^2}$	KV 11.6821	Density 2119.5512	HHV 93.2453	OS 10.4284	AV 1.0211	FP 357.2692	CFPP 26.5141	CN 127.3897	IV 249.3950	MUFA 128.2070	PUFA 73.0026	LCSF 15.0502
$\bar{X}_{ij}$	PSO	0.3022	0.3963	0.4128	0.5380	0.4113	0.3135	−0.6412	0.3791	0.4647	0.3782	0.5346	0.2120
	SFO	0.3647	0.4034	0.4251	0.6856	0.2448	0.2939	−0.5657	0.3960	0.4198	0.4979	0.3541	0.1880
	JBD	0.4451	0.4084	0.3700	0.2896	0.4897	0.4898	0.3772	0.4003	0.3970	0.3526	0.4411	0.3495
	BLT	0.4862	0.4099	0.4223	0.3433	0.3330	0.3961	0.3017	0.4239	0.3448	0.3019	0.3822	0.7734
	RSB	0.3938	0.4161	0.4022	0.1918	0.2938	0.4059	−0.1509	0.4317	0.4371	0.3448	0.4329	0.3375
	WCB	0.4314	0.4150	0.4146	0.0451	0.5778	0.5038	−0.1131	0.4160	0.3746	0.5242	0.2466	0.2924

Table 10
TOPSIS: Weighted normalized criteria (v_{ij}) and alternatives ranking.

(a) Equal weightage method:																	
Alternative	Criteria	KV	Density	HHV	OS	AV	FP	CFPP	CN	IV	MUFA	PUFA	LCSF	S_i^+	S_i^-	$S_i^+ + S_i^-$	P_i	Rank
(6 biodiesels)	Weightage (%)	8.333	8.333	8.333	8.333	8.333	8.333	8.333	8.333	8.333	8.333	8.333	8.333					
	PSO	0.0252	0.0330	0.0344	0.0448	0.0343	0.0261	−0.0534	0.0316	0.0387	0.0315	0.0445	0.0177	0.0585	0.0982	0.1567	0.6268	2
	SFO	0.0304	0.0336	0.0354	0.0571	0.0204	0.0245	−0.0471	0.0330	0.0350	0.0415	0.0295	0.0157	0.0559	0.1000	0.1559	0.6417	1
	JBD	0.0371	0.0340	0.0308	0.0241	0.0408	0.0408	0.0314	0.0333	0.0331	0.0294	0.0367	0.0291	0.1021	0.0339	0.1361	0.2494	6
	BLT	0.0405	0.0341	0.0352	0.0286	0.0277	0.0330	0.0251	0.0353	0.0287	0.0251	0.0318	0.0644	0.0871	0.0626	0.1496	0.4181	4
	RSB	0.0328	0.0347	0.0335	0.0160	0.0245	0.0338	−0.0126	0.0360	0.0364	0.0287	0.0361	0.0281	0.0713	0.0570	0.1283	0.4440	3
	WCB	0.0359	0.0346	0.0345	0.0038	0.0481	0.0420	−0.0094	0.0347	0.0312	0.0437	0.0205	0.0244	0.0876	0.0485	0.1362	0.3565	5
Ideal best (Vj+)		0.0252	0.0330	0.0354	0.0571	0.0204	0.0420	−0.0534	0.0360	0.0387	0.0251	0.0205	0.0644					
Ideal worst (Vj−)		0.0405	0.0347	0.0308	0.0038	0.0481	0.0245	0.0314	0.0330	0.0287	0.0437	0.0367	0.0157					
(b) Critic weightage method:																	
Alternative	Criteria	KV	Density	HHV	OS	AV	FP	CFPP	CN	IV	MUFA	PUFA	LCSF	S_i^+	S_i^-	$S_i^+ + S_i^-$	P_i	Rank
(6 biodiesels)	Weightage (%)	6.788	7.316	8.687	9.810	7.996	8.635	8.057	7.614	9.604	9.958	8.389	7.147					
	PSO	0.0205	0.0290	0.0359	0.0528	0.0329	0.0271	−0.0517	0.0289	0.0446	0.0377	0.0449	0.0151	0.0541	0.0992	0.1532	0.6470	2
	SFO	0.0248	0.0295	0.0369	0.0673	0.0196	0.0254	−0.0456	0.0302	0.0403	0.0496	0.0297	0.0134	0.0512	0.1031	0.1543	0.6682	1
	JBD	0.0302	0.0299	0.0321	0.0284	0.0392	0.0423	0.0304	0.0305	0.0381	0.0351	0.0370	0.0250	0.1000	0.0370	0.1370	0.2701	6
	BLT	0.0330	0.0300	0.0367	0.0337	0.0266	0.0342	0.0243	0.0323	0.0331	0.0301	0.0321	0.0553	0.0863	0.0604	0.1467	0.4115	4
	RSB	0.0267	0.0304	0.0349	0.0188	0.0235	0.0350	−0.0122	0.0329	0.0420	0.0343	0.0363	0.0241	0.0727	0.0565	0.1292	0.4375	3
	WCB	0.0293	0.0304	0.0360	0.0044	0.0462	0.0435	−0.0091	0.0317	0.0360	0.0522	0.0207	0.0209	0.0911	0.0474	0.1385	0.3425	5
Ideal best (Vj+)		0.0205	0.0290	0.0369	0.0673	0.0196	0.0435	−0.0517	0.0329	0.0446	0.0301	0.0207	0.0553					
Ideal worst (Vj−)		0.0330	0.0304	0.0321	0.0044	0.0462	0.0254	0.0304	0.0302	0.0331	0.0522	0.0370	0.0134					
(c) Entropy weightage method:																	
Alternative (6 biodiesels)	Criteria	KV	Density	HHV	OS	AV	FP	CFPP	CN	IV	MUFA	PUFA	LCSF	S_i^+	S_i^-	$S_i^+ + S_i^-$	P_i	Rank
	Weightage (%)	2.126	0.027	0.200	39.213	8.144	3.779	12.527	0.185	0.913	3.930	4.881	24.074					
	PSO	0.0064	0.0001	0.0008	0.2109	0.0335	0.0118	−0.0803	0.0007	0.0042	0.0149	0.0261	0.0510	0.1485	0.2322	0.3807	0.6099	2
	SFO	0.0078	0.0001	0.0008	0.2689	0.0199	0.0111	−0.0709	0.0007	0.0038	0.0196	0.0173	0.0453	0.1418	0.2789	0.4207	0.6630	1
	JBD	0.0095	0.0001	0.0007	0.1136	0.0399	0.0185	0.0472	0.0007	0.0036	0.0139	0.0215	0.0841	0.2265	0.1042	0.3307	0.3151	4
	BLT	0.0103	0.0001	0.0008	0.1346	0.0271	0.0150	0.0378	0.0008	0.0031	0.0119	0.0187	0.1862	0.1792	0.1847	0.3639	0.5076	3
	RSB	0.0084	0.0001	0.0008	0.0752	0.0239	0.0153	−0.0189	0.0008	0.0040	0.0136	0.0211	0.0813	0.2289	0.0979	0.3268	0.2996	5
	WCB	0.0092	0.0001	0.0008	0.0177	0.0471	0.0190	−0.0142	0.0008	0.0034	0.0206	0.0120	0.0704	0.2858	0.0675	0.3533	0.1911	6
Ideal best (Vj+)		0.0064	0.0000	0.0008	0.2689	0.0199	0.0190	−0.0803	0.0008	0.0042	0.0119	0.0120	0.1862					
Ideal worst (Vj−)		0.0103	0.0001	0.0007	0.0177	0.0471	0.0111	0.0472	0.0007	0.0031	0.0206	0.0215	0.0453					

Table 11
Summary of results.

Biodiesel	PROMETHEE II			WSM			WPM			TOPSIS			Average values	Average Ranks	Mode Ranks
	Eq	Cr	En	Eq	Cr	En	Eq	Cr	En	Eq	Cr	En			
PSO	1	1	1	2	2	2	3	3	3	2	2	2	2.4	2	2
SFO	2	2	2	1	1	1	2	1	1	1	1	1	1.6	1	1
JBD	6	6	4	6	6	5	4	4	4	6	6	4	6.1	5	6
BLT	5	5	3	4	4	3	1	2	2	4	4	3	4	3	4
RSB	3	3	5	3	3	4	5	5	5	3	3	5	4.7	4	3
WCB	4	4	6	5	5	6	6	6	6	5	5	6	6.4	6	6

where Eq is equal weight method, Cr is critic weight method and En is entropy weight method.

JBD and WCB were found to be the least favourable feedstocks to be considered.

9. Conclusion

In this study, the screening of six biodiesel feedstocks from non-edible sources was analysed in terms of their compositional structure and physico-chemical properties. Four different multiple-criteria decision analysis (MCDA) methods, namely PROMETHEE GAIA, WSM, WPM, and TOPSIS have been used for screening the six feedstocks. Twelve fuel properties of KV, density, HHV, OS, AV, FP, CFPP, CN, IV, MUFA, PUFA, and LCSF were selected as criteria, while all six biodiesel feedstocks were the alternatives. Three different weightage (%) determination methods of EQUAL, CRITIC and ENTROPY were used to emphasise the relative importance of each criterion. The summary of the findings of this study are as follows:

- Physico-chemical and compositional properties of all six biodiesel feedstocks are within the ASTM, EU and AU standards.
- The PROMETHEE GAIA MCDA method, when utilised in combination with all three weightage methods, indicated that PSO biodiesel ranked at the top of the list for producing biodiesel, while SFO came in second.
- SFO was found to rank first and PSO came second when combining all weightage methods with the WSM MCDA method. Both equal weightage and critic weightage methods showed an exact match of the rankings of all biodiesel feedstocks, whereas entropy weightage showed slightly different lower rankings.
- WPM indicated PSO as third best (all weightage methods), while SFO was second best under the equal weightage method and first under the critic and entropy methods. However, both critic weightage and entropy weightage methods showed an exact match of all rankings of biodiesel feedstocks, whereas equal weightage showed different first and second rankings.
- TOPSIS ranked SFO first and PSO second for all different weightage methods. Both equal weightage and critic weightage methods showed an exact match of all biodiesel feedstocks rankings, whereas entropy weightage showed slightly different lower rankings.
- The average ranking shows that the SFO ranked first and PSO second, followed by BLT, RSB, JBD and WCB.
- The mode ranking indicated that SFO was the first choice followed by PSO, RSB, and BLT. Both JBD and WCB were found to be equal lowest in the list as a tie.

Further research is required before these results can be recommended as sources of commercial biodiesel. It is recommended that the above-mentioned biodiesels be tested using a fully equipped diesel engine for engine performance, emission characteristics, combustion characteristics, corrosion, tribological performance and long-term engine durability.

References

[1] Banković-Ilić IB, Stamenković OS, Veljković VB. Biodiesel production from non-edible plant oils. Renew Sustain Energy Rev 2012;16(6):3621–47.
[2] Mofijur M, Masjuki HH, Kalam MA, Hazrat MA, Liaquat AM, Shahabuddin M, et al. Prospects of biodiesel from Jatropha in Malaysia. Renew Sustain Energy Rev 2012;16(7):5007–20.
[3] Anwar M, Rasul M, Ashwath N. A systematic multivariate analysis of carica papaya biodiesel blends and their interactive effect on performance. Energies 2018;11(11):2931.
[4] Mahmudul HM, Hagos FY, Mamat R, Adam AA, Ishak WFW, Alenezi R. Production, characterization and performance of biodiesel as an alternative fuel in diesel engines – a review. Renew Sustain Energy Rev 2017;72:497–509.
[5] Atabani AE, Mahlia TMI, Anjum Badruddin I, Masjuki HH, Chong WT, Lee KT. Investigation of physical and chemical properties of potential edible and non-edible feedstocks for biodiesel production, a comparative analysis. Renew Sustain Energy Rev 2013;21:749–55.
[6] Ahmad FB, Zhang Z, Doherty WOS, O'Hara IM. A multi-criteria analysis approach for ranking and selection of microorganisms for the production of oils for biodiesel production. Bioresour Technol 2015;190:264–73.
[7] Nwokoagbara E, Olaleye AK, Wang M. Biodiesel from microalgae: the use of multi-criteria decision analysis for strain selection. Fuel 2015;159:241–9.
[8] Samanlioglu F. A multi-criteria decision making approach to feedstock selection. Am Sci Res J 2018;49(1):15. 2018.
[9] Javier Martínez RANC. Use of Multicriteria decision making (MCDM) methods for biomass selection aimed to Fischer Tropsch processes. Int J Eng Trends Technol (IJETT) 2016;V34(6):266–72.
[10] Sharma SK, Mitra SK, Saran S. Papaya production in india – history, present status and future prospects. Leuven, Belgium: International Society for Horticultural Science (ISHS); 2016.
[11] Farming, A., Agri Farming # 1 source for farming in India. Available from : < http ://www.agrifarming.in/papaya-farming > ; 2017 [accessed 13.10.17].
[12] Salunkhe DK, Kadam SS. Handbook of Fruit Science and Technology: Production, Composition, Storage, and Processing. Taylor & Francis; 1995.
[13] Chan HT, Heu RA, Tang CS, Okazaki EN, Ishizaki SM. Composition of papaya seeds. J Food Sci 1978;43(1):255–6.
[14] Daryono ED, Sinaga EJ. Rapid in situ transesterification of papaya seeds to biodiesel with the aid of co-solvent. Int J Renew Energy Res 2017;7(1):379–85.
[15] Anwar M, Rasul M, Ashwath N. Optimization of biodiesel production from stone fruit kernel oil. Energy Proc 2019;160:268–76.
[16] Sharma R, Gupta A, Abrol GS, Joshi VK. Value addition of wild apricot fruits grown in North-West Himalayan regions: a review. J Food Sci Technol 2012.
[17] Atabani AE, Silitonga AS, Ong HC, Mahlia TMI, Masjuki HH, Badruddin IA, et al. Non-edible vegetable oils: a critical evaluation of oil extraction, fatty acid compositions, biodiesel production, characteristics, engine performance and emissions production. Renew Sustain Energy Rev 2013;18(Supplement C):211–45.
[18] Mohibbe Azam M, Waris A, Nahar NM. Prospects and potential of fatty acid methyl esters of some non-traditional seed oils for use as biodiesel in India. Biomass Bioenergy 2005;29(4):293–302.
[19] Silitonga AS, Atabani AE, Mahlia TMI, Masjuki HH, Badruddin IA, Mekhilef S. A review on prospect of Jatropha curcas for biodiesel in Indonesia. Renew Sustain Energy Rev 2011;15(8):3733–56.
[20] Gui MM, Lee KT, Bhatia S. Feasibility of edible oil vs. non-edible oil vs. waste edible oil as biodiesel feedstock. Energy 2008;33(11):1646–53.
[21] Friday JB, Okano D. Calophyllum inophyllum (kamani). Available from: http:// www.agroforestry.net/tti/Calophyllum-kamani.pdf; 2011 [accessed on 20.03.19].
[22] Anwar M, Rasul MG, Ashwath N. Production optimization and quality assessment of papaya (Carica papaya) biodiesel with response surface methodology. Energy Convers Manage 2018;156:103–12.
[23] Anwar M, Rasul M, Ashwath N, Rahman M. Optimisation of second-generation biodiesel production from australian native stone fruit oil using response surface method. Energies 2018;11(10):2566.
[24] Pramanik K. Properties and use of jatropha curcas oil and diesel fuel blends in compression ignition engine. Renewable Energy 2003;28(2):239–48.
[25] Datta A, Palit S, Mandal BK. An experimental study on the performance and emission characteristics of a CI engine fuelled with Jatropha biodiesel and its blends with diesel. J Mech Sci Technol 2014;28(5):1961–6.
[26] Jahirul MI, Brown RJ, Senadeera W, Ashwath N, Rasul MG, Rahman MM, et al.

Physio-chemical assessment of beauty leaf (Calophyllum inophyllum) as second-generation biodiesel feedstock. Energy Rep 2015;1:204–15.
[27] Ashwath N. Evaluating biodiesel potential of Australian native and naturalised plant species. Rural Industries. Res Develop Corp 2010:96. Canberra.
[28] Encinar JM, Pardal A, Sánchez N, Nogales S. Biodiesel by transesterification of rapeseed oil using ultrasound: a kinetic study of base-catalysed reactions. Energies 2018;11(9):2229.
[29] Kannan GR, Balasubramanian KR, Anand R. Artificial neural network approach to study the effect of injection pressure and timing on diesel engine performance fueled with biodiesel. Int J Automot Technol 2013;14(4):507–19.
[30] Ong HC, Masjuki HH, Mahlia TMI, Silitonga AS, Chong WT, Leong KY. Optimization of biodiesel production and engine performance from high free fatty acid Calophyllum inophyllum oil in CI diesel engine. Energy Convers Manage 2014;81:30–40.
[31] Dharma S, Masjuki HH, Ong HC, Sebayang AH, Silitonga AS, Kusumo F, et al. Optimization of biodiesel production process for mixed Jatropha curcas–Ceiba pentandra biodiesel using response surface methodology. Energy Convers Manage 2016;115:178–90.
[32] de Almeida VF, García-Moreno PJ, Guadix A, Guadix EM. Biodiesel production from mixtures of waste fish oil, palm oil and waste frying oil: optimization of fuel properties. Fuel Process Technol 2015;133:152–60.
[33] Hamze H, Akia M, Yazdani F. Optimization of biodiesel production from the waste cooking oil using response surface methodology. Process Saf Environ Prot 2015;94:1–10.
[34] Boonmee K, Chuntranuluck S, Punsuvon V, Silayoi P. Optimization of biodiesel production from Jatropha oil (Jatropha curcas L.) using response surface methodology. Kasetsart J Natural Sci 2010;44(2):290–9.
[35] Jahirul M, Koh W, Brown R, Senadeera W, Hara I, Moghaddam L. biodiesel production from non-edible beauty leaf (Calophyllum inophyllum) oil: process optimization using response surface methodology (RSM). Energies 2014;7(8):5317.
[36] Yuan X, Liu J, Zeng G, Shi J, Tong J, Huang G. Optimization of conversion of waste rapeseed oil with high FFA to biodiesel using response surface methodology. Renew Energy 2008;33(7):1678–84.
[37] Mofijur M, Rasul MG, Hassan NMS, Masjuki HH, Kalam MA, Mahmudul HM. Chapter fourteen – assessment of physical, chemical, and tribological properties of different biodiesel fuels. In: Rasul MG, Azad AK, Sharma SC, editors. Clean Energy for Sustainable Development. Academic Press; 2017. p. 441–63.
[38] Anwar M, Rasul MG, Ashwath N. Optimization of biodiesel production process from papaya (Carica papaya) seed oil. 2017 IEEE 7th International Conference on Power and Energy Systems (ICPES). 2017.
[39] Wakil MA, Kalam MA, Masjuki HH, Atabani AE, Rizwanul Fattah IM. Influence of biodiesel blending on physicochemical properties and importance of mathematical model for predicting the properties of biodiesel blend. Energy Convers Manage 2015;94:51–67.
[40] Giakoumis EG. A statistical investigation of biodiesel physical and chemical properties, and their correlation with the degree of unsaturation. Renewable Energy 2013;50:858–78.
[41] McCormick RL, Graboski MS, Alleman TL, Herring AM, Tyson KS. Impact of biodiesel source material and chemical structure on emissions of criteria pollutants from a heavy-duty engine. Environ Sci Technol 2001;35(9):1742–7.
[42] Ramos MJ, Fernández CM, Casas A, Rodríguez L, Pérez Á. Influence of fatty acid composition of raw materials on biodiesel properties. Bioresour Technol 2009;100(1):261–8.
[43] Fernando S, Karra P, Hernandez R, Jha SK. Effect of incompletely converted soybean oil on biodiesel quality. Energy 2007;32(5):844–51.
[44] El-Kasaby M, Nemit-allah MA. Experimental investigations of ignition delay period and performance of a diesel engine operated with Jatropha oil biodiesel. Alexandria Eng J 2013;52(2):141–9.
[45] Anwar M, Rasul MG, Ashwath N, Nabi MDN. The potential of utilising papaya seed oil and stone fruit kernel oil as non-edible feedstock for biodiesel production in Australia—a review. Energy Rep 2019;5:280–97.
[46] Monirul IM, Masjuki HH, Kalam MA, Zulkifli NWM, Rashedul HK, Rashed MM, et al. A comprehensive review on biodiesel cold flow properties and oxidation stability along with their improvement processes. RSC Adv 2015;5(105):86631–55.
[47] Gumus M, Kasifoglu S. Performance and emission evaluation of a compression ignition engine using a biodiesel (apricot seed kernel oil methyl ester) and its blends with diesel fuel. Biomass Bioenergy 2010;34(1):134–9.
[48] Rizwanul FIM, Masjuki HH, Kalam MA, Wakil MA, Ashraful AM, Shahir SA. Experimental investigation of performance and regulated emissions of a diesel engine with Calophyllum inophyllum biodiesel blends accompanied by oxidation inhibitors. Energy Convers Manage 2014;83:232–40.
[49] Demirbas A. Biodiesel production from vegetable oils via catalytic and non-catalytic supercritical methanol transesterification methods. Prog Energy Combust Sci 2005;31(5):466–87.
[50] Diakoulaki D, Mavrotas G, Papayannakis L. Determining objective weights in multiple criteria problems: the critic method. Comput Oper Res 1995;22(7):763–70.
[51] Srđević B, Medeiros Y, Faria A, Schaer M. Objective evaluation of performance criteria for a reservoir system. Vodoprivreda 2003;35(3–4):163–76.
[52] Brans J-P, Mareschal B. The PROMCALC & GAIA decision support system for multicriteria decision aid. Decis Support Syst 1994;12(4):297–310.
[53] Kolios A, Mytilinou V, Lozano-Minguez E, Salonitis K. A comparative study of multiple-criteria decision-making methods under stochastic inputs. Energies 2016;9(7):566.
[54] Triantaphyllou E, Mann SH. An examination of the effectiveness of multi-dimensional decision-making methods: a decision-making paradox. Decis Support Syst 1989;5(3):303–12.
[55] Podvezko V. The comparative analysis of MCDA methods SAW and COPRAS. Eng Econ 2011;22(2):134–46.
[56] Hwang CL, Yoon K. Multiple attribute decision making: methods and applications. Berlin Heidelberg New York: Springer-Verlag; 1981.
[57] Figueira J, Greco S, Ehrogott M, editors. International Series in Operations Research & Management Science 78 ed.New York: Springer; 2005. https://doi.org/10.1007/b100605. no. 78.

{this page is intentionally left blank}

Declaration of Co-authorship and Contribution

Research Division

CHAPTER 4: Part A- Biodiesel Production Process Optimisation

Title of the paper	Production optimization and quality assessment of papaya (Carica papaya) biodiesel with response surface methodology
Full bibliographic reference	Anwar, M., M.G. Rasul, and N. Ashwath, Production optimization and quality assessment of papaya (Carica papaya) biodiesel with response surface methodology. Energy Conversion and Management, 2018. 156: p. 103-112. https://www.sciencedirect.com/science/article/pii/S0196890417310439
Status	Published

Nature of Candidate's Contribution, including percentage of total
I was responsible for conducted the experiments, performed data analysis and drafted the manuscript. [80%]

Nature of all Co-Authors' Contributions, including percentage of total
My co-authors, Prof. Mohammad Rasul and A/Professor Nanjappa Ashwath, were supervised the project and reviewed the manuscript. [20%]

Has this paper been submitted for an award by another research degree candidate (Co- Author), either at CQUniversity or elsewhere? (if yes, give full details)
No

Candidate's Declaration

I declare that the publication above meets the requirements to be included in the thesis as outlined in the Research Higher Degree Theses Policy and Procedure.

Mohammad Anwar

Energy Conversion and Management 156 (2018) 103–112

Contents lists available at ScienceDirect

Energy Conversion and Management

journal homepage: www.elsevier.com/locate/enconman

Production optimization and quality assessment of papaya (*Carica papaya*) biodiesel with response surface methodology

Mohammad Anwar[a,*], Mohammad G. Rasul[a], Nanjappa Ashwath[b]

[a] Central Queensland University, School of Engineering and Technology, North Rockhampton, Queensland 4702, Australia
[b] Central Queensland University, School of Health, Medical and Applied Sciences, North Rockhampton, Queensland 4702, Australia

ARTICLE INFO

Keywords:
Response surface methodology
Papaya seed oil
Biodiesel
Pawpaw
Optimization
RSM

ABSTRACT

Optimization of biodiesel production from non-edible papaya seed oil was investigated in this study. Biodiesel production process parameters such as catalyst concentration, methanol:oil molar ratio and reaction temperature were optimized by using the Response Surface methodology based on the Box-Behnken experimental design. Optimization of the transesterification process was conducted by varying three factors each at three different levels and this required a total of fifteen runs. A quadratic model was created to predict the biodiesel yield where the R^2 value was found to be 0.99 which indicates the satisfactory accuracy of the model. Based on the results, the optimum process parameters for transesterification of the papaya seed oil mixture at an agitation speed of 600 rpm over a period of 60 min were found to be a methanol:oil molar ratio 10:1, KOH catalyst concentration of 1 wt% and reaction temperature of 45 °C. At these reaction conditions, the predicted and experimental biodiesel yield were 96.12% and 96.48% respectively which shows less than 0.5% variation. The biodiesel properties were characterized and the results obtained were found to satisfy both ASTM D6751 and EN14214 standards. The statistical tool MINITAB 17 was used to draw both 3D surface plots and 2D contour plots to predict the optimum biodiesel yield.

1. Introduction

About 88% of the global energy supply is dependent on petroleum-derived fuels (oils, natural gas & coal) [1]. These fossil fuels play an important role in the transportation and power generation sectors, and are a significant burden on the economies of those underprivileged countries that do not have any natural resources. It is expected that global oil production will be the highest between 2015 and 2030 [2]. Due to the uncertainty and political imbalance situation in major oil producing countries as well as price hiking of fossil fuels and depletion of those fuel reserves, a need has arisen for identifying alternative fuel sources [3]. Furthermore, combustion of fossil fuels results in greenhouse gas emission, which leads to climate change. Fossil fuels also release pollutants such as nitrogen oxides and unburned hydrocarbons into the atmosphere, causing health hazards and acid rain [4].

Biofuel (e.g., biodiesel) is becoming popular as an alternative energy source due to its excellent environmental attributes. Biodiesel is a clean burning ester-based oxygenated fuel, renewable, sulphur free, biodegradable and non-toxic [5–8]. It has the potential to minimize environmental pollution and global warming significantly [9,10]. Biodiesel can be derived from vegetable oils or animal fat. Vegetable oils are becoming attractive as a renewable source for biodiesel production due to their availability and low cost [11,12]. Vegetable oils usually have higher cetane numbers and lower calorific values which restrict them from use as fuel directly in the diesel engine. Additionally, their brake thermal efficiency is poor compared to petro-diesel which leads to problems of high smoke, HC (hydrocarbon) and CO (carbon monoxide) emissions [6]. Some crude oils or vegetable oils have high viscosity and high molecular weight that cause poor fuel flow. This will result in incomplete combustion and severe engine deposits, injector coking and piston ring sticking [13,14]. Several techniques have been deployed to overcome these problems, including preheating the oil, diluting the oil with other conventional fuels or additives, oil microemulsification, transesterification or thermal cracking/pyrolysis [15].

Transesterification is the most widely used technique to reduce viscosity and oxygen content of oil. An alkali catalysed transesterification reaction is the most widely used method for producing biodiesel due to its higher conversion efficiency. This process is suitable for oils that contain low free fatty acid content (< 4%). Oils that have > 4% free fatty acids are converted by an acid catalysed transesterification process. Transesterification is influenced by several process parameters such as reaction temperature, catalyst type, catalyst

* Corresponding author.
E-mail address: m.anwar@cqu.edu.au (M. Anwar).

https://doi.org/10.1016/j.enconman.2017.11.004
Received 17 July 2017; Received in revised form 31 October 2017; Accepted 2 November 2017

concentration, type of alcohol and their oil molar ratio, reaction time and agitation speed. Optimization of those process parameters will result in higher yields and better quality of the biodiesel.

Biodiesel feedstock should be chosen from the sources that are locally available and easily accessible, economically feasible and technically viable [16]. More than 350 oil-bearing crops have been identified for biodiesel production in the last decade [17,18]. Some conventional biodiesel sources are beauty leaf tree, palm, jatropha, coconut, sunflower, soybean, rapeseed, jojoba, neem, karanja, moringa, cotton, castor oil and microalgae [10,19–22]. Among those feedstocks, many of them are first generation which is produced from edible oils (human food) and some of them are 2nd generation which is produced from non-edible vegetable oils and fats. This 2nd generation feedstocks cover a wider range of biomass resources such as agriculture to forestry and waste materials. This non-edible biodiesel is attracting increasing attention worldwide due to their excellent environmentally friendly attributes.

Biodiesel consists of simple alkyl esters of fatty acids derived from renewable lipid feedstocks such as animal fat and vegetable oil. Many researchers have studied the production of biodiesel from different feedstocks, but very few researchers [11,23,24] have studied the production of *Carica papaya* biodiesel. Wong et al. [11] produced papaya biodiesel via enzymatic transesterification using lipase at methanol:oil molar ratio of 6:1. Agunbiade et al. [23] have shown that the crude papaya seed oil can be transesterified by two-stage catalysis using methanol:oil molar ratio of 9:1. Mohan et al. [24] used CaO as the catalyst and analysed the emissions of a single cylinder diesel engine using 20% papaya biodiesel and 80% chicken biodiesel blend. De Melo et al. [25] have used alkaline transesterification with 0.5% sodium methoxide with methanol:oil maolar ratio of 8:1. Daryono et al. [26] has used sodium hydroxide as an alkaline catalyst for transesterification process for production of biodiesel from papaya seed. They have all claimed that the physicochemical properties of papaya seed oil biodiesel were very close to those of petro diesel. Based on these information, it was decided to use single stage alkaline transesterification for biodiesel production in this study. However, the potential of papaya seed oil biodiesel as a source of future generation biodiesel is yet to be established due to a lack of knowledge on its optimum production processes.

The papaya (*Carica papaya*) originates from the tropics of the Americas and is mainly cultivated in tropical climates of Asia, South America, Africa and Polynesia. India is the largest papaya fruit producer in the world contributing 42% of world production that is nearly 3 million tonnes of papaya produced annually [27,28]. Fig. 1 shows global papaya production in 2014. Papaya being a tropical fruit grows well in sub-tropical regions. Papaya fruit can weigh from 200 g to more than 3000 g and its seed content can be approximately 15% of the wet weight of the fruit [29,30]. Since seeds are not consumed, 15% of the biomass (i.e. amount of seeds) is discarded [26,30]. This seeds can be utilized as the feedstock for biodiesel synthesis. However, in order to make more use of papaya seeds, it is important to investigate and test the processes of papaya seed oil extraction and its conversion into biodiesel. This paper addresses the optimization of PSO conversion into PSO biodiesel using Response Surface Methodology (RSM).

RSM is a set of mathematical and statistical methods used for modelling and problem solving, where the response is influenced by several operating or process parameters [31]. RSM is very effective when designing the experiments for maximizing yield and minimizing production cost.

In this study, the Box-Behnken design matrix was used to explore optimum experimental conditions for biodiesel production from PSO using the alkaline transesterification process. In the design matrix, the parameters of methanol:oil ratio, KOH catalyst concentration and temperature were each varied within different ranges of three levels to predict the optimum biodiesel yield.

2. Materials and methods

Papaya seed oil (PSO) was purchased from Katyani Exports Company in India. They produce mass quantity of Papaya seed oil and export globally. The methods they used for extracting PSO were as follows: Papaya fruits were first cut into two longitudinal halves and the seeds were removed, washed and dried in an oven at 60 °C for 24 h [11,33]. The dried seeds were ground into fine powder. The powdered seeds were treated with n-hexane in a Soxhlet extractor at 40–60 °C for 8 h. The oil was recovered by evaporating the solvent using a rotary evaporator and the remaining solvent was removed by drying the oil in an oven at 60 °C for 1 h [34]. After filtration, the papaya seed oil was shipped to Australia within 3 months of extraction. The biodiesel conversion experiments were conducted at Central Queensland University (Australia) using small scale three-neck laboratory reactors (0.5 L or 1 L). Methanol (reagent grade), potassium hydroxide, sodium hydroxide and Whatman 541 grade filter paper (pore size 22 μm) used in this experiment were supplied by School of Engineering and Technology, Central Queensland University.

2.1. Biodiesel production process

Small scale three-neck laboratory reactors (0.5 L or 1 L) were used in the transesterification process. The reactor was equipped with a reflux condenser, thermocouple, and magnetic stirrer. The acid value of PSO was found to be around 0.98, which indicated that only the transesterification process is adequate to convert PSO to biodiesel. In this experiment, 40 g of preheated PSO was reacted with a defined amount of alcohol (methanol:oil molar ratio 4:1, 7:1 and 10:1) in the presence of KOH catalysts (0.5, 1 and 1.5 wt%). These combinations were tested at different temperatures (45, 55 and 65 °C) for 60 min at an agitation speed of 600 rpm.

At first, 40 g of PSO was preheated in the reactor at 40 °C and the known quantity of methanol and measured amount of catalyst were added and stirred vigorously at 40 °C. This resulted in the production of potassium methoxide. The potassium methoxide was then poured into the reactor that contained PSO at 45 or 55 or 65 °C. After set times, the product was transferred into a separating funnel for layer separation. Two clear layers were observed, the upper red layer being methyl ester and the lower dark brown layer consisting of glycerol and excess methanol. The glycerol was drained followed by the methyl ester. The methyl ester was heated to 70 °C to remove any remaining methanol. Then it was washed with warm distilled water to remove any dissolved glycerol or impurities. The washed methyl ester was dried using Sodium Sulphate (Na_2SO_4) and filtered through a Whatman No 541 paper filter. The resulting methyl ester was collected and stored at room temperature. The graphical abstract of PSO production process is shown in Fig. 2.

The biodiesel yield was calculated using the Fatty acid methyl ester (FAME) percentage from Gas Chromatogram (GC) analysis multiplied with the ratio of weight of methyl ester produced to weight of oil used initially. Many researchers [20,35–38] have used another simplified Eq. (1) to obtain biodiesel yield that is as follows:

$$Yield\ \% = \frac{Weight\ of\ methyl\ ester\ produced}{Weight\ of\ Oil\ used} \times 100 \quad (1)$$

2.2. Characterization of PSO and PSO biodiesel

The physicochemical properties of crude PSO and PSO methyl ester were tested according to ASTM Standard D6751. Fatty acid composition was determined using a gas chromatograph (Thermo Trace 1310 GC). The PSO biodiesel (25 mg) was dissolved in 10 ml of high purity hexane and then transferred to 2 ml auto-sampler vials. The PSO biodiesel samples were analysed using the Thermo Trace 1310 GC with a split-splitless injector, flame ionization detector and TriPlus auto-sampler.

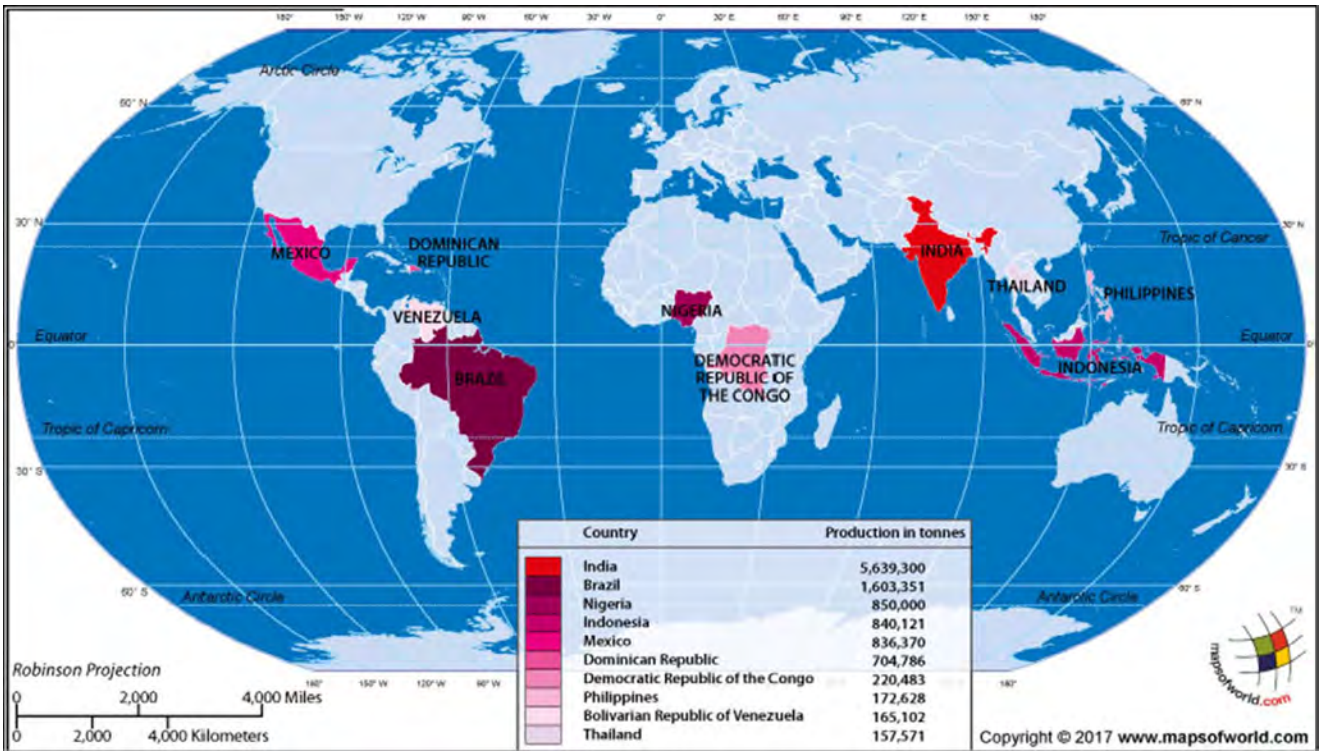

Fig. 1. Global papaya production in 2014 [32].

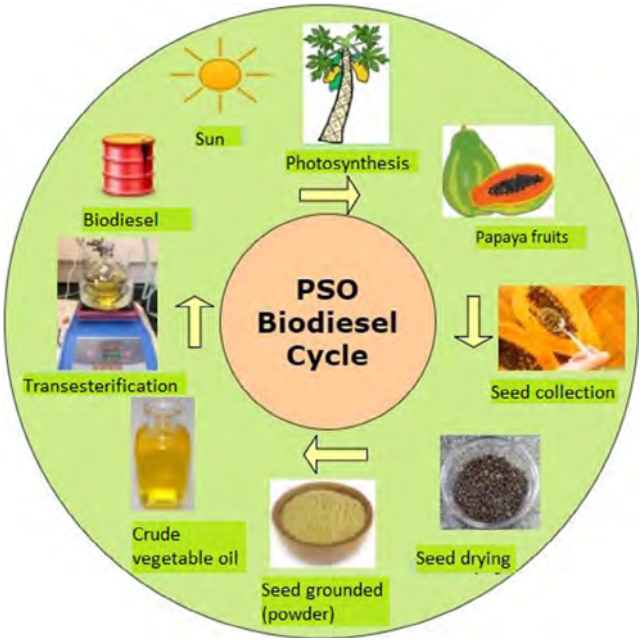

Fig. 2. Graphical abstract of PSO biodiesel production.

One microliter sample was injected in split mode (40:1) at 240 °C with a constant helium flow of 1.2 ml/min. FAMEs were separated using a BPX-70 column (60 m × 250 µm × 0.25 µm film) with a temperature program: 110 °C (4 min) – 10 °C/min – 150 – 3.9 °C/min – 230 °C (5 min). Individual components of the PSO biodiesel were identified by retention time compared to a standard FAME mixture that had certified concentrations, namely Supelco CRM18920 (FAME C8-C22). Data were acquired and processed using Chromeleon 7.2 software.

Fourier transform infrared (FT-IR) analysis of the PSO biodiesel was performed to identify the long chain fatty acid esters. Attenuated total reflectance (ATR) infrared spectra were recorded using a Spectrum 100 FT-IR spectrometer with a universal ATR sampling accessory (Perkin Elmer, Melbourne, Australia). PSO biodiesel samples were placed directly on the ATR window, and the spectra were recorded (four scans, 4000–650 cm^{-1}) at approximately 40% transmission. Data were acquired and processed using the Spectrum 6.2.0 software following ATR correction.

Cetane number (CN), saponification value (SV), iodine value (IV), long chain saturated factor (LCSF) and degree of unsaturation (DU) were determined using the following equations [39,40]:

$$CN = 46.3 + \left(\frac{5458}{SV}\right) - (0.225 \times IV) \quad (2)$$

$$SV = \sum \frac{(560 \times A_i)}{MW_i} \quad (3)$$

$$IV = \sum \frac{(254 \times DxA_i)}{MW_i} \quad (4)$$

$$LCSF = 0.1 \times (C16{:}\ 0\ wt\%) + 0.5 \times (C18{:}\ 0\ wt\%) + 1 \times (C20{:}\ 0\ wt\%) + 1.5 \times (C22{:}\ 0\ wt\%) + 2.0 \times (C24{:}\ 0\ wt\%) \quad (5)$$

$$DU = \sum MUFA + (2 \times PUFA) \quad (6)$$

where D is the number of double bonds, A_i is the percentage of each fatty acid in the FAME, and MW_i is the molecular weight. Mono-unsaturated fatty acid (*MUFA)* and polyunsaturated fatty acid (*PUFA)* concentrations were used to calculate degree of unsaturation.

3. Results and discussion

3.1. Characterization of fatty acid composition of PSO

PSO properties were determined before the optimization process was undertaken. The oil was characterized for viscosity, density, specific gravity, acid value, refractive index, angular rotation, stability oxidative and Iodine value. The properties of PSO biodiesel and the petro diesel are compared and presented in Table 1.

Table 1
Physical and chemical properties of PSO.

Serial no.	Properties	PSO	Petro diesel
1	Kinematic Viscosity ($m^2 s^{-1}$) @ 40 °C	27.3	3.23
2	Density (kg/m^3)	885	830
3	Specific Gravity @ 15 °C	0.885	0.83
4	Acid Value (mg KOH/g)	0.98	0.11
5	Refractive Index @ 25 °C	1.457	–
6	Angular Rotation (°) @ 20 °C	−8.75	–
7	Stability Oxidative (hour)	77.97	–
8	Iodine Value ($g.I.100\,g^{-1}$)	79.95	–

Table 2
Fatty acid composition of PSO.

Fatty Acid	PSO (wt%)
Palmitic Acid (C16:0)	6.07
Stearic Acid (C18:0)	3.13
Oleic Acid (C18:1)	47.73
Linoleic Acid (C18:2)	37.25
Linolenic Acid (C18:3)	1.78
Eicosenoic Acid (C20:1)	0.76
Behenic Acid (C22:0)	0.68
Erucic Acid (C22:1)	1.51
Others	1.09
Saturated Acid	9.88
Unsaturated Acid	87.52

The compositional analysis set out in Table 2 shows that the PSO contains a high level (87.5%) of unsaturated fatty acid (such as polysaturated and monosaturated fatty acid methyl esters). Among these, the oleic acid (C18:1) was found to be the dominant fatty acid (47.7%). Linoleic acid (C18:2) was found at 37.3% and the saturated fatty acids such as palmitic acid (C16:0) was found at 6.1%. This high-level unsaturated fatty acid is prone to autoxidation. Moreover, oxidation degradation has a negative impact on acid value and kinematic viscosity [41]. However, high amount of unsaturated fatty acid ensures good flow properties compared with saturated fatty acids. Saturated fatty acids limit the application of biodiesel in cold countries due to poor cold flow.

3.2. Optimization of reaction conditions by response surface methodology (RSM)

The experiments were carried out in accordance with the Box-Behnken response surface design. The statistical analysis was carried out using Minitab 17, and experimental optimization was reached via analysis of variance (ANOVA). Optimization of the transesterification process was carried out using 3 factors at three levels which required a total of fifteen runs. The factors and the ranges and levels of the investigated variables are listed in Table 3.

The factors were methanol to oil molar ratio (M), KOH catalyst concentration (C) and reaction temperature (T). Methanol to oil molar ratio ranged from 4:1 to 10:1, catalyst concentration levels were 0.5–1.5% by weight of oil and the upper-temperature level was chosen at 65 °C (boiling point of methanol) and the lower temperature level was 45 °C. Once the experiments were completed, the response variable

Table 3
Experimental range and levels coded for ANOVA.

Factors	Unit	Symbol coded	Range and levels		
			−1	0	1
Methanol to Oil ratio	mol/mol	M	4:1	7:1	10:1
KOH catalyst concentration	wt%	C	0.5	1.00	1.5
Temperature	°C	T	45	55	65

(biodiesel yield) was applied in a full quadratic model to correlate the response variable to the independent variable. The form of the full quadratic model is shown in Eq. (7).

$$Y = b_0 + b_1c_1 + b_2c_2 + b_3c_3 + b_{1,2}c_1c_2 + b_{1,3}c_1c_3 + b_{2,3}c_2c_3 + b_{1,1}c_1^2 + b_{2,2}c_2^2 + b_{3,3}c_3^2 \quad (7)$$

where Y is the response factor (biodiesel yield); b_0 is a constant; b_1, b_2, b_3 are regression coefficients and c_1, c_2, c_3 are independent variables.

Table 4 shows the complete experimental design matrix of Box-Behnken design for factorial design. The order in which the runs were made was randomized to avoid systematic errors. In the transesterification experiments, the biodiesel yield ranged from 79.7% to 96.5% with the highest content resulting from reaction conditions of methanol oil molar ratio of 10:1, KOH catalyst concentration of 1 wt% and reaction temperature of 45 °C.

Based on the coded parameters, a quadratic regression model with determined coefficients for statistical prediction as defined by Eq. (8) was developed using Minitab 17 to predict papaya biodiesel yield percentages as a function of methanol oil molar ratio, catalyst concentration, and reaction temperature. Table 5 summarizes the resulting regression coefficients, computed T-values and corresponding P-values.

$$Y = 79.96 + 4.094M - 0.079C - 1.575\,T + 7.601M^2 + 1.901C^2 - 0.656T^2 - 0.337MC - 3.555MT + 0.320CT \quad (8)$$

The analysis of variance (ANOVA) was performed to determine statistical significance and fitness of the model equation. ANOVA also determined the effects of significant individual terms and their interaction on the selected response. These results are shown in Table 6. The results show that the model is highly significant at the 95% confidence level due to the higher F value (58.45) and lower P value (< .0001). The P value indicates the probability of error and it is used to check the significance of each regression coefficient. The P value is also revealing of the interaction effect of each cross product. The P value of .0001 indicates that a probability of getting a large F value due to noise is only 0.01%. In this case, M (methanol:oil molar ratio), T (reaction temperature), M^2 (quadratic effect of methanol amount), C^2 (quadratic effect of catalyst concentration) and MT (methanol amount with reaction temperature) have significant effects on biodiesel production. The methanol:oil molar ratio (M) is the most important variable in the production of biodiesel from PSO due to its higher F value (163.33) and lower P value (< .0001). According to regression model Eq. (8), both catalyst concentration (C) and reaction temperature (T) have negative effects on PSO biodiesel yield. This means that increasing both the catalyst concentration (C) and reaction temperature (T) will slow the speed of the transesterification reaction. The “Lack of Fit” indicates that the model does not sufficiently describe the relationship between the independent variables (M, C and T) and the dependent variable (PSO Biodiesel yield). In this study, it is found the F value and P value lack of fit parameters are 17.30 and .055 respectively. The P value (.055) lack of fit parameter is slightly greater than .50, indicating that there is good fit between the quadratic model and the experimental data.

The quality of the model fitness was verified by the coefficient of determination (R^2). The coefficient of determination (R^2) was 99% and the adjusted coefficient of determination (Adj. R^2) was 97.4%. The determined value of the coefficient indicates the good accuracy of the model. In conclusion, the model is quite appropriate for experimental relationships between the variables and the response.

Fig. 3 shows the accuracy of the prediction model as indicated by the comparison of experimental and predicted biodiesel yields. All points are close to the straight line indicating that a good agreement exits between the experimental and predicted values.

3.3. Response surface plots for PSO biodiesel production

The interactive effects of the process variables on the

Table 4
Experimental matrix for Box–Behnken design and the results.

Exp. number	Run order	M	C	T	Methanol:oil (molar ratio)	KOH (wt%)	Temp (°C)	PSO biodiesel yield (%)	
								Experimental	Predicted
1	6	0	−1	1	7	0.5	45	82.30	83.18
2	7	1	0	−1	10	0.5	55	94.50	93.97
3	10	1	0	1	7	1	55	80.25	79.96
4	13	−1	1	0	4	1	45	81.67	80.83
5	1	−1	0	−1	***10***	***1***	***45***	***96.48***	***96.12***
6	2	0	0	0	4	0.5	55	85.15	85.11
7	8	0	0	0	4	1.5	55	85.10	85.63
8	9	0	1	1	7	1	55	79.70	79.96
9	11	0	−1	−1	7	1	55	79.93	79.96
10	14	1	−1	0	7	1.5	45	82.07	82.38
11	15	−1	−1	0	10	1.5	55	93.10	93.14
12	3	0	0	0	10	1	65	85.03	85.87
13	4	1	1	0	4	1	65	84.44	84.79
14	5	−1	0	1	7	0.5	65	79.70	79.39
15	12	0	1	−1	7	1.5	65	80.75	79.87

Table 5
Regression coefficient of predicted quadratic polynomial model.

Term	Coefficients	Standard errors	Computed T-value	P value
Constant	76.960	0.523	152.86	.000
M	4.094	0.320	12.78	.000
C	−0.079	0.320	−0.25	.816
T	−1.575	0.320	−4.92	.004
M * M	7.601	0.471	16.12	.000
C * C	1.901	0.471	4.03	.010
T * T	−0.656	0.471	−1.39	.223
M * C	−0.337	0.453	−0.75	.490
M * T	−3.555	0.453	−7.85	.001
C * T	0.320	0.453	0.71	.511

transesterification efficiency were studied by plotting three-dimensional surface curves against any two independent variables while keeping other variables at their central level. The surface plots and contour plots of the yield obtained by Eq. (8) are shown in Figs. 4–6. The response surface curves were plotted to understand the interaction of the variables and to determine the optimum level of each variable for maximum response.

3.3.1. Interaction effect of methanol:oil molar ratio and catalyst concentration

Fig. 4 shows the 3D response surface and 2D contour plot between methanol:oil molar ratio and KOH catalyst concentration for different fixed parameters (reaction temperature 45 °C and time 60 min) under experimental conditions defined by the Box-Behnken matrix. Biodiesel yield (%) increases with the increase of Methanol:oil molar ratio up to 10:1 with the mid-value of catalyst concentration. The maximum PSO methyl ester was found to be 96.48% at KOH 1 wt%. However, the Box-Behnken experimental matrix in Table 4 indicates that, when the methanol:oil molar ratio remains unchanged at (10:1) and the catalyst concentration is highest (1.5 wt%), the PSO methyl ester decreases to 93.10%. Again at methanol:oil molar ratio of up to 10:1 and mid-value of catalyst concentration 1 wt% and high temperature (65 °C), the yield drops to 85.03%. Thus catalyst concentration is one of the important factors in improving biodiesel yield, although high concentrations of catalyst can produce emulsion and result in phase separation [42]. From ANOVA results in Table 6, it was observed that there was a less significant interaction between the methanol:oil molar ratio and KOH catalyst concentration.

3.3.2. Interaction effect of catalyst concentration and temperature

The effects of catalyst concentration and reaction temperature on the biodiesel yield are shown in 3D surface plots and 2D contour plots in Fig. 5. While keeping the factors of Methanol:oil molar ratio of 10:1 and reaction time of 60 min constant, an increase in reaction temperature (45 °C) and the mid-level of KOH catalyst concentration (1 wt %) can improve the biodiesel yield up to 96.48%. Increasing the reaction temperature to 55 °C and catalyst concentration to 1.5 wt% resulted in the decline in biodiesel yield to 93.10%. Similarly, decreasing the catalyst concentration to the lower level (0.5 wt%) and increasing temperature to the mid-level (55 °C) resulted in a stepwise decline in biodiesel yield to 94.50%. Moreover, keeping the catalyst concentration at mid-level (1 wt%) and increasing the reaction temperature to high

Table 6
ANOVA results for papaya methyl ester.

Source	Sum of squares	Degree of freedom	Mean square	F-value	P-value	Remarks
Model	431.812	9	47.979	58.45	< .0001	Highly significant
M-Methanol	134.070	1	134.07	163.33	< .0001	Highly significant
C-Catalyst	0.050	1	0.050	0.06	.816	Not significant
T- Temperature	19.845	1	19.845	24.18	.004	Significant
M^2	213.338	1	213.338	259.90	< .001	Significant
C^2	13.347	1	13.347	16.26	.010	Significant
T^2	1.590	1	1.590	1.94	.223	Not significant
MC	0.456	1	0.456	0.56	.490	Not significant
MT	50.552	1	50.552	61.59	.001	Significant
CT	0.410	1	0.410	0.50	.511	Not significant
Lack of Fit	3.952	3	1.317	17.30	.055	Not Significant
Pure Error	0.153	2	0.076			
Total	435.916	14				
R^2 = 0.9906	Adj R^2 = 0.9736					

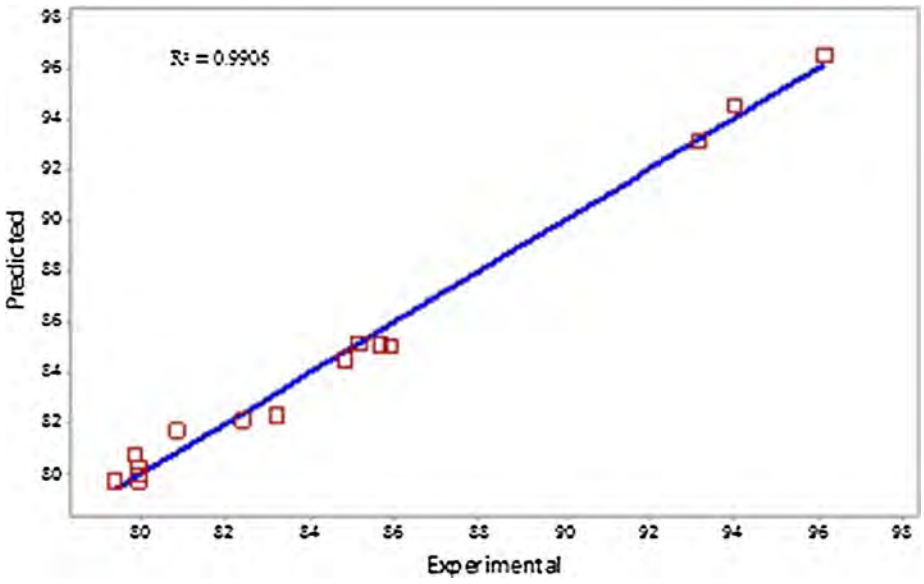

Fig. 3. Predicted versus actual (%) of yield values.

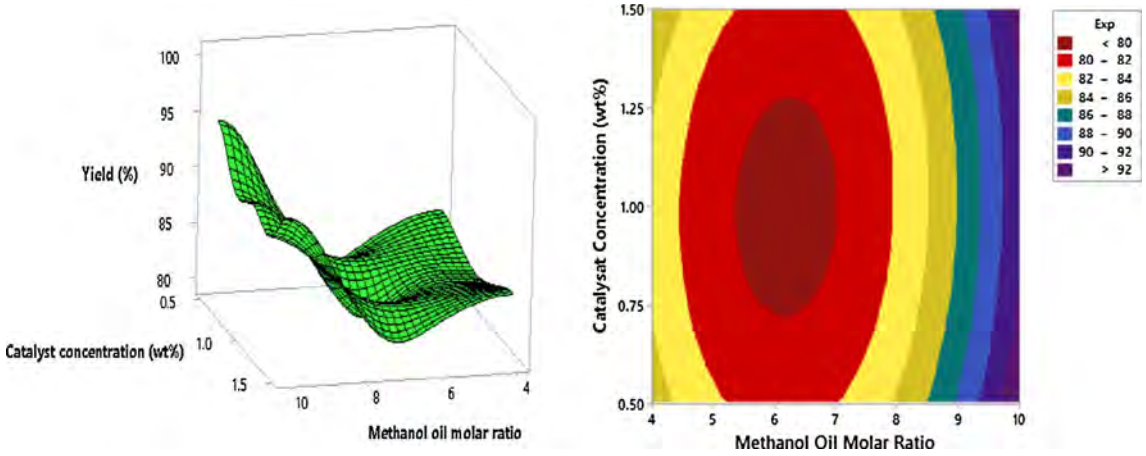

(a) 3D response surface plot (b) 2D contour plot

Fig. 4. Combined effects of methanol:oil molar ratio (M) and catalyst concentration (C) on the biodiesel yield.

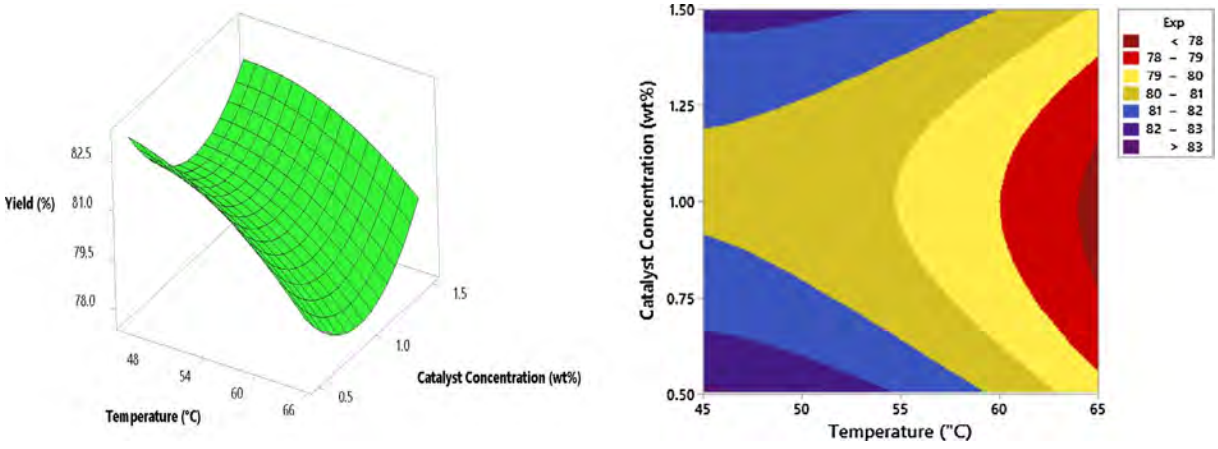

(a) 3D response surface plot (b) 2D contour plot

Fig. 5. Combined effects of reaction temperature (T) and catalyst concentration (C) on the biodiesel yield.

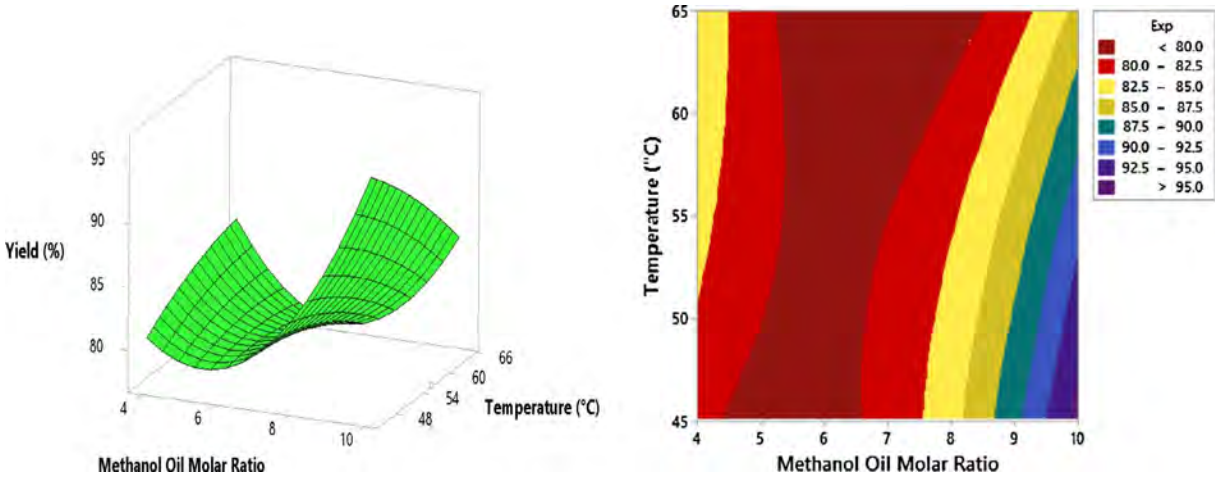

(a) 3D response surface plot (b) 2D contour plot

Fig. 6. Combined effects of methanol:oil molar ratio (M) and reaction temperature (T) on the biodiesel yield.

Table 7
Comparison of PSO methyl ester with other non-edible methyl esters.

Non-edible methyl esters	Density (kg/m^3)	Viscosity at 40 °C, m^2 s^{-1}	Acid value, mg KOH/g	Cetane number (CN)	Higher heating value, MJ/kg	Flash point, °C	Iodine value (IV)	Oxidation stability (OS), h
PSO	840.0	3.53	0.42	48.29	38.49	112	115.89	5.61
Petro diesel	827.2	3.23	0.05	48.00	45.30	68.5	38.3	39.0
Tobacco [46,48]	888.5	4.23	–	51.60	–	165.4	136	0.80
Jatropha [46]	879.5	4.80	0.40	51.60	39.23	135	104	2.30
Rapeseed [48]	882.0	4.43	–	54.40	37.00	170	–	7.60
Cottonseed [48]	875.0	4.07	0.16	54.13	40.43	150	–	1.83
Neem [46,48]	868.0	5.21	0.65	–	39.81	76	–	7.10
Karanja [46]	931.0	6.13	0.42	55.00	43.42	95	–	–
Moringa [48]	883.0	5.00	0.18	67.07	–	160	74	2.30
ASTM D6751	880.0	1.9–6.0	Max. 0.5	Min. 47	–	100–170	–	Min. 3
EN14214	860–900	3.5–5.0	Max. 0.5	Min. 51	35	> 120	Max. 120	Min. 6

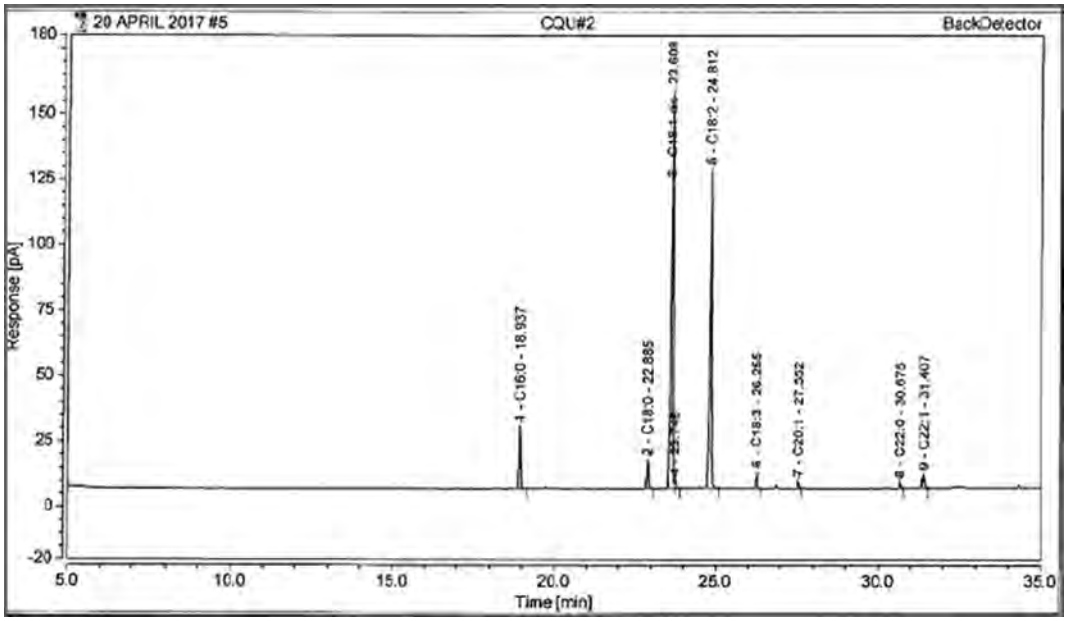

Fig. 7. GC Chromatogram of PSO methyl ester.

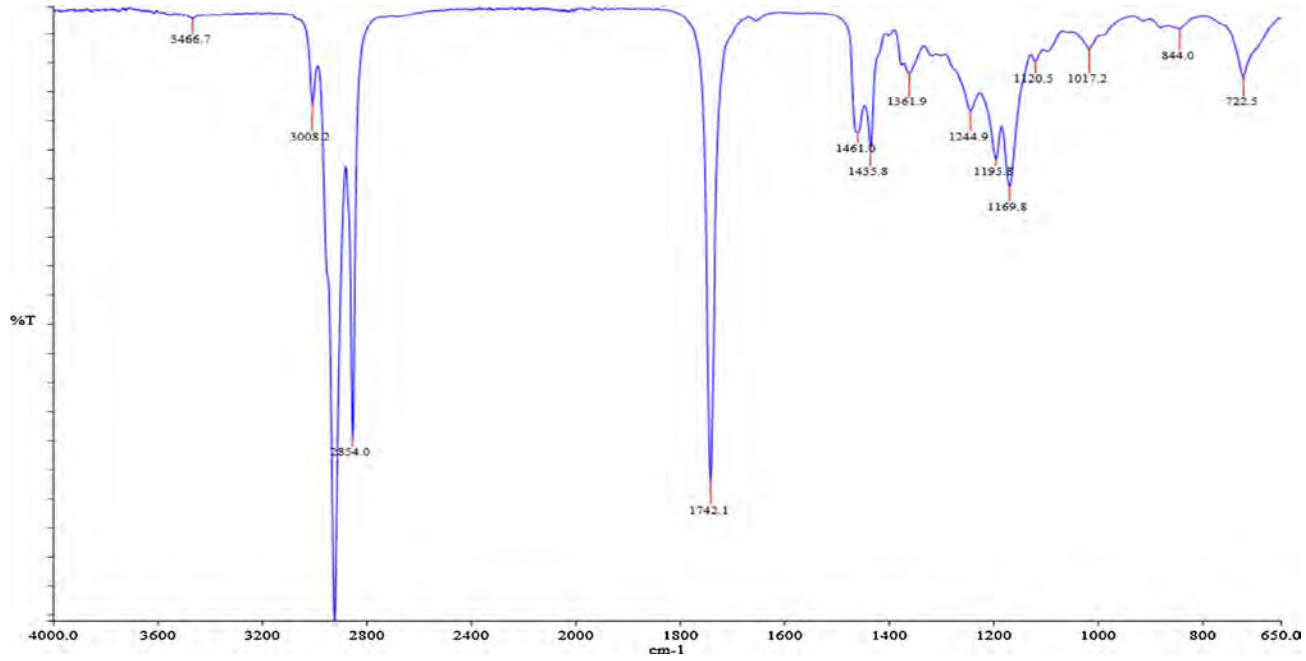

Fig. 8. Fourier transform infrared (FT-IR) spectrum of PSO methyl ester.

Table 8
Wavenumber, functional group, band assignment and absorption intensity of the absorption peaks detected in the FT-IR spectrum of PSO methyl ester.

Wavenumber (cm^{-1})	Group attribution	Vibration type	Absorption intensity
2924	=C−H	Asymmetric stretching vibration	Strong
2854	$-CH_2$	Symmetric stretching vibration	Strong
1742.1	−C=O	Stretching	Strong
1461	$-CH_2$	Shear-type vibration	Weak
1244.9	$-CH_3$	Bending vibration	Weak
1195.8	C−O−C	Anti-symmetric stretching vibration	Middling
1169.8	C−O−C	Anti-symmetric stretching vibration	Middling
1120.5	C−O−C	Anti-symmetric stretching vibration	Weak
1017.2	C−O−C	Anti-symmetric stretching vibration	Weak
722.5	$-CH_2$	Plane rocking vibration	Weak

level (65 °C) decreased biodiesel yield significantly to 85.03%. The high temperature and catalyst concentration may favour the triglycerides saponification and end up forming soap which may significantly affect biodiesel yield production [43]. From ANOVA results in Table 6, it was observed that the interaction between KOH catalyst concentration and reaction temperature is not significant.

3.3.3. Interaction effect of temperature and methanol:oil molar ratio

Fig. 6 shows that increase in reaction temperature decreases the biodiesel yield. Higher temperatures (above 45 °C) decelerated the transesterification process resulting in less biodiesel yield production. Methanol:oil molar ratio also played an important role in increasing the biodiesel yield. The optimum methanol:oil molar ratio was found to be 10:1 and decreasing the molar ratio (< 10) lowered the biodiesel yield. At the lower reaction temperature (45 °C), biodiesel yield was the highest (96.48%) with an increased molar ratio (10:1). The overall biodiesel yield decreased significantly (85.03%) when the reaction temperature reached 65 °C. The main reason for lower biodiesel yield is the volatilization of methanol at 65 °C [36]. It can thus be concluded that the reaction temperature is a significant factor in biodiesel production. The optimum reaction temperature was identified to be 45 °C. From ANOVA results in Table 6, it was observed that the interaction between reaction temperature and methanol:oil molar ratio is significant.

Methanol:oil molar ratio was the most significant process variable that affected PSO biodiesel yield as indicated by the highest F-values in the ANOVA results (Table 6). The optimum conditions are reaction temperature 45 °C, KOH Catalyst concentration 1 wt% and methanol: oil molar ratio 10:1 and optimum biodiesel yield was predicted to be 96.48%. In order to validate the predicted optimum values, experiments were carried out at these optimum conditions and the experimental values (96.48%) closely matches the predicted values (96.12%) from the regression model.

3.4. Properties and qualities of PSO methyl ester

The properties of produced PSO methyl ester is compared with other non-edible methyl esters and petro diesel according to ASTM D6751 and EN14214 standard in Table 7. The properties and qualities of PSO methyl ester adhere with the international standards such as American standard ASTM D6751 and European Union EN14214. American standard ASTM D6751 identifies that the parameters of the pure biodiesel (B100) should satisfy before being used as a blend with diesel or pure fuel. Whereas European Union EN14214 describes the minimum requirements for FAME [44]. Density is one of the important property of biodiesel that influences the efficiency of fuel atomization in airless combustion systems [45]. According to ASTM and EN standard, density of methyl ester at 15 °C should be between 860 and 900 kg/m^3. The density of PSO and Karanja was found to be 840 and 931 kg/m^3 respectively whereas petro diesel was found to be 827.2 kg/m^3. Generally methyl ester or biodiesel fuel has slightly higher density than petro diesel fuel. The viscosity of methyl ester is ranged from 1.9 to 6.0 $m^2 s^{-1}$ and all methyl esters in Table 7 fulfils this requirement. Acid values of methyl ester can be very vital as it can affect and cause corrosion of internal combustion engine and some other metal parts. Therefore both ASTM and EN standard only approves a maximum acid value of 0.5 mg KOH/g. All methyl esters except Neem met the standards. Higher heating value is another important properties in the

selection of any fuel. It is noticed that all methyl esters have slightly less heating value than petro diesel although they are within the international standards. According to ASTM standard flash point should be 100–170 °C and most of methyl esters in Table 7 met that requirement as well. Oxidation stability is an indication of the degree of oxidation and can determine the need for antioxidants. Low oxidation stability can affect the quality of any biodiesel [46]. PSO methyl ester has oxidation stability of 5.61 h which fall in range of both ASTM and EN standards 3–6 h. Biodiesel with poor oxidation stability such as tobacco, cottonseed and moringa can be easily remedied by adding antioxidants such as butylated hydroxytoluene (BHT) and butylated hydroxyanisole (BHA), synthetic antioxidants such as di-tertbutylhydroquinone and poly (1,2-dihydro-2,2,4-tri methylquinoline) and natural oxidants such as sage and thyme extracts [47].

The chromatogram of PSO methyl ester shows the presence of derivatives of C16:0 (palmitic acid), C18:0 (stearic acid), C18:1 (oleic acid), C18:2 (linoleic acid), C18:3 (linolenic acid), C20:0 (eicosenoic acid), C22:1 (behenic acid) and C22:2 (erucic acid) as shown in Fig. 7. The chromatogram of PSO biodiesel confirmed the formation of methyl ester.

3.5. Fourier transform infrared analysis (FTIR)

PSO biodiesel was analysed using FT-IR to identify the characteristic peaks of different methyl esters. The sample PSO methyl ester was applied directly to the Attenuated Total Reflectance (ATR) window and spectra were recorded (four scans, 4000–650 cm^{-1}) at approximately 40% transmission. Fig. 8 shows the FT-IR spectrum of the PSO methyl ester.

Table 8 presents the wavenumber, functional group, band assignment and absorption intensity of absorption peaks detected in the FT-IR spectrum of PSO methyl ester. This result reflects the conversion of triglycerides to methyl ester. The peak of stretching C=O is 1742.1 cm^{-1} located in the region of 1800–1700 cm^{-1} which is common for esters. The region of 1500–900 cm^{-1} is the major region of the spectrum from PSO methyl ester (known as 'fingerprint') and the peak at 1244.9 cm^{-1} corresponds to the bending vibration of $-CH_3$ [5].

4. Conclusions

Papaya seed oil is a promising source of biodiesel production as it is not currently used as edible oil. The purpose of this study was to test if this oil can be used as an alternative source for biodiesel to optimise the conditions needed for producing PSO biodiesel production and to identify the optimum reaction conditions for an alkaline transesterification process. A response surface method based Box-Behnken design was employed to understand the relation between the process variables and biodiesel yield. The Box-Behnken design was used to determine the experimental plan/matrix to optimize the papaya biodiesel conversion process. In that design matrix, three parameters were each varied within different ranges to predict biodiesel yield. A statistical model was derived and used to predict optimum conditions for transesterification methanol: oil molar ratio, catalyst concentration, and reaction temperature were 10:1, 1 wt% and 45 °C respectively. Conditions of reaction time and reaction agitation speed were fixed at 60 min and 600 rpm respectively. Based on these conditions, the highest biodiesel yield was predicted at 96.12% volume of the oil. The experimental maximum yield was obtained at 96.48% under these same parameters. ANOVA statistics indicated that the methanol:oil molar ratio has a significant effect on the papaya biodiesel yield. Physicochemical properties of the papaya biodiesel meet both ASTM D6751 and EN14214 standards. Finally, Papaya biodiesel could be used as a potential alternative to diesel and is an environment-friendly fuel.

References

[1] Jahirul M, Koh W, Brown R, Senadeera W, Hara I, Moghaddam L. Biodiesel production from non-edible beauty leaf (*Calophyllum inophyllum*) oil: process optimization using response surface methodology (RSM). Energies 2014;7(8):5317.
[2] Jahirul M, Brown R, Senadeera W, Hara I, Ristovski Z. The use of artificial neural networks for identifying sustainable biodiesel feedstocks. Energies 2013;6(8):3764.
[3] Azad AK, Rasul MG, Khan MMK, Sharma SC, Hazrat MA. Prospect of biofuels as an alternative transport fuel in Australia. Renew Sustain Energy Rev 2015;43:331–51.
[4] Dharma S, Masjuki HH, Ong HC, Sebayang AH, Silitonga AS, Kusumo F, et al. Optimization of biodiesel production process for mixed *Jatropha curcas–Ceiba pentandra* biodiesel using response surface methodology. Energy Convers Manage 2016;115:178–90.
[5] Dincer K. Lower emissions from biodiesel combustion. Energy Sources, Part A: Recovery Utilization Environ Effects 2008;30(10):963–8.
[6] Mosarof MH, Kalam MA, Masjuki HH, Alabdulkarem A, Ashraful AM, Arslan A, et al. Optimization of performance, emission, friction and wear characteristics of palm and *Calophyllum inophyllum* biodiesel blends. Energy Convers Manage 2016;118:119–34.
[7] Ganjehkaviri A, Mohd Jaafar M, Hosseini S, Musthafa A. Performance evaluation of palm oil-based biodiesel combustion in an oil burner. Energies 2016;9(2):97.
[8] Rahman SMA, Masjuki HH, Kalam MA, Abedin MJ, Sanjid A, Rahman MM. Assessing idling effects on a compression ignition engine fueled with Jatropha and Palm biodiesel blends. Renew Energy 2014;68:644–50.
[9] Mofijur M, Hazrat MA, Rasul MG, Mahmudul HM. Comparative evaluation of edible and non-edible oil methyl ester performance in a vehicular engine. Energy Proc 2015;75:37–43.
[10] Bhuiya MMK, Rasul MG, Khan MMK, Ashwath N, Azad AK. Prospects of 2nd generation biodiesel as a sustainable fuel—Part: 1 selection of feedstocks, oil extraction techniques and conversion technologies. Renew Sustain Energy Rev 2016;55:1109–28.
[11] Wong CS, Othman R. Biodiesel production by enzymatic transesterification of papaya seed oil and rambutan seed oil. Int J Eng Technol (IJET) 2014;6(6):2773–7.
[12] Jamil F, Al-Muhtaseb AaH, Al-Haj L, Al-Hinai MA, Hellier P, Rashid U. Optimization of oil extraction from waste "Date pits" for biodiesel production. Energy Convers Manage 2016;117:264–72.
[13] Pramanik K. Properties and use of *Jatropha curcas* oil and diesel fuel blends in compression ignition engine. Renew Energy 2003;28(2):239–48.
[14] Ramadhas AS, Jayaraj S, Muraleedharan C. Characterization and effect of using rubber seed oil as fuel in the compression ignition engines. Renew Energy 2005;30(5):795–803.
[15] Lin L, Cunshan Z, Vittayapadung S, Xiangqian S, Mingdong D. Opportunities and challenges for biodiesel fuel. Appl Energy 2011;88(4):1020–31.
[16] Lim S, Teong LK. Recent trends, opportunities and challenges of biodiesel in Malaysia: an overview. Renew Sustain Energy Rev 2010;14(3):938–54.
[17] Mofijur M, Masjuki HH, Kalam MA, Atabani AE. Evaluation of biodiesel blending, engine performance and emissions characteristics of *Jatropha curcas* methyl ester: Malaysian perspective. Energy 2013;55:879–87.
[18] Mofijur M, Masjuki HH, Kalam MA, Atabani AE, Fattah IMR, Mobarak HM. Comparative evaluation of performance and emission characteristics of *Moringa oleifera* and Palm oil based biodiesel in a diesel engine. Ind Crops Prod 2014;53:78–84.
[19] Mihaela P, Josef R, Monica N, Rudolf Z. Perspectives of safflower oil as biodiesel source for South Eastern Europe (comparative study: Safflower, soybean and rapeseed). Fuel 2013;111:114–9.
[20] Ogaga Ighose B, Adeleke IA, Damos M, Adeola Junaid H, Ernest Okpalaeke K, Betiku E. Optimization of biodiesel production from *Thevetia peruviana* seed oil by adaptive neuro-fuzzy inference system coupled with genetic algorithm and response surface methodology. Energy Convers Manage 2017;132:231–40.
[21] Onoji SE, Iyuke SE, Igbafe AI, Nkazi DB. Rubber seed oil: a potential renewable source of biodiesel for sustainable development in sub-Saharan Africa. Energy Convers Manage 2016;110:125–34.
[22] Teo SH, Rashid U, Taufiq-Yap YH. Biodiesel production from crude *Jatropha curcas* oil using calcium based mixed oxide catalysts. Fuel 2014;136:244–52.
[23] Agunbiade FO, Adewole TA. Methanolysis of *Carica papaya* seed oil for production of biodiesel. J Fuels 2014;2014:6.
[24] Mohan A, Kollam K, SS SS. Emission analysis of the biodiesel from papaya and chicken blends. Int J Inf Futuristic Res 2015;2(7):6.
[25] De Melo MLS, Santos NA, Rosenhaim R, Souza AG, Athayde Filho PF. Use of thermal analysis techniques for evaluation of the stability and chemical properties of papaya biodiesel (*Carica papaya* L.) at low temperatures. J Therm Anal Calorim 2011;106(3):831–6.
[26] Sinaga EJ, Daryono ED. Rapid in situ transesterification of papaya seeds to biodiesel with the aid of co-solvent. J Renew Energy Res 2017;7(1):379–85.
[27] Sharma SK, Mitra SK, Saran S. Papaya production in India - history, present status and future prospects. Leuven (Belgium): International Society for Horticultural Science (ISHS); 2016.
[28] Farming A. Agri farming # 1 source for farming in India; 2017. Available from: < http://www.agrifarming.in/papaya-farming > [accessed 13.10.17].
[29] Salunkhe DK. Kadam SS. Handbook of fruit science and technology: production, composition, storage, and processing. Taylor & Francis; 1995.
[30] Chan HT, Heu RA, Tang CS, Okazaki EN, Ishizaki SM. Composition of papaya seeds. J Food Sci 1978;43(1):255–6.
[31] Hamze H, Akia M, Yazdani F. Optimization of biodiesel production from the waste cooking oil using response surface methodology. Process Saf Environ Prot

2015;94:1–10.
[32] World MO. World map of top ten papaya producing countries; 2014. Available from: < https://www.mapsofworld.com/world-top-ten/papaya-producing-countries.html > [accessed 31.10.17].
[33] Marfo EK, Oke OL, Afolabi OA. Chemical composition of papaya (*Carica papaya*) seeds. Food Chem 1986;22:259–66.
[34] Puangsri T, Abdulkarim SM, Ghazali HM. Properties of *Carica papaya* L. (papaya) seed oil following extractions using solvent and aqueous enzymatic methods. J Food Lipids 2004;12:62–76.
[35] Ezekannagha CB, Ude CN, Onukwuli OD. Optimization of the methanolysis of lard oil in the production of biodiesel with response surface methodology. Egypt J Pet 2017. [in press].
[36] Muthukumaran C, Praniesh R, Navamani P, Swathi R, Sharmila G, Manoj Kumar N. Process optimization and kinetic modeling of biodiesel production using non-edible *Madhuca indica* oil. Fuel 2017;195:217–25.
[37] Bello EI, Ogedengbe TI, Lajide L, Daniyan IA. Optimization of process parameters for biodiesel production using response surface methodology. Am J Energy Eng 2016;4(2):8–16.
[38] Onukwuli DO, Emembolu LN, Ude CN, Aliozo SO, Menkiti MC. Optimization of biodiesel production from refined cotton seed oil and its characterization. Egypt J Pet 2017;26(1):103–10.
[39] Rahman Md Mofijur, Rasul M, Hassan Nur Md Sayeed, Hyde Justin. Prospects of biodiesel production from macadamia oil as an alternative fuel for diesel engines. Energies 2016;9(403).
[40] Islam MA, Brown RJ, Brooks PR, Jahirul MI, Bockhorn H, Heimann K. Investigation of the effects of the fatty acid profile on fuel properties using a multi-criteria decision analysis. Energy Convers Manage 2015;98:340–7.
[41] Atabani AE, César AdS. *Calophyllum inophyllum* L. -a prospective non-edible biodiesel feedstock. Study of biodiesel production, properties, fatty acid composition, blending and engine performance. Renew Sustain Energy Rev 2014;37(Suppl. C):644–55.
[42] Silva GF, Camargo FL, Ferreira ALO. Application of response surface methodology for optimization of biodiesel production by transesterification of soybean oil with ethanol. Fuel Process Technol 2011;92(3):407–13.
[43] Vicente G, Martínez M, Aracil J. Optimisation of integrated biodiesel production. Part I. A study of the biodiesel purity and yield. Biores Technol 2007;98(9):1724–33.
[44] Silitonga AS, Masjuki HH, Mahlia TMI, Ong HC, Chong WT, Boosroh MH. Overview properties of biodiesel diesel blends from edible and non-edible feedstock. Renew Sustain Energy Rev 2013;22(Suppl. C):346–60.
[45] Silitonga AS, Ong HC, Mahlia TMI, Masjuki HH, Chong WT. Biodiesel conversion from high FFA crude *Jatropha curcas*, *Calophyllum inophyllum* and *Ceiba pentandra* oil. Energy Proc 2014;61(Suppl C):480–3.
[46] Hasni K, Ilham Z, Dharma S, Varman M. Optimization of biodiesel production from *Brucea javanica* seeds oil as novel non-edible feedstock using response surface methodology. Energy Convers Manage 2017;149(Suppl. C):392–400.
[47] Amini Z, Ong HC, Harrison MD, Kusumo F, Mazaheri H, Ilham Z. Biodiesel production by lipase-catalyzed transesterification of *Ocimum basilicum* L. (sweet basil) seed oil. Energy Convers Manage 2017;132(Suppl. C):82–90.
[48] Atabani AE, Silitonga AS, Badruddin IA, Mahlia TMI, Masjuki HH, Mekhilef S. A comprehensive review on biodiesel as an alternative energy resource and its characteristics. Renew Sustain Energy Rev 2012;16(4):2070–93.

Declaration of Co-authorship and Contribution

Research Division

CHAPTER 4: Part B- Biodiesel Production Process Optimisation

Title of the paper	Optimisation of second-generation biodiesel production from Australian native stone fruit oil using response surface method
Full bibliographic reference	Anwar, M., M. Rasul, N. Ashwath, and M. Rahman, Optimisation of Second-Generation Biodiesel Production from Australian Native Stone Fruit Oil Using Response Surface Method. Energies, 2018. 11(10): p. 2566. https://www.mdpi.com/1996-1073/11/10/2566
Status	Published

Nature of Candidate's Contribution, including percentage of total
I was responsible for collected oil, produced and characterised biodiesel, optimised the biodiesel, and drafted the manuscript. [80%]

Nature of all Co-Authors' Contributions, including percentage of total
My co-authors, Prof. Mohammad Rasul, A/Professor Nanjappa Ashwath, and Dr. Md Mofijur Rahman, were designed the experimentation, reviewed, revised and improved the manuscript. [20%]

Has this paper been submitted for an award by another research degree candidate (Co- Author), either at CQUniversity or elsewhere? (if yes, give full details)
No

Candidate's Declaration

I declare that the publication above meets the requirements to be included in the thesis as outlined in the Research Higher Degree Theses Policy and Procedure.

Mohammad Anwar

energies

MDPI

Article

Optimisation of Second-Generation Biodiesel Production from Australian Native Stone Fruit Oil Using Response Surface Method

Mohammad Anwar [1], Mohammad G. Rasul [1], Nanjappa Ashwath [2] and Md Mofijur Rahman [1,*]

[1] School of Engineering and Technology, Central Queensland University, North Rockhampton, Queensland 4702, Australia; m.anwar@cqu.edu.au (M.A.); m.rasul@cqu.edu.au (M.G.R.)

[2] School of Health, Medical and Applied Sciences, Central Queensland University, North Rockhampton, Queensland 4702, Australia; n.ashwath@cqu.edu.au

* Correspondence: m.rahman@cqu.edu.au or m.anwar@cqu.edu.au; Tel.: +617-4930-6371

Received: 13 August 2018; Accepted: 25 September 2018; Published: 26 September 2018

Abstract: In this study, the production process of second-generation biodiesel from Australian native stone fruit have been optimised using response surface methodology via an alkali catalysed transesterification process. This process optimisation was performed varying three factors, each at three different levels. Methanol: oil molar ratio, catalyst concentration (wt %) and reaction temperature were the input factors in the optimisation process, while biodiesel yield was the key model output. Both 3D surface plots and 2D contour plots were developed using MINITAB 18 to predict optimum biodiesel yield. Gas chromatography (GC) and Fourier transform infrared (FTIR) analysis of the resulting biodiesel was also done for biodiesel characterisation. To predict biodiesel yield a quadratic model was created and it showed an R^2 of 0.98 indicating the satisfactory performance of the model. Maximum biodiesel yield of 95.8% was obtained at a methanol: oil molar ratio of 6:1, KOH catalyst concentration of 0.5 wt % and a reaction temperature of 55 °C. At these reaction conditions, the predicted biodiesel yield was 95.9%. These results demonstrate reliable prediction of the transesterification process by Response surface methodology (RSM). The results also show that the properties of the synthesised Australian native stone fruit biodiesel satisfactorily meet the ASTM D6751 and EN14214 standards. In addition, the fuel properties of Australian native stone fruit biodiesel were found to be similar to those of conventional diesel fuel. Thus, it can be said that Australian native stone fruit seed oil could be used as a potential second-generation biodiesel source as well as an alternative fuel in diesel engines.

Keywords: response surface methodology; RSM; second-generation biodiesel; stone fruit; optimisation; biodiesel testing; transesterification

1. Introduction

Global climate change and the resulting desire for renewable energy sources has generated the interests for using biofuel in the transport sector [1]. Due to the higher production of biofuel in recent years, it currently contributes 1.5% global transportation fuel. It has been reported that nearly 40% of the total worldwide biofuel supply comes from emerging and developing countries. However, the expansion of biofuel production around the world has raised major concerns, for example the existence of several first-generation biofuels. Biofuels that are produced from edible sources are termed first-generation biofuels [2], and these have been increasingly questioned over some concerns such as food-fuel controversy, environmental pollution, and climate change. The increasing concern regarding the sustainability of several first-generation biofuels has led to investigations into the potential of producing biodiesel from non-food crops which are termed as second-generation biodiesel.

The potential benefits offered by the second-generation biodiesels are that they consume waste oils, make use of abandoned land and do not compete with food crops [3].

In addition, second-generation biofuel from locally available sources can play a great role in economic development of rural and emerging region of a country [4]. Despite significant socio-economic advantages and continuous support from government and non-government organisations, the market for biofuel production around the world has not expanded very much over the last few years. Many countries have announced second-generation biofuel support policies, e.g., the United States has adopted the policies to produce 60 billion litres by 2022 and the European Union set their target to use 20% renewable energy in the transport sector by 2020 [5]. Both the US and EU policies could play an important role for the worldwide biofuel development because of their market size and considerable amount of biofuel imports. In addition, the Australian Federal Government and its State Governments have developed relevant policies to promote a sustainable biofuel industry to ensure Australian's long-term energy security. Leading oil companies such as Caltex, Shell, BP, and Exxon Mobile are also coming forward in second-generation biofuel research with more investment. A few plants with research activities are going to be established soon in emerging countries.

Biodiesel is one of the biofuels and has proved its potential as an alternative fuel worldwide. Biodiesel is biodegradable, renewable and environmentally friendly [6,7]. The feedstock selection of biodiesel is very important as 75% of the total cost of biodiesel production is associated with obtaining feedstocks alone. A high oil yield of any feedstock ensures a commercial scale biodiesel production at reasonable prices [8]. Feedstock security of supply, feedstock cost of supply and feedstock storage are the important factors to consider when choosing the biodiesel feedstock [9]. In addition, biodiesel should be produced from the feedstock that is consistently available, economically viable and locally available. Currently, the major feedstocks for biodiesel production in Australia are waste cooking oil, animal tallow, macadamia, beauty leaf, canola and mustard oils [10]. However, stone fruit such as *Prunus armeniaca* L. is widely cultivated in Australia, and it yields 22–38% of kernels which contain up to 54.2% oil. Australia produces about 100,000 tons of summer stone-fruit from October to April each year and, in 2008, about 16,917 tons of *Prunus armeniaca* L. fruit were produced from all six mainland states in Australia. This could therefore be a potential second-generation biodiesel feedstock in Australia. The main aim of this research was to investigate and optimise the production process of second-generation biofuel from this Australian native feedstock as the research on it is still far behind that into other feedstocks. This biodiesel could overcome the limitations associated with first-generation biodiesels and be used as an alternative to conventional fossil fuels.

2. Literature Review

Stone fruit is similar to a small peach, generally 1.5–2.5 cm in diameter, with its colour varying from yellow to orange or red. Its single seed is enclosed in a hard stony shell. During fruit processing, the seeds are discarded due to the presence of hydro-cyanic acid [11]. To utilise this waste product, it is important to optimise the procedures involved in oil extraction and its conversion into biodiesel.

Many researchers [12–17] have optimised the production of biodiesel from different first- and second-generation feedstocks using various methods. For example, Saydu et al. [13] optimised the process of biodiesel production from hazelnut and sunflower oil using single step transesterification with methanol, and employing potassium hydroxide as a catalyst. Razack and Duraiarasan [12] optimised the waste cooking oil biodiesel production process using response surface methodology using encapsulated mixed enzyme as a catalyst. Dharma et al. [17] optimised the biodiesel production process of *Jatropha curcas* and *Ceiba pentandra* oil using response surface methodology as also did Ong et al. [16] for the *Calophyllum inophyllum* biodiesel production process.

A few studies have been done on the optimisation of the stone fruit oil (SFO) biodiesel production process but none of them used any statistical modelling. For instance, Gumus et al. [18] used alkali transesterification with methanol and potassium hydroxide catalyst for producing SFO methyl

ester. Abdelrahman [19] produced SFO biodiesel via alkali transesterification with 0.75% potassium hydroxide catalyst and at a methanol: oil molar ratio of 6:1. Faizan et al. [20] showed that the wild *Prunus Armeniaca* L. oil can be transesterified by a single step process via the use of sodium hydroxide catalyst at a methanol: oil molar ratio of 6:1, and reported a biodiesel yield of 93%. Ashok et al. [21] performed single step alkali transesterification using 1% potassium hydroxide as a catalyst at 55 °C and 60 min reaction time with a constant stirring at 400 rpm and obtained a biodiesel yield of 96.5%. Thus, many process parameters, including reaction temperature, catalyst type and catalyst concentration, type of alcohol used, the oil to methanol molar ratio, reaction time and agitation speed have been found to influence the optimum transesterification process [22–26]. From the above literature, it is obvious that no/limited investigation has been done on the optimisation of second-generation biodiesel production process from *Prunus Armeniaca* L. oil using any statistical modelling. Thus, this study has explored optimisation of the biodiesel production processes from Australian native stone fruit oil using response surface methodology.

3. Materials and Methods

3.1. Materials

Stone fruit (*Prunus armeniaca* L. species) seed oil was purchased from a local producer named Chromium Group Pty Ltd. of Eumundi, Queensland, Australia. The chemicals used in this study were methanol (99.9% purity), potassium hydroxide (KOH pellets, 99% purity) and sodium hydroxide (NaOH pellets, 99% purity). All were of analytical reagent grade (AR) and were procured from the School of Engineering and Technology, Central Queensland University, Rockhampton, Australia. A three-neck laboratory reactor (1 L) along with a reflux condenser and a thermocouple placed on a magnetic heater/stirrer were used in the SFO biodiesel conversion experiments. In this experiment, methanol, KOH, NaOH and Whatman 541 grade filter paper (pore size 22 μm) were used.

3.2. Oil Extraction

The stone fruits were collected and the fleshy parts were separated manually for drying purposes. The seeds were separated for kernel collection and oil extraction. For easy breaking of the hard shell, seeds were softened by immersing in water for 10–20 min. The broken shell can be used as fertilizer or firewood after the oil extraction process [27]. Kernels were separated from the broken shells and were crushed using a pestle and mortar and sieved through a 40 mesh or 0.8 mm sieve [19,28]. The ground kernel was placed in a Soxhlet apparatus and the oil was extracted using petroleum ether (40–60 °C) over 6–8 h until the extraction was completed [19]. After oil extraction, the petroleum ether was evaporated using a rotary evaporator at 25 °C [29]. The oil was placed in an oven at 60 °C for 60 min to remove the remaining solvent. The oil was filtered using Whatman 541 filter paper. After filtration, the SFO was kept in a sealed container for characterisation. The oil yield was calculated using Equation (1).

$$\text{Oil Yield } (\%\text{wt/wt dry kernels}) = \frac{\text{weight of oil extracted } (\text{g})}{\text{weight of dry kernels used } (\text{g})} \times 100 \quad (1)$$

3.3. Biodiesel Production

The acid value of raw SFO was determined as 1.65 mg KOH/g. After transesterification using KOH catalyst transesterification, the acid value of SFO biodiesel was found to be 0.25 mg KOH/g. This trial experiment suggested that only the single stage alkyl catalyst transesterification process was satisfactory for SFO biodiesel production. Thus, in each experiment, the experiment was performed by reacting a known quantity of SFO with methanol and the catalyst.

Initially, the SFO was poured into a three-neck laboratory reactor and heated to the desired temperature. The measured quantities (molar basis) of methanol and catalyst (KOH) were poured into a separate beaker and stirred vigorously using a magnetic stirrer at 50 °C at 600 rpm for 10 min

to produce methoxide. This solution was slowly poured into the three-neck reactor containing SFO. The blend was agitated continuously at 600 rpm and the temperature and reaction time were varied as per the experimental design. At the end of the transesterification reaction, the blend was transferred into a separating funnel. Although the separation of glycerol and biodiesel occurred instantaneously, the funnel was left undisturbed for 24 h. Two separate liquid phases were formed, with the top layer being methyl ester (biodiesel) and the bottom layer of red viscous glycerol and impurities. The bottom layer was drained off while the top layer was collected and washed with warm (50 °C) distilled water. This moist biodiesel was then heated to 110 °C for 15 min to remove residual water that would have been retained by the biodiesel during the washing process. The Whatman® qualitative Grade 1 filter paper was used to filter the biodiesel and finally stored in an airtight container at room temperature until its characterisation. Biodiesel yield was calculated using Equation (2) and its composition was determined using a Gas Chromatogram [22]. The graphical illustration of the SFO production process is shown in Figure 1.

$$\text{SFO Biodiesel Yield} = \text{FAME percent from GC analysis} \times \frac{\text{weight of SFO biodiesel}}{\text{weight of Stone fruit oil}} \quad (2)$$

Figure 1. Graphical representation of producing biodiesel from SFO biodiesel.

3.4. Physicochemical Characterisation of SFO

This section discusses the international standards used in characterising the SFO biodiesel and its composition via Gas Chromatography (GC) and Fourier Transform Infrared (FTIR) spectroscopy.

3.4.1. Fuel Properties

The physicochemical properties and fatty acid compositions of crude SFO and SFO biodiesel were tested according to ASTM and EN standards. The properties studied were density at 15 °C (ASTM D1298), kinematic viscosity at 40 °C (ASTM D445), acid value (ASTM D664), calorific value (ASTM D240), flash point (ASTM D93) and oxidation stability (ASTM D2274). The fatty acid compositions were determined using a gas chromatograph according to EN 14103.

Fuel properties calculated based on the fatty acid composition of the SFO biodiesel were cetane number (CN), saponification value (SV), iodine value (IV), long-chain saturated factor (LCSF) and degree of unsaturation (DU). The numerical calculations were determined using the following equations [30]:

$$\mathrm{CN} = 46.3 + \left(\frac{5458}{\mathrm{SV}}\right) - (0.225 \times \mathrm{IV}) \tag{3}$$

$$\mathrm{SV} = \sum \frac{(560 \times \mathrm{A_i})}{\mathrm{MW_i}} \tag{4}$$

$$\mathrm{IV} = \sum \frac{(254 \times \mathrm{D} \times \mathrm{A_i})}{\mathrm{MW_i}} \tag{5}$$

$$\begin{aligned}\mathrm{LCSF} = {} & 0.1 \times (\mathrm{C16:0\ wt\ \%}) + 0.5 \times (\mathrm{C18:0\ wt\ \%}) + 1 \times (\mathrm{C20:0\ wt\ \%}) \\ & + 1.5 \times (\mathrm{C22:0\ wt\ \%}) + 2.0 \times (\mathrm{C24:0\ wt\ \%})\end{aligned} \tag{6}$$

$$\mathrm{DU} = \sum \mathrm{MUFA} + (2 \times \mathrm{PUFA}) \tag{7}$$

where D indicates the number of double bonds, A_i is the percentage of each fatty acid in the FAME, and MW_i is the molecular mass of each component. MUFA denotes monounsaturated fatty acid and PUFA refers to polyunsaturated fatty acid. The degree of unsaturation was calculated using both MUFA and PUFA concentrations. Fatty acids of C16:0, C18:0, C20:0, C22:0 and C24:0 stand for palmitic acid, stearic acid, arachidic acid, behenic acid and lignoceric acid, respectively, and were used for measuring the long chain saturated factor.

3.4.2. Gas Chromatography

According to EN14103, a gas chromatograph (GC) (Thermo Scientific Trace 1310 GC) was used to determine the fatty acid composition of the SFO. 25 mg of the SFO biodiesel was dissolved in high purity hexane (10 mL). Then, this solution was poured to 2 mL auto-sampler vials. The equipment for the GC test included Thermo Scientific Trace 1310 GC with a split/split less (SSL) injector, flame ionisation detector, and TriPlus auto-sampler. At 240 °C, a 1 µL sample was injected in split mode (40:1) by maintaining a constant helium flow of 1.2 mL/min. The conditions for separating FAMEs were: using a BPX-70 column (60 m × 250 µm × 0.25 µm film) with a temperature program: 110 °C (4 min); 10 °C/min, 150 °C; 3.9 °C/min, 230 °C (5 min). In this study, SFO biodiesel individual components were identified by retention time compared to a standard FAME mixture that had certified concentrations, namely Supelco CRM18920 (FAME C8-C22). Chromeleon 7.2 software was used for data acquisition and processing.

3.4.3. Fourier Transform Infrared (FTIR) Spectroscopy

The various functional groups present in the crude oil and the biodiesel sample were determined with Fourier transform infrared (FTIR) spectroscopy. The Spectrum 100 FTIR spectrometer with a universal Attenuated total reflectance (ATR) sampling accessory (Perkin Elmer, Melbourne, Australia) was used to record ATR infrared spectra. SFO biodiesel samples were placed directly on the ATR window at approximately 40% transmission to record the spectra with four scans, 4000–650 cm^{-1}. After ATR correction, Spectrum 6.2.0 software was used to acquire data and processing.

3.5. Design of Experiments

Box-Behnken is one of the most commonly used responses surface methodology designs. This design was used for designing and statistical analysis of this experiment. The Box-Behnken design matrix was utilised to find the optimum conditions for maximum biodiesel yield production. The experimental optimisation was achieved via analysis of variance (ANOVA) using Minitab 18 software. The effects of process factors such as methanol: oil molar ratio, KOH catalyst concentration, and reaction temperature were tested. Using these three factors at three levels required a total of 15 runs for identifying the optimum conditions for transesterification. The coded symbols, ranges, and levels of the investigated factors are listed in Table 1. The design matrix for the three factors was varied at three levels, namely −1, 0 and +1. The range levels of the factors investigated were chosen by considering the initial tests carried out on the effect of individual factors on biodiesel yield as well as the operating limits of the biodiesel production process conditions as evidenced from the literature.

Table 1. Experimental range and levels coded for independent factors.

Factors/Variables	Unit	Symbol Coded	Range and Levels		
			−1	**0**	**+1**
Methanol: Oil ratio	mol/mol	M	4:1	5:1	6:1
KOH catalyst concentration	wt %	C	0.5	1.00	1.5
Temperature	°C	T	45	55	65

Methanol: oil molar ratio ranged from 4:1 to 6:1, catalyst concentrations were 0.5–1.5% by weight of oil and the reaction temperature was varied from 45 °C to 65 °C (boiling point of methanol). Once the experiments were completed, the response factor (biodiesel yield) was applied in a full quadratic model to correlate the response factor to the independent factors. The general form of the full quadratic model is shown in Equation (8).

$$Y = P_0 + P_1Q_1 + P_2Q_2 + P_3Q_3 + P_{1,2}Q_1Q_2 + P_{1,3}Q_1Q_3 + P_{2,3}Q_2Q_3 + P_{1,1}{Q_1}^2 + P_{2,2}{Q_2}^2 + P_{3,3}{Q_3}^2 \quad (8)$$

where Y is the response factor (biodiesel yield, %); P_0 is a constant; P_1, P_2, and P_3 are regression coefficients; $P_{1,1}$, $P_{1,2}$, $P_{1,3}$, $P_{2,2}$, $P_{2,3}$, and $P_{3,3}$ are quadratic coefficient; and Q_1, Q_2, and Q_3 are independent variables.

4. Results and Discussion

This section includes the results of the characterisation of both crude SFO and SFO biodiesel, fatty acid compositions of SFO biodiesel, optimisation of reaction conditions by response surface methodology and response surface plots for SFO biodiesel production.

4.1. Characterisation of Crude SFO

The properties of crude stone fruit seed oil used in this study were evaluated prior to the optimisation process. Physicochemical properties are the most important features to check the quality of any crude oil. The SFO was characterised by viscosity, density, specific gravity, acid value, calorific value, saponification number and iodine value. The properties of SFO from this study along with those from other studies and those of petro diesel were compared and are presented in Table 2. The density of the oil was found to be 910 kg/m^3 which matches with that reported in the literature. Again, the acid value of SFO was determined to be 1.65 mg KOH/g, indicating the presence of low levels of free fatty acids in the oil. The kinematic viscosity of the oil was found to be 34.54 m^2/s and the calorific value was 38.45 MJ/kg, which is within the values found in the literature [18]. Based on above results, it is clear that Australian native SFO oil have similar fuel properties including fatty acid, calorific value

and viscosity with the data of other researchers, thus it is expected that Australian native SFO may serve as a good feedstock for biodiesel production.

Table 2. Physical and chemical properties of SFO.

Properties	Units	SFO This Study	SFO [18]	SFO [21]	SFO [11]	Petro Diesel
Kinematic Viscosity @ 40 °C	m^2/s	34.54	34.82	20.53	26.22	3.23
Density	kg/m^3	910	920	913	916.6	827.2
Specific Gravity @ 15 °C	g/cm^3	0.91	0.91	0.91	0.91	0.83
Acid value	mg KOH/g	1.65		2.60	0.68	0.05
Calorific value	MJ/kg	38.4	39.6	31.5		45.3
Saponification number	mg KOH/g	173		188	187	
Iodine value	$mgI_2/100$ g	103		90	101	

4.2. Properties and Qualities of SFO Biodiesel

The physical and chemical properties of SFO biodiesel from this study, along with results from other researchers' work on SFO biodiesel, are compared with other non-edible biodiesels and petrodiesel in Table 3. It was found that all the properties and qualities of the SFO biodiesel fulfilled the international standards (USA ASTM D6751 and European Union EN14214). Many researchers [31–34] showed that densities of biodiesels do not vary considerably, as the density of methanol and oil are close to the density of produced biodiesel, which usually varies between 850 and 900 kg/m^3. The density of SFO and papaya seed oil (PSO) was found to be 855 and 840 kg/m^3 respectively, whereas that of petrodiesel was found to be 827.2 kg/m^3. Densities of other SFO biodiesels also matched with the international standards. Karanja biodiesel has a density of 931 kg/m^3, which is outside the ASTM and EN standards specification, thus limiting its efficiency of fuel atomisation in airless combustion systems [35]. However, other biodiesels (Table 3) have slightly higher densities than petrodiesel fuel, but they are within the range of the international standards. The viscosity of SFO biodiesel was determined to be 4.26 mm^2/s and other biodiesels (except Karanja) ranged from 1.9–6.0 mm^2/s and also fulfil the requirements of the standards. The viscosity of SFO biodiesels of other studies was found to be within the range as well. The acid values of biodiesels (except Neem) were also in line with requirements of ASTM and EN biodiesel standards which are less than 0.5 mg KOH/g. Higher acid values can cause corrosion of IC engines and internal metal parts. Cetane number is an important fuel property for diesel engines. A higher speed diesel engine works more efficiently with a fuel with a higher cetane number. A lower cetane number fuel has longer ignition delays providing more time to complete the combustion process. The cetane number of biodiesel increases with an increase in fatty acid proportion. Longer fatty acid chains and higher saturated fatty acid content will lead to a higher cetane number [36,37]. Moringa biodiesel has the highest cetane number of 67.1 compared with all other biodiesels in Table 3 and is within the international standard limit. All calorific values are lower than those of petrodiesel fuel (45.3 MJ/kg). The SFO biodiesel calorific value was found to be 39.64 MJ/kg in this study, thus meeting the minimum EN standard requirement of 35 MJ/kg. All other SFO biodiesels have similar calorific values as well. The flashpoint of this SFO biodiesel was found to be 105 °C, whereas the ASTM standard specifies 100–170 °C and petrodiesel fuel is 68.5 °C. This suggests that SFO biodiesel fuel is safer to handle and store than petroleum diesel. The iodine value for this SFO was recorded as 104.7 mgI_2 which met the range of the EN standard. The higher the iodine value, the more unsaturated double bonds are present in the methyl ester, leading to better biodiesel fuel quality. Biodiesel with higher oxidation stability is preferable as low oxidation stability can affect the quality of biodiesel [38]. This SFO biodiesel has an oxidation stability of 7.15 h, which falls above the minimum values of both the ASTM (minimum 3 h) and EN standards (minimum 6 h). Some biodiesels with poor oxidation stability such as Tobacco, Cottonseed, Jatropha and Moringa biodiesel can be easily remedied by adding antioxidants.

Table 3. Comparison of SFO biodiesel with other non-edible biodiesels.

Non-Edible Biodiesels	Density (kg/m^3)	Viscosity at 40 °C, mm^2/s	Acid Value, mg KOH/g	Cetane Number (CN)	Calorific Value, MJ/Kg	Flash Point, °C	Iodine Value (IV) $mgI_2/100$ g	Oxidation Stability (OS), h
SFO this study	855.0	4.26	0.25	50.45	39.64	105	104.70	7.15
SFO [18]	884.3	4.92			39.95	111		
SFO [21]	857.0	5.20	0.32	58.70	38.93	180	100.70	6.30
SFO [11]	879.4	4.21	0.08		39.12	170	100.66	
Petro diesel [39]	827.2	3.23	0.05	48.00	45.30	68.5	38.3	39.0
Tobacco [23,38]	888.5	4.23		51.60		165.4	136	0.80
PSO [39]	840.0	3.53	0.42	48.29	38.49	112	115.89	5.61
Jatropha [38]	879.5	4.80	0.40	51.60	39.23	135	104	2.30
Rapeseed [23]	882.0	4.43		54.40	37.00	170		7.60
Cottonseed [23]	875.0	4.07	0.16	54.13	40.43	150		1.83
Neem [23,38]	868.0	5.21	0.65		39.81	76		7.10
Karanja [38]	931.0	6.13	0.42	55.00	43.42	95		
Moringa [23]	883.0	5.00	0.18	67.1		160	74	2.3
ASTM D6751	880.0	1.9~6.0	maximum 0.5	minimum 47		93~170		minimum 3
EN14214	860~900	3.5~5.0	maximum 0.5	minimum 51	35	>120	maximum 120	minimum 6

4.3. The Fatty Acid Composition of SFO Biodiesel

The fatty acid composition of any biodiesel feedstock is an important fuel property. The fatty acid composition is highly dependent on the quality of the feedstock, its growth condition and the geographic location in which the plant has grown. The chromatogram of the SFO biodiesel produced in this study shows the existence of derivatives of C16:0 (palmitic acid), C18:0 (Stearic acid), C18:1 (oleic acid), C18:2 (linoleic acid), C18:3 (linolenic acid), and C22:1 (behenic acid) in Figure 2. GC chromatogram of SFO biodiesel ensured the formation of methyl ester.

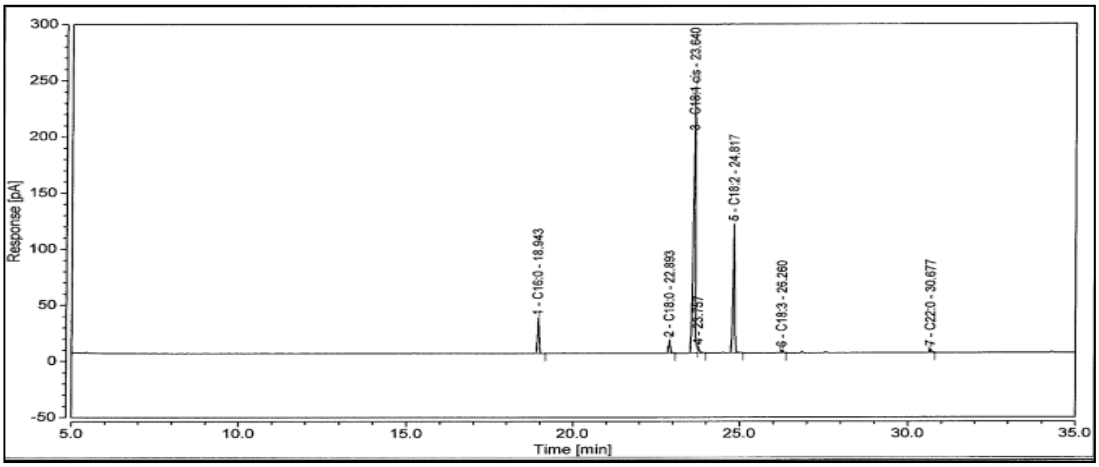

Figure 2. GC Chromatogram of SFO biodiesel.

The fatty acid compositional analysis of SFO biodiesel produced in this study is shown in Table 4, which indicates a high level (89.7%) of unsaturated fatty acids made up of both polyunsaturated and monounsaturated fatty acids. Saturated fatty acids such as palmitic acid, stearic acid, and behenic acid were found to be present at 5.85%, 2.51%, and 0.66%, respectively. Monounsaturated fatty acids (MUFA) such as oleic acid were found to be the dominant fatty acids (63.84%), whereas polyunsaturated fatty acids (PUFA) such as linoleic acid and linolenic acid were 25.34% and 0.51%, respectively. Pedro et al. [40] indicated that the degree of unsaturation of biodiesel did not significantly affect the engine performance and the start of injection, but it had a significant influence on combustion characteristics and emissions. The degree of unsaturation was recorded as 115.54% in this study. Altun [41] indicated that degree of unsaturation and cetane number of biodiesel could highly influence NO_x formation in biodiesel-fuelled diesel engines. Generally, higher degrees of saturation relate to higher cetane numbers of biodiesel. Unsaturated biodiesel produces higher NO_x and lowers HC

emissions than saturated biodiesels [40]. Furthermore, higher degrees of unsaturation in crude oil results in the production of less viscous biodiesel.

Table 4. The fatty acid composition of SFO.

Fatty Acids.	Formula	Molecular Weight	Structure	wt %
Palmitic	$C_{16}H_{32}O_2$	256	16:0	5.85
Stearic	$C_{18}H_{36}O_2$	284	18:0	2.51
Oleic	$C_{18}H_{34}O_2$	282	18:1	63.8
Linoleic	$C_{18}H_{32}O_2$	280	18:2	25.3
Linolenic	$C_{18}H_{30}O_2$	278	18:3	0.51
Behenic	$C_{22}H_{44}O_2$	340	22:0	0.66
Others				1.29
Total Saturated Fatty Acids (SFA)				9.02
Total Monounsaturated Fatty Acids (MUFA)				63.84
Total Polyunsaturated Fatty Acids (PUFA)				25.85
The degree of Unsaturation (DU)				115.5
Long Chain Saturated Factor (LCSF)				2.83

The distribution of the main fatty acids of some non-edible biodiesel feedstocks (including the SFO in this study and those from other research works on SFO) are shown in Table 5. Gas chromatography (GC) analysis of those biodiesels shows that the most abundant fatty acids are oleic acid, linoleic acid, and palmitic acid. The SFO biodiesel produced in this study shows similar results compared with those of previous research [18,21,28,42,43] on SFO biodiesel fuel. The presence of higher MUFA and PUFA can contribute to lower oxidative stability. As mentioned earlier, low oxidative stability could affect the quality of produced biodiesel. This low oxidation has a negative impact on both kinematic viscosity and acid value [44]. However, the presence of high contents of MUFA and PUFA ensures biodiesel with good fuel flow properties (especially in cold prone countries) compared with saturated fatty acids (SFA).

Table 5. Variations in the main fatty acid compositions of selected biodiesel feedstocks.

Non-Edible Biodiesels	Fatty Acids (% *w*/*w*)						Ref.
	C16:0	C18:0	C18:1	C18:2	C18:3	Others	
SFO this study	5.85	2.51	63.84	25.34	0.51	1.95	
SFO	5.62	1.27	67.31	24.68	0.08	1.04	[18]
SFO	4.20	2.32	71.00	20.15	1.20	1.13	[21]
SFO	3.87	0.92	67.21	27.12	0.11	0.77	[28]
SFO	3.79	1.01	65.23	28.92	0.14	0.91	[42]
SFO			66.20	28.20		5.60	[43]
PSO	6.07	3.13	47.73	37.25	1.78	4.04	[39]
Tobacco	8.90	3.50	14.10	70.10	1.00	2.40	[45]
Jatropha	16.20	8.20	38.40	36.80	0.40	0	[46]
Rapeseed	3.49	0.85	64.40	22.30	8.23	0.73	[47]
Cottonseed	28.70	0.90	13.00	57.40	0	0	[48]
Neem	12.00	10.00	61.00	16.00	0	1.00	[49]
Karanja	9.80	6.20	72.20	11.80	0	0	[50]
Moringa	6.50	6.00	72.20	1.0	0.65	13.65	[51]

The comparison of different non-edible biodiesels and SFO biodiesel fatty acid compositions are shown in Figure 3. It can be seen that MUFA-oleic acid (C18:1) dominates most of the feedstocks (except tobacco and cottonseed), followed by PUFA-linoleic acid (C18:2) and SFA-palmitic acid (C16:0). Both tobacco and cottonseed had high proportions of PUFA and it can be seen in Table 3 that their oxidation stabilities are very poor (0.8 h and 1.83 h, respectively). Oxidation occurs due to the presence of high proportions of unsaturated fatty acid chains and double bonds, i.e., PUFA in the parent molecule reacts

with oxygen as soon as it is exposed to air [23,52]. Therefore, biodiesels with high linoleic acid (C18:2) and linolenic acids (C18:3) such as tobacco and cottonseed tend to have lower oxidation stabilities.

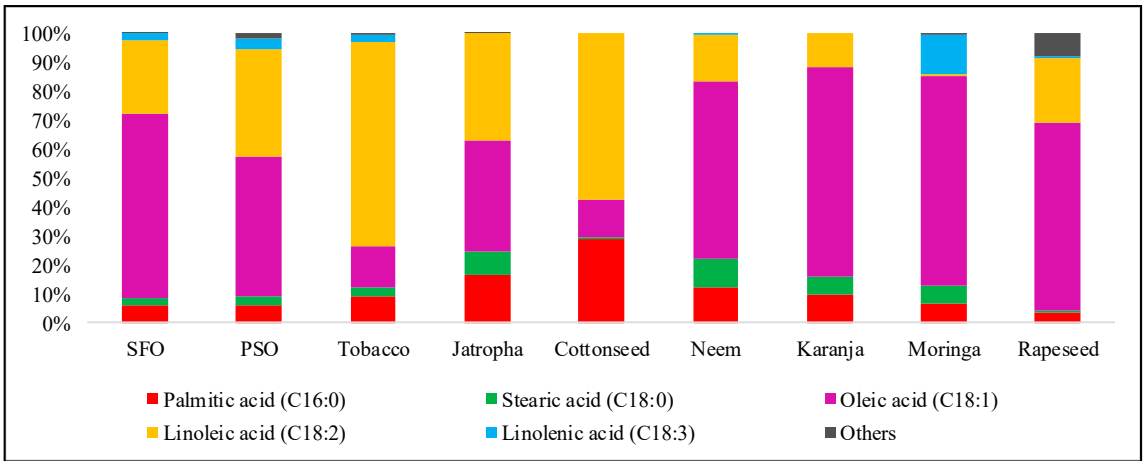

Figure 3. Comparison of the fatty acid composition of SFO and other non-edible vegetable oils.

Figure 4 shows the FTIR spectrum of the SFO methyl ester produced in this study. The advantages of using the FTIR method compared with GC is the ability to analyse whole samples, including precipitated fractions, without any further preparation [53].

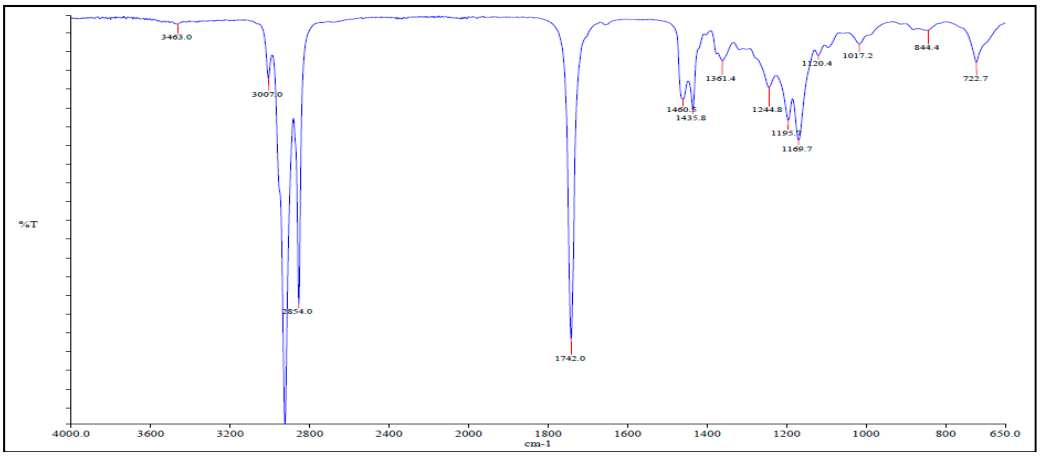

Figure 4. Fourier transforms infrared (FTIR) spectrum of SFO biodiesel.

The most important functional groups, wave number, band assignment and absorption intensity of absorption peaks detected in the FTIR spectrum of the SFO methyl ester are presented in Table 6. The peak at 1435.8 cm^{-1} corresponds to the asymmetric stretching of $–CH_3$ present in the SFO biodiesel sample, which is shown in Figure 4. The peak in the region of 2800–3000 cm^{-1} represents the CH_3 asymmetric stretching vibration. The peak of stretching of the carbonyl group (–C=O) is 1742 cm^{-1} located in the region of 1800–1700 cm^{-1} which is common for esters. The fingerprint region of 1500–900 cm^{-1} is the major spectrum from the SFO methyl ester which has a peak at 1244.8 cm^{-1}, corresponding to the bending vibration of $–CH_3$ [5]. These results reflect the conversion of triglycerides to methyl ester.

Table 6. Functional groups of SFO biodiesel detected in the FTIR spectrum.

Wavenumber (cm^{-1})	Group Attribution	Vibration Type	Functional Groups	Absorption Intensity
2924	=C–H	Asymmetric stretching vibration	Alkyl	Strong
2854	$–CH_2$	Symmetric stretching vibration	Aromatic	Strong
1742	–C=O	Stretching	Carbonyl	Strong
1460.5	$–CH_2$	Shear-type vibration	Alkanes	Weak
1244.8	$–CH_3$	Bending vibration	Alkanes	Weak
1195.7	C–O–C	Anti-symmetric stretching vibration	Ethers	Middling
1169.7	C–O–C	Anti-symmetric stretching vibration	Ethers	Middling
1120.4	C–O–C	Anti-symmetric stretching vibration	Ethers	Weak
1017.2	C–O–C	Anti-symmetric stretching vibration	Ethers	Weak
722.7	$–CH_2$	Plane rocking vibration	Aromatic	Weak

4.4. Optimisation of Reaction Conditions by RSM

The results of the Box–Behnken design model to optimise biodiesel production process parameters are shown in Table 7. In the transesterification experiments, the SFO biodiesel yield ranged from 75.2% to 95.8%. This design matrix also shows the experimental run order, experimental yields and predicted yields. These results show that the biodiesel yield varies with the production process. To avoid systematic errors, all run orders were randomised.

Table 7. Experimental matrix and results for Box-Behnken design model. The combination in italics shows the best combination for SFO biodiesel production.

Exp. Number	Run Order	M	C	T	Methanol: Oil (Molar Ratio)	KOH (wt %)	Temp (°C)	SFO Biodiesel Yield (%)	
								Experimental	Predicted
1	7	0	−1	−1	5	0.5	45	86.65	85.27
2	*13*	*1*	*−1*	*0*	*6*	*0.5*	*55*	*95.75*	*95.89*
3	14	0	0	0	5	1	55	91.65	92.98
4	12	−1	0	−1	4	1	45	80.34	80.85
5	15	1	0	−1	6	1	45	87.71	88.95
6	6	−1	−1	0	4	0.5	55	75.24	76.12
7	9	−1	1	0	4	1.5	55	82.27	82.13
8	11	0	0	0	5	1	55	93.65	92.98
9	5	0	0	0	5	1	55	93.65	92.98
10	8	0	1	−1	5	1.5	45	84.58	84.21
11	4	1	1	0	6	1.5	55	82.11	81.23
12	3	1	0	1	6	1	65	89.33	88.82
13	2	−1	1	1	4	1	65	79.30	78.06
14	1	0	−1	1	5	0.5	65	86.71	87.08
15	10	0	1	1	5	1.5	65	78.10	79.48

The predicted biodiesel yield values were generated from a quadratic regression model as obtained from Minitab software version 18.0 through response surface methodology (RSM) statistical analysis of the experimental data. The Minitab 18 program was used to calculate the effects of each parameter and its interactions with other parameters. The response parameter (biodiesel yield %) was correlated with other parameters using a full quadratic regression model shown in Equation (9). The model represents SFO biodiesel predicted yield (Y) as a function of methanol: oil molar ratio (M), catalyst concentration (wt %) (C) and reaction temperature (T).

$$Y = 92.983 + 4.719M - 2.161C - 0.730T - 4.490M^2 - 4.650C^2 - 4.323T^2 - 5.168MC + 0.665MT - 1.635CT \quad (9)$$

Figure 5a shows the line of a perfect fit with points corresponding to zero error as indicated by the comparison of experimental and predicted biodiesel yields. Points closer to the straight line indicate a good agreement between the experimental and predicted values. Figure 5b shows that there is an adequate correlation between RSM predicted values and experimental values, which verifies the acceptability of the model. The model represents a relatively good description of the experimental data regarding the SFO yield.

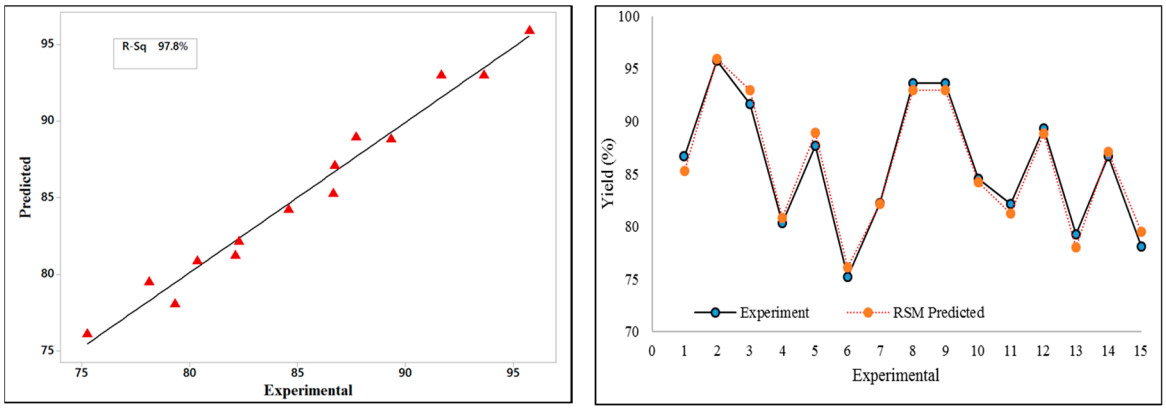

(**a**) (**b**)

Figure 5. Biodiesel yield values (%): (**a**) Experimental versus (**b**) RSM predicted.

The linear, quadratic and interaction effects of the parameters were considered to investigate the impacts on the biodiesel yield. Table 8 displays the significance of those parameters in terms of the probability value (p value). It also summarises the resulting regression coefficients and computed T-values. In the model, positive coefficients M and MT showed a linear effect on biodiesel yield, whereas quadratic terms of M^2, C^2, T^2, MC, and CT had adverse effects that reduce the biodiesel yield. At the 95% confidence level, the p values were less than 0.05, indicating significant effects of those parameters. The analysis of variance (ANOVA) was used to determine the significance and fitness of the quadratic model.

Table 8. Regression coefficient of the predicted quadratic polynomial model.

Term.	Coefficients	Standard Errors	Computed T-Value	p Value
Constant	92.983	0.893	104.17	0.000
M	4.719	0.547	8.63	0.000
C	−2.161	0.547	−3.95	0.011
T	−0.730	0.547	−1.34	0.239
M × M	−4.490	0.805	−5.58	0.003
C × C	−4.650	0.805	−5.78	0.002
T × T	−4.323	0.805	−5.37	0.003
M × C	−5.168	0.773	−6.69	0.001
M × T	0.665	0.773	0.86	0.429
C × T	−1.635	0.773	−2.12	0.088

Table 9 shows the level of significance of individual terms and their interactions on the selected response. The quadratic regression model has higher F value (24.76) and lower p value (0.001) than significance level ($p < 0.05$), which indicates that the model is significant at the 99.9% confidence level. The p value represents the probability of error and is used to check the significance of each regression coefficient. The interaction effect of each cross product can be revealed through the p value. It is found, M (methanol: oil molar ratio), C (catalyst concentration), M^2 (quadratic effect of methanol amount), C^2 (quadratic effect of catalyst concentration), T^2 (quadratic effect of reaction temperature) and MC (methanol amount with catalyst) have significant effects on SFO biodiesel production. Among all other

parameters, methanol: oil molar ratio (M) has the lowest p value (0.000) and highest F value (74.53). These results show that M is the most important parameter in SFO biodiesel production. According to the regression model in Equation (9), M has a positive effect and both C and reaction temperature (T) have negative effects on SFO biodiesel yield. This implies that increasing M will increase the speed of the transesterification process. However, increase in C and T will slow the speed of the transesterification reaction. The square term of T^2 was also significant although it has a smaller F value compared to its corresponding linear term which indicated its weaker influence in the model. Again, the ANOVA results showed that the linear term of T with p value was not significant (more than 0.05) and its quadratic term T^2 with p value was significant (less than 0.05). ANOVA also showed that both C and C^2 terms were significant with their F values (15.63 and 27) which indicated their medium effect in the model. The Lack of Fit was also determined for this regression model. F value and p value of Lack of Fit parameters were found to be 2.32 and 0.315 respectively. The p value (0.315) of the Lack of Fit parameter is greater than 0.050, which indicated the quadratic model has an insignificant Lack of Fit, i.e., the model sufficiently described a relationship between independent parameters such as M, C and T, with the dependent parameter (SFO biodiesel yield). The coefficient of determination (R^2) was employed to identify the quality of the model fitness. R^2 also indicates the good correlation between the independent parameters. In this study, R^2 was found to be 97.8% and the adjusted coefficient of determination (Adj. R^2) was 93.9%. This means that the model explains 97.8% of the variation in the experimental data. In conclusion, the regression model developed for SFO biodiesel yield was valid and showed a satisfactory experimental relationship between the response and parameters.

Table 9. ANOVA results for SFO biodiesel.

Source	Sum of Squares	Degree of Freedom	Mean Square	F-Value	p-Value	Remarks
Model	532.603	9	59.178	24.76	0.001	Significant
M-Methanol	178.123	1	178.123	74.53	0.000	Highly significant
C-Catalyst	37.364	1	37.364	15.63	0.011	Significant
T-Temperature	4.263	1	4.263	1.78	0.239	Not significant
M^2	74.447	1	74.447	31.15	0.003	Significant
C^2	79.847	1	79.847	27.00	0.002	Significant
T^2	69.004	1	69.004	28.87	0.003	Significant
MC	106.823	1	106.823	44.69	0.001	Significant
MT	1.769	1	1.769	0.74	0.429	Not significant
CT	10.693	1	10.693	4.47	0.088	Not significant
Lack of Fit	9.284	3	3.095	2.32	0.315	Not Significant
Pure Error	2.667	2	1.333			
Total	544.553	14				
R^2 = 0.9781			Adj R^2 = 0.9386			

4.5. Response Surface Plots for SFO Biodiesel Production

The interactive effect of the two factors on the transesterification process for biodiesel production is necessary for interpreting the impact of independent variables used in the optimisation process. Figures 6–8 show both surface plots and contour plots of SFO biodiesel yield obtained by the regression model in Equation (9). Surface plots were produced by plotting three-dimensional (3D) surface curves against any two independent variables while keeping the other variables fixed at their medium values. The interaction effect of the two parameters plotted while the third parameter was fixed at a medium value in the contour plot. Contour plots can identify the variation in biodiesel yield with any change in experimental conditions.

4.5.1. Interaction Effect of Methanol: Oil Molar Ratio and Catalyst Concentration

Figure 6a shows the 3D response surface for SFO biodiesel yield production as a function of methanol: oil molar ratio, and KOH catalyst concentration under the current conditions of Box-Behnken

design matrix. With an increase of methanol: oil molar ratio up to 6:1 (highest) and 0.5 wt % of catalyst concentration (lowest), biodiesel yield percentage increases. The maximum SFO biodiesel yield of 95.8% was found for KOH 0.5 wt % (Run 13). Table 7 design matrix indicated that highest KOH concentration at 1.5 wt % and unchanged methanol: oil ratio at 6:1 resulted in lower SFO biodiesel yield to 82.1% (Run 4). When the methanol:oil molar ratio remains unchanged at 6:1, and the catalyst concentration is at the highest value of 1.5 wt %, the SFO biodiesel decreases to 82.1% (Run 4). When the methanol: oil molar ratio was reduced to 4:1 (lowest level), and with the highest value of catalyst concentration of 1.5 wt %, the biodiesel yield was found to be 82.3% (Run 9). Again, at methanol: oil molar ratio of 6:1, and with the mid-value of catalyst concentration of 1wt %, the yield was found to be 89.3% (Run 3). On the other hand, when the methanol: oil molar ratio was reduced to 4:1, and with the mid-value of catalyst concentration of 1 wt %, the yield dropped to 80.3% (Run 12). Methanol: oil molar ratio affected total biodiesel yield production. ANOVA from Table 9 confirmed that both M, C and MC interaction were significant. The 2D contour plot with MC interaction along with biodiesel yield is shown in Figure 6b. It is easy to identify the optimum operating conditions and the related response values (yield) through the 2D contour plot. Therefore, both M and C are significant factors for higher biodiesel yield. Although literature showed that higher amount of C could result in less biodiesel yield production, and eventually produce emulsion and phase separation [54].

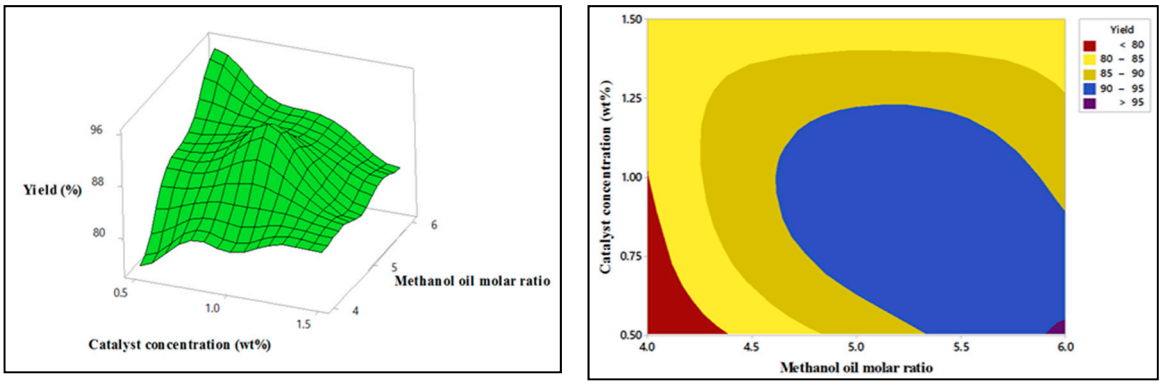

(**a**) 3D response surface plot (**b**) 2D contour plot

Figure 6. Interaction effect of methanol: oil molar ratio (M) and catalyst concentration (C) on the SFO biodiesel yield.

4.5.2. Interaction Effect of Catalyst Concentration and the Reaction Temperature

The interaction effect of catalyst concentration, C and reaction temperature, T on the SFO biodiesel yield in 3D surface plots is shown in Figure 7a. An increase in T to mid-level (55 °C), and the low-level of C (0.5 wt %) can enhance the SFO biodiesel yield up to 95.8% (Run 13), considering M of 6:1 and reaction time of 60 min constant, which is presented in Table 7 of the Box–Behnken design matrix. It is found that increasing the T to 65 °C and C to 1 wt % resulted in the decline in biodiesel yield to 89.3% (Run 3). Similarly, increasing C to the highest level of 1.5 wt % and increasing T to the mid-level of 55 °C resulted in a stepwise decline in biodiesel yield to 82.1% (Run 11). Figure 7a displays the interaction between C and T on biodiesel yield production up to 92%, keeping the experimental conditions of T at 55 °C and C at 1 wt %. ANOVA results in Table 9 confirms that the interaction between C and T is not significant. Moreover, the higher amount of C and higher T might induce saponification of triglycerides as well as form soap at the end [55]. Figure 7b shows the 2D contour plots of CT interaction, which is not significant for SFO biodiesel yield production.

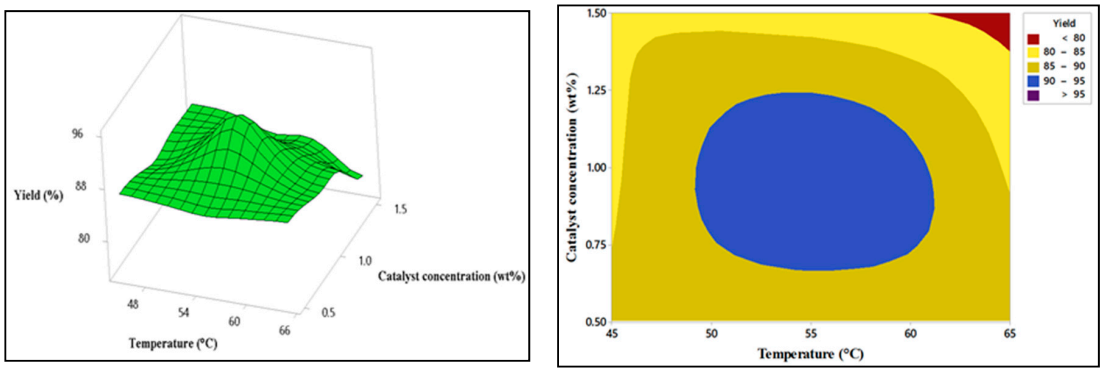

(**a**) 3D response surface plot (**b**) 2D contour plot

Figure 7. Interaction effect of reaction temperature (T) and catalyst concentration (C) on SFO biodiesel yield.

4.5.3. Interaction Effect of Reaction Temperature and Methanol: Oil Molar Ratio

Figure 8a shows the 3D surface plot of reaction temperature, T and methanol: oil molar ratio, M with SFO biodiesel yield. The T at mid-level (55 °C) and mid-level M of 5:1 shows the maximum yield. Table 7 Box–Behnken design matrix shows that, at the mid-level T and mid-level M, a biodiesel yield of 93% can be achieved. However, at mid-level T and the highest level M, biodiesel yield was optimised and found to be 95.8%. The overall biodiesel yield decreased significantly to 89.3% when T reached 65 °C (Run 3). Any change in T either by an increase or decrease from its mid-level (55 °C) resulted in reduced biodiesel yield. The optimum M was found to be 6:1 and any decreasing the molar ratio (<6) lowered the biodiesel yield. Figure 8b shows the contour plot of interaction between M and T. It shows that, at the mid-level of both T and M, biodiesel yield is maximum. Therefore, ANOVA results in Table 9 confirms that both T and TM are not significant in SFO biodiesel production.

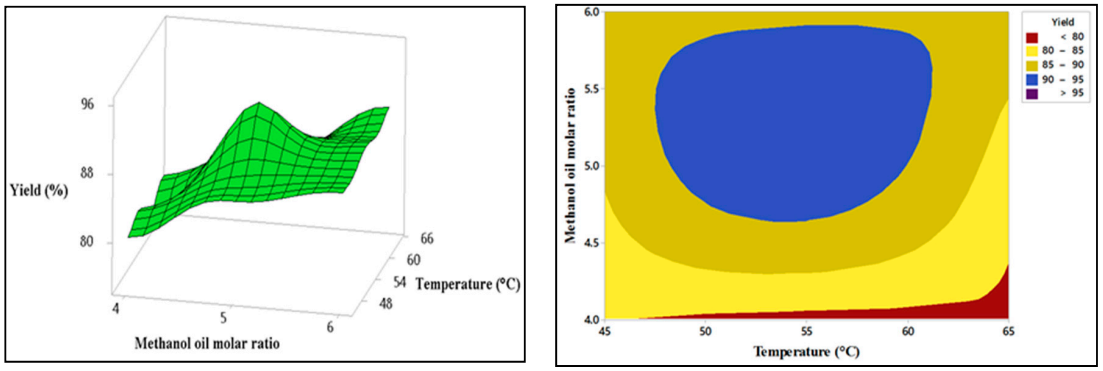

(**a**) 3D response surface plot (**b**) 2D contour plot

Figure 8. Interaction effect of methanol: oil molar ratio (M) and reaction temperature (T) on SFO biodiesel yield.

From ANOVA results in Table 9, it is found that M is the only highly significant process factor that affects the production of SFO biodiesel. Interaction of MC is also a significant process factor for biodiesel production. Both the M and MC have higher F values of 74.5 and 44.7, respectively. Therefore, the optimum reaction conditions are M of 6:1, KOH C of 0.5 wt % and a T of 55 °C and the optimum SFO biodiesel yield is predicted to be 95.9%. To check the validity of the regression model (Equation (9)), experiments were carried out under predicted optimum conditions. The results of the experimental values under the optimum conditions indicated the highest (95.8%) conversion of SFO to SFO biodiesel. This matches very closely with the predicted value (95.9%). Finally, this small degree of error (<0.5%) indicates the high accuracy of the model.

5. Conclusions

A response surface methodology-based Box–Behnken design matrix was employed to achieve the optimum operating parameters for second-generation biodiesel production from SFO. Three major parameters were varied individually within different ranges to anticipate biodiesel yield in that matrix. Based on the results, optimum operating parameters for transesterification of stone fruit seed oil were found to be methanol: oil molar ratio of 6:1, catalyst concentration 0.5 wt %, and a reaction temperature of 55 °C, considering both reaction time and reaction agitation speed were fixed at 60 min and 600 rpm. The maximum biodiesel yield under such conditions was 95.8%, which also confirmed the RSM model prediction of 95.9%. ANOVA statistics of this study confirmed that methanol: oil molar ratio has the most significant effect on the stone fruit biodiesel yield, whereas catalyst concentration and reaction temperature does not seem to have any significant impact. The results show a significant improvement in fuel properties of stone fruit biodiesel with kinetic viscosity 4.26 (mm^2/s), density 0.855 (kg/m^3), acid value 0.25 (mg/KOH/g), flash point 105 (°C), cloud point −4 (°C), pour point −8 (°C), higher heating value 39.04 (MJ/kg), cetane number 50.45 and oxidation stability 7.15 (h), all of which meet both the ASTM D6751 and EN14214 standards. In conclusion, stone fruit oil is a potential for biodiesel production, and this environment-friendly biodiesel can be used as an alternative to diesel fuel.

Author Contributions: M.A. collected oil, produced and characterised biodiesel, optimised the biodiesel, and drafted the manuscript; M.G.R. contributed to the experimental design and thoroughly revised the paper; N.A. helped revise and improve the paper; and M.M.R. checked and revised the manuscript.

Funding: This research received no external funding.

Acknowledgments: The authors would like to acknowledge Tim Mcsweeney, Adjunct Research Fellow, Tertiary Education Division at Central Queensland University, Australia for his contribution in proofreading of this article.

Conflicts of Interest: The authors declare no conflict of interest.

References

1. Rahman, M.M.; Rasul, M.G.; Hassan, N.M.S.; Azad, A.K.; Uddin, M.N. Effect of small proportion of butanol additive on the performance, emission, and combustion of Australian native first-and second-generation biodiesel in a diesel engine. *Environ. Sci. Pollut. Res.* **2017**, *24*, 22402–22413. [CrossRef] [PubMed]
2. Rahman, M.; Rasul, M.; Hassan, N. Study on the tribological characteristics of Australian native first generation and second generation biodiesel fuel. *Energies* **2017**, *10*, 55. [CrossRef]
3. Bhuiya, M.M.K.; Rasul, M.G.; Khan, M.M.K.; Ashwath, N.; Azad, A.K.; Hazrat, M.A. Second generation biodiesel: Potential alternative to-edible oil-derived biodiesel. *Energy Procedia* **2014**, *61*, 1969–1972. [CrossRef]
4. Bhuiya, M.M.K.; Rasul, M.G.; Khan, M.M.K.; Ashwath, N.; Azad, A.K.; Hazrat, M.A. Prospects of 2nd generation biodiesel as a sustainable fuel—Part 2: Properties, performance and emission characteristics. *Renew. Sustain. Energy Rev.* **2016**, *55*, 1129–1146.
5. Popp, J.; Lakner, Z.; Harangi-Rákos, M.; Fári, M. The effect of bioenergy expansion: Food, energy, and environment. *Renew. Sustain. Energy Rev.* **2014**, *32*, 559–578. [CrossRef]
6. NguyenThi, T.; Bazile, J.-P.; Bessières, D. Density measurements of waste cooking oil biodiesel and diesel blends over extended pressure and temperature ranges. *Energies* **2018**, *11*, 1212. [CrossRef]
7. Yusop, A.; Mamat, R.; Yusaf, T.; Najafi, G.; Yasin, M.; Khathri, A. Analysis of particulate matter (pm) emissions in diesel engines using palm oil biodiesel blended with diesel fuel. *Energies* **2018**, *11*, 1039. [CrossRef]
8. Ali, O.; Mamat, R.; Najafi, G.; Yusaf, T.; Safieddin Ardebili, S. Optimization of biodiesel-diesel blended fuel properties and engine performance with ether additive using statistical analysis and response surface methods. *Energies* **2015**, *8*, 14136–14150. [CrossRef]
9. Silitonga, A.S.; Atabani, A.E.; Mahlia, T.M.I.; Masjuki, H.H.; Badruddin, I.A.; Mekhilef, S. A review on prospect of jatropha curcas for biodiesel in Indonesia. *Renew. Sustain. Energy Rev.* **2011**, *15*, 3733–3756. [CrossRef]
10. Rahman, M.; Rasul, M.; Hassan, N.; Hyde, J. Prospects of biodiesel production from macadamia oil as an alternative fuel for diesel engines. *Energies* **2016**, *9*, 403.

11. Sharma, R.; Gupta, A.; Abrol, G.S.; Joshi, V.K. Value addition of wild apricot fruits grown in north-west himalayan regions: A review. *J. Food Sci. Technol.* **2012**, *51*, 2917–2924. [CrossRef] [PubMed]
12. Razack, S.A.; Duraiarasan, S. Response surface methodology assisted biodiesel production from waste cooking oil using encapsulated mixed enzyme. *Waste Manag.* **2016**, *47*, 98–104. [CrossRef] [PubMed]
13. Saydut, A.; Erdogan, S.; Kafadar, A.B.; Kaya, C.; Aydin, F.; Hamamci, C. Process optimization for production of biodiesel from hazelnut oil, sunflower oil and their hybrid feedstock. *Fuel* **2016**, *183*, 512–517. [CrossRef]
14. Martínez, S.L.; Romero, R.; Natividad, R.; González, J. Optimization of biodiesel production from sunflower oil by transesterification using Na_2O/NaX and methanol. *Catal. Today* **2014**, *220*, 12–20. [CrossRef]
15. Kostić, M.D.; Djalović, I.G.; Stamenković, O.S.; Mitrović, P.M.; Adamović, D.S.; Kulina, M.K.; Veljković, V.B. Kinetic modeling and optimization of biodiesel production from white mustard (*Sinapis alba* L.) seed oil by quicklime-catalyzed transesterification. *Fuel* **2018**, *223*, 125–139. [CrossRef]
16. Ong, H.C.; Masjuki, H.H.; Mahlia, T.M.I.; Silitonga, A.S.; Chong, W.T.; Leong, K.Y. Optimization of biodiesel production and engine performance from high free fatty acid *Calophyllum inophyllum* oil in Ci diesel engine. *Energy Convers. Manag.* **2014**, *81*, 30–40. [CrossRef]
17. Dharma, S.; Masjuki, H.H.; Ong, H.C.; Sebayang, A.H.; Silitonga, A.S.; Kusumo, F.; Mahlia, T.M.I. Optimization of biodiesel production process for mixed *Jatropha curcas–Ceiba pentandra* biodiesel using response surface methodology. *Energy Convers. Manag.* **2016**, *115*, 178–190. [CrossRef]
18. Gumus, M.; Kasifoglu, S. Performance and emission evaluation of a compression ignition engine using a biodiesel (apricot seed kernel oil methyl ester) and its blends with diesel fuel. *Biomass Bioenergy* **2010**, *34*, 134–139. [CrossRef]
19. Fadhil, A.B. Evaluation of apricot (*Prunus armeniaca* L.) seed kernel as a potential feedstock for the production of liquid bio-fuels and activated carbons. *Energy Convers. Manag.* **2017**, *133*, 307–317. [CrossRef]
20. Ullah, F.; Nosheen, A.; Hussain, I.; Bano, A. Base catalyzed transesterification of wild apricot kernel oil for biodiesel production. *Afr. J. Biotechnol.* **2009**, *8*, 3309–3313.
21. Yadav, A.K.; Pal, A.; Dubey, A.M. Experimental studies on utilization of *Prunus armeniaca* L. (wild apricot) biodiesel as an alternative fuel for CI engine. *Waste Biomass Valoriz.* **2017**, 1–9. [CrossRef]
22. Hamze, H.; Akia, M.; Yazdani, F. Optimization of biodiesel production from the waste cooking oil using response surface methodology. *Process Saf. Environ. Prot.* **2015**, *94*, 1–10. [CrossRef]
23. Atabani, A.E.; Silitonga, A.S.; Badruddin, I.A.; Mahlia, T.M.I.; Masjuki, H.H.; Mekhilef, S. A comprehensive review on biodiesel as an alternative energy resource and its characteristics. *Renew. Sustain. Energy Rev.* **2012**, *16*, 2070–2093. [CrossRef]
24. Atadashi, I.M.; Aroua, M.K.; Abdul Aziz, A.R.; Sulaiman, N.M.N. The effects of water on biodiesel production and refining technologies: A review. *Renew. Sustain. Energy Rev.* **2012**, *16*, 3456–3470. [CrossRef]
25. Banerjee, A.; Chakraborty, R. Parametric sensitivity in transesterification of waste cooking oil for biodiesel production—A review. *Resour. Conserv. Recycl.* **2009**, *53*, 490–497. [CrossRef]
26. Yaakob, Z.; Mohammad, M.; Alherbawi, M.; Alam, Z.; Sopian, K. Overview of the production of biodiesel from waste cooking oil. *Renew. Sustain. Energy Rev.* **2013**, *18*, 184–193. [CrossRef]
27. Targais, K.; Stobdan, T.; Yadav, A.; Singh, S.B. Extraction of apricot kernel oil in cold desert Ladakh, India. *Indian J. Tradit. Knowl.* **2011**, *10*, 304–306.
28. Wang, L. Properties of manchurian apricot (*Prunus mandshurica* Skv.) and siberian apricot (*Prunus sibirica* L.) seed kernel oils and evaluation as biodiesel feedstocks. *Ind. Crops Prod.* **2013**, *50*, 838–843. [CrossRef]
29. Fan, S.; Liang, T.; Yu, H.; Bi, Q.; Li, G.; Wang, L. Kernel characteristics, oil contents, fatty acid compositions and biodiesel properties in developing siberian apricot (*Prunus sibirica* L.) seeds. *Ind. Crops Prod.* **2016**, *89*, 195–199. [CrossRef]
30. Rahman, M.M.; Hassan, M.H.; Kalam, M.A.; Atabani, A.E.; Memon, L.A.; Rahman, S.M.A. Performance and emission analysis of *Jatropha curcas* and *Moringa oleifera* methyl ester fuel blends in a multi-cylinder diesel engine. *J. Clean. Prod.* **2014**, *65*, 304–310. [CrossRef]
31. Kafuku, G.; Mbarawa, M. Alkaline catalyzed biodiesel production from moringa oleifera oil with optimized production parameters. *Appl. Energy* **2010**, *87*, 2561–2565. [CrossRef]
32. Alptekin, E.; Canakci, M. Determination of the density and the viscosities of biodiesel–diesel fuel blends. *Renew. Energy* **2008**, *33*, 2623–2630. [CrossRef]
33. Encinar, J.M.; González, J.F.; Rodríguez-Reinares, A. Biodiesel from used frying oil. Variables affecting the yields and characteristics of the biodiesel. *Ind. Eng. Chem. Res.* **2005**, *44*, 5491–5499. [CrossRef]

34. Graboski, M.S.; McCormick, R.L. Combustion of fat and vegetable oil derived fuels in diesel engines. *Prog. Energy Combust. Sci.* **1998**, *24*, 125–164. [CrossRef]
35. Silitonga, A.S.; Ong, H.C.; Mahlia, T.M.I.; Masjuki, H.H.; Chong, W.T. Biodiesel conversion from high FFA crude *Jatropha curcas*, *Calophyllum inophyllum* and *Ceiba pentandra* oil. *Energy Procedia* **2014**, *61*, 480–483. [CrossRef]
36. Silitonga, A.S.; Ong, H.C.; Masjuki, H.H.; Mahlia, T.M.I.; Chong, W.T.; Yusaf, T.F. Production of biodiesel from *Sterculia foetida* and its process optimization. *Fuel* **2013**, *111*, 478–484. [CrossRef]
37. Keera, S.T.; El Sabagh, S.M.; Taman, A.R. Transesterification of vegetable oil to biodiesel fuel using alkaline catalyst. *Fuel* **2011**, *90*, 42–47. [CrossRef]
38. Hasni, K.; Ilham, Z.; Dharma, S.; Varman, M. Optimization of biodiesel production from *Brucea javanica* seeds oil as novel non-edible feedstock using response surface methodology. *Energy Convers. Manag.* **2017**, *149*, 392–400. [CrossRef]
39. Anwar, M.; Rasul, M.G.; Ashwath, N. Production optimization and quality assessment of papaya (*Carica papaya*) biodiesel with response surface methodology. *Energy Convers. Manag.* **2018**, *156*, 103–112. [CrossRef]
40. Benjumea, P.; Agudelo, J.R.; Agudelo, A.F. Effect of the degree of unsaturation of biodiesel fuels on engine performance, combustion characteristics, and emissions. *Energy Fuels* **2011**, *25*, 77–85. [CrossRef]
41. Altun, Ş. Effect of the degree of unsaturation of biodiesel fuels on the exhaust emissions of a diesel power generator. *Fuel* **2014**, *117*, 450–457. [CrossRef]
42. Wang, L.; Yu, H. Biodiesel from siberian apricot (*Prunus sibirica* L.) seed kernel oil. *Bioresour. Technol.* **2012**, *112*, 355–358. [CrossRef] [PubMed]
43. Kate, A.E.; Lohani, U.C.; Pandey, J.P.; Shahi, N.C.; Sarkar, A. Traditional and mechanical method of the oil extraction from wild apricot kernel: A comparative study. *Res. J. Chem. Environ. Sci.* **2014**, *2*, 54–60.
44. Atabani, A.E.; César, A.D.S. *Calophyllum inophyllum* L.—A prospective non-edible biodiesel feedstock. Study of biodiesel production, properties, fatty acid composition, blending and engine performance. *Renew. Sustain. Energy Rev.* **2014**, *37*, 644–655. [CrossRef]
45. García-Martínez, N.; Andreo-Martínez, P.; Quesada-Medina, J.; de los Ríos, A.P.; Chica, A.; Beneito-Ruiz, R.; Carratalá-Abril, J. Optimization of non-catalytic transesterification of tobacco (*Nicotiana tabacum*) seed oil using supercritical methanol to biodiesel production. *Energy Convers. Manag.* **2017**, *131*, 99–108. [CrossRef]
46. Goyal, P.; Sharma, M.P.; Jain, S. Optimization of conversion of high free fatty acid *Jatropha curcas* oil to biodiesel using response surface methodology. *ISRN Chem. Eng.* **2012**, *2012*, 8. [CrossRef]
47. Lin, L.; Zhou, C.; Vittayapadung, S.; Shen, X.; Dong, M. Opportunities and challenges for biodiesel fuel. *Appl. Energy* **2011**, *88*, 1020–1031. [CrossRef]
48. Demirbaş, A. Biodiesel fuels from vegetable oils via catalytic and non-catalytic supercritical alcohol transesterifications and other methods: A survey. *Energy Convers. Manag.* **2003**, *44*, 2093–2109. [CrossRef]
49. Shankar, V.; Jambulingam, R. Waste crab shell derived CaO impregnated Na-ZSM-5 as a solid base catalyst for the transesterification of neem oil into biodiesel. *Sustain. Environ. Res.* **2017**, *27*, 273–278. [CrossRef]
50. Patel, R.L.; Sankhavara, C.D. Biodiesel production from karanja oil and its use in diesel engine: A review. *Renew. Sustain. Energy Rev.* **2017**, *71*, 464–474. [CrossRef]
51. Rashid, U.; Anwar, F.; Moser, B.R.; Knothe, G. Moringa oleifera oil: A possible source of biodiesel. *Bioresour. Technol.* **2008**, *99*, 8175–8179. [CrossRef] [PubMed]
52. Silitonga, A.S.; Masjuki, H.H.; Mahlia, T.M.I.; Ong, H.C.; Chong, W.T.; Boosroh, M.H. Overview properties of biodiesel diesel blends from edible and non-edible feedstock. *Renew. Sustain. Energy Rev.* **2013**, *22*, 346–360. [CrossRef]
53. Gupta, J.; Agarwal, M.; Dalai, A.K. Optimization of biodiesel production from mixture of edible and nonedible vegetable oils. *Biocatal. Agric. Biotechnol.* **2016**, *8*, 112–120. [CrossRef]
54. Silva, G.F.; Camargo, F.L.; Ferreira, A.L.O. Application of response surface methodology for optimization of biodiesel production by transesterification of soybean oil with ethanol. *Fuel Process. Technol.* **2011**, *92*, 407–413. [CrossRef]
55. Vicente, G.; Martínez, M.; Aracil, J. Optimisation of integrated biodiesel production. Part I. A study of the biodiesel purity and yield. *Bioresour. Technol.* **2007**, *98*, 1724–1733. [CrossRef] [PubMed]

{this page is intentionally left blank}

Declaration of Co-authorship and Contribution

Research Division

CHAPTER 5: Part A- Interactive Effects of Operating Parameters on Engine Performance

Title of the paper	A comparative study of engine performance and emission characteristics of biodiesels produced from the waste seeds of papaya and stone fruit
Full bibliographic reference	Anwar, M., M. Rasul, N. Ashwath, A comparative study of engine performance and emission characteristics of biodiesels produced from the waste seeds of papaya and stone fruit, IEEE 2nd International Conference on Renewable Energy and Power Engineering. 2019. Toronto.
Status	Published

Nature of Candidate's Contribution, including percentage of total
I was responsible for conducted the experiment, data analysis and drafted the manuscript. [80%]

Nature of all Co-Authors' Contributions, including percentage of total
My co-authors, Prof. Mohammad Rasul, and A/Professor Nanjappa Ashwath, were designed the experimentation, reviewed, revised and improved the manuscript. [20%]

Has this paper been submitted for an award by another research degree candidate (Co- Author), either at CQUniversity or elsewhere? (if yes, give full details)
No

Candidate's Declaration

I declare that the publication above meets the requirements to be included in the thesis as outlined in the Research Higher Degree Theses Policy and Procedure.

Mohammad Anwar

A comparative study of engine performance and emission characteristics of biodiesels produced from the waste seeds of papaya and stone fruit

M. Anwar* and M.G. Rasul
School of Engineering and Technology
Central Queensland University
Rockhampton, QLD 4702, Australia
*E-mail: m.anwar@cqu.edu.au
E-mail: m.rasul@cqu.edu.au

N. Ashwath
School of Heath, Medical and Applied Sciences
Central Queensland University
Rockhampton, QLD 4702, Australia
E-mail: n.ashwath@cqu.edu.au

***Abstract*— This paper investigates the engine performance and emission characteristics of the biodiesels synthesised from papaya seed oil (PSO), stone fruit kernel oil (SFO) blends using a diesel engine. All experiments were carried out at full load condition with different engine speeds ranging from 1200 rpm to 2400 rpm at an interval of 200 rpm. Diesel (100%) and its four blends such as 10% biodiesel with 90% diesel (PSO10, SFO10), and 20% biodiesel with 80% diesel (PSO20, SFO20) were considered for comparative analysis. Engine performance results showed that the SFO biodiesel blends differed marginally (0.6% ▲Brake Power (BP), 0.3% ▲torque, 3% ▲ Brake thermal efficiency (BTE) and 2.3% ▼Brake specific fuel consumption (BSFC) from PSO biodiesel blends. However, SFO biodiesel blends produced higher exhaust emissions than PSO biodiesel blends, in the order of 2.1%▲NO_x, 3%▲PM, 10.1%▲HC, 5.4%▲CO_2, and 13.3%▲CO. Both biodiesel blends produced considerably reduced emissions of PM (max. 34%), HC (max. 33%), and CO (max. 31%) as compared to diesel, while a slight in NO_x (max. 6.8%) and CO_2 (max. 8.7%) was observed. These results demonstrate that both SFO and PSO could be effectively used in a diesel engine without any modifications.**

Keywords- Carica papaya, apricot, stone fruit, brake power, NO_x, emission.

I. INTRODUCTION

Petroleum-derived fuel such as diesel is one of the most wanted energy sources in the modern world, and many countries are solely dependent on diesel fuel for their energy needs, especially by the transportation sector. The world has seen a major oil crisis in 1973, 1979, and 1981 [1]. The supply of petroleum-derived fuels fluctuates along with the price if there are any issues such as political unrest, war, conflict, and sanctions [2]. Furthermore, the resources required for producing fuel are depleting every day, and an alternative source of fuel is required. Burning petroleum-derived fuel in the transportation sector results in serious environmental issues such as global warming, air pollution, changes in rainfall pattern, acid rain and changes in the frequency of extreme weather events [2-4]. Researchers are working hard to find suitable alternatives from different renewable sources to replace these uncertainties. Biodiesel is one of the renewable energy sources that can be used as a direct or blended source of fuel in any diesel engine.

There are 350 oil-bearing crops that are known to act as biodiesel feedstocks. A sustainable feedstock should be non-edible, locally sourced, easily accessible, economical, and technically viable [5, 6]. This study explores the opportunity of waste papaya seed and stone fruit kernel seed as potential biodiesel feedstocks. Papaya (Carica papaya) is mainly cultivated in the tropical climates of Asia, South America, Africa, and Polynesia. The papaya fruit can weigh up to 3 kg and about 15% its wet weight is discarded as non-consumable, i.e., waste seeds. This waste seed contains 30-34% oil [5]. Stone fruits such as apricot (*Prunus armeniaca L.*) originates from cool frost-free regions of India and Armenia. Each stone fruit yields 22-38% of kernels, which contain 54% oil [4]. It is shown that both papaya seed oil (PSO) and stone fruit (apricot) kernel oil (SFO) can be successfully converted into biodiesels using single stage transesterification, with an estimated conversion rate of up to 96% and 96% respectively [2, 4]. Fuel properties of both biodiesels were found similar and within the limits of international standard. In this study, a comparison is made between the PSO and SFO derived biodiesels for engine performance (BP, torque, BET and BSFC) and emission characteristics (NO_x, PM, HC, CO_2, and CO) of a diesel engine using four fuel blends, viz., PSO10, PSO20, SFO10, SFO20 and neat diesel fuel, with the view to assessing their relative performances.

II. MATERIALS AND METHODS

Diesel fuel was sourced from a local fuel station in Rockhampton which contained less than 10 ppm of sulphur, with a calorific value of 45.3 MJ/kg and cetane number of 48. The referenced papaya seed oil biodiesel and stone fruit kernel oil biodiesel had oleic acid (C18:1) of 47.7% and 63.8%; linoleic acid (C18:2) of 37.3% and 25.3%; cetane number of 48.3 and 50.5; calorific values of 38.5 MJ/kg and 39.6 MJ/kg; Iodine value of 115.9 mg I2/100 g and 104.7 mg I2/100 g respectively. The following treatments were considered for this comparative analysis (i) diesel, (ii) diesel with 10% PSO biodiesel (PSO10), (iii) diesel with 20% PSO biodiesel (PSO20), (iv) diesel with 10% SFO biodiesel (SFO10), and (v) diesel with 20% SFO biodiesel (SFO20).

Kubota V3300 diesel engine was fuelled with those blends at full load condition. The engine speed was incremented at 200 rpm from 1200 rpm to 2400 rpm. The engine was coupled with an eddy current dynamometer. The exhaust gas emissions (NO_x, HC, and CO_2) were measured using a CODA 5 gas analyser, and MAHA MPM-4M apparatus was used for measuring particulate matter (PM).

III. COMPARATIVE ANALYSIS OF PSO AND SFO

A. Engine performance analysis

The variation in engine speeds with brake power (BP) for all five treatments at full load condition is presented in Figure 1. BP increased steadily with an increase in engine speeds for all blending conditions. It was found that lower the biodiesel content, the higher was the BP value. At any given engine speed, diesel had higher BP value followed by SFO10, PSO10, SFO20, and PSO20. The average BP values of PSO10, PSO20, SFO10, SFO20, and diesel were 37.7, 37.3, 37.9, 37.4, and 39.3 kW. The BP values of both PSO and SFO blends were found to be nearly identical, with SFO10 and SFO20 having 0.56% and 0.34% higher BP than PSO10 and PSO20. Average BP value reduction for PSO10, PSO20, SFO10, and SFO20 in comparison with diesel were 3.9%, 5.1%, 3.4% and 4.7% owing to biodiesel blends having lower calorific values, higher viscosities and higher densities [7-9].

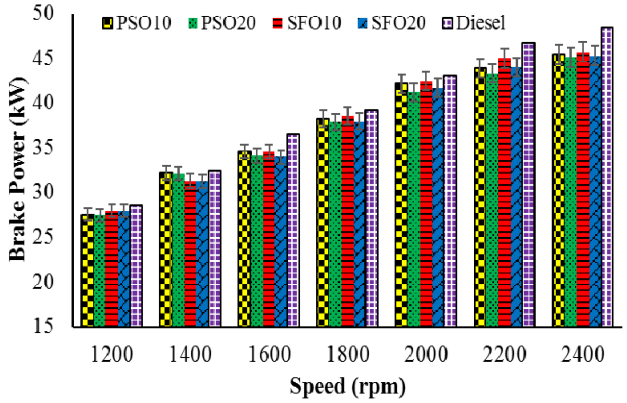

Figure 1. Variation of engine speeds of BP.

Figure 2 shows the relationship between the engine torque and variation in engine speeds at full load conditions. The torque increased with an increase in engine speed up to 1400 rpm and then decreased continuously until the maximum speed of 2400 rpm for all five treatments. The reason behind this is the Kubota engine has the maximum rated torque recorded at 1400 rpm. This can also be attributed to mechanical friction loss and lower volumetric efficiency of the engine [7, 10, 11]. Torque decreased with increased concentration of biodiesel in the blends. As expected, diesel had the highest torque at all engine speeds followed by SFO10, SFO20, PSO10, and PSO20. The average torque values of PSO10, PSO20, SFO10, SFO20, and diesel were 202.7, 199.9, 203.2, and 200.5 N.m. The torque values of both PSO and SFO blends were found similar, with the SFO10 and SFO20 having 0.22% and 0.32% higher torque than PSO10 and PSO20. Average torque value reduction for PSO10, PSO20, SFO10, and SFO20 in comparison with the diesel was 2.5%, 3.9%, 2.3% and 3.5%. Researchers show that lower densities and viscosities, and higher calorific values of the diesel result in diesel having higher engine torque than biodiesel [9, 11].

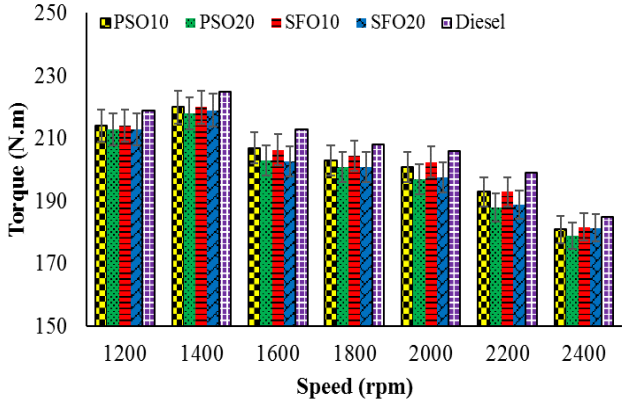

Figure 2. Variation of engine speeds of torque.

The variation in BTE with engine speeds for all five treatments at full load condition is shown in Figure 3. The BTE decreased with an increase in engine speed over the entire range. It is known that the BTE decreases at higher speeds due to a lack of sufficient air that causes uneven combustion of fuel [12]. Again, higher BTE depends on higher calorific value, lower density, and lower viscosity. A higher BTE is observed in biodiesel blends that contain lower proportion of biodiesel such as PSO10 and SFO10 as compared to PSO20 and SFO20 respectively Researchers show that lower viscosity and higher volatility results in better air-fuel mixture leading to better combustion [12, 13]. As expected, diesel had the highest BTE at all engine speeds followed by SFO10, PSO10, SFO20, and PSO20. The average BTE values of PSO10, PSO20, SFO10, SFO20 and diesel were 28.6%, 27.2%, 29.6%, 27.8% and 31.3%. Both SFO10 and SFO20 had a BTE of 2.96% and, this was 1.9% higher than that of PSO10 and PSO20 respectively. Again, average BTE value reduction for PSO10, PSO20, SFO10, and SFO20, as compared to diesel were 8.8%, 13.1%, 6%, and 11.4%.

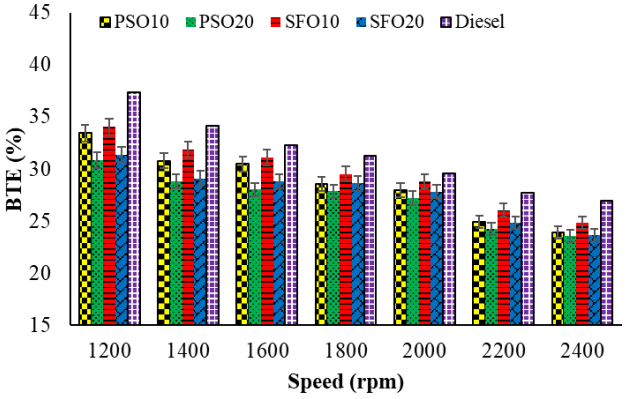

Figure 3. Variation of engine speeds of BTE.

Figure 4 shows that the BSFC increases with an increase in engine speed. Ong et al. [13] show that friction heat losses occur at higher speeds, and this leads to deterioration of combustion, leading to higher BSFC. Other researchers show that the fuel injection system, density, viscosity, and calorific value affect the BSFC value [6, 14]. Due to the lower calorific value of the biodiesel, it had higher BSFC values, as biodiesel needed more fuel for producing the same power as compared to diesel. Again, diesel had the lowest BSFC at all engine speeds followed by SFO10, PSO10, SFO20, and PSO20. The average BSFC values of PSO10, PSO20, SFO10, SFO20, and diesel were 282.6, 300.5, 276.1, 296 and 256.5 g/kWh. Both SFO10 and SFO20 had 2.4% and 1.5% lower BSFC than PSO10 and PSO20, respectively. The average BSFC value for PSO10, PSO20, SFO10 and SFO20, as compared to diesel were 10.2%, 17.1%, 7.6% and 15.4%, respectively.

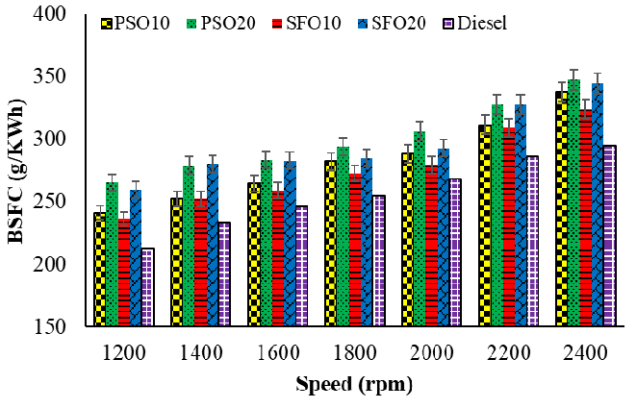

Figure 4. Variation of engine speeds of BSFC.

B. *Engine emission analysis*

The variation in NO_x emissions with changing engine speeds for PSO and SFO blends with diesel at full load conditions is shown in Figure 5. The NO_x increased with the increase of engine speeds for all fuels due to higher combustion temperature and stoichiometry of the mixture [15]. At full load condition, the air-fuel ratio increases, and this resulted in higher gas temperature in the combustion chamber, leading to higher NO_x emissions [16]. The increased biodiesel content in the blends produced higher NO_x emissions where higher cetane number of a low biodiesel blend can initiate a short ignition delay that causes lower combustion temperature and pressure leading to reduced NO_x emission [17]. The average NO_x emission produced by PSO10, PSO20, SFO10, SFO20, and diesel is 349.4, 354.3, 353.7, 361.7, and 337.9 ppm respectively. The SFO10 and SFO20 blends showed higher NO_x than PSO10 and PSO20 by 1.2% and 2.1% respectively. The average NO_x emission for PSO10, PSO20, SFO10, and SFO20, as compared with diesel were 3.4%, 4.9%, 4.7%, and 7.1%, respectively.

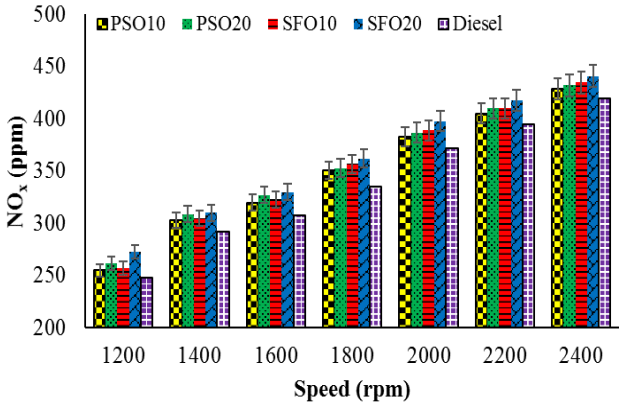

Figure 5. Variation with engine speeds of NOx.

Generally, PM emission is lower in biodiesel blends than in diesel due to lower volatility and higher oxygen content in the biodiesel [18]. Figure 6 shows variation in PM emissions over engine speeds at full load conditions for all five fuel blends. Lin et al. [19] demonstrate that the higher cetane number of biodiesel blends can cause shorter ignition delay and longer combustion, and this would have resulted in lower PM emissions. The average PM emission produced by the PSO10, PSO20, SFO10, SFO20, and diesel were 40.4, 36.8, 41.3, 37.9 and 55.6 mg/m3 respectively. SFO10 and SFO20 blends showed higher PM as compared to PSO10 and PSO20 by 2.3% and 3%, respectively. The average PM emission was reduced for PSO10, PSO20, SFO10, and SFO20 as compared diesel, and were 27.4%, 33.9%, 25.7%, and 32%, respectively.

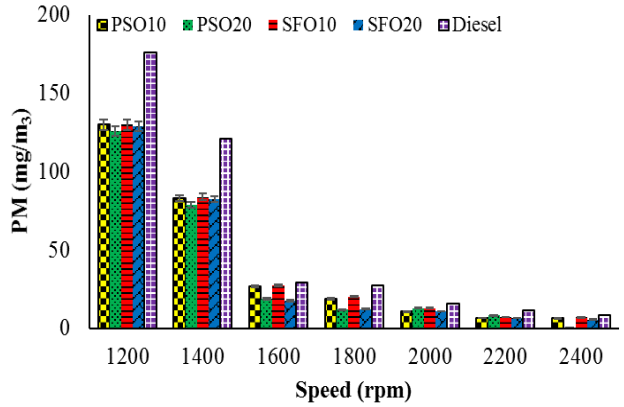

Figure 6. Variation with engine speeds of PM.

The HC emission mainly occurs due to incomplete combustion of the fuel, and the flame quenching happens in the cylinder walls and crevices. The variation in HC emission with engine speeds for all five blends are shown in Figure 7 at full load condition. HC emission decreases with an increase in engine speed. Kocak et al. [20] show that at lower engine speeds, the higher fuel density and viscosity critically affect the fuel atomisation and ignition in the combustion chamber leading to higher HC emission. The average HC emission for PSO10, PSO20, SFO10, SFO20, and diesel were 16.9, 15.1, 17.1, 16.7 and 22.6 ppm,

respectively. The SFO10 and SFO20 blends showed higher HC emission as compared to PSO10 and PSO20 at 1.7% and 10.1% respectively. The average HC emission reduction for PSO10, PSO20, SFO10, and SFO20, as compared to diesel were 25.3%, 32.9%, 24.1%, and 26.1%.

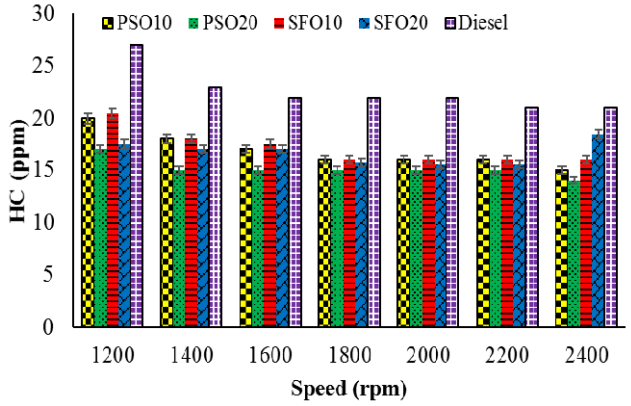

Figure 7. Variation with engine speeds of HC.

The CO_2 emission is an important parameter that indicates the combustion efficiency of fuel, as higher CO_2 refers to better combustion. The CO_2 emission over the entire engine speeds are shown in Figure 8. At 1400 rpm maximum rated torque, CO_2 emission was recorded as the highest for all blends. It can be seen that the higher the biodiesel content in the blend, the higher was the CO_2 emission. This is due to the higher oxygen content and cetane number in the biodiesel blends. The average CO_2 emission produced by PSO10, PSO20, SFO10, SFO20 and diesel were 12.4%, 12.5%, 12.9% and 13.2% respectively. The SFO10 and SFO20 blends showed higher CO_2 emission producer in comparison with PSO10 and PSO20 by 4.5% and 5.4% respectively. The average CO_2 emission increase for PSO10, PSO20, SFO10, and SFO20, as compared to diesel were 1.8%, 3.1%, 6.4% and 8.7%.

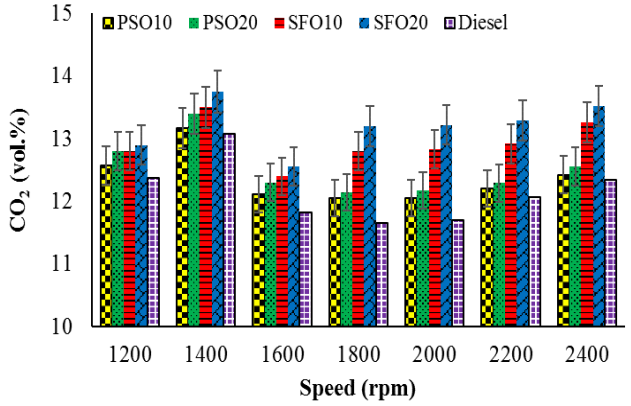

Figure 8. Variation of engine speeds of CO_2.

Carbon monoxide (CO) is a toxic gas that can result from two processes of incomplete combustion, such as (i) an excessively lean air-fuel mixture and (ii) an excessively rich air-fuel mixture. CO emission directly relates to types of fuel, engine speed, air-fuel mixture, injection pressure, and injection timing [21]. Generally, biodiesel blends have higher O_2 content and higher cetane number that enable complete combustion to produce lower CO emission. Figure 9 shows the variation in CO emission over different engine speeds. CO emission drops drastically after 1400 rpm, with little change in the concentration from 1600 to 2400 rpm. This is due to a better air-fuel mixture that occurred at higher engine speeds. The average CO emission produced by PSO10, PSO20, SFO10, SFO20 and diesel were 0.15%, 0.11%, 0.15%, 0.13% and 0.16% respectively. The SFO10 and SFO20 blends showed higher CO emission in comparison with PSO10 and PSO20 by 4.9% and 13.3% respectively. Average CO emission reduction for PSO10, PSO20, SFO1, and SFO20 as compared to diesel were 10.4%, 31.3%, 6.1%, and 22.2%.

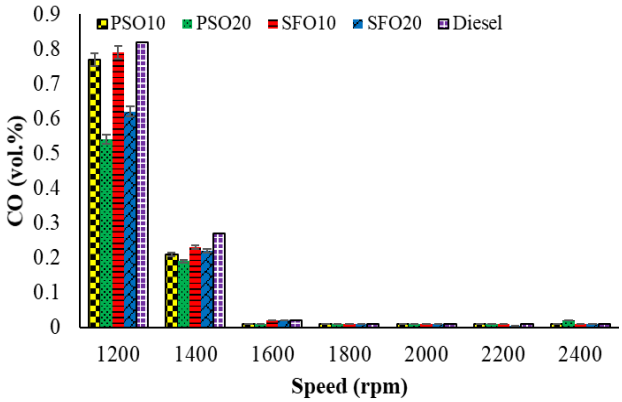

Figure 9. Variation with engine speeds of CO.

IV. CONCLUSION

Biodiesel produced from papaya seed oil and stone fruit kernel oil were evaluated in a diesel engine. Based on the results, the following inferences can be drawn:

- The performance of both PSO and SFO biodiesels is comparable with that of neat diesel fuel. The performance of SFO biodiesel blends is slightly better than that of PSO biodiesel blends. The BP and torque produced by these biodiesels blends were almost identical with a deviance of less than 0.5%. However, the BTE of SFO biodiesel blend was 3.2% higher than that of PSO. In contrast, the BSFC of SFO was 2.4% lower than that of PSO.
- The SFO biodiesel blends produced higher NO_x emissions than PSO biodiesel blends by a maximum of 2.1%. An increase in NO_x emission compared with diesel was observed for all PSO and SFO biodiesel blend, and this ranged from 3.4% to 7.1%.
- The SFO biodiesel blends produced higher PM emissions than PSO biodiesel blends by a maximum of 3%. The highest reduction in PM emission was recorded for PSO20, and this was found to be 34% lower than diesel fuel.
- The SFO biodiesel blends produced higher HC emissions compared with PSO blends by max. 10%. The PSO20 can reduce the HC emission by 33%.

- A maximum of 5.4% more CO_2 emission was produced by the SFO biodiesel blends as compared to PSO blends. An average increase in CO_2 for PSO10, PSO20, SFO10, and SFO20, compared with diesel was 1.8%, 3.1%, 6.5% and 8.7%, respectively
- SFO biodiesel blends produced a maximum of 13.3% higher CO emission than PSO biodiesel blends. In comparison with the diesel fuel, the PSO20 produced 31.3% lower CO emissions.

Although the SFO biodiesel blends have better performance than PSO biodiesel blends, the PSO biodiesel blends prove to be a better choice due to their excellent environmental-friendly attributes that can reduce the exhaust emission to a great extent. Therefore, PSO biodiesel blends can be used as an excellent source of alternative fuel in a diesel engine improve air quality via a significant reduction in exhaust emissions into the environment with a marginal reduction in the engine performance.

REFERENCES

[1] Kettell, S. Oil crisis. [cited 2019 April 28]; Available from: https://www.britannica.com/topic/oi l-crisis.

[2] Anwar, M., M.G. Rasul, and N. Ashwath, Production optimization and quality assessment of papaya (Carica papaya) biodiesel with response surface methodology. Energy Conversion and Management, 2018. 156: p. 103-112.

[3] Rizwanul Fattah, I.M., M.A. Kalam, H.H. Masjuki, and M.A. Wakil, Biodiesel production, characterization, engine performance, and emission characteristics of Malaysian Alexandrian laurel oil. RSC Advances, 2014. 4(34): p. 17787-17796.

[4] Anwar, M., M. Rasul, N. Ashwath, and M. Rahman, Optimisation of Second-Generation Biodiesel Production from Australian Native Stone Fruit Oil Using Response Surface Method. Energies, 2018. 11(10): p. 2566.

[5] Anwar, M., M.G. Rasul, N. Ashwath, and M.D.N. Nabi, The potential of utilising papaya seed oil and stone fruit kernel oil as non-edible feedstock for biodiesel production in Australia—A review. Energy Reports, 2019. 5: p. 280-297.

[6] Mofijur, M., H.H. Masjuki, M.A. Kalam, and A.E. Atabani, Evaluation of biodiesel blending, engine performance and emissions characteristics of Jatropha curcas methyl ester: Malaysian perspective. Energy, 2013. 55: p. 879-887.

[7] Bhuiya, M., M. Rasul, M. Khan, and N. Ashwath, Performance and Emission Characteristics of Binary Mixture of Poppy and Waste Cooking Biodiesel. Energy Procedia, 2017. 110: p. 523-528.

[8] Sanjid, A., M.A. Kalam, H.H. Masjuki, M. Varman, N.W.B.M. Zulkifli, and M.J. Abedin, Performance and emission of multi-cylinder diesel engine using biodiesel blends obtained from mixed inedible feedstocks. Journal of Cleaner Production, 2016. 112: p. 4114-4122.

[9] Rahman, M.M., M.G. Rasul, N.M.S. Hassan, A.K. Azad, and M.N. Uddin, Effect of small proportion of butanol additive on the performance, emission, and combustion of Australian native first- and second-generation biodiesel in a diesel engine. Environmental science and pollution research international, 2017. 24(28): p. 22402-22413.

[10] Anwar, M., M. Rasul, and N. Ashwath, A Systematic Multivariate Analysis of Carica papaya Biodiesel Blends and Their Interactive Effect on Performance. Energies, 2018. 11(11): p. 2931.

[11] Liaquat, A.M., H.H. Masjuki, M.A. Kalam, M. Varman, M.A. Hazrat, M. Shahabuddin, and M. Mofijur, Application of blend fuels in a diesel engine. Energy Procedia, 2012. 14(Supplement C): p. 1124-1133.

[12] Sajjad, H., H.H. Masjuki, M. Varman, M.A. Kalam, M.I. Arbab, S. Imtenan, and A.M. Ashraful, Influence of gas-to-liquid (GTL) fuel in the blends of Calophyllum inophyllum biodiesel and diesel: An analysis of combustion–performance–emission characteristics. Energy Conversion and Management, 2015. 97: p. 42-52.

[13] Ong, H.C., H.H. Masjuki, T.M.I. Mahlia, A.S. Silitonga, W.T. Chong, and K.Y. Leong, Optimization of biodiesel production and engine performance from high free fatty acid Calophyllum inophyllum oil in CI diesel engine. Energy Conversion and Management, 2014. 81: p. 30-40.

[14] Qi, D.H., H. Chen, L.M. Geng, and Y.Z. Bian, Experimental studies on the combustion characteristics and performance of a direct injection engine fueled with biodiesel/diesel blends. Energy Conversion and Management, 2010. 51(12): p. 2985-2992.

[15] Devan, P.K. and N.V. Mahalakshmi, Performance, emission and combustion characteristics of poon oil and its diesel blends in a DI diesel engine. Fuel, 2009. 88(5): p. 861-867.

[16] Godiganur, S., C. Suryanarayana Murthy, and R.P. Reddy, Performance and emission characteristics of a Kirloskar HA394 diesel engine operated on fish oil methyl esters. Renewable Energy, 2010. 35(2): p. 355-359.

[17] Yongcheng, H., Z. Longbao, W. Shangxue, and L. Shenghua, Study on the Performance and Emissions of a Compression Ignition Engine Fuelled with Fischer-Tropsch Diesel Fuel. Proceedings of the Institution of Mechanical Engineers, Part D: Journal of Automobile Engineering, 2006. 220(6): p. 827-835.

[18] Tse, H., C.W. Leung, and C.S. Cheung, Investigation on the combustion characteristics and particulate emissions from a diesel engine fueled with diesel-biodiesel-ethanol blends. Energy, 2015. 83: p. 343-350.

[19] Lin, L., Z. Cunshan, S. Vittayapadung, S. Xiangqian, and D. Mingdong, Opportunities and challenges for biodiesel fuel. Applied Energy, 2011. 88(4): p. 1020-1031.

[20] Koçak, M.S., E. Ileri, and Z. Utlu, Experimental Study of Emission Parameters of Biodiesel Fuels Obtained from Canola, Hazelnut, and Waste Cooking Oils. Energy & Fuels, 2007. 21(6): p. 3622-3626.

[21] Gumus, M. and S. Kasifoglu, Performance and emission evaluation of a compression ignition engine using a biodiesel (apricot seed kernel oil methyl ester) and its blends with diesel fuel. Biomass and Bioenergy, 2010. 34(1): p. 134-139.

Declaration of Co-authorship and Contribution

Research Division

CHAPTER 5: Part B- Interactive Effects of Operating Parameters on Engine Performance

Title of the paper	A systematic multivariate analysis of *Carica papaya* biodiesel blends and their interactive effect on performance
Full bibliographic reference	Anwar, M., M. Rasul, and N. Ashwath, A Systematic Multivariate Analysis of Carica papaya Biodiesel Blends and Their Interactive Effect on Performance. Energies, 2018. 11(11): p. 2931. https://www.mdpi.com/1996-1073/11/11/2931
Status	Published

Nature of Candidate's Contribution, including percentage of total
I was responsible for collected oil, produced and characterised biodiesel, optimized the biodiesel and drafted the manuscript. [80%]

Nature of all Co-Authors' Contributions, including percentage of total
My co-authors, Prof. Mohammad Rasul, and A/Professor Nanjappa Ashwath, were designed the experimentation, reviewed, revised and improved the manuscript. [20%]

Has this paper been submitted for an award by another research degree candidate (Co- Author), either at CQUniversity or elsewhere? (if yes, give full details)
No

Candidate's Declaration

I declare that the publication above meets the requirements to be included in the thesis as outlined in the Research Higher Degree Theses Policy and Procedure.

Mohammad Anwar

energies

MDPI

Article

A Systematic Multivariate Analysis of *Carica papaya* Biodiesel Blends and Their Interactive Effect on Performance

Mohammad Anwar [1,*], Mohammad G. Rasul [1] and Nanjappa Ashwath [2]

[1] School of Engineering and Technology, Central Queensland University, North Rockhampton, QLD 4702, Australia; m.rasul@cqu.edu.au

[2] School of Health, Medical and Applied Sciences, Central Queensland University, North Rockhampton, QLD 4702, Australia; n.ashwath@cqu.edu.au

* Correspondence: m.anwar@cqu.edu.au; Tel.: +61-7-4930-6371

Received: 11 October 2018; Accepted: 25 October 2018; Published: 26 October 2018

Abstract: This paper investigates the interactive relationship between three operating parameters (papaya seed oil (PSO) biodiesel blends, engine load, and engine speed) and four responses (brake power, BP; torque; brake specific fuel consumption, BSFC; and, brake thermal efficiency, BTE) for engine testing. A fully instrumented four cylinder four-stroke, naturally aspirated agricultural diesel engine was used for all experiments. Three different blends: B5 (5% PSO biodiesel +95% diesel), B10 (10% PSO biodiesel + 90% diesel), and B20 (20% PSO biodiesel + 80% diesel) were tested. Physicochemical properties of these blends and pure PSO biodiesel were characterised, and the engine's performance characteristics were analysed. The results of the engine performance experiments showed that, in comparison with diesel, the three PSO biodiesel blends caused a slight reduction in BP, torque, and BTE, and an increase in BSFC. The analysis of variance and quadratic regression modelling showed that both load and speed were the most important parameters that affect engine performance, while PSO biodiesel blends had a significant effect on BSFC.

Keywords: diesel; *Carica papaya*; engine performance; biodiesel; characterisation

1. Introduction

Diesel fuel has successfully contributed to all sectors of human life, especially to transportation, industry, and agricultural sectors due to its availability, reliability, adaptability, higher combustion efficiency, and excellent handling/storage properties. However, fossil reserves (oil, gas, and coal) are limited, therefore, researchers have been exploring an alternative source for diesel for many years, and, over the last decade, biofuel (i.e., mainly biodiesel) has drawn massive attention for its excellent environmental and sustainability attributes [1,2]. Biodiesel is biodegradable, non-toxic, non-explosive, non-flammable, renewable, and an environmentally friendly (produces fewer emissions) fuel. Although the biodiesel energy content is about 10–12% less than diesel, it can be mixed with diesel at specific proportions to make the blended fuel properties close to diesel [3,4]. Furthermore, researchers are working hard to find suitable sustainable biodiesels and their blends, which can be used as fuel in unmodified diesel engines.

Numerous researchers have explored the production of biodiesel from different feedstocks focusing on non-edible oil, but very few investigations [5–10] have been performed on papaya seed oil (PSO) biodiesel. Among these, most of the articles deal with only the biodiesel production process when using different catalysts and methanol: oil molar ratios. Asokan et al. [2] examined engine performance in a single cylinder diesel engine fuelled with a mixture of papaya seed oil and watermelon seed oil and found that B20 performed close to diesel. Prabhakaran et al. [11] analysed

engine performance of a single cylinder Kirloskar-TV1 diesel engine with PSO biodiesel blends and found B25 blend has lower BSFC than all other blends. Sundar Raj and Karthikayan [12] did diesel engine (single cylinder) performance analysis with PSO-diesel blends with/without additives and found PSO-diesel blends with additives have better combustion and emission characteristics. However, no other literature has been found on engine performance analysis of a fully instrumented four cylinder four-stroke diesel engine fuelled with PSO biodiesel.

PSO is non-edible and converting the waste product (seeds) of the fruit into biodiesel is a sensible option. *Carica papaya* was originally native to the tropics of the Americas and it is now primarily grown in tropical-subtropical climates of Asia (in particular, India with 42% of world production), South America (mainly Brazil), Africa (Nigeria and Congo), and Polynesia [13,14]. Therefore, the evaluation of papaya seed oil as biodiesel feedstock will contribute to the development of regional communities and their overall economy. In this study, papaya seed oil was used as feedstock to produce biodiesel and investigate its suitability as an alternative fuel source. Determining the fuel properties of PSO and its various blends with diesel were also undertaken. Finally, interactive relationships between several operating parameters (PSO biodiesel blends, load, and speed) and engine performance are evaluated and discussed.

2. Materials and method

2.1. Materials

The raw PSO was obtained from a supplier in Eumundi, Queensland, Australia. The chemicals that were utilised for this study were methanol (99.9% purity), potassium hydroxide (KOH pellets, 99% purity), and sodium hydroxide (NaOH pellets, 99% purity). All chemicals were of analytical reagent grade (AR) and they were procured from the School of Engineering and Technology, Central Queensland University. A reflux condenser and a thermocouple fitted on 0.5 L and 1 L three-neck laboratory reactors were used for the PSO biodiesel conversion experiments.

2.2. Equipment List

The PSO properties were characterised for density, viscosity, refractive index, angular rotation, acid value, oxidation stability, and iodine value. These properties were measured before the biodiesel conversion and optimisation process. Table 1 summarises the equipment used in this study to measure the properties of PSO, PSO biodiesel, and the biodiesel-diesel blends, and the relevant standards applied. The properties studied were density at 15 °C, kinematic viscosity at 40 °C, acid value, calorific value, flash point, and oxidation stability. A gas chromatograph was used to determine the fatty acid compositions by EN 14103.

Table 1. Equipment used for measuring properties of papaya seed oil (PSO) and related products in this study.

Property	Equipment	Standard Applied	Accuracy
Kinematic viscosity	NVB classic (Normalab, France)	ASTM D445	±0.01 mm^2/s
Density	DM40 LiquiPhysics™ density meter (Mettler Toledo, Switzerland)	ASTM D1298	±0.1 kg/m^3
Flash point	NPM 440 Pensky-Martens flash point tester (Normalab, France)	ASTM D93	±0.1 °C
Acid value	Automation titration Rondo 20 (Mettler Toledo, Switzerland)	ASTM D664	±0.001 mg KOH/g
Calorific value	6100EF semi-auto bomb calorimeter (Perr, USA)	ASTM D240	±0.001 MJ/kg
Oxidation stability at 110 °C	873 Rancimat (Metrohm, Switzerland)	ASTM D2274	±0.01 h
Refractive index	RM 40 Refractometer	-	±0.0001

2.3. Biodiesel Production

The acid value of raw PSO was determined to be 0.98 mg KOH/g. After transesterification using the KOH catalyst, the acid value of PSO biodiesel was found to be 0.42 mg KOH/g. This trial experiment suggested that only the single-stage alkyl catalyst transesterification process was necessary for satisfactory PSO biodiesel production. Further, only a few researchers [6–10] have found that the single-stage transesterification process was sufficient for PSO biodiesel conversion. Based on these researches and the trial experiment, it was decided to use single-stage alkaline transesterification for biodiesel production. Thus, in each experiment, the conversion was performed by reacting a known quantity of PSO with methanol and the catalyst.

In each of these experiments, PSO was poured into a three-neck laboratory reactor and was heated to the preferred temperature. The catalyst (KOH) was dissolved in methanol in a separate beaker, and a magnetic stirrer was used to provide vigorous agitation at 600 rpm for 10 min at 50 °C to produce methoxide. This solution was then poured into the reactor that contained heated PSO to allow the transesterification reaction at a constant speed of agitation of 600 rpm. Other reaction conditions, such as temperature and time, were adjusted as per the individual experimental designs determined from the optimisation process of PSO biodiesel [14]. At the end of the transesterification reaction, the blend was poured into a separating funnel and left to settle 24 h for layer separation. Under gravity, two distinct liquid phases were formed; the upper layer was methyl ester (biodiesel), and the bottom dark brown layer consisted of glycerol and impurities. The glycerol and impurities were drawn off, whence the methyl ester layer was collected and washed with warm (50 °C) distilled water. The methyl ester was then heated to 110°C for 15 min to remove any water that would have been retained from the washing process. A Whatman® qualitative Grade 1 filter paper was used to filter the methyl ester (i.e., biodiesel) and was stored at laboratory temperature for characterisation. Figure 1 shows the PSO production process.

Figure 1. PSO biodiesel production.

PSO biodiesel yield was calculated using Equation (1).

$$\text{PSO Biodiesel Yield} = \text{FAME percent (from GC analysis)} \times \frac{\text{weight of PSO biodiesel}}{\text{weight of PSO}} \quad (1)$$

2.4. Fatty Acid Composition

Fatty acids with a double bond are known as unsaturated fatty acids, while those without a double bond are called saturated fatty acids. High unsaturated fatty acid levels make biodiesel prone to autoxidation [14]. However, high unsaturated fatty acid levels do ensure good flow properties as compared with saturated fatty acids. The major drawback of high saturated fatty acid levels in biodiesel is its poor fuel filterability, particularly in cold weather conditions. The PSO biodiesel fatty acid composition was determined using a gas chromatograph (GC), (Thermo Trace 1310 GC) according to EN14103. Table 2 shows the operating condition details of the GC.

Table 2. Gas chromatograph (GC) operating conditions.

Property	Details
Brand, model	Thermo Scientific Trace 1310 GC
Carrier gas	Helium
Flow rates	Air: 350 mL/min, H_2: 35 mL/min, N_2: 30 mL/min
Detector temperature	240 °C
Column dimensions	60 m × 250 μm × 0.25 μm
Column head pressure	23.8 psi
Injector	Split injector, 40:1 ratio, split flow 48 mL/min, constant flow 1.2 mL/min, 1 μL injection volume
Temperature ramp 1	110 °C hold for 4 min
Temperature ramp 2	10 °C/min to 230 °C, hold for 3 min

The compositional analysis that is detailed in Table 3 shows that PSO biodiesel contains a high level (87.5%) of unsaturated fatty acid methyl esters (FAME) made up of polyunsaturated fatty acid (PUFA) at 39.03% and monounsaturated fatty acid (MUFA) at 48.49%. Amongst these, the dominant fatty acids were found to be oleic acid (C18:1) at 47.7% and linoleic acid (C18:2) at 37.3%. The saturated fatty acids included palmitic acid (C16:0) at 6%.

Table 3. PSO biodiesel fatty acid composition.

Fatty Acids	Formula	Molecular Weight	Structure	wt%
Palmitic	$C_{16}H_{32}O_2$	256	16:0	6.07
Stearic	$C_{18}H_{36}O_2$	284	18:0	3.13
Oleic	$C_{18}H_{34}O_2$	282	18:1	47.73
Linoleic	$C_{18}H_{32}O_2$	280	18:2	37.25
Linolenic	$C_{18}H_{30}O_2$	278	18:3	1.78
Eicosenoic	$C_{20}H_{38}O_2$	310	20:1	0.76
Behenic	$C_{22}H_{44}O_2$	340	22:0	0.68
Erucic	$C_{22}H_{42}O_2$	338	22:1	1.51
Others				1.09
Total Saturated Fatty Acids (SFA)				9.88
Total Monounsaturated Fatty Acids (MUFA)				48.49
Total Polyunsaturated Fatty Acids (PUFA)				39.03
Degree of Unsaturation (DU)				126.55
Long Chain Saturated Factor (LCSF)				3.19

2.5. Properties Analysis

The properties of the produced PSO methyl ester (i.e., pure biodiesel or B100) are compared with those of diesel (B0) and PSO biodiesel-diesel blends (B5, B10, and B20) in Table 4. The properties and qualities of PSO biodiesel and the diesel blends comply with the requirements of international standards ASTM D6751 and EN14214. The USA's ASTM D6751 ensures that the parameters of any pure biodiesel (B100) satisfy the standard before being used as a blend with diesel or pure fuel, whereas the European Union's EN14214 defines the minimum standards for FAME [14,15]. The PSO biodiesel was found to comply with both standards.

Table 4. Comparison of PSO biodiesel and blends with diesel.

Properties	Units	PSO	B100	B20	B10	B5	B0	ASTM D6751-2	EN14214-03
Density	Kg/m^3	885	840	829.76	828.48	827.84	827.2	870–890	860–900
Viscosity at 40 °C	mm^2/s	27.3	3.53	3.29	3.26	3.25	3.23	1.9–6.0	3.5–5.0
Acid value	mg KOH/g	0.98	0.42	0.12	0.09	0.07	0.05	max. [1] 0.5	max. 0.5
Cetane number (CN)	-	-	48.29	48.06	48.03	48.01	48.00	min. [2] 47	min. 51
Calorific value	MJ/kg	-	38.49	43.94	44.62	44.96	45.30	-	35.00
Flash point	(°C)	-	112	77.20	72.85	70.68	68.50	min. 93	>120
Iodine value (IV)	-	79.95	115.89	53.82	46.06	42.18	38.30	-	max. 120
Oxidation stability (OS)	Hour	77.97	5.61	32.32	35.66	37.33	39	min. 3	min. 6

[1] max. = maximum; [2] min. = minimum.

2.6. Fourier Transform Infrared (FTIR) Analysis

The various functional groups that are present in the pure PSO biodiesel sample were determined with FTIR spectroscopy. In this study, a Spectrum 100 series FTIR spectrometer with a universal Attenuated total reflectance (ATR) sampling accessory was used. Samples of the PSO biodiesel were inserted directly on the ATR window to record the spectra over the frequency range of 4000–650 cm^{-1} with four scans at approximately 40% transmission. Spectrum analysis program (Spectrum version 6.2.0, Perkin-Elmer Life and Analytical Sciences, Bridgeport, CT, USA) was used to acquire data and for processing. Figure 2 shows the FTIR spectrum of the pure PSO biodiesel (B100).

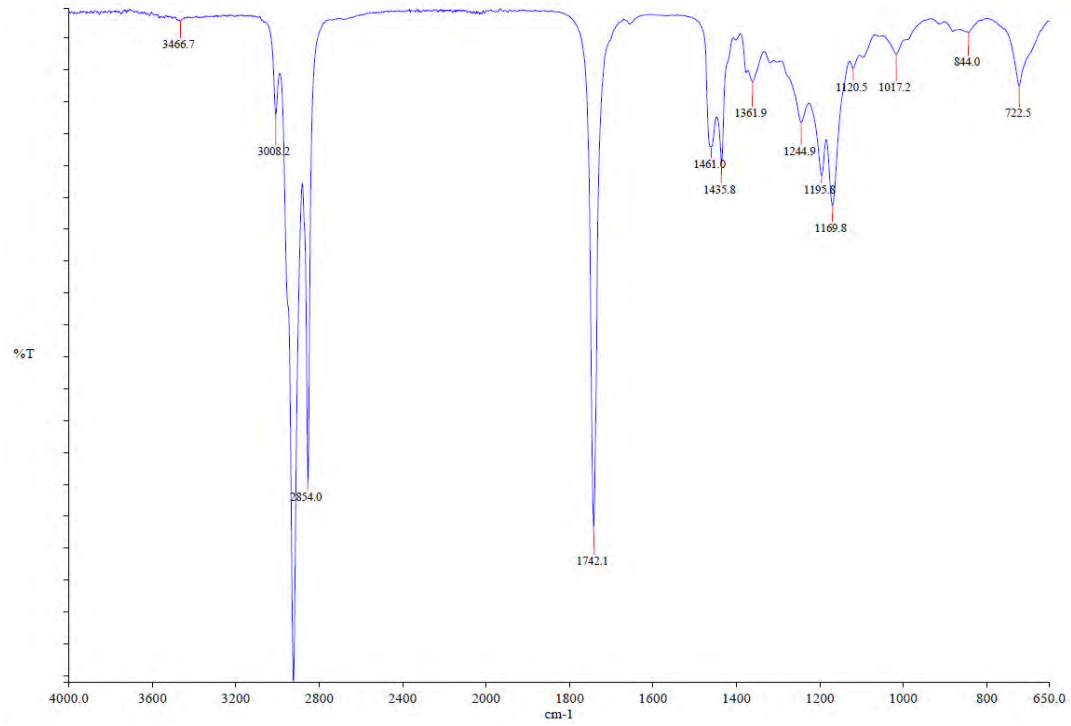

Figure 2. PSO methyl ester investigation Fourier Transform Infrared (FTIR) spectrum.

2.7. Blending of Biodiesel

The pure PSO biodiesel (B100) was mixed with pure diesel (B0) to prepare various blends. Those blends comprised homogeneous mixtures of 5% vol. of biodiesel with 95% vol. of diesel denoted by B5, 10% vol. of biodiesel with 90% vol. of diesel indicated by B10 and 20% vol. of biodiesel with 80% vol. of diesel meant by B20. The blends were prepared in a 2 L flask and were agitated at 2000 rpm with a magnetic stirrer for 60 min.

2.8. Experimental Setup for Engine Testing

This experimental investigation was carried out using pure diesel (B0) and PSO biodiesel-diesel blends (B5, B10, and B20) in an agricultural tractor four-stroke diesel engine with four cylinders (model: Kubota V3300) coupled with an eddy current dynamometer. Table 5 details the engine specification. This tractor engine was used for testing PSO biodiesel-diesel blends with regard to engine performance and characteristics of exhaust emissions. The engine performance and emissions data were collected under full load (100%) condition, keeping the throttle 100% wide open and varying speeds in the range from 1200 to 2400 rpm with an increment of 200 rpm. A photograph of the engine and test bed and a schematic of the setup of the engine along with the data acquisition system are shown in Figure 3. The engine is connected with the test bed along with instrumentation consoles that measure engine speed, torque, air, and fuel consumption and temperature. A Dynolog data acquisition system was used to convert the console-measured data to a display in the computer monitor. The exhaust gas emissions of NO_x and HC in ppm, and CO and CO_2 in vol. %, were measured with a CODA 5 gas analyser (CODA Products Pty Ltd., Hamilton NSW 2303, Australia). For measuring Particulate Matter (PM) emissions, a PM meter (MPM-4M) (MAHA Maschinenbau Haldenwang GmbH & Co. KG, Haldenwang, Germany) was used. Table 6 shows the specification of the gas analyser and PM meter. Before taking any data from the diesel engine, it was run with pure diesel (B0) for 20 min at full load to ensure that the engine was warmed up. The biodiesel-diesel blend (B5, B10, and B20) was then fuelled into the engine for analysis and data acquisition. At the end of any test or experiment with blended fuel, the engine was again flushed out with pure diesel to clear the fuel line of blended fuel and the injection system. All of the tests were repeated three times to minimise any possible error.

(**a**) Photograph of test bed and diesel engine

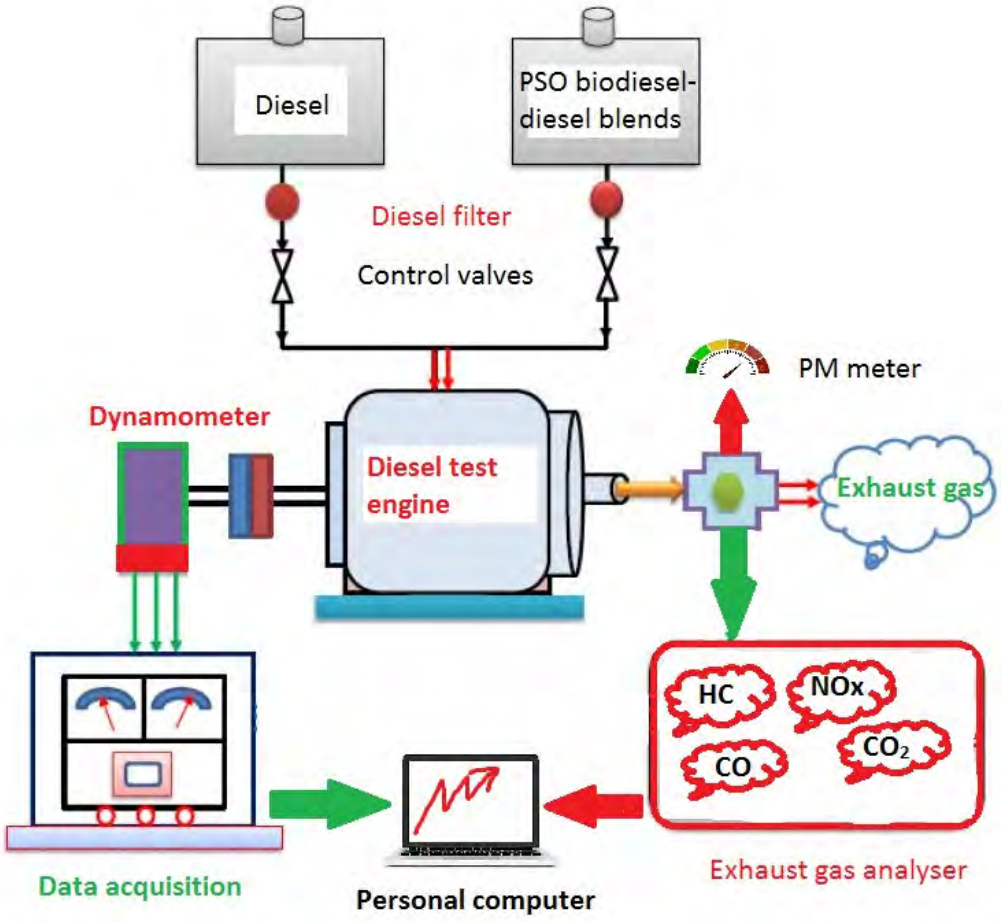

(**b**) Schematic of test procedure setup

Figure 3. Test engine set up.

Table 5. Details of the test engine.

Property	Apparatus, Model
Engine Model	Kubota V3300 Indirect injection
Type	Vertical, 4 cycle liquid cooled diesel
Number of cylinders	4
Total displacement (L)	3.318
Bore × Stroke (mm)	98 × 110

Combustion system	Spherical type (E-TVCS) (three vortex combustion system)
Intake system	Natural aspired
Rated power output (KW/rpm)	53.9/2600
Rated torque (Nm/rpm)	230/1400
Compression ratio	22.6
Emissions certification	Tier 2

Table 6. Exhaust gas analyser, PM meter specification, and error analysis.

Measured Gas	**Measurement**		
	Range	**Resolution**	**Accuracy**
HC	0–30,000 ppm (n-hexane)	1 ppm	±1 ppm
CO	0–15%	0.001%	±0.02%
CO_2	0–20%	0.001%	±0.3%
NOx	0–5000 ppm	1 ppm	±1 ppm
Meter	**Particle Size**	**Particle Concentration Range**	**Resolution**
Particulate Matter	<100 nm to >10 μm	0.1 to >700 mg/m^3	±0.1 mg/m^3
Measurements	**Accuracy**	**Relative Uncertainty (%)**	**Average Reading for B0**
BP	±0.41 kW	0.0105	39.20
BSFC	±5 g/kWh	0.0195	256

There are a large number of studies available in literatures on different biodiesels, and their engine performance and emission characteristics, but a very few researchers have analysed the engine performance or emission characteristics in terms of multivariate analysis. This study focuses on the multivariate analysis of PSO biodiesel blends and their interactive effect on engine performance.

3. Results and discussion

3.1. Characterisation of PSO Biodiesel-Diesel Blends

While the engine performance experiments in this study investigated B5, B10, and B20 biodiesel blends, the characteristics of a much broader series of PSO biodiesel-diesel blends has been investigated. A total of 10 PSO biodiesel-diesel blends (from B5-B90) were prepared, and their individual fuel properties of density, viscosity, flash point, calorific value, and oxidation stability have been analysed and are presented in Figure 4a–e.

Density is one of the vital properties of biodiesel that affects fuel atomisation efficiency in an airless combustion system [16]. According to relevant ASTM and EN standards, the density of biodiesel at 15 °C should be in the range of 860–900 kg/m^3. The densities of B5 (827.84 kg/m^3), B10 (828.48 kg/m^3), and B20 (829.76 kg/m^3) were very close to that of B0 diesel (827.20 kg/m^3). Generally, biodiesel has a slightly higher density than diesel. In addition, density increased as the percentage of PSO biodiesel in the blends increased (Figure 4a).

Some vegetable oils have a higher viscosity, which causes poor fuel flow. Raw PSO has a viscosity of 27.3 mm^2/s, which is 8–9 times higher than diesel (B0). However, after the transesterification process, the viscosity of PSO drops to an acceptable limit. Generally, the viscosity of biodiesel ranges from 1.9–6.0 mm^2/s, and all PSO biodiesel-diesel blends in Figure 4b fulfill this requirement. However, the viscosity of B5 (3.25 mm^2/s), B10 (3.26 mm^2/s), B20 (3.29 mm^2/s), and B30 (3.32 mm^2/s) were very close to B0 (3.23 mm^2/s). Therefore, those blends (B10–B30) can be used as a diesel engine fuel without any modifications to the engine.

According to ASTM D6751, the flashpoint should be 100–170 °C, and all of the biodiesel-diesel blends met that requirement as well. The flash point of B0 was recorded as 68.50 °C, whereas B5, B10, and B20 were found to be 70.68 °C, 72.85 °C, and 77.20 °C, respectively. Biodiesel tends to a higher flash point than diesel, and Figure 4c shows the pattern of the increased flash point with increased biodiesel blends. The more the flashpoint is above 66 °C is indicative of a safer fuel with better

storage ability [1,17]. From that perspective, all PSO biodiesel-diesel blends can be stored safely and they can be used to fuel a diesel engine without any modifications.

Calorific value is another important property in the selection of any fuel. Figure 4d shows that pure PSO biodiesel and all of its blends have slightly lower calorific values than diesel although they are within the requirements of international standards. Biodiesel has nearly 10% more oxygen content than diesel, and less hydrogen-carbon content hence will produce less thermal energy [17]. Calorific values of B5 (44.96 MJ/kg), B10 (44.62 MJ/kg), and B20 (43.94 MJ/kg) blends are very close to B0 (45.30 MJ/kg).

Another vital fuel property is oxidation stability (OS), as it indicates the degree of oxidation that occurs during prolonged storage. Hasni et al. [18] mentioned that lower oxidation stability could adversely affect fuel quality. The higher the oxidation stability, the better the fuel quality. As the PSO biodiesel (unsaturated fatty acid) percentage increases, the OS decreases, which is shown in Figure 4e. As per European standard EN 590, the minimum OS of any fuel should be 20 h (indicated by the red line on the Figure 4e). PSO biodiesel-diesel blends B5 to B50 meet that standard. B5 has an OS value of 37.33 h and B50 is 22.31 h, while B0 has an OS value of 39 h. According to ASTM D6751 and EN14214, the minimum OS values are 3 and 6 h respectively. This study found the 100% PSO biodiesel has an OS value of 5.61 h, which falls within the ASTM and close to EN standards.

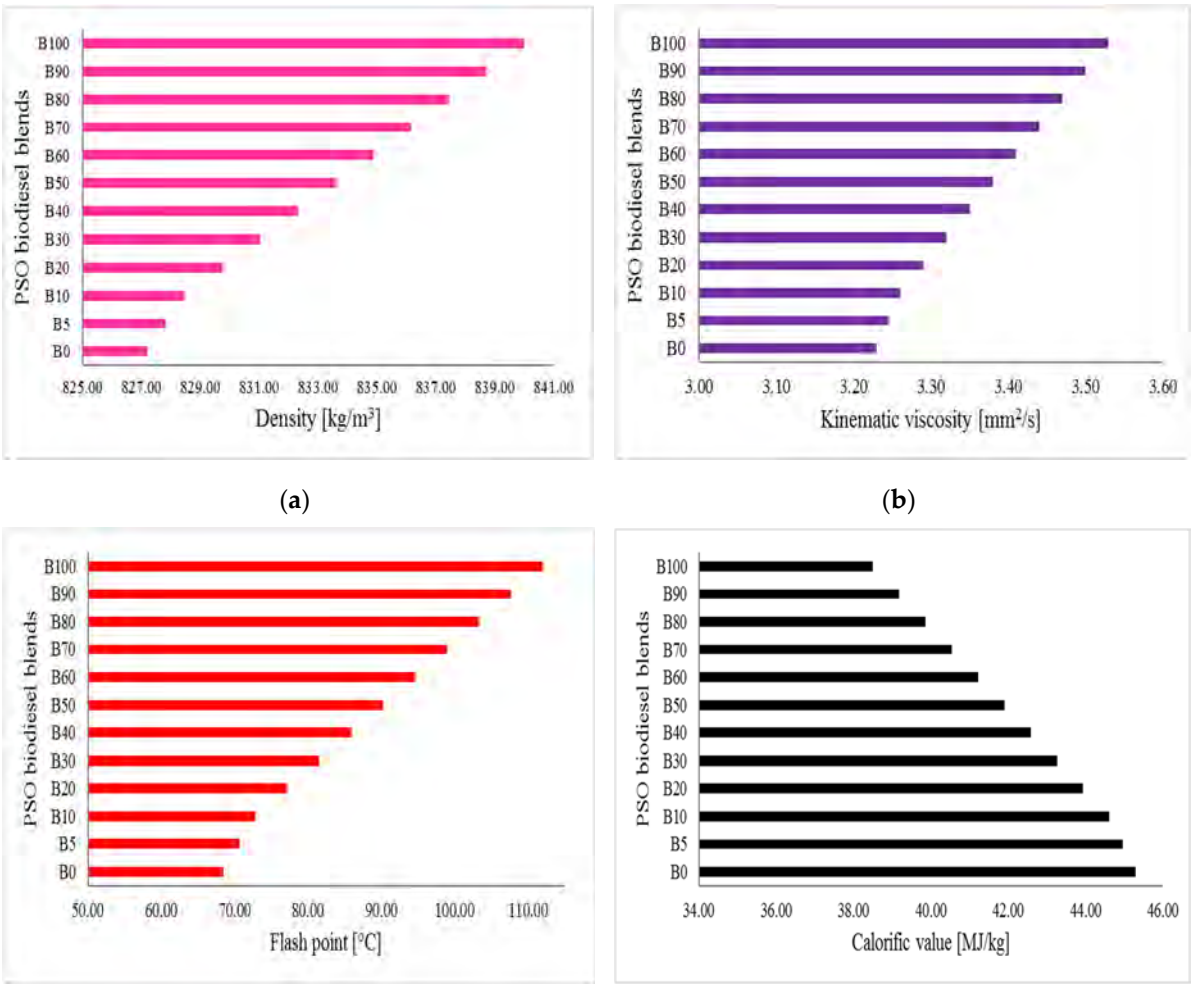

(**a**) (**b**)

(**c**) (**d**)

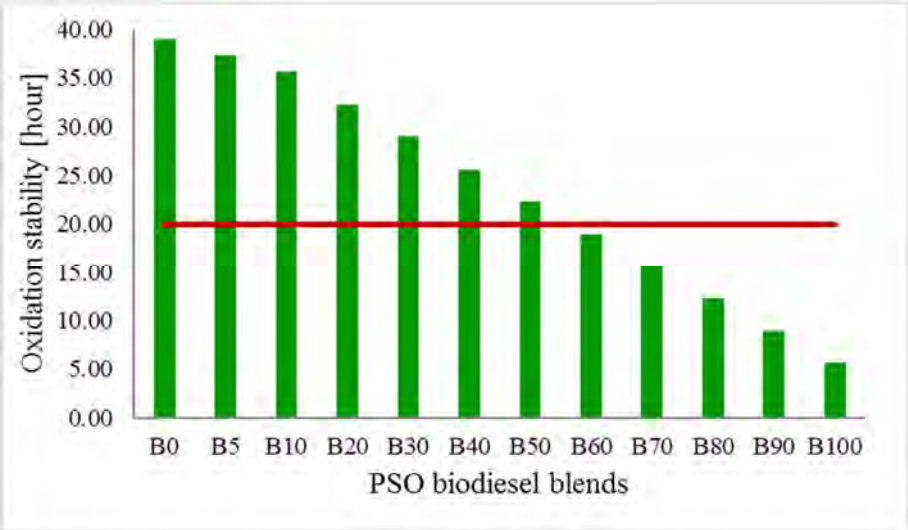

(**e**)

Figure 4. PSO biodiesel-diesel blending effects on: (**a**) density, (**b**) kinematic viscosity, (**c**) flash point, (**d**) calorific value, and (**e**) oxidation stability.

3.2. Analysis of Engine Performance

3.2.1. Brake Power (BP)

The brake power (BP) outputs from the diesel engine fuelled with diesel (B0) and PSO B5, B10, and B20 blends are shown in Figure 5a. It can be seen that the BP gradually increases with the increase of engine speed. Maximum BP was observed at 2400 rpm and was 45.9 kW, 45.4 kW, 45.08 kW, and 48.34 kW for B5, B10, B20, and B0, respectively. Several factors, such as calorific value and viscosity, can have the effect of uneven combustion that results in lowering the BP value. In this study, the viscosity of diesel (B0) and PSO biodiesel-diesel blends were very close. Only the difference in calorific values of blends and diesel caused the variations in BP values. Average BP value reductions for B5, B10, and B20 in comparison with B0 were 2.88%, 3.87%, and 5.13%, respectively.

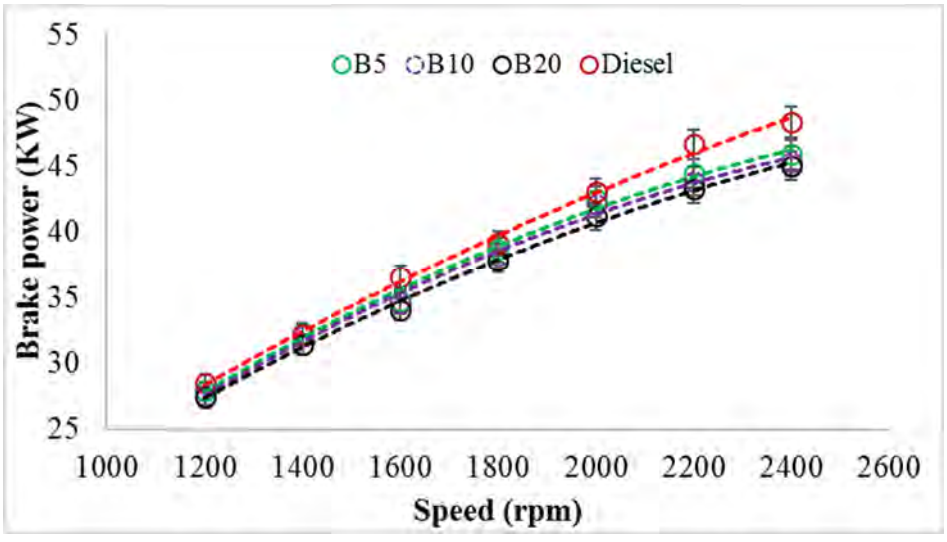

(**a**)

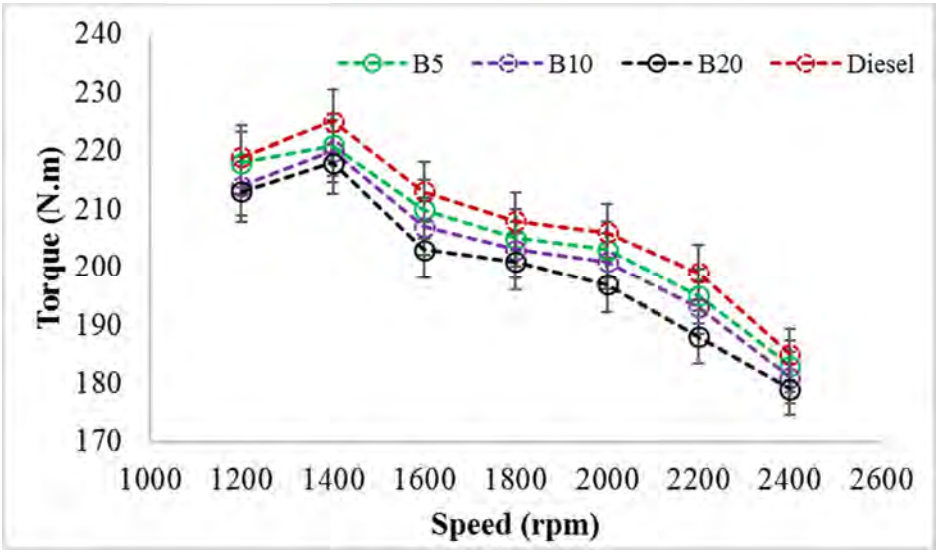

(**b**)

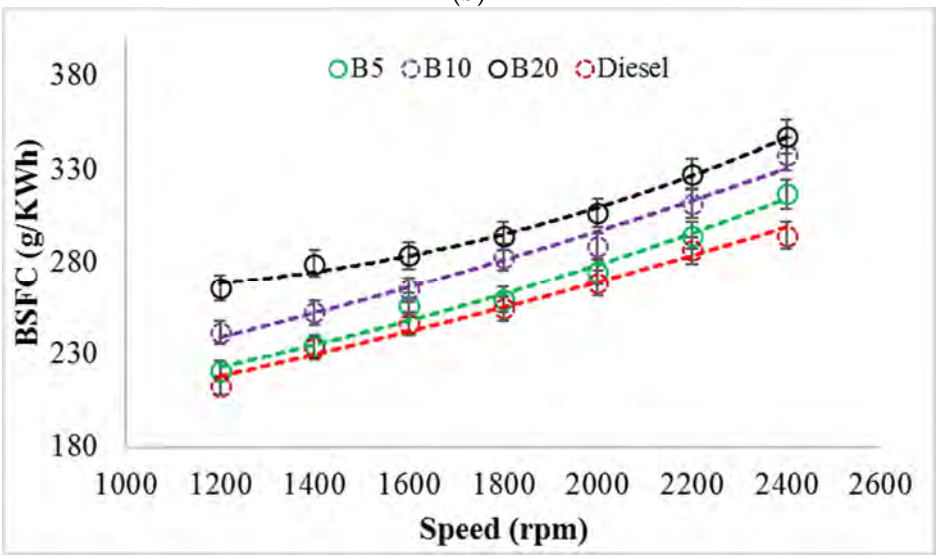

(**c**)

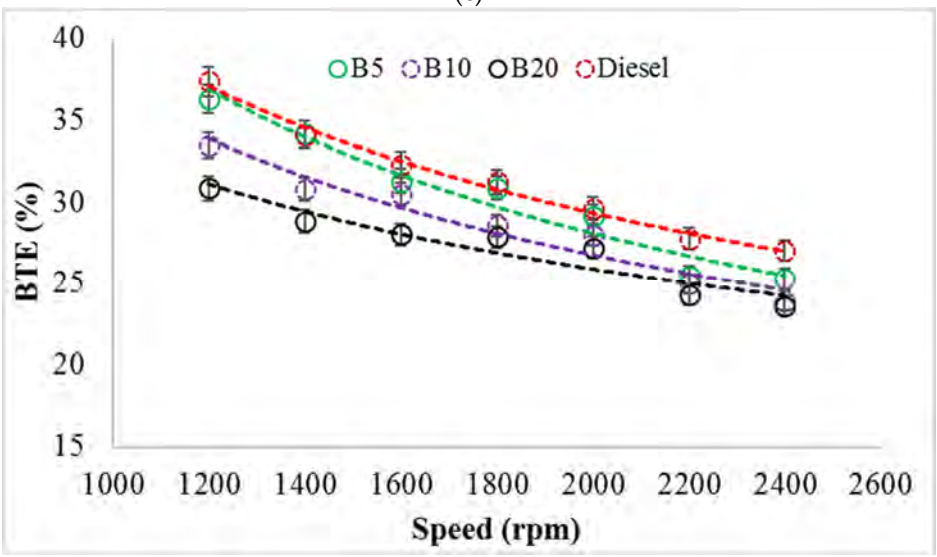

(**d**)

Figure 5. Variation of: (**a**) brake power, (**b**) torque, (**c**) brake specific fuel consumption (BSFC), and (**d**) brake thermal efficiency (BTE) for all PSO biodiesel-diesel blends and diesel with respect to engine speed at full load condition.

3.2.2. Torque

Figure 5b shows that torque increases initially with speed increase up to 1400 rpm when the maximum level is achieved and then decreases continuously until the maximum speed of 2400 rpm for all biodiesel blends and B0. B5 had the highest torque among the biodiesel blends due to its higher calorific value and lower density and viscosity. As expected, B0 (diesel) had the highest torque followed by B5, B10, and B20. The maximum torques were recorded at 1400 rpm, and these were 225 Nm, 221 Nm, 220 Nm, and 218 Nm for B0, B5, B10, and B20, respectively. The average torque reduction for B5, B10, and B20 as compared with B0 was 1.37%, 2.47%, and 3.85%, respectively.

3.2.3. Brake Specific Fuel Consumption (BSFC)

Brake specific fuel consumption (BSFC) is the ratio of fuel flow rate and brake power. According to Mofijur et al. [17], BSFC values depend on the relationship between the fuel injection system, fuel density, calorific value, and viscosity. Figure 5c shows the variation of BSFC for all PSO biodiesel-diesel blends and diesel with respect to engine speed. It is found that diesel has the lowest BSFC value in comparison with PSO biodiesel-diesel blends (B5, B10, and B20). The average BSFC value of B0 was measured as 256.5 g/kWh, whereas those for blends of B5, B10, and B20 were 265 g/kWh, 282.6 g/kWh, and 300.4 g/kWh, respectively. As mentioned earlier, the combined effects of fuel properties, such as density, viscosity, and calorific values of biodiesel may result in higher BSFC. Besides, biodiesel needs more fuel for producing the same power due to its lower calorific value in comparison with diesel. The average increase in BSFC values for B5, B10, and B20 as compared with B0 (diesel) were 3.35%, 10.16%, and 17.13%, respectively.

3.2.4. Brake Thermal Efficiency (BTE)

Brake thermal efficiency (BTE) is the ratio of the brake power and heat energy that is produced by fuel. Figure 5d shows that BTE decreases with the increase of biodiesel in the blends from B5 to B20. A higher BTE value (%) depends on some specific fuel properties such as higher calorific value, and lower density and viscosity. When compared with other blends, the properties of B5 were matched closely with diesel. The average BTE value of B5 was measured as 30.35%, whereas diesel was recorded as 31.33%. The lower calorific values and higher fuel consumptions of both B10 and B20 resulted in BTE values of 28.59% and 27.23%, respectively. The average reduction in BTE values for B5, B10, and B20 as compared with B0 (diesel) were 3.1%, 8.76%, and 13.1%, respectively.

3.3. Interaction Effects of Operating Parameters on PSO Engine Performance

The complex interaction effects of operating parameters, such as biodiesel blends, load, and speed, on each engine output response (BP, torque, BSFC, and BTE) could not be analysed independently. The significance of each of the various parameters in the model was obtained via analysis of variance (ANOVA). The experiments were carried out by use of the Box-Behnken response surface design. Minitab 18 was used to carry out the statistical analysis. Table 7 shows the factors and the range and levels of the investigated variables.

Table 7. Experimental range and levels coded for analysis of variance (ANOVA).

Factors	Unit	Symbol Coded	Range and Levels		
			–1	**0**	**1**
Biodiesel blends	%	BL	0	10	20
Load	%	LD	0	50	100
Speed	rpm	SP	1200	1800	2400

Once the experiments were completed, a full quadratic model was applied for the correlation of the response variable to the independent variables. The form of the full quadratic model is shown in Equation (2).

$$R = P_0 + P_1Q_1 + P_2Q_2 + P_3Q_3 + P_{1,2}Q_1Q_2 + P_{1,3}Q_1Q_3 + P_{2,3}Q_2Q_3 + P_{1,1}Q_1^2 + P_{2,2}Q_2^2 + P_{3,3}Q_3^2 \quad (2)$$

where R is the response factor; P_0 is a constant; P_1, P_2, P_3 are regression coefficients, $P_{1,1}$, $P_{1,2}$, $P_{1,3}$, $P_{2,2}$, $P_{2,3}$, and $P_{3,3}$ are quadratic coefficient; and, Q_1, Q_2, and Q_3 are independent variables.

Consideration was given to the linear, quadratic and combined effects of operating parameters to identify their impacts on the response. Each parameter's the significance was evaluated by the probability value (*p*-value) from ANOVA. At the 95% confidence level, the *p*-values less than 0.05 indicate a 'significant' effect of those parameters on the response. In other words, *p*-values more than 5% or 0.05 indicate 'not-significant' effects of those parameters on the response.

3.3.1. Effects of Biodiesel Blends, Load and Speed on Brake Power (BP)

The relationships between brake power and three operating parameters of biodiesel blends, load, and speed were analysed. A quadratic regression model based on the coded parameters with determined coefficients for statistical prediction as defined by Equation (3) was developed using Minitab 18 to predict BP (kW) as a function of biodiesel blends (BL), load (LD), and speed (SP).

$$BP = 20 - 0.018BL + 17.945\ LD + 4.41\ SP + 0.501\ BL^2 - 0.324\ LD^2 - 0.799\ SP^2 - 0.267\ BL \times LD - 2.177\ BL \times SP + 4.093\ LD \times SP \quad (3)$$

p-values from Table 8 show that the model is highly significant with an insignificant lack of fit. When considering the linear, quadratic, and combined effects, BL is not significant as a linear parameter; also, none of the quadratic terms is significant. Only the combined effects of LD and SP are highly significant, whereas BL and SP have a significant effect on BP. The ANOVA results in Table 8 also show that both LD and SP have the lowest *p*-values (<0.0001 each) and highest F-values (3307.29 and 199.74). According to the quadratic Equation (3), both LD and SP have positive effects on BP. This means that increasing the LD and SP will increase BP as well. The coefficient of determination (R^2) and the adjusted coefficient of determination (adj. R^2) were 99.86% and 99.61%, respectively, which indicates a high accuracy for the model.

Table 8. ANOVA results of the interactive effect of biodiesel blends, load, and speed on brake power.

Source	DF	Adj. SS	Adj. MS	F-Value	*p*-Value	Significant
Model	9	2821.89	313.54	402.53	<0.0001	Highly
Biodiesel blends (BL)	1	0.00	0.00	0.00	0.957	No
Load (LD)	1	2576.18	2576.18	3307.29	<0.0001	Highly
Speed (SP)	1	155.58	155.58	199.74	<0.0001	Highly
BL×BL	1	0.93	0.93	1.19	0.325	No
LD×LD	1	0.39	0.39	0.50	0.512	No
SP×SP	1	2.36	2.36	3.02	0.143	No
BL×LD	1	0.29	0.29	0.37	0.571	No
BL×SP	1	18.97	18.97	24.35	0.004	Yes
LD×SP	1	66.99	66.99	86.01	<0.0001	Highly
Lack-of-Fit	3	3.58	1.19	7.71	0.117	No
Pure Error	2	0.31	0.15	-	-	-
Total	14	2825.79	-	-	-	-
R^2 = 0.9986			Adj. R^2 = 0.9961			-

The ANOVA results in Table 8 for both LD × SP, and BL × SP interaction effects on BP are shown graphically in Figure 6. The three-dimensional (3D) surface plot and two-dimensional (2D) contour plot of LD and SP effects on BP are presented in Figure 6a,b respectively. BP (kW) increases with the increase of LD up to 100% and exceeds 40 kW with SP of 2000 rpm onwards. The maximum BP was found to be 45 kW at 2400 rpm. At 50% LD, the average BP value was recorded at about 20

kW with minimum effects from SP. However, the combined effects of LD and SP on BP are more significant with an increase of LD above 50%. Figure 6c,d present the 3D surface plot and 2D contour plot, respectively, which show only minor influences of changes of BL and SP on BP. It is therefore concluded that BL has a slight effect on BP, irrespective of SP changes.

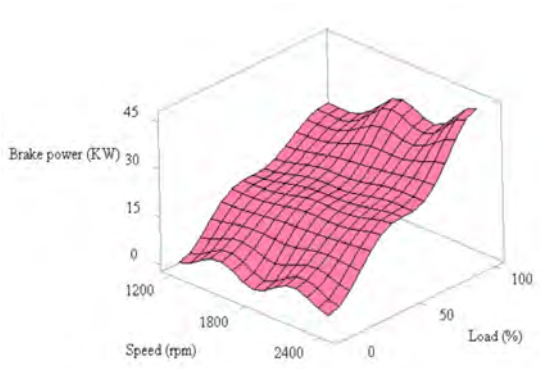

(**a**) Three-dimensional (3D) surface plot of load and speed on brake power (BP)

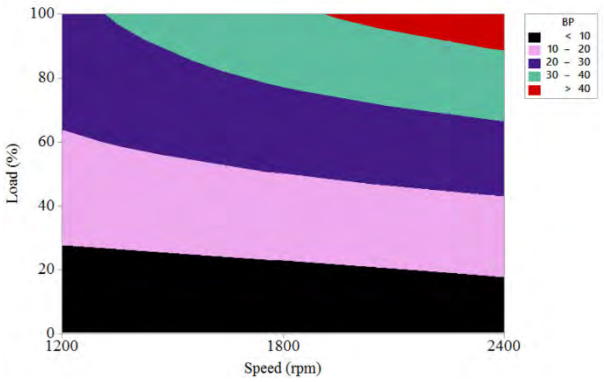

(**b**) Two-dimensional (2D) contour plot of load and speed on BP

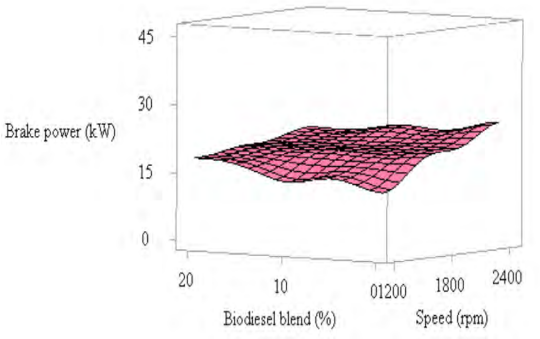

(**c**) 3D surface plot of biodiesel blends and speed on BP

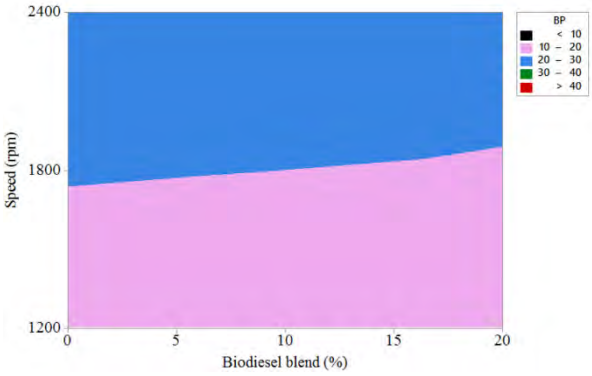

(**d**) 2D contour plot of biodiesel blends and speed on BP

Figure 6. Combined effects of biodiesel blends, load, and speed on BP (kW).

3.3.2. Effects of Biodiesel Blends, Load, and Speed on Torque

The relationships between torque and three operating parameters of biodiesel blend, load, and speed were analysed. Based on the coded parameters, a quadratic regression model with determined coefficients for statistical prediction, as defined by Equation (4), was developed using Minitab 18 to predict torque (N.m) as a function of biodiesel blend (BL), load (LD), and speed (SP).

$$T = 137.47 + 4.596BL + 95.884\ LD - 8.105\ SP - 16.6\ BL^2 - 15.06\ LD^2 - 18.13\ SP^2 - 0.53\ BL \times LD - 11.42\ BL \times SP - 12\ LD \times SP \quad (4)$$

p-values from Table 9 show that the model is highly significant with an insignificant lack of fit. When considering the linear, quadratic, and combined effects, only the combined effects of BL and LD are not significant. The ANOVA results in Table 9 show that LD is not significant, as it has the lowest *p*-value and highest F-value, while BL is found to be significant and all other parameters are highly significant. According to the quadratic Equation (4), both LD and BL have positive effects on torque. This means that increasing the LD and BL will increase torque as well. The coefficient of determination (R^2) and the adjusted coefficient of determination (adj. R^2) were 99.96% and 99.89%, respectively, which indicates the high accuracy of the model.

Table 9. ANOVA results of the interactive effect of biodiesel blends, load, and speed on torque.

Source	DF	Adj. SS	Adj. MS	F-Value	*p*-Value	Significant
Model	9	78,005.7	8667.3	1352.54	<0.0001	Highly
BL	1	169.0	169.0	26.37	0.004	Yes
LD	1	73,549.5	73,549.5	11,477.45	<0.0001	Highly
SP	1	525.5	525.5	82.01	<0.0001	Highly
BL × BL	1	1017.2	1017.2	158.73	<0.0001	Highly
LD × LD	1	837.8	837.8	130.73	<0.0001	Highly
SP × SP	1	1213.7	1213.7	189.40	<0.0001	Highly
BL × LD	1	1.1	1.1	0.18	0.691	No
BL × SP	1	521.7	521.7	81.41	<0.0001	Highly
LD × SP	1	575.5	575.5	89.81	<0.0001	Highly
Lack-of-Fit	3	30.4	10.1	12.13	0.077	No
Pure Error	2	1.7	0.8	-	-	-
Total	14	78,037.7	-	-	-	-
$R^2 = 0.9996$			Adj. $R^2 = 0.9989$			

The ANOVA results in Table 9 for LD × SP, and BL × SP interaction effects on torque are shown graphically in Figure 7. The 3D surface plot and 2D contour plot of LD and SP effects on torque are presented in Figure 7a,b, respectively. Torque (Nm) decreases with the increase of SP at 100% LD. The maximum torque was found to be 220 Nm at 1400 rpm. At 50% LD, the average torque was recorded as about 120 Nm with minimum effects from SP. However, the combined effects of LD and SP on torque are more significant with an increase of LD above 50%. Figure 7c,d present the 3D surface plot and 2D contour plot, respectively, which show only minor influences of changes of BL and SP on torque. It is therefore concluded that BL has a slight effect on torque, irrespective of SP changes.

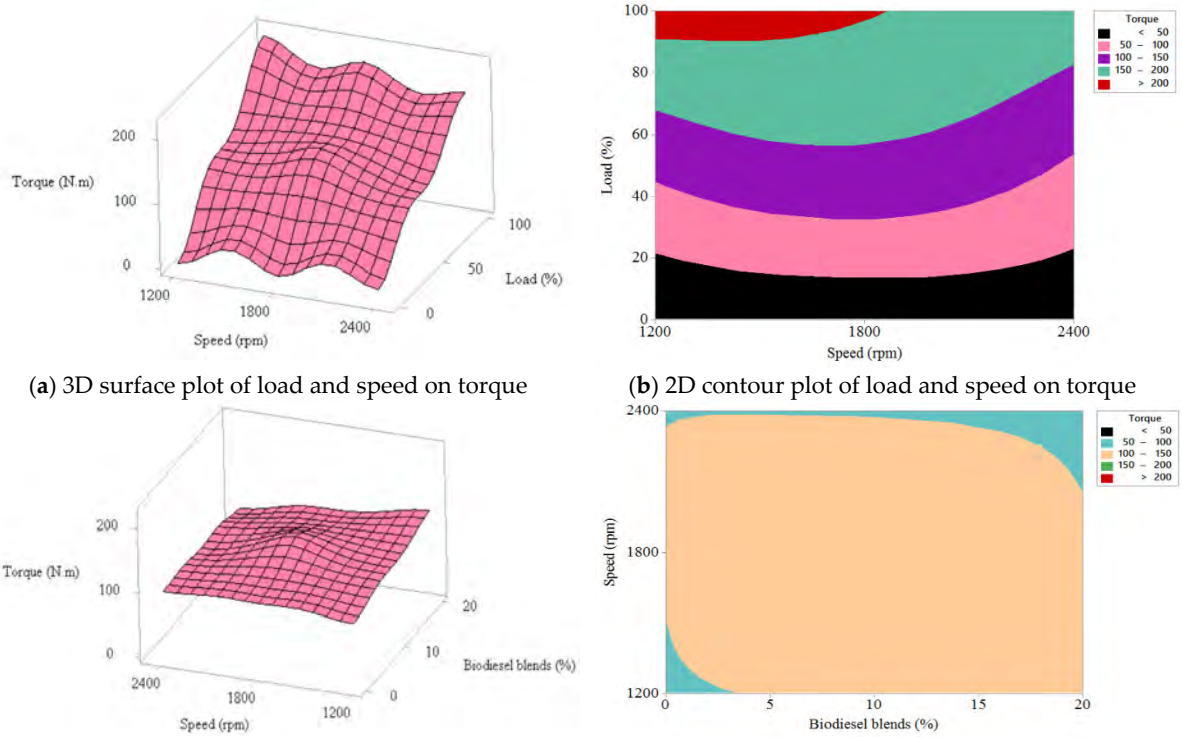

(**a**) 3D surface plot of load and speed on torque

(**b**) 2D contour plot of load and speed on torque

(**c**) 3D surface plot of biodiesel blends and speed on torque.

(**d**) 2D contour plot of biodiesel blends and speed on torque.

Figure 7. Combined effects of biodiesel blends, load, and speed on torque (Nm).

3.3.3. Effects of Biodiesel Blends, Load, and Speed on Brake Specific Fuel Consumption (BSFC)

The relationships between three operating parameters of biodiesel blend, load, and speed with brake specific fuel consumption (BSFC) were analysed. Based on the coded parameters, a quadratic regression model with determined coefficients for statistical prediction, as defined by Equation (5), was developed using Minitab 18 to predict BSFC (gm/kWh) as a function of biodiesel blends (BL), load (LD), and speed (SP).

$$BSFC = 252.17 + 138.13\ BL - 526.25\ LD - 30.43\ SP + 62.5\ BL^2 + 488.88\ LD^2 + 71.66\ SP^2 - 125.71\ BL \times LD - 38.55\ BL \times SP + 78.67\ LD \times SP \quad (5)$$

p-values in Table 10 show that the model is highly significant with an insignificant lack of fit. When considering the linear, quadratic, and combined effects, all of the parameters are highly significant. Among all parameters, LD is the parameter with the lowest *p*-value and highest F-value (20,429.23). According to the quadratic Equation (5), both LD and SP have a negative effect on BSFC. This means that increasing the LD will decrease BSFC, whereas decreasing the LD will increase BSFC. The SD parameter has less influence in changing BSFC. The coefficient of determination (R^2) and the adjusted coefficient of determination (adj. R^2) were 99.98% and 99.95%, respectively, which indicates the high accuracy of the model.

Table 10. ANOVA results of the interactive effect of biodiesel blends, load and speed on brake specific fuel consumption (BSFC).

Source	DF	Adj. SS	Adj. MS	F-Value	*p*-Value	Significant
Model	9	3,358,105	373,123	3440.61	<0.0001	Highly
BL	1	152,631	152,631	1407.43	<0.0001	Highly
LD	1	2,215,481	2,215,481	20,429.23	<0.0001	Highly
SP	1	7408	7408	68.31	<0.0001	Highly
BL × BL	1	14,424	14,424	133.00	<0.0001	Highly
LD × LD	1	882,480	882,480	8137.45	<0.0001	Highly
SP × SP	1	18,960	18,960	174.83	<0.0001	Highly
BL × LD	1	63,215	63,215	582.91	<0.0001	Highly
BL × SP	1	5944	5944	54.81	0.001	Highly
LD × SP	1	24,756	24,756	228.28	<0.0001	Highly
Lack-of-Fit	3	521	174	16.38	0.058	No
Pure Error	2	21	11	-	-	-
Total	14	3,358,647	-	-	-	-
R^2 = 0.9998			Adj. R^2 = 0.9995			

The ANOVA results in Table 10 for LD × SP, BL × LD, and BL × SP interaction effects on BSFC are shown graphically in Figure 8. The 3D surface plot and 2D contour plot of LD and SP effects on BSFC are presented in Figure 8a,b respectively. BSFC decreases with the increase of LD, irrespective of SP. The maximum BSFC was found to be 1450 gm/kWh at 0% LD and 1200 rpm SP. At 50% LD, the average BSFC was recorded at about 400 gm/kWh with almost no effect from changes in SP (rpm). Figure 8c,d present the 3D surface plot and 2D contour plot, respectively, of BL and LD effects on BSFC. At 0% LD, BL has a significant effect on BSFC. The 20% biodiesel blend (BL20) shows the maximum BSFC of 1450 gm/kWh at 0% LD. BSFC values decrease with the increase of LD, irrespective of BL. From Figure 8d, it can be seen that, at 36% LD, the 0–10% biodiesel blends (BL0, BL5, and BL10) have low BSFC values whereas, at 60% LD, BL20 also has achieved a lower BSFC. It is therefore concluded that BL has a minor effect on BSFC, irrespective of SP changes. Figure 8e,f show the 3D surface plot and 2D contour plot respectively of BL and SP effects on BSFC. BSFC values for BL0 have recorded for SP values in the range of 1200 to 2400 rpm and found to be less than 400 gm/kWh. Changes in both BL and SP influence BSFC values. From Figure 8f, it can be seen that

both BL at 5% and BL at 10% have low BSFC for SP values in the range of 1600 to 2000 rpm. Higher BL percentages with higher SP values (up to 2000 rpm) result in higher values of BSFC.

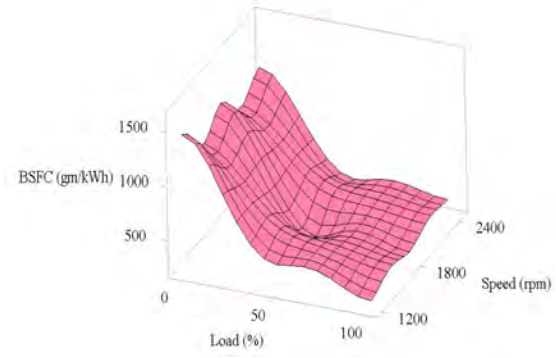

(**a**) 3D surface plot of load and speed on BSFC

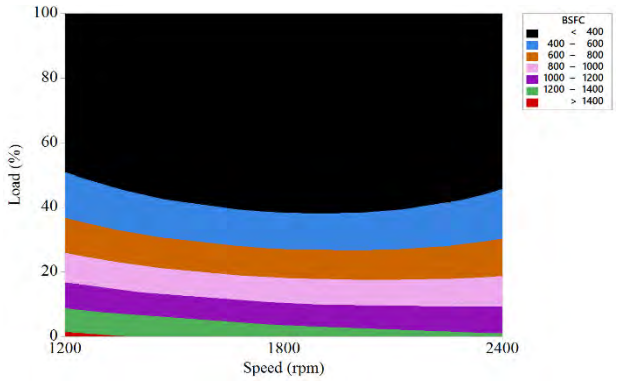

(**b**) 2D contour plot of load and speed on BSFC

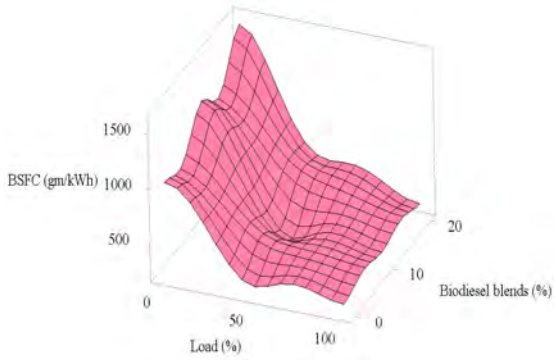

(**c**) 3D surface plot of biodiesel blends and load on BSFC

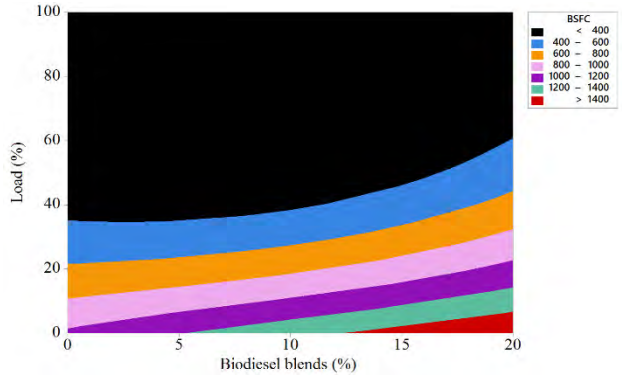

(**d**) 2D contour plot of biodiesel blends and load on BSFC

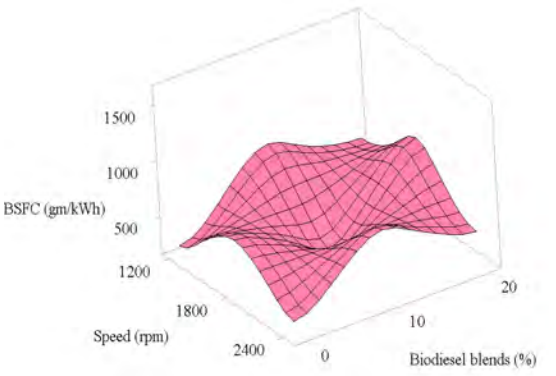

(**e**) 3D surface plot of biodiesel blends and speed on BSFC

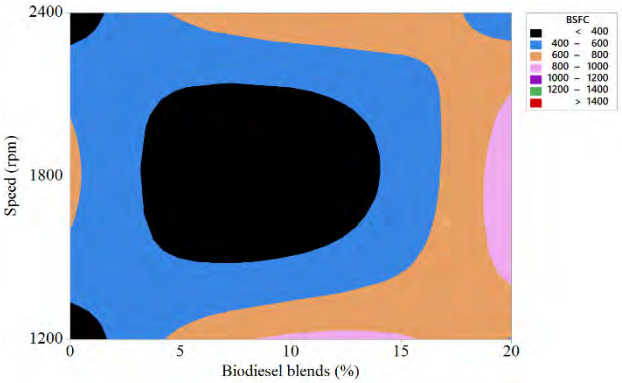

(**f**) 2D contour plot of biodiesel blends and speed on BSFC

Figure 8. Combined effects of biodiesel blends, load, and speed on BSFC (gm/kWh).

3.3.4. Effects of Biodiesel Blends, Load, and Speed on Brake Thermal Efficiency (BTE)

The relationships between brake thermal efficiency (BTE) and three operating parameters of biodiesel blends, load, and speed were analysed. Based on the coded parameters, a quadratic regression model with determined coefficients for statistical prediction, as defined by Equation (6), was developed using Minitab 18 to predict BTE (%) as a function of biodiesel blends (BL), load (LD), and speed (SP).

$$\text{BTE} = 32.283 - 1.36\,\text{BL} + 11.752\,\text{LD} - 1.71\,\text{SP} - 2.795\,\text{BL}^2 - 12.05\,\text{LD}^2 - 1.9\,\text{SP}^2 + 1.038\,\text{BL} \times \text{LD} + 0.267\,\text{BL} \times \text{SP} - 2.097\,\text{LD} \times \text{SP} \quad (6)$$

p-values in Table 11 show that the model is highly significant with an insignificant lack of fit. When considering the linear, quadratic, and combined effects, only the BL × LD and BL × SP

combined parameters are not significant; all other parameters are significant. Only the combined effects of LD × SP are significant, whereas the quadratic terms LD × LD, BL × BL, and SP × SP were all found to have significant effects on BTE. The ANOVA results in Table 11 also show that LD has both the lowest *p*-values (<0.0001) and highest F-value (940.76). According to the quadratic Equation (6), only LD has a positive effect on BTE. This means that increasing the LD will increase BTE as well. The coefficient of determination (R^2) and the adjusted coefficient of determination (adj. R^2) were 99.66% and 99.05%, respectively, which indicates the high accuracy of the model.

Table 11. ANOVA results of the interactive effect of biodiesel blends, load, and speed on brake thermal efficiency (BTE).

Source	DF	Adj. SS	Adj. MS	F-Value	*p*-Value	Significant
Model	9	1717.12	190.79	162.44	<0.0001	Highly
BL	1	14.80	14.80	12.60	0.016	Yes
LD	1	1104.97	1104.97	940.76	<0.0001	Highly
SP	1	23.39	23.39	19.92	0.007	Yes
BL × BL	1	28.85	28.85	24.57	0.004	Yes
LD × LD	1	536.17	536.17	456.49	<0.0001	Highly
SP × SP	1	13.34	13.34	11.35	0.020	Yes
BL × LD	1	4.31	4.31	3.67	0.114	Not
BL × SP	1	0.29	0.29	0.24	0.642	No
LD × SP	1	17.60	17.60	14.98	0.012	Yes
Lack-of-Fit	3	5.48	1.83	9.26	0.099	No
Pure Error	2	0.39	0.20	-	-	-
Total	14	1722.99	-	-	-	-
R^2 = 0.9966			Adj. R^2 = 0.9905			

The ANOVA results in Table 11 for LD × SP interaction effects on BTE are shown graphically in Figure 9. The 3D surface plot and 2D contour plot of LD and SP effects on BTE are presented in Figure 9a,b, respectively. BTE increases with the increase of LD with minimum impacts from SP. The maximum BTE was found to be 33.43% at 1200 rpm. However, the combined effects of LD and SP on BTE are affected by an increase of LD above 50%. It is therefore concluded that SP has a minor impact on BTE, irrespective of LD changes.

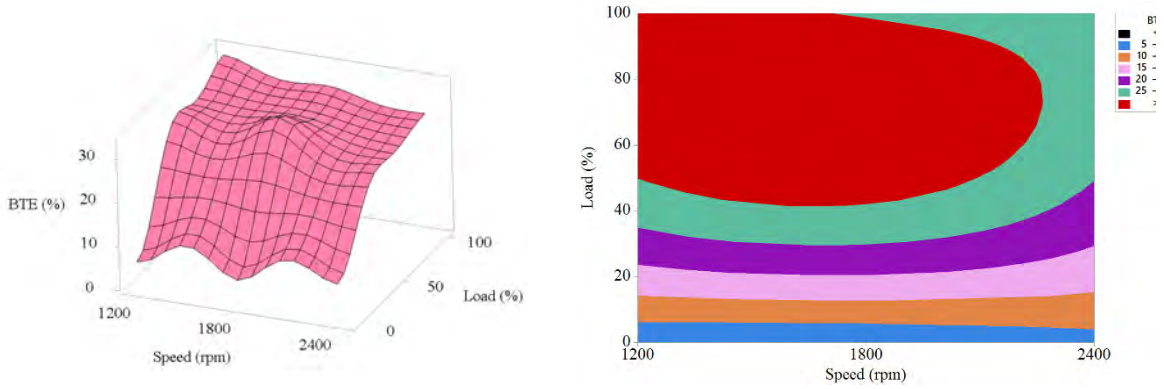

(**a**) 3D surface plot of load and speed on BTE

(**b**) 2D contour plot of load and speed on BTE

Figure 9. Combined effects of biodiesel blends, load, and speed on BTE (%).

4. Conclusions

This study investigated the effect of papaya seed oil (PSO) biodiesel in an agricultural diesel engine with various biodiesel-diesel blends and the resulting engine performance outcomes as

compared with those from the use of a reference diesel. A response surface methodology was introduced to analyse and describe the performance of this engine. The results of this investigation can be summarised, as follows:

- PSO biodiesel-diesel blends (B5–B50) meet the European standard EN 590 for having minimum oxidation stability of 20 h.
- Over the entire speed range of 1200 to 2400 rpm, the average BP value reductions for B5, B10, and B20 in comparison with B0 were 2.88%, 3.87%, and 5.13%, respectively.
- The average torque reductions for B5, B10, and B20 in comparison with B0 were 1.37%, 2.47%, and 3.85%, respectively.
- The average increase in BSFC values for B5, B10, and B20 in comparison with B0 were 3.35%, 10.16%, and 17.13%, respectively.
- The average BTE value of B5 was measured as 30.35%, whereas B0 (diesel) was recorded as 31.33%.
- The interactive relationships between three operating parameters (biodiesel blends, load, and speed) and four responses (BP, torque, BSFC, and BTE) were analysed. ANOVA and a statistical regression model show that load and speed were the two most important parameters that affect all four responses. The biodiesel blends parameter had a significant effect on BSFC.

These results show that B5 and B10 PSO biodiesel-diesel blends can be used to fuel diesel engines without further engine modification. Therefore, it can be concluded that papaya seed oil can be considered as a promising source of biodiesel production. However, before recommending as a future alternative energy source in commercial scale, further research needs to be conducted in terms of engine emissions, in-cylinder pressure, burn rate data, combustion analysis, and tribological performance analysis.

Author Contributions: The contributions of each author are as follows: M.A. produced and characterised biodiesel-diesel blends, conducted and analysed engine performance, and drafted the manuscript; M.G.R. contributed to the experimental design and thoroughly revised the paper, and N.A. helped to revised and improved the paper.

Funding: This research received no external funding.

Acknowledgments: The authors would like to acknowledge Tim McSweeney, Adjunct Research Fellow, Tertiary Education Division at Central Queensland University, Australia for his contribution in proof reading of this article.

Conflicts of Interest: The authors declare no conflict of interest.

References

1. Bhuiya, M.M.K.; Rasul, M.G.; Khan, M.M.K.; Ashwath, N.; Azad, A.K.; Hazrat, M.A. Second Generation Biodiesel: Potential Alternative to-edible Oil-derived Biodiesel. *Energy Procedia* **2014**, *61*, 1969–1972.
2. Asokan, M.A.; prabu, S.S.; Kamesh, S.; Khan, W. Performance, combustion and emission characteristics of diesel engine fuelled with papaya and watermelon seed oil bio-diesel/diesel blends. *Energy* **2018**, *145*, 238–245.
3. Tüccar, G.; Tosun, E.; Özgür, T.; Aydın, K. Diesel engine emissions and performance from blends of citrus sinensis biodiesel and diesel fuel. *Fuel* **2014**, *132*, 7–11.
4. Ozsezen, A.N.; Canakci, M.; Turkcan, A.; Sayin, C. Performance and combustion characteristics of a DI diesel engine fueled with waste palm oil and canola oil methyl esters. *Fuel* **2009**, *88*, 629–636.
5. Agunbiade, F.O.; Adewole, T.A. Methanolysis of Carica papaya Seed Oil for Production of Biodiesel. *J. Fuels* **2014**, *2014*, 904076.
6. Wong, C.S.; Othman, R. Biodiesel Production by Enzymatic Transesterification of Papaya Seed Oil and Rambutan Seed Oil. *Int. J. Eng. Technol.* **2014**, *6*, 2773–2777.
7. Mohan, A.; Sen, S.S.S. Emission Analysis Of The Biodiesel from Papaya and Chicken Blends. *Int. J. Inform. Futurist. Res.* **2015**, *2*, 2258–2264.

8. De Melo, M.L.S.; Santos, N.A.; Rosenhaim, R.; Souza, A.G.; Filho, P.F.A. Use of thermal analysis techniques for evaluation of the stability and chemical properties of papaya biodiesel (*Carica papaya* L.) at low temperatures. *J. Therm. Anal. Calorim.* **2011**, *106*, 831–836.
9. Daryono, E.D.; Sinaga, E.J. Rapid In Situ Transesterification of Papaya Seeds to Biodiesel with the Aid of Co-solvent. *Int. J. Renew. Energy Res.* **2017**, *7*, 379–385.
10. Anwar, M.; Rasul, M.G.; Ashwath, N. Optimization of biodiesel production process from papaya (*Carica papaya)* seed oil. In Proceedings of the 2017 IEEE 7th International Conference on Power and Energy Systems (ICPES), Toronto, ON, Canada, 1–3 November 2017.
11. Prabhakaran, P.; Saravanan, C.G.; Aalam, C.S. Effects of Papaya Methyl Ester on DI Diesel Engine Combustion, Emission and Performance Characteristics. *Int. Res. J. Eng. Technol.* **2016**, *3*, 319–325.
12. Sundar Raj, C.; Karthikayan, M. Effect of additive on the performance, emission and combustion characteristics of a diesel engine run by diesel-papaya methyl ester blends. *Int. J. Chem. Sci.* **2016**, *14*, 2823–2834.
13. Sharma, S.K.; Mitra, S.K.; Saran, S. *Papaya Production in India—History, Present Status and Future Prospects*; International Society for Horticultural Science (ISHS): Leuven, Belgium, 2016; Volume 1111, pp. 87–94.
14. Anwar, M.; Rasul, M.G.; Ashwath, N. Production optimization and quality assessment of papaya (*Carica papaya*) biodiesel with response surface methodology. *Energy Convers. Manag.* **2018**, *156*, 103–112.
15. Silitonga, A.S.; Masjuki, H.H.; Mahlia, T.M.I.; Ong, H.C.; Chong, W.T.; Boosroh, M.H. Overview properties of biodiesel diesel blends from edible and non-edible feedstock. *Renew. Sustain. Energy Rev.* **2013**, *22* (Suppl. C), 346–360.
16. Silitonga, A.S.; Ong, H.C.; Mahlia, T.M.I.; Masjuki, H.H.; Chong, W.T. Biodiesel Conversion from High FFA Crude Jatropha Curcas, Calophyllum Inophyllum and Ceiba Pentandra Oil. *Energy Procedia* **2014**, *61* (Suppl. C), 480–483.
17. Mofijur, M.; Masjuki, H.H.; Kalam, M.A.; Atabani, A.E. Evaluation of biodiesel blending, engine performance and emissions characteristics of Jatropha curcas methyl ester: Malaysian perspective. *Energy* **2013**, *55*, 879–887.
18. Hasni, K.; Ilham, Z.; Dharma, S.; Varman, M. Optimization of biodiesel production from Brucea javanica seeds oil as novel non-edible feedstock using response surface methodology. *Energy Convers. Manag.* **2017**, *149* (Suppl. C), 392–400.

{this page is intentionally left blank}

Declaration of Co-authorship and Contribution

Research Division

CHAPTER 6: Interactive Effects of Operating Parameters on Emission Characteristics

Title of the paper	A pragmatic and critical analysis of engine emissions for biodiesel blended fuels
Full bibliographic reference	Anwar, M., M. Rasul, and N. Ashwath, 2020, A pragmatic and critical analysis of engine emissions for biodiesel blended fuels. Fuel, 2020. 270: p. 117513. https://www.sciencedirect.com/science/article/pii/S0016236120305081?dgcid=rss_sd_all
Status	Published

Nature of Candidate's Contribution, including percentage of total
I was responsible for designed the study, performed the experiments and wrote the first draft of the manuscript. [80%]

Nature of all Co-Authors' Contributions, including percentage of total
My co-authors, Prof. Mohammad Rasul, and A/Professor Nanjappa Ashwath, were designed the experimentation, reviewed, revised and improved the manuscript. [20%]

Has this paper been submitted for an award by another research degree candidate (Co- Author), either at CQUniversity or elsewhere? (if yes, give full details)
No

Candidate's Declaration

I declare that the publication above meets the requirements to be included in the thesis as outlined in the Research Higher Degree Theses Policy and Procedure.

Mohammad Anwar

Fuel 270 (2020) 117513

Contents lists available at ScienceDirect

Fuel

journal homepage: www.elsevier.com/locate/fuel

Full Length Article

A pragmatic and critical analysis of engine emissions for biodiesel blended fuels

Mohammad Anwar[a,*], Mohammad G. Rasul[a], Nanjappa Ashwath[b]

[a] Central Queensland University, School of Engineering and Technology, North Rockhampton, Queensland 4702, Australia
[b] Central Queensland University, School of Health, Medical and Applied Sciences, North Rockhampton, Queensland 4702, Australia

ARTICLE INFO

Keywords:
Carica papaya
Exhaust
Emissions
Biodiesel
Diesel engine
Response surface methodology
RSM

ABSTRACT

This paper explores the impact of non-edible biodiesel blends on emission characteristics under various loading conditions in a naturally aspirated four-strokes multi-cylinder diesel engine. A comparative analysis of the emissions characteristics of four non-edible biodiesel (beauty leaf biodiesel, papaya seed biodiesel, stone fruit biodiesel and tomato seed biodiesel) blends (20% vol. = B20) and diesel was performed by varying engine loads (0, 50 and 100%) and speeds (1200, 1800 and 2400 rpm). The aim was to optimise operating parameters such as biodiesel blends, engine loads and speed on engine emissions such as nitrogen oxide (NO_x), carbon dioxide (CO_2), hydrocarbon (HC), particulate matter (PM), carbon monoxide (CO) and exhaust gas temperature (EGT). A statistical model and analysis of variance (ANOVA) were used to optimise various parameters. At full load condition and 2400 rpm, the minimum and maximum increase in NO_x and CO_2 emissions were found to be 4.1% to 23.6% and 1.7% to 19% for papaya seed biodiesel PB20 and beauty leaf biodiesel BTL20 respectively. The results reveal that the engine load and speed were the two most imperative parameters that affected emissions (NO_x, HC, PM and CO). Both biodiesel blend and the load were responsible for changing the EGT and NO_x emissions. While NO_x emissions were unaffected by variations in biodiesel blends, load or speed, the CO_2 emissions were not affected by the operating parameters. To conclude, papaya seed oil can be a plausible biodiesel feedstock and its diesel blends with varying engine speeds, and loads can provide optimal engine testing characteristics for negotiating NO_x, CO_2, HC, PM, CO, and EGT concentration.

1. Introduction

Both outdoor and household air pollution levels remain seriously elevated in many parts of the world, leading to a shocking death toll of 7 million people every year. Outdoor air pollution itself accounts for 4.2 million deaths every year due to stroke, chronic respiratory diseases, heart diseases and lung cancer [1]. One of the major causes of this mortality is the exposure to small particulate matter (PM) of 2.5 μm or less in diameter. The sources that are responsible for this outdoor air pollution are manufacturing industries, power generation, municipal and agricultural wastes, and transportation. There are many sub-sources of transportation air pollution such as light/heavy duty vehicles and motorcycles representing on-road causes, whereas aircraft, diesel equipment, marine engine/ocean vessels, locomotives, and recreation vehicles and lawn mower are non-road contributors. Both on-road and non-road transportation sources are mostly accountable for air quality deterioration. Ready availability and easy affordability of fossil fuels such as the fuel derived from petroleum sources has triggered the rapid growth of the transportation industry, and resulted in substantial increases in air pollution, i.e., exhaust gas emissions. These exhaust gas emissions are not only adversely affecting our clean environment and human health but can increase the rate of global warming. The fifth assessment report of the United Nations Intergovernmental panel on climate change (IPCC) indicated that the transport sector produced 7.0 Gigatonnes of equivalent carbon dioxide ($GtCO_2eq$) of direct greenhouse gas emissions including non-CO_2 gases in 2010. Vehicle emissions could increase at a rate faster than any other emissions generating sectors and reach around 12 $GtCO_2eq$ per year by 2050 [2]. The greenhouse gas emissions of the transport sector has grown 250% from 2.8 $GtCO_2eq$ in 1970 to 7.0 $GtCO_2eq$ in 2010 [2]. The most common vehicle power units, i.e., compression ignition (CI) engines, emit NO_x, CO, HC, formaldehyde (HCHO), PM and non-methane organic gases (NMOG) as well.

The consequences of excessive use of fossil fuel greatly affect the whole planet's health and quality of living. Apart from global warming, other results include that NO_x emissions lead to ground level ozone

* Corresponding author.
E-mail address: m.anwar@cqu.edu.au (M. Anwar).

https://doi.org/10.1016/j.fuel.2020.117513
Received 13 August 2019; Received in revised form 14 January 2020; Accepted 29 February 2020

Nomenclature

ANOVA	Analysis of variance
B20	20% Biodiesel + 80% diesel
BTL20	20% Beauty leaf biodiesel + 80% diesel
CO	Carbon monoxide
EGT	Exhaust gas temperature
HC	Hydrocarbon
NO_x	Nitrogen oxide
PB10	10% Papaya seed biodiesel + 90% diesel
PM	Particulate matter
SFO20	20% Stone fruit biodiesel + 80% diesel
TMT20	20% Tomato seed biodiesel + 80% diesel
B0	100% diesel
BL	Biodiesel blends
CI	Compression Ignition
CO_2	Carbon dioxide
GtCO2eq	Gigatonnes of equivalent carbon dioxide
LD	Engine Load
PB5	5% Papaya seed biodiesel + 95% diesel
PB20	20% Papaya seed biodiesel + 80% diesel
PSO	Papaya seed oil
SP	Engine Speed

formation which is severely harmful to human beings and animal life as well as for vegetation; CO_2 and CO cause ozone layer depletion; sulphuric oxides and NO_x trigger acidification; heart and nervous system disorders are caused by CO; unburnt HC can cause serious coughing, eye irritation and drowsiness; and NO_x and PM cause respiratory problem, asthma and lung cancer [3–6]. However, biofuel or biodiesel can be used as alternatives to fossil fuel in CI engines to reduce their HC, smoke and CO emissions [7,8]. As biodiesels are considered to be oxygenated fuels, the excess oxygen content in biodiesel ensures complete combustion, resulting in higher exhaust gas temperature as well as higher NO_x formation. Nabi et al. [9] reported that PM generation from biodiesel combustion is significantly reduced due to the higher oxygen content and absence of aromatics in the fuel.

In recent decades, many researchers have been investigating alternative biodiesels and their blends on engine performance and technical feasibility. Sathiyamoorthi et al. [10] investigated palmarosa oil biodiesel at different blends with diesel, and found lower CO, HC, smoke emissions and slightly higher NO_x emissions generation in all biodiesel blends compared with pure diesel. Castor biodiesel can reduce CO and HC by 9% and 8.8% respectively. In addition, a considerable reduction in oxides of nitrogen was claimed by Arunkumar et al. [11]. They also mentioned the increase in BSFC by 4% and decrease in BTE by 2.2%. Patel et al. [12] reported that waste cooking oil biodiesel exhibited a slightly higher heat release rate than diesel at 1500 rpm speed. They found HC and NO_x emissions were lower for waste cooking, karanja and jatropha biodiesels compared to diesel, while CO emissions were higher. Roy et al. [13] used canola oil biodiesel at different blends and found there was no increase in NO_x emissions as well as lower CO and HC emissions at 5% biodiesel blend. Uyumaz [14] investigated mustard seed oil biodiesel and found remarkable reductions in CO and smoke emissions at 30% biodiesel blend, whereas NO_x emissions were increased by 22.1%. They also showed that, for a 10% biodiesel blend, the indicated thermal efficiency decreased 6.8% while BSFC increased 4.8%. Kakati and Gogoi [15] produced biodiesel from kutkura and found the engine performance of 10% and 20% biodiesel blends gave almost similar fuel consumption rates with diesel. They found that BTE was higher while smoke was recorded lower at all biodiesel blends. Rashed et al. [16] investigated palm, jatropha and moringa oil biodiesel and found palm biodiesel was better in terms of engine performance and minimum emissions compared with jatropha and moringa biodiesel fuel. Sanjid et al. [17] mixed two non-edible feedstocks, kapok and moringa, and found average NO_x and CO_2 emissions for that mixed blends were 14–17% and 1–3% higher respectively than for diesel. Again, for the mixed blends, the average HC and CO emissions were found to be 23–38% and 16–31% lower respectively than for diesel.

However, very limited literature is available on emissions studies of papaya seed oil (PSO) biodiesel. Researchers have mixed PSO biodiesel with other biodiesels, but none have done engine emissions analysis in a full instrumented four stroke, multi-cylinder engine. For example, Asokan et al. [18] reported that the emissions characteristics of mixed watermelon and papaya seed biodiesel (20% vol. = B20) were found to be better than diesel, as the emissions of CO, HC, and smoke were 27.3%, 23.8%, and 8.3% less for B20 than diesel. Prabhakaran et al. [19] recommended PSO B25 to be an acceptable biodiesel blend, for the intent of lower emissions of CO and NO_x emissions. Sundar Raj et al. [20] and Anwar et al. [21] concluded that PSO biodiesel-diesel blends with additives have better combustion and emissions characteristics, with lower smoke density and reductions in NO_x. Mohan and Sen [22] used biodiesel mix blends (20% vol. of papaya biodiesel with 80% vol. of chicken biodiesel) and found a marginal increase in NO_x emissions while CO, HC and smoke were reduced compared with diesel.

The literature search provided no clear understanding of the influence of PSO biodiesel blends, engine loads and speeds on the NO_x, CO_2, HC, CO and PM emissions and EGT of a CI engine. Therefore, this work aims to determine the optimum level of biodiesel blends, engine loads and speeds using papaya biodiesel blends and assessing their contribution on a fully instrumented four stroke, four cylinder diesel engine using mathematical modeling and ANOVA methods in achieving lower emissions. The main objective is to gain a detailed understanding of the PSO biodiesel blends' emissions characteristics under varied engine load conditions (0–100%) and engine speed (1200 rpm), engine mid speed (1800 rpm) and engine high speed (2400 rpm).

2. Materials and methods

2.1. Biodiesel production

PSO was supplied from an approved local supplier (The Reliable Convenience Store) of vegetable oils in Central Queensland, Australia. The transesterification method was used to convert the oil to biodiesel. Anwar et al. [23,24] discussed the optimisation process and biodiesel conversion techniques in details. In the transesterification reaction, potassium hydroxide (KOH pellets, 99% purity) was used as a catalyst and methanol (99.9% purity) was chosen as the alcohol. KOH was dissolved in methanol at 50 °C to produce methoxide. This methoxide was then poured into a three-neck laboratory reactor that contained pre-heated PSO for performing the transesterification reaction. Reaction time, temperature and agitation speed were controlled as per the experimental design from the optimisation process. At the end of the reaction, the mixture was moved to a separation funnel to separate the phase and held for one day. Impurities and glycerol formed at the bottom and drained away. The upper layer (biodiesel) was transferred into a beaker and heated for 15 min at 110 °C to remove any methanol and water content. Before stored at laboratory environment, biodiesel was filtered through Whatman® qualitative Grade 1 filter paper (pore size: 11 μm). Three PSO biodiesel blends were prepared comprising homogeneous mixtures of 5%, 10% and 20% vol. of biodiesel with 95%, 90% and 80% vol. of diesel respectively, denoted by PB5, PB10 and PB20. Several ASTM standards and equipment were used to identify different fuel properties such as kinematic viscosity (ASTM D445) with *NVB classic* equipment (accuracy ± 0.01 mm^2/s); density (ASTM D1298) with *DM40 LiquiPhysics*™ density meter (accuracy ± 0.1 kg/

m^3); flash point (ASTM D93) with *NPM 440 Pensky-Martens flash point tester* (accuracy ± 0.1 °C); acid value (ASTM D664) with *Automation titration Rondo 20* (accuracy ± 0.001 mg KOH/g); calorific value (ASTM D240) with *6100EF semi-auto bomb calorimeter* (accuracy ± 0.001 MJ/kg) and oxidation stability (ASTM D2274) with *873 Rancimat* (accuracy ± 0.01 h). Table 1 shows the physico-chemical properties of raw PSO, pure PSO biodiesel (PB100) and PB20 that were used in this study.

2.2. Experimental engine setup

Four-cylinder, four stroke indirect injection Kubota V3300 series diesel engine was fuelled with PSO biodiesel blends (PB5, PB10 and PB20) and reference pure diesel fuel (B0). The detail engine technical specifications are listed in Table 2. The engine emissions data using the PSO biodiesel blends and pure diesel were collected under different load (25–100%) conditions and at 1400 rpm (maximum rated torque). A comparative emissions analysis of different non-edible biodiesels and PSO biodiesel was performed under different load conditions (0–100%) and at different speeds (1200, 1800 and 2400 rpm). Fig. 1 shows the schematic of the engine along with its data acquisition system. Exhaust gas emissions such as, NO_x (ppm), HC (ppm), CO (vol.%) and CO_2 (vol. %) were measured using a CODA5 gas analyzer. The gas analyzer uses a non-dispersive infrared sensor for measuring exhaust gas emissions. A MPM-4M branded particulate matter (PM) meter was used for measuring PM (mg/m^3) emissions. The engine was warmed up prior to every test by running with pure diesel (B0) at full load. For technical analysis and acquisition of data, the desired biodiesel blend was fuelled on the engine. The engine was flushed with pure diesel immediately following each test to prevent contamination with other biodiesel blends.

Experimental error and uncertainty could arise in several ways while tests were conducted. Some possible ways to minimize errors are proper planning, condition monitoring, right instrument selection, reading and observing, calibration and controlled experimental environment. Table 3 provides technical information about gas analyser, PM meter and error tolerances.

3. Results and discussion

The viscosity, density, acid value, IV and CN of PSO biodiesel are higher than diesel. PSO biodiesel has higher oxygen content that resulted in a reduced (15% less than diesel) calorific value of the fuel. Such intrinsic attributes of PSO biodiesel influence significantly the emission characteristics of the engine. This section presents a detailed emissions analysis of PSO biodiesel and its comparison with other non-edible biodiesels (beauty leaf, stone fruit oil, tomato oil biodiesel). Interactive effects of engine parameters such as PSO biodiesel blend concentration, engine load and speed on emissions characteristics are also presented in this section.

Table 2
Specification of the diesel engine.

Items	Unit	Specifications
Model		Kubota V3300, Indirect injection
Type	–	Vertical, 4 cycle liquid cooled diesel
No. of cylinders	–	4
Total displacement	L	3.318
Bore × Stroke	mm	98 × 110
Combustion type	–	Spherical type [E-TVCS (Three vortex combustion system)]
Intake system	–	Natural aspired
Rated power output	kW/rpm	53.9/2600
Rated torque	Nm/rpm	230/1400
Compression ratio	–	22.6:1
Fuel injection timing	–	16° before TDC
Injection pressure	MPa	13.73
Emissions certification	–	Tier 2

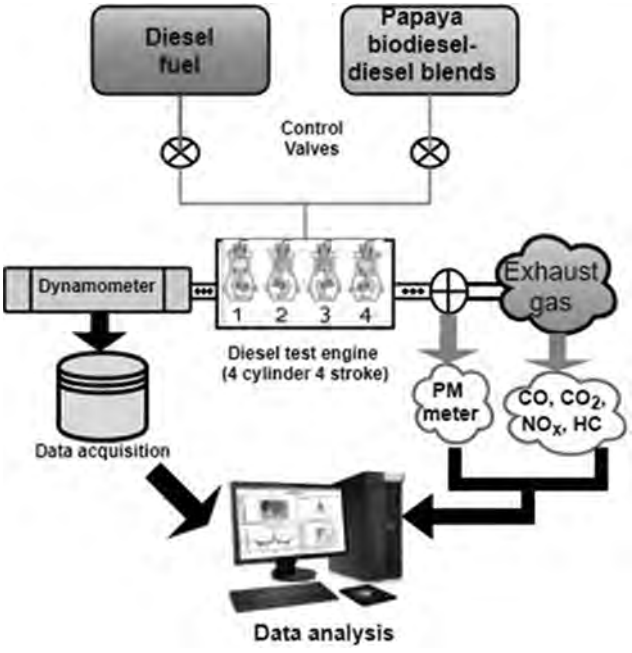

Fig. 1. The test engine schematic.

3.1. Engine emissions analysis

3.1.1. Nitrogen oxide (NO_x) emissions

In the combustion chamber, high temperatures break down the nitrogen molecular bonds and cause a sequence of oxygen reactions to create nitrogen oxide (NO_x). Yatish et al. [25] mentioned that several factors in the flame front and post-flame zone, including the content of oxygen, in-cylinder temperature and residence time, are responsible for NO_x formation. The variation in NO_x emissions with changes in load for PSO biodiesel and diesel at 1400 rpm is shown in Fig. 2(a). It has been

Table 1
Physico-chemical properties of PSO biodiesel (PB100), PB20 with diesel (B0).

Properties	Units	PSO	PB100	PB20	B0	ASTM D6751-2	EN14214-03	Australian Fuel Standard (Biodiesel)
Density	kg/m^3	885	840	829.76	827.2	870–890	860–900	860–890
Viscosity at 40 °C	mm^2/s	27.3	3.53	3.29	3.23	1.9–6.0	3.5–5.0	3.5–5.0
Acid value	mg KOH/g	0.98	0.42	0.12	0.05	Maximum 0.5	Maximum 0.5	Maximum 0.8
Cetane number (CN)	–	–	48.29	48.06	48.00	Minimum 47	Minimum 51	–
Calorific value	MJ/kg	–	38.49	43.94	45.30	–	35.00	–
Flash point	(°C)	–	112	77.20	68.50	Minimum 93	> 120	–
Iodine value (IV)	–	79.95	115.89	53.82	38.30	–	Maximum 120	Maximum 120
Oxidation stability (OS)	Hour	77.97	5.61	32.32	39	Minimum 3	Minimum 6	Minimum 6

Table 3
Exhaust gas analyser, PM meter specification and error tolerances [23].

Measured gas	Measurement				
	Range	Resolution	Accuracy	Relative uncertainty	Average reading for B0
HC	0–30,000 ppm (n-hexane)	1 ppm	± 1 ppm abs.	(± 1/22.57) = 0.044	22.57
CO	0–15%	0.001%	± 0.02% abs.	(± 0.02/0.2) = 0.1	0.2
CO_2	0–20%	0.001%	± 0.3% abs.	(± 0.3/12.28) = 0.024	12.28
NO_x	0–5000 ppm	1 ppm	± 1 ppm abs.	(± 1/354) = 0.0028	354
Meter	*Particle size*	*Particle concentration range*	*Resolution*		
Particulate Matter	< 100 nm to > 10 μm	0.1 to > 700 mg/m^3	± 0.1 mg/m^3	(± 0.1/55.2) = 0.0018	55.2

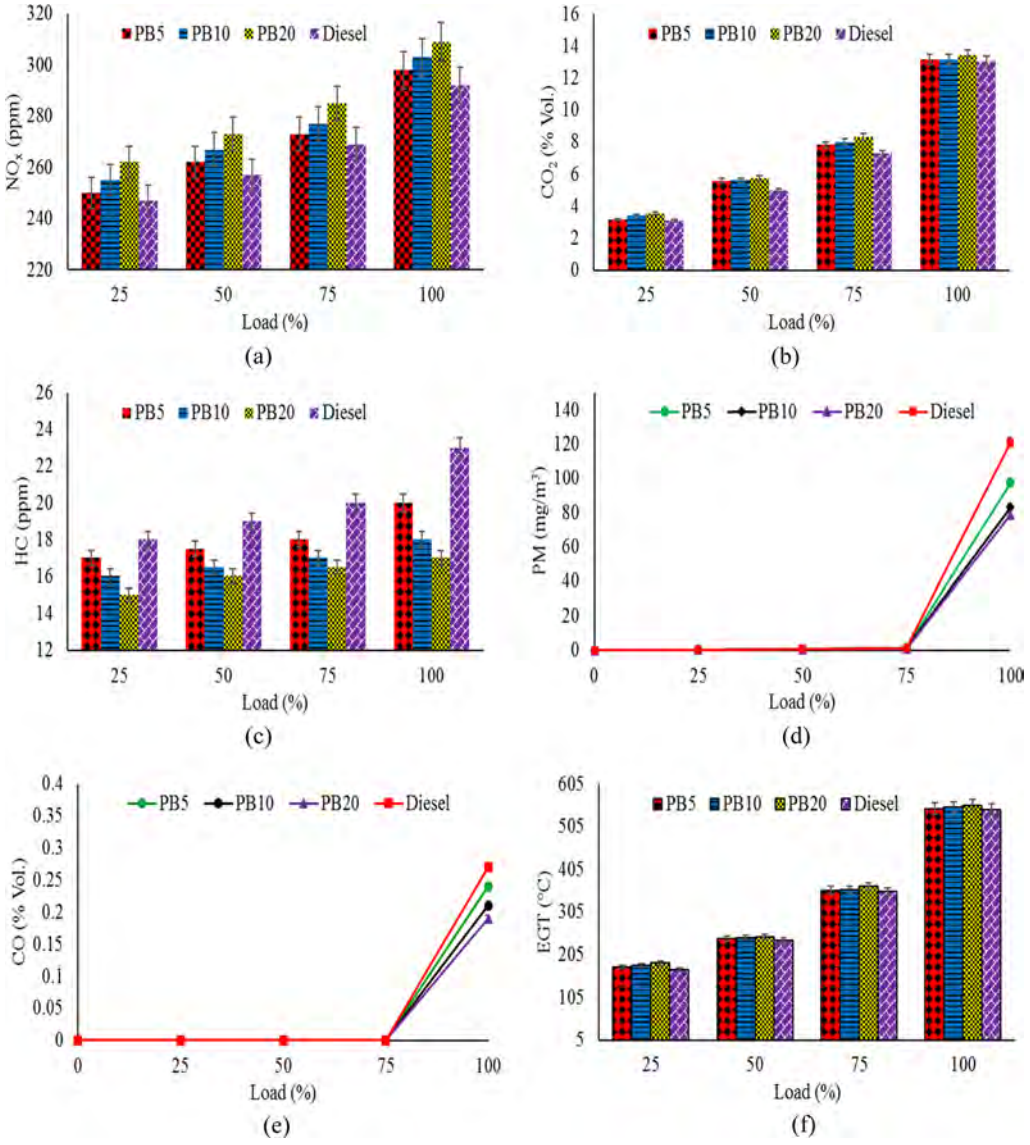

Fig. 2. Variation in: (a) NO_x, (b) CO_2, (c) HC, (d) PM, (e) CO, and (f) EGT with changing load for PSO biodiesel blends and pure diesel at 1400 rpm.

found that the NO_x emissions rise as load rises for all fuels. Devan et al. [26] and Abed et al. [27] reported that increased combustion temperatures and the stoichiometry of mixtures resulted in higher NO_x emissions with load changes. Godiganur et al. [28] indicated that the air-fuel ratio increases with the increase in engine load, resulting in a higher combustion chamber gas temperature and producing higher NO_x emissions. Under all loading conditions, PB5, PB10 and PB20 produced higher NO_x emissions than diesel. The greater the biodiesel content in the biodiesel blends, the higher the levels of NO_x produced. Some researchers found that the higher cetane numbers for a lower biodiesel blend could lead to a short delay in ignition leading to lower combustion temperature and pressure, which resulted in reduced NO_x emissions [29,30]. The average NO_x increases of PB5, PB10 and PB20 was 1.7%, respectively 3.47% and 6% compared to diesel.

3.1.2. Carbon dioxide (CO_2) emissions

CO_2 emissions increased as engine loads increased for all biodiesel blends and pure diesel (Fig. 2(b)). At all load conditions, the higher the

biodiesel content in the biodiesel blends from PB5 to PB20, the higher the CO_2 emissions produced. Imdadul et al. [31] mentioned that CO is converted into CO_2 with the reaction being facilitated by an oxidising agent, hydroxyl radical (OH), when adequate O_2 is available. Mofijur et al. [32] indicated that CO_2 emissions increased due to the higher O_2 content and higher cetane number of biodiesel blends. PB20 shows the highest CO_2 emissions under all loads compared with other biodiesel blends and diesel due to the higher O_2 content in its chemical structure

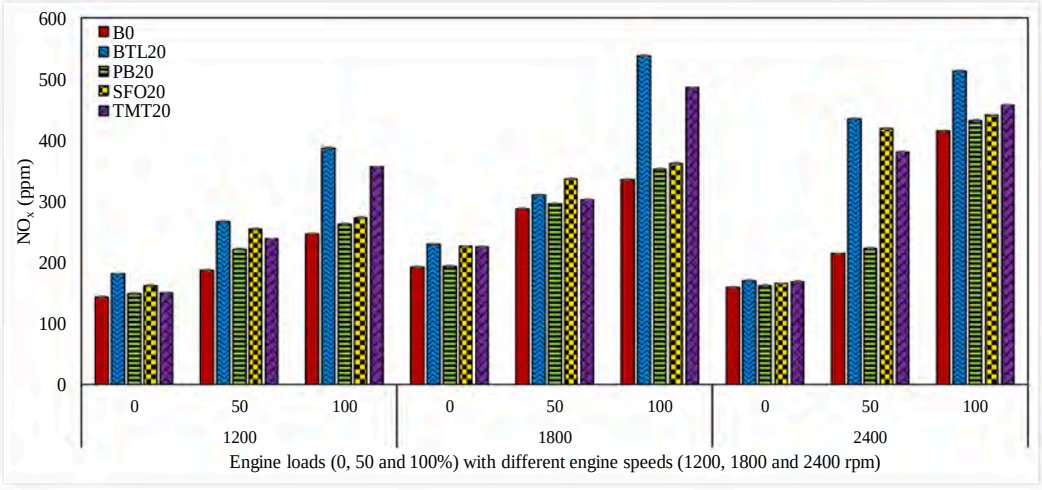

(a) Engine loads and speed vs NO_x.

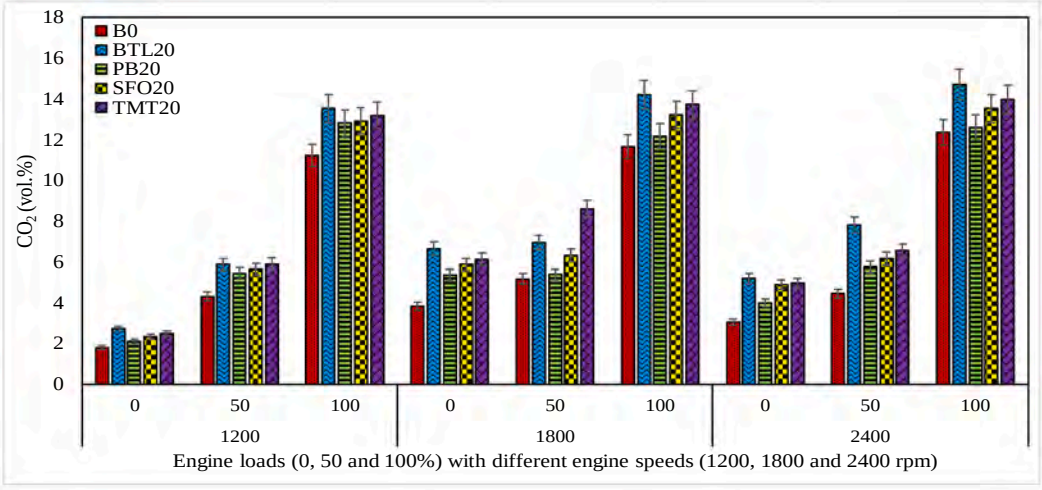

(b) Engine loads and speed vs CO_2.

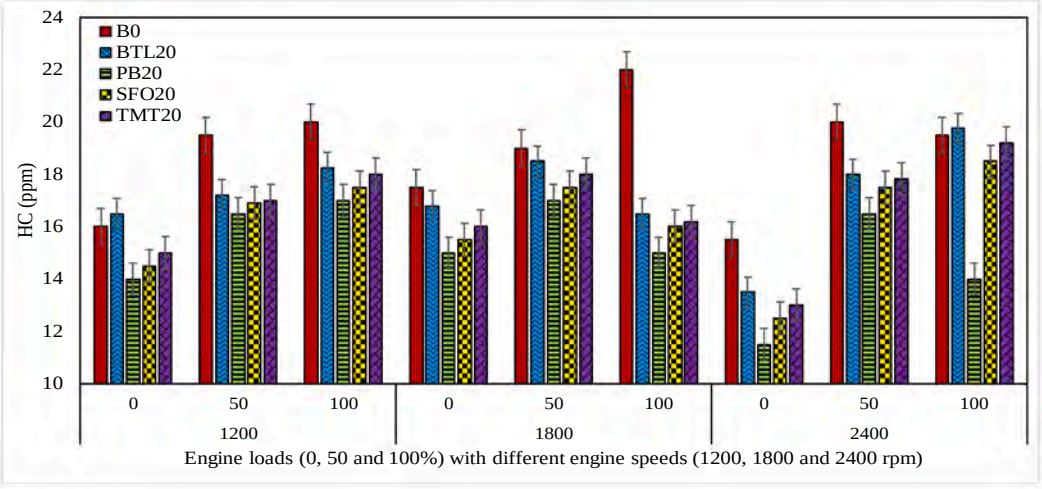

(c) Engine loads and speed vs HC.

Fig. 3. Variation of emissions with different engine loads and speeds.

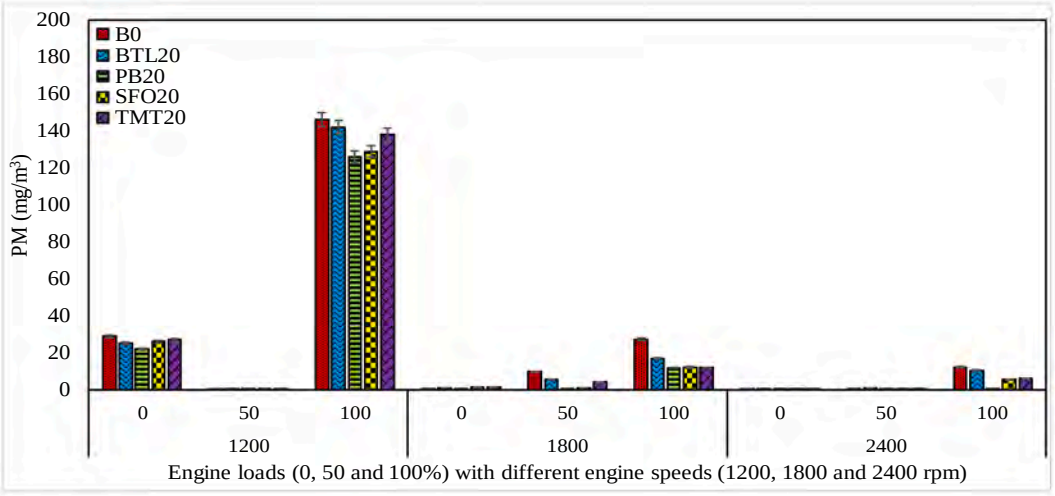

(d) Engine loads and speed vs PM.

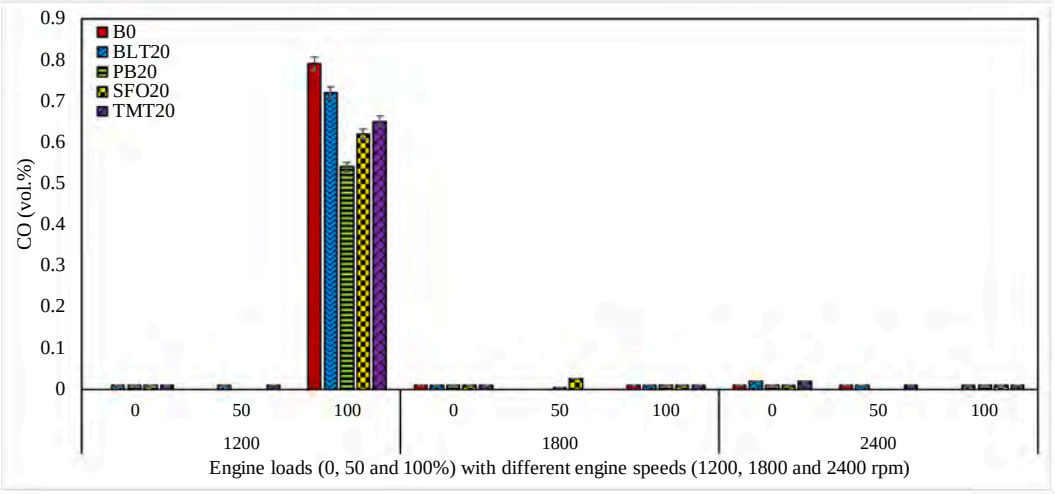

(e) Engine loads and speed vs CO.

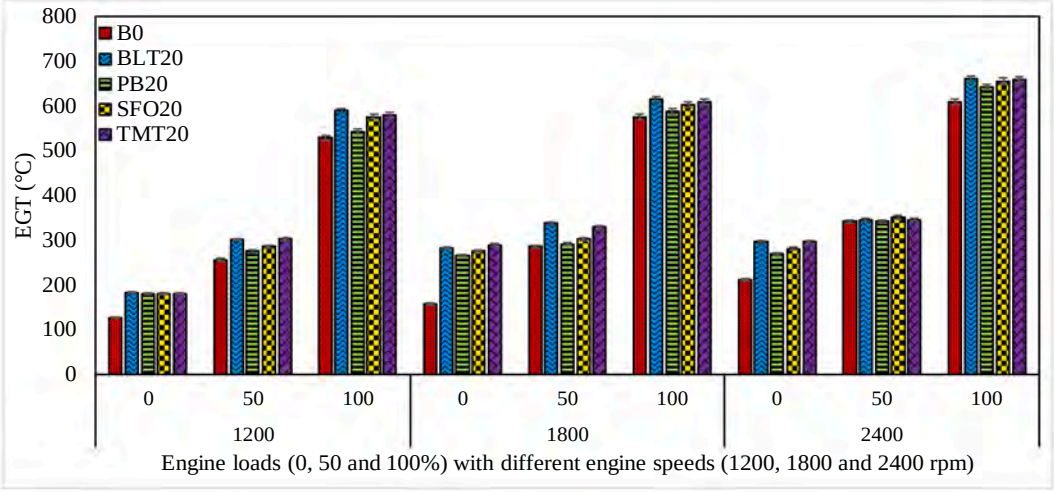

(f) Engine loads and speed vs EGT.

Fig. 3. (*continued*)

which assists in completing combustion. The average CO_2 increases for PB5, PB10 and PB20 were 4.5%, 6.3%, and 9% respectively in comparison to Diesel.

3.1.3. Hydrocarbon emissions (HC)

Fig. 2(c) shows the variation in hydrocarbon (HC) emissions over the whole load ranges at 1400 rpm. With the increase in engine load for all PSO biodiesel blends and diesel, HC emissions are rising. Nantha

Table 4
Overall emissions generation and EGTs of biodiesel (BD) blends over B0 at full load on different engine speeds.

Emissions Generation and EGT	Full load (100%)			Comparison of BD with B0	
	1200 rpm	1800 rpm	2400 rpm	Min. ▲/▼ (%)	Max.▲/▼ (%)
NO_x emissions	BD > B0	BD > B0	BD > B0	PB20 (▲4.1%)	BTL20 (▲23.6%)
CO_2 emissions	BD > B0	BD > B0	BD > B0	PB20 (▲1.7%)	BTL20 (▲19%)
HC emissions	B0 > BD	B0 > BD	B0 > BD	BTL20 (▼1.3%)	PB20 (▼28.2%)
PM emissions	B0 > BD	B0 > BD	B0 > BD	BTL20 (▼2.7%)	PB20 (▼13.7%)
CO emissions	B0 > BD	–	–	BTL20 (▼8.8%)	PB20 (▼31.6%)
EGT	BD > B0	BD > B0	BD > B0	PB20 (▲5.4%)	BTL20 (▲8.7%)

Note: ▲ = increase and ▼ = decrease.

Table 5
Experimental range and levels of operating parameters.

Operating parameters	Symbol coded	Range and Levels		
		−1	0	1
Biodiesel blends (%)	BL	0	10	20
Load (%)	LD	0	50	100
Speed (rpm)	SP	1200	1800	2400

Gopal et al. [33] reported that the fuel mass entering into the cylinder greater at higher engine loads, hence fuel to air ratio increases. Other researchers have testified to similar outcomes that confirm HC emissions increase as engine loads increase [27,34–36]. Higher HC emissions at low engine speeds are obtained by high fuel density and viscosity that affect the atomisation and ignition of fuel in the combustion chamber [37,38]. Imdadul et al. [31] also mentioned that fuel being trapped in the crevice volumes of the combustion chamber may contribute to higher HC emissions. Vijay Kumar et al. [39] mentioned that higher levels of oxygen and cetane number can reduce HC emissions. Relative to diesel, the average HC decreases are 9.3%, 15.6% and 19.3%, respectively in PB5, PB10 and PB20.

3.1.4. Particulate matter emission (PM)

Fig. 2(d) shows particulate matter (PM) emissions variation with engine load changes for both PSO biodiesel blends and diesel at 1400 rpm. A significant increase in PM occurred with an increase in engine load from 75% to 100%. Generally, biodiesel has lower PM emissions in comparison with diesel. Tse et al. [40] mentioned that the lower volatility and higher oxygen content of biodiesel led to lower PM emissions. Lin et al. [41] mentioned that lower PM emissions can be obtained using biodiesel with a higher cetane number due to the shorter ignition delay and longer combustion. Imdadul et al. [31] also mentioned that PM emissions increase significantly at higher engine load as fuel burns in diffusion mode due to the high fuel quantity being injected in a combustion chamber to provide soot oxidation with less combustion time. Conversely, few researchers [40,42] stated that the lower PM emissions at lower engine load may be attributed to the premixed fuel consumption which requires more combustion time for soot oxidation. At 100% full load, PB5, PB10 and PB20 decreases in PM values are 19.5%, 31.4% and 34.9%, respectively, compared with diesel.

3.1.5. Carbon monoxide emissions (CO)

Incomplete combustion is the main reason for elevated carbon monoxide (CO) in the exhaust emissions. Both excessively lean and rich air-fuel ratio blends can cause CO in the engine cylinder. Inadequate or low air fuel in a rich combustion mix may also cause high CO emissions. Ong et al. [43] mentioned that CO forms in the rich blend of air-fuel mixture regions due to lack of accessibility to oxygen (O_2) needed to oxidise all CO in the fuel. CO emissions are determined by the air-fuel ratio, engine speed, injection timing, pressure and fuel types [32,34,43,44]. Fig. 2(e) shows the variation in CO emissions by PSO biodiesel blends and diesel over the whole load ranges. The CO emissions increase with an increase in the load from 75% to 100% for all biodiesel blends and diesel. Over the entire range of loads, CO emissions were highest at 100% full load. Biodiesel generally contains 12% greater oxygen content than pure diesel [45]. The higher the O_2 content (i.e., the greater the biodiesel concentration in the biodiesel diesel blend), the lower the CO emissions. Improved combustion occurred due to increase in O_2 content in the air-fuel mixture in the biodiesel blends [13,46,47]. Murillo et al. [48] noted that CO emissions from biodiesel blends are lower because they have greater oxidation than pure diesel. At 100% full load, CO levels of PB5, PB10, and PB20 decreased by 11.1%, 22.2% and 29.6%, respectively, compared to diesel.

Table 6
Experimental matrix and results for the model of response values for Box-Behnken.

Run no	Operating parameters			Experimental response values						Predicted response values					
	BL (vol. %)	LD (%)	SP (rpm)	NO_x (ppm)	CO_2 (vol. %)	HC (ppm)	PM (mg/m^3)	CO (vol. %)	EGT (°C)	NO_x (ppm)	CO_2 (vol. %)	HC (ppm)	PM (mg/m^3)	CO (vol.%)	EGT (°C)
1	20	50	2400	223.0	5.75	16.50	0.20	0.000	343	226.0	5.78	16.25	0.20	0.003	404
2	20	100	1800	353.0	12.15	15.00	12.0	0.010	589	235.0	12.15	15.00	12.0	0.010	540
3	10	50	1800	317.0	5.17	15.00	0.20	0.000	298	316.0	5.25	15.25	0.10	0.000	311
4	10	50	1800	313.0	5.23	15.33	0.20	0.000	287	323.0	5.13	15.45	0.20	0.000	300
5	20	50	1200	221.0	5.44	16.50	0.10	0.000	276	291.4	5.43	17.00	0.10	0.000	269
6	0	100	1800	335.0	11.65	22.00	27.4	0.010	576	178.0	11.65	20.00	27.4	0.010	528
7	10	100	2400	429.0	12.42	15.00	6.50	0.010	624	338.0	12.42	15.00	6.50	0.010	612
8	10	50	1800	314.0	5.14	16.00	0.20	0.000	292	327.0	5.55	15.75	0.20	0.000	283
9	10	100	1200	255.0	12.57	20.00	130.0	0.770	537	192.0	12.57	20.50	130.0	0.4876	505
10	10	0	1200	369.0	5.63	16.00	0.10	0.000	153	294.0	5.43	16.55	0.1	0.000	148
11	0	50	2400	214.0	4.45	20.00	0.12	0.010	346	333.6	5.45	21.00	0.1	0.000	329
12	0	0	1800	192.0	3.85	18.67	0.01	0.010	159	178.0	4.07	19.00	0.0	0.010	156
13	0	50	1200	187.0	4.31	19.50	0.55	0.000	257	144.0	4.82	22.00	0.7	0.000	220
14	20	0	1800	193.0	5.38	15.00	0.30	0.010	267	164.0	4.00	14.25	0.2	0.000	249
15	10	0	2400	145.0	3.92	13.00	54.0	0.200	253	140.0	3.96	16.25	56.5	0.2954	250

3.1.6. Exhaust gas temperature (EGT)

Fig. 2(f) demonstrates EGT variations for PSO biodiesel blends as well as diesel for the entire range of engine loads. Devan et al. [26] mentioned that EGT depends significantly on the fuel injection rate in the combustion chamber. Ong et al. [43] again found that EGT increases due to the heat energy generated in the combustion chamber increasing with the increase in engine speed with increasing load for all biodiesel blends and diesel. Low biodiesel concentration in the biodiesel diesel blend such as for PB5 results in a higher cetane number, so the oxygenated fuel mixture it produced assisted in improving combustion [49]. In contrast, lower calorific value and higher viscosity of the PB10 and PB20 lead to poor atomisation and incomplete combustion, resulting in higher EGTs [50]. Ong et al. [43] state that diesel generally has higher heating values and shorter combustion phases, resulting in lower EGTs compared to all biodiesel blends. Some researchers also found that a higher EGT of biodiesel can result from lower volatility of biodiesel blends that affect spray formation in the combustion chamber, leading to slower combustion [26,51]. A higher EGT suggests a biodiesel-fuelled engine's poor performance. The EGT values for PB5, PB10 or PB20 increased on average as compared to diesel by 1.2% by 2% and 3.7% respectively.

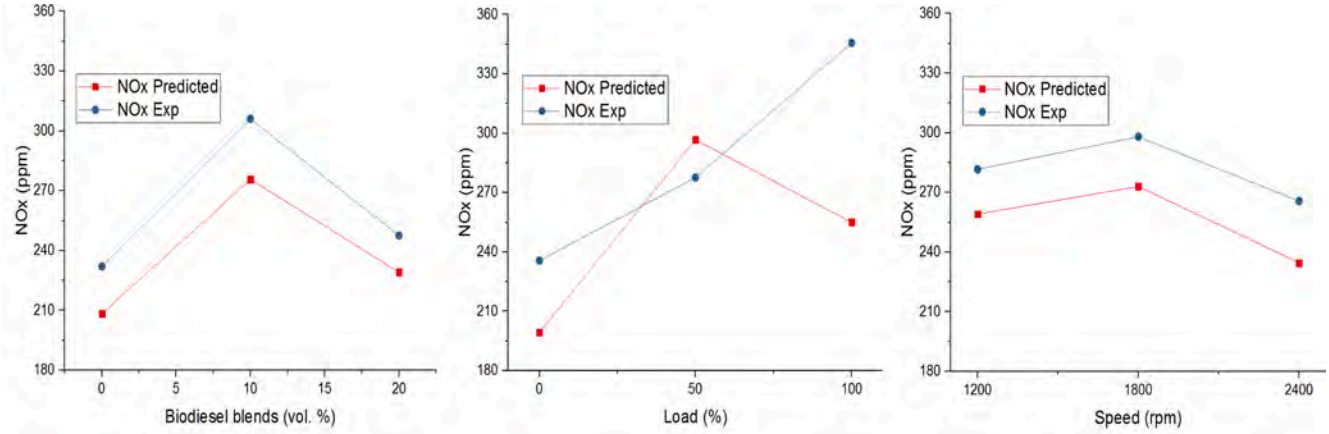

(a) Design matrix for mean NO_x emissions.

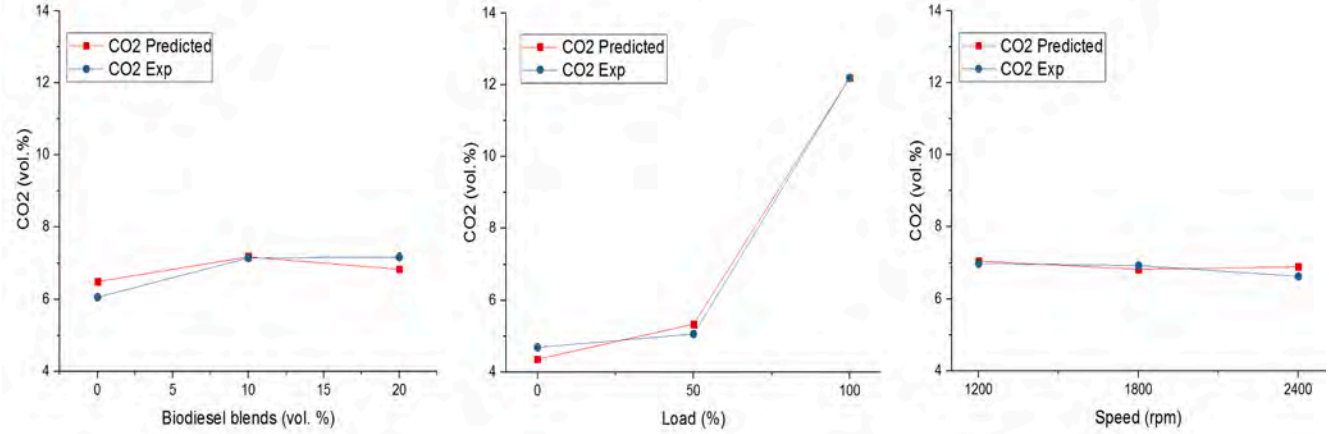

(b) Design matrix for mean CO_2 emissions.

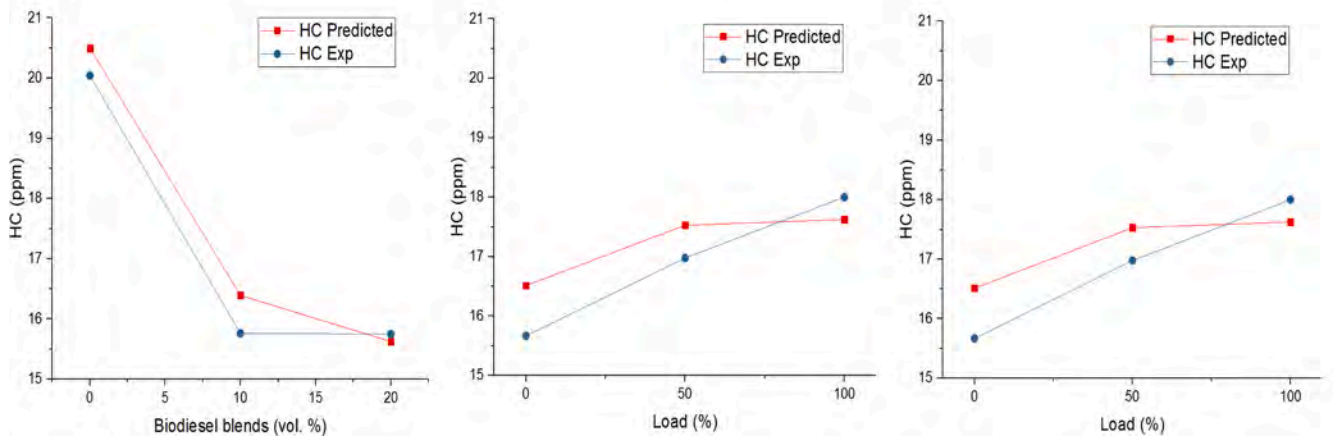

(c) Design matrix for mean HC emissions.

Fig. 4. Output responses of Box-Behnken design matrix for mean emissions.

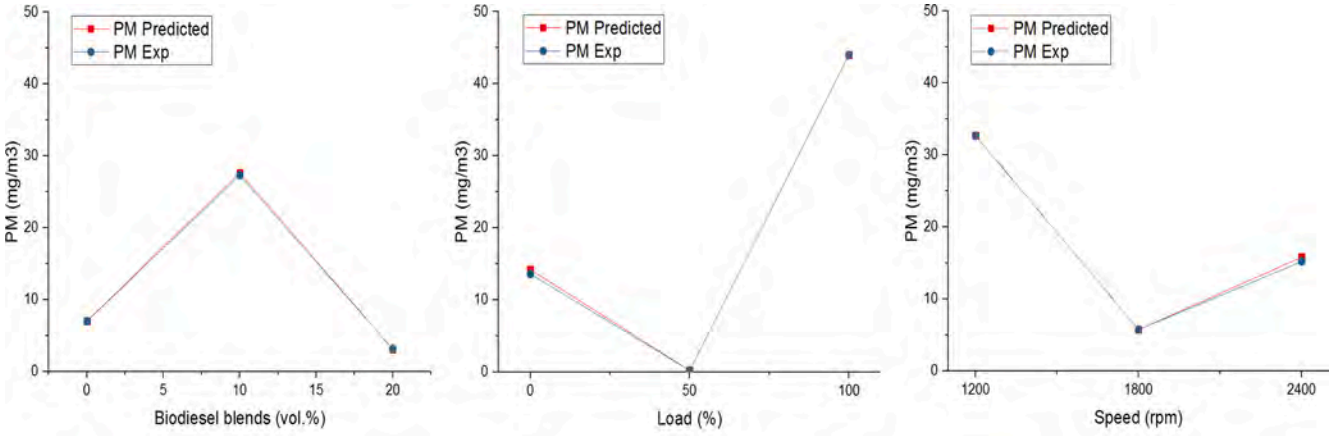

(d) Design matrix for mean PM emissions.

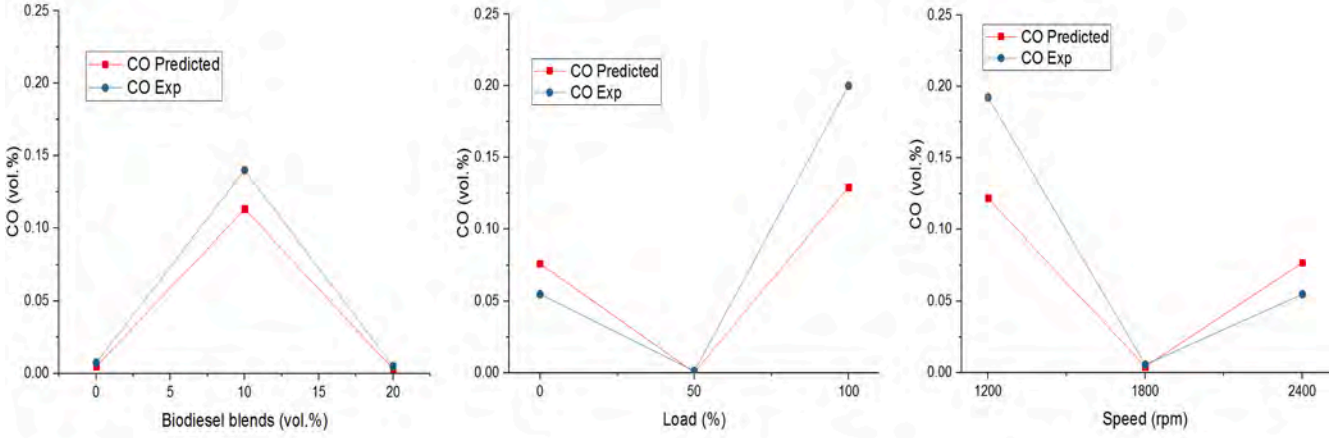

(e) Design matrix for mean CO emissions.

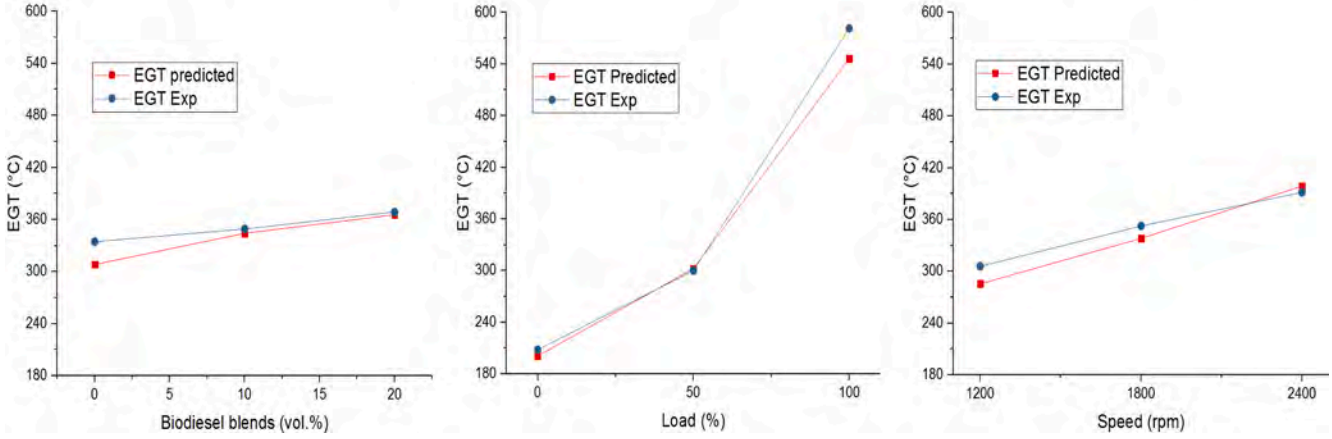

(f) Design matrix for mean EGTs.

Fig. 4. (*continued*)

3.2. Comparative analysis of engine emissions from PSO and other non-edible biodiesels

Fig. 3 shows the comparative analysis of diesel (B0), PSO biodiesel engine emission characteristics and three other non-edible biodiesels related to NO_x, CO_2, HC, PM, CO and EGT. Three engine loads (0, 50 and 100%) were tested at three engine speeds (1200, 1800 and 2400 rpm) to investigate emissions characteristics. Biodiesel content of 20% vol. (B20) of all four biodiesel blends (beauty leaf biodiesel-BTL20, papaya seed biodiesel-PB20, stone fruit biodiesel-SFO20 and tomato seed biodiesel-TMT20) were considered in this analysis.

Fig. 3(a) compares the NO_x emissions characteristics of pure diesel (B0) and four 20% biodiesel blend concentrations (B20) with varying engine loads and speeds. NO_x emissions increased with increases in engine loads and speeds due to higher biodiesel oxygen content, which increases the combustion temperature, leading to better combustion [26,47]. Over the entire engine speed range (1200, 1800 and 2400 rpm), CO_2 emissions for all B20 biodiesel blends increased with each load increase (0%, 50% and 100%) (Fig. 3(b)). PB20 was found to emit the minimum NO_x and CO_2 emissions at any combination of load condition and engine speed, followed by SFO20, TMT20 and BTL20. Again, at all load conditions, both NO_x and CO_2 emissions of all biodiesel blends are higher than those of B0.

Fig. 3(c) demonstrates B0 and B20 biodiesel emissions of HC with

Table 7
Variation of output responses of Box-Behnken design matrix for mean emissions generation.

Mean emissions generation and EGT	Optimum parameter level		
	Biodiesel blends (vol.%)	Load (%)	Speed (rpm)
NO_x emissions	PB20	50	2400
CO_2 emissions	PB20	50	2400
HC emissions	PB20	50	2400
PM emissions	PB20	50	1800
CO emissions	PB20	50	1800
EGT	PB10	0	1200

increasing engine loads and speeds. Godiganur et al. [28] reported that lower HC emissions from biodiesel blends were found due to better combustion of the blends. Over the whole range of engine speeds (1200, 1800 and 2400 rpm), the HC emissions of PB20 were found to be lowest at any of the tested load conditions (0%, 50% and 100%). Fig. 3(d) shows the PM emissions decreased with engine speed up to 2400 rpm. Some literature has shown that PM is higher at lower speeds because of incomplete combustion and intense lubricating oil burning [52,53]. However, PM emissions decrease drastically in biodiesel blends at higher engine speeds because of better combustion in oxygenated fuels [54,55]. Again, the absence of aromatic content in biodiesel can reduce PM emission. At all loads, both the HC and PM emissions of all biodiesel blends are lower than those of B0. The lowermost HC and PM emitters were found to be PB20, followed by SFO20, TMT20 and BTL20 at any combination of engine loading conditions and speeds.

Fig. 3(e) shows that incomplete combustion at lower engine speed (1200 rpm) and higher engine load (100%) causes higher CO emissions generation for all biodiesels and B0. CO emissions have been reduced as engine loads and speeds have increased. Higher oxygen content and cetane number of biodiesel blends led to total combustion. This finding is compatible with the research available [32,56]. PB20 was found to produce the lowest CO emissions, followed by SFO20, TMT20 and BTL20.

With increasing engine loads and speeds in B0 and with all biodiesel blends, the exhaust gas temperature (EGT) increases as shown in Fig. 3(f). Lower calorific values and increased viscosity of biodiesels lead to poor atomisation and incomplete combustion, leading to more EGTs [49,51]. The B0, PB20, followed by SFO20, TMT20 and BTL20, are found to produce the lowest EGT. With a full load (100%) and 2400 rpm, the highest EGT was obtained.

Table 4 describes the overall scenarios of emissions generation and EGT of biodiesel blends (BD) compared with pure diesel (B0) at full engine load conditions at different speeds. The minimum and maximum increase in NO_x and CO_2 emissions were found to be 4.1% and 1.7% for PB20, and 23.6% and 19% for BTL20 respectively, compared with B0 at full load (100%) condition and 2400 rpm. The highest and lowest decrease in HC, PM and CO emissions were found to be PB20 (28.2%, 13.7% and 31.6%) and BTL20 (1.3%, 2.7% and 8.8%) respectively. Moreover, the minimum and maximum increases in EGT were found to be 5.4% for PB20 and 8.7% for BTL20 respectively.

3.3. Interactive effects of PSO biodiesel on emissions

3.3.1. Design of experiments

The intricate relationships of operating parameters such as PSO biodiesel blends, engine load and engine speed on the output responses, i.e., exhaust gas emissions (NO_x, CO_2, HC, PM, CO and EGT), could not be explored individually. Anwar et al. [23] have shown the interaction effects of operating parameters with engine performance using PSO biodiesel. However, no research is available on the correlation between the operational parameters (biodiesel blends, load and engine speed),

Table 8
ANOVA results of the interactive effects of operating parameters on NO_x, CO_2 and HC.

Interactive effect of operating parameters on NO_x				Interactive effect of operating parameters on CO_2				Interactive effect of operating parameters on HC			
Source	DF	F-Value	P-Value	Remarks	Source	DF	F-Value	P-Value	Remarks	Source	DF	F-Value	P-Value	Remarks
Model	9	52.26	< 0.0001	***	Model	9	89.34	< 0.0001	***	Model	9	21.03	0.002	**
BL	1	0.03	0.861	NS	BL	1	1.21	0.322	NS	BL	1	103.79	< 0.0001	***
LD	1	28.00	0.003	**	LD	1	630.36	< 0.0001	***	LD	1	5.41	0.068	NS
SP	1	2.86	0.151	NS	SP	1	0.26	0.630	NS	SP	1	15.56	0.011	*
BL*BL	1	105.69	< 0.0001	***	BL*BL	1	1.53	0.271	NS	BL*BL	1	25.64	0.004	*
LD*LD	1	92.56	< 0.0001	***	LD*LD	1	164.10	< 0.0001	***	LD*LD	1	0.34	0.587	NS
SP*SP	1	2.66	0.164	NS	SP*SP	1	2.24	0.195	NS	SP*SP	1	26.00	0.004	**
BL*LD	***1***	***16.10***	***0.010***	*	BL*LD	1	0.42	0.547	NS	BL*LD	1	0.03	0.861	NS
BL*SP	***1***	***121.57***	***< 0.0001***	***	BL*SP	1	0.10	0.764	NS	BL*SP	1	0.03	0.861	NS
LD*SP	***1***	***117.62***	***< 0.0001***	***	LD*SP	1	2.24	0.195	NS	***LD*SP***	***1***	***14.76***	***0.012***	**
Lack of Fit	3	9.62	0.096	NS	Lack-of-Fit	3	6.27	0.141	NS	Lack-of-Fit	3	11.38	0.082	NS
Pure Error	2				Pure Error	2				Pure Error	2			
Total	14				Total	14				Total	14			
R^2 = 0.9895			Adj. R^2 = 0.9705		R^2 = 0.9938			Adj. R^2 = 0.9827		R^2 = 0.9743			Adj. R^2 = 0.9279	

Note: NS = Not significant (P > 0.05), * = Significant (P < 0.05), ** = Moderately significant (P < 0.001), *** = Highly significant (P < 0.0001).

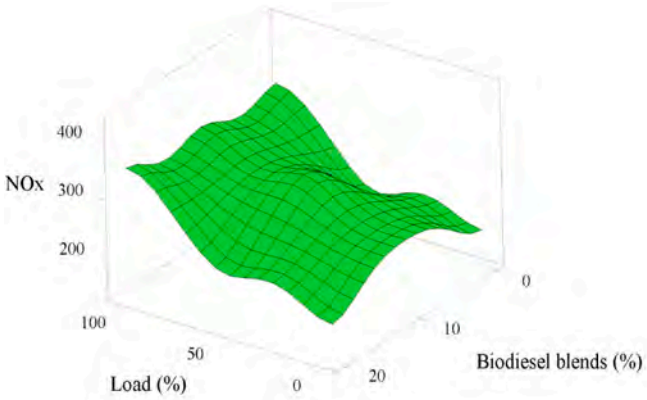

(a) 3D surface plot of load and biodiesel blends on NO_x (ppm).

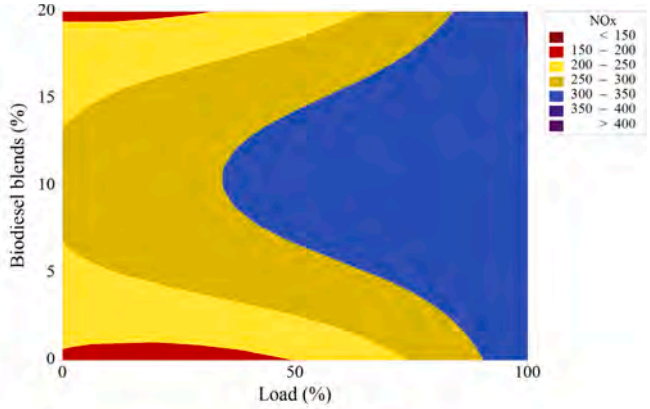

(b) 2D contour plot of load and biodiesel blends on NO_x (ppm).

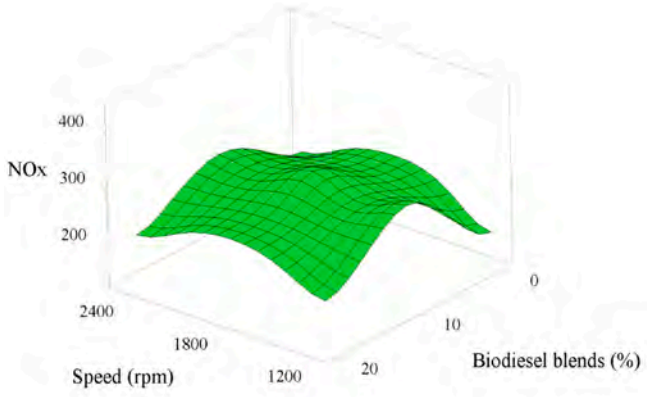

(c) 3D surface plot of biodiesel blends and speed on NO_x (ppm).

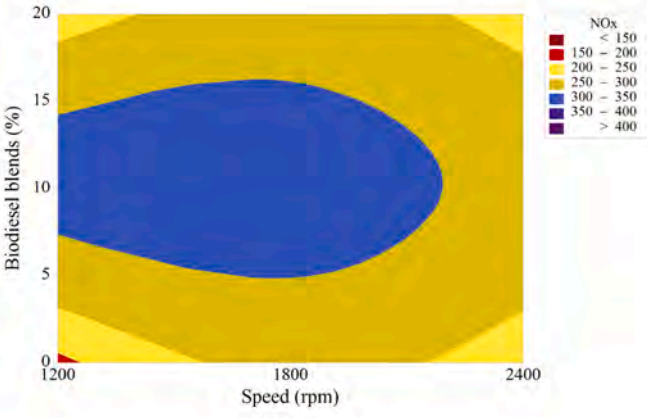

(d) 2D contour plot of biodiesel blends and speed on NO_x (ppm).

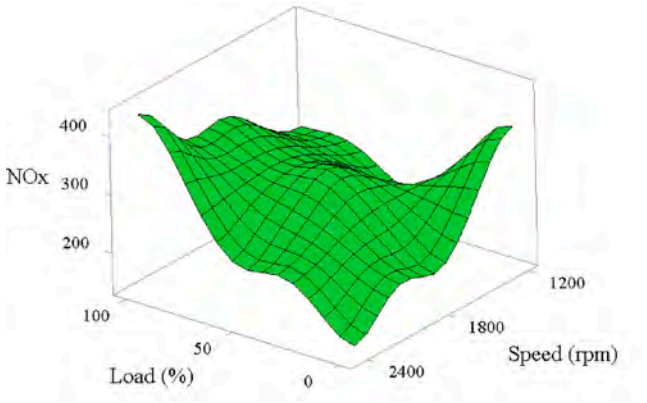

(e) 3D surface plot of load and speed on NO_x (ppm).

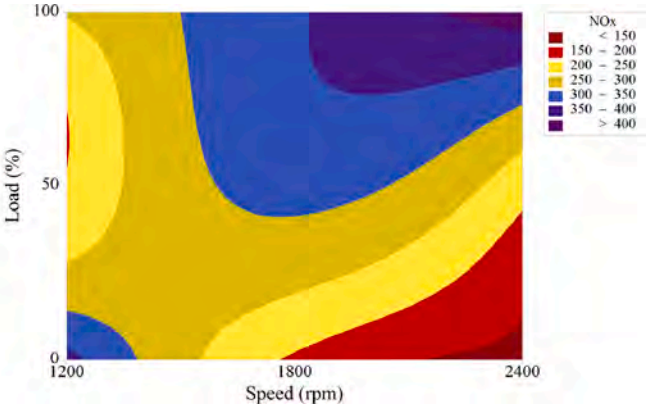

(f) 2D contour plot of load and speed on NO_x (ppm).

Fig. 5. Interactive effects of biodiesel blends, engine load, and speed on NO_x (ppm).

and the output responses (exhaust gas emissions) of PSO biodiesel blends. This study focuses on the interactive relationships between three operational parameters (PSO biodiesel blends, load and engine speed) and six responses (NO_x, CO_2, HC, PM, CO and EGT). The Minitab 18 software package was used for statistical analysis. A response surface design based on the Box-Behnken module was used in all experiments. The operating parameters and the ranges and levels used in this study are listed in Table 5.

To compare the response variable with the operating parameters, a complete quadratic model was developed. Eq. (1) shows the form of this model.

$$R = P_0 + \sum_{i=1}^{n} P_i Q_i + \sum_{i=1}^{n} P_{ii} Q_i 2 + \sum_{i=1}^{n-1} \sum_{j=i+1}^{n} P_{ij} Q_i Q_j \quad (1)$$

where R is the predicted response factor; P_0 is a constant; P_i is the linear effect; P_{ii} is the quadratic effect; P_{ij} is the interaction effect of Q_i (the ith

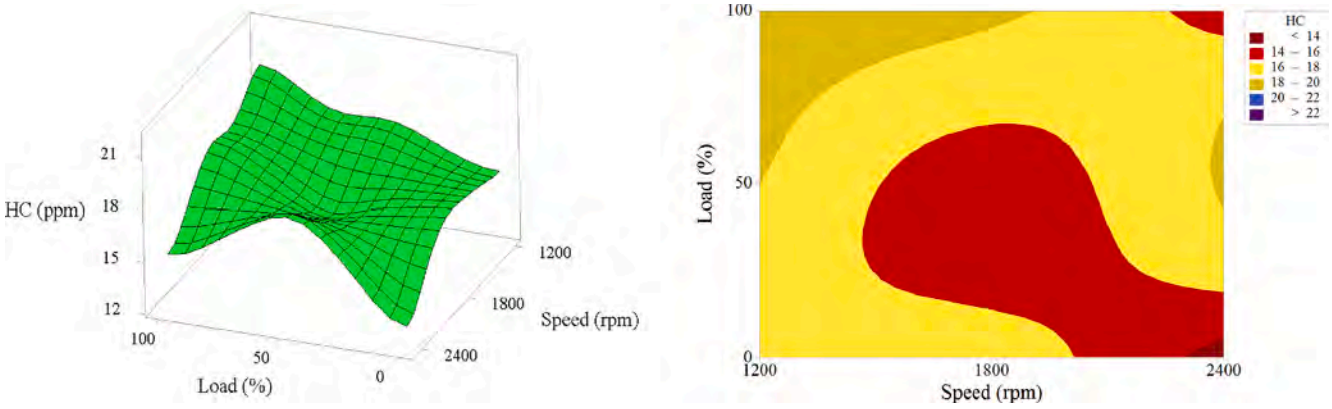

(a) 3D surface plot of speed and loads on HC (ppm)

(b) 2D contour plot of speed and loads on HC (ppm)

Fig. 6. Interactive effects of biodiesel blends, load, and speed on HC (ppm).

operating parameter) and Q_j (the jth operating parameter).

For investigating the relationships between the six responses of NO_x, CO_2, HC, PM, CO emissions and EGT and the three operating parameters of biodiesel blend, load and speed, these were fitted by a regression quadratic model. Based on the coded parameters, as shown in the following equations, this model was developed to predict individual responses as a function of biodiesel blend (BL), load (LD) and speed (SP):

$$NO_x = 322 - -0.9BL + 25.87LD + 8.28SP - 74BL^2 - 69.25LD^2 - 11.75SP^2 + 27.75BL * LD - -76.25BL * SP + 75LD*SP \quad (2)$$

$$CO_2 = 5.31 + 0.17BL + 3.92LD - -0.08SP - -0.28BL^2 + 2.94LD^2 + 0.34SP^2 + 0.14BL * LD - -0.07BL * SP + 0.33LD*SP \quad (3)$$

$$HC = 15.48 - -2.44BL + 0.56LD - 0.94SP + 1.78BL^2 - -0.2LD^2 + 1.8SP^2 - -0.06BL * LD + 0.06BL * SP - -1.3LD*SP \quad (4)$$

$$PM = 2.5 - -1.96BL + 14.89LD - -8.45SP - -20.3BL^2 + 27.7LD^2 + 18.07SP^2 - -3.9BL * LD + 0.17BL * SP - -44.97LD*SP \quad (5)$$

$$CO = 0.0265LD - -0.0224SP - 0.095BL^2 + 0.1025LD^2 + 0.0958SP^2 + 0.0025BL * LD + 0.0007BL * SP - 0.1932LD*SP \quad (6)$$

$$EGT\,(^{\circ}C) = 298 + 28.63BL + 172.75LD + 56.63SP - -1.5BL^2 + 71.75LD^2 + 9SP^2 - -20.25BL * LD + 6.5BL * SP + 1.25LD * SP \quad (7)$$

To identify the impact of operating parameters on the response, the linear, quadratic and combined effects have been considered on operating parameters. The probability value (P-value) is utilized as a tool to evaluate the significance of each parameter from the analysis of variance (ANOVA). P-values lower than 0.05 are known at the confidence level of 95% as a 'significant' impact of these parameters on the response. P-values above 0.05 suggest that these parameters have a 'non-significant' effect on response. The effects of the Box-Behnken development method for predicting response values are shown in Table 6.

Fig. 4 shows the variation of output responses in accordance with Box-Behnken design matrix for mean NO_x, CO_2, HC, PM and CO emissions and EGT. The lowering of all emissions is better for the global environment. From the response shown in Fig. 4(a), it is found that the theoretical parameter levels of biodiesel blends (PB20) with 0% engine load at 2400 rpm can generate minimum NO_x emissions after diesel (B0). NO_x emissions are inversely proportional to biodiesel blends and speeds. With an increase in both biodiesel blend (PB10 to PB20) and speed (1800 rpm to 2400 rpm), NO_x drops drastically. However, engine load has a consistent trend in its effect on NO_x emissions generation as the higher the engine load, the higher are the NO_x emissions. The optimum parameter levels to minimise NO_x emissions would be PB20 with 50% engine load at 2400 rpm speed. Fig. 4(b) shows the theoretical parameter levels that can produce minimum CO_2 emissions after diesel (B0) are biodiesel blend (PB10) with 0% engine load at 2400 rpm. However, the change in CO_2 value is insignificant by varying biodiesel blends PB10 to PB20 as well as increasing engine load 0% to 50%. Engine load increases from 50% to 100% caused a peak rise in CO_2 generation. The other significant factor that affects CO_2 emissions for PSO biodiesel blends is engine speed. With the increase of engine speed from 1800 rpm to 2400 rpm, CO_2 emission dropped by 4.4%. Fig. 4(c) shows the variation in biodiesel blends between PB10 and PB20 does not have any significant effect on HC emissions level changes. HC emissions are inversely proportional with engine speed. With an increase in speed (1800 rpm to 2400 rpm), HC drops drastically. Nevertheless, engine load has a positive effect on HC emissions generation as the higher the engine load, the higher are the HC emissions. Again, the optimum parameter level would be PB20 with 50% engine load at 2400 rpm speed, whereas the theoretical parameter levels are biodiesel blends (PB10 or PB20) with 0% engine load at 2400 rpm. PM emissions are inversely proportional with biodiesel blends as shown in Fig. 4(d). With an increase in biodiesel content in the blends (PB10 to PB20), PM drops drastically. However, both engine load and speed have mixed effects on PM emissions generation as PM drops with the increase of load (0% to 50%) and speed (1200 rpm to 1800 rpm). Any increase in load and speed caused higher PM emissions. Fig. 4(e) shows that the CO emissions level was found to be the same at B0 and PB20. Both engine load and speed have mixed effects on CO emissions generation as CO drops with the increase of load (0% to 50%) and speed (1200 rpm to 1800 rpm). Any increase in engine load and speed caused higher CO emissions. However, engine load (50% to 100%) has a significant effect on increasing CO emissions. Biodiesel has a higher oxygen content that ensures better combustion, which resulted in generating higher EGTs. At higher engine loads and speeds, the EGT was found to be higher. Biodiesel content in the blends, engine loads and speeds are proportional in changes in EGT, as expected. From the response shown in Fig. 4(f), it is found that the optimum parameter levels are biodiesel blends (PB20) with 0% engine load at 1200 rpm.

The optimum parameter levels of biodiesel blends, engine load and speed are summarized in Table 7. All mean emissions were found to be optimum at PB20 biodiesel blends with 50% load while keeping the speed at 2400 rpm or 1800 rpm. However, EGT was found to be lowest at PB10 blends with 0% loading condition and the lower speed of 1200 rpm. A change in biodiesel blends (PB10 to PB20) and speed (1200 to 2400 rpm) will incur 5.6% and 28% increases in EGT respectively.

Table 9
ANOVA emerges from the interactive effects on PM, CO and EGT of the operating parameters.

Interactive effect of operating parameters on PM					Interactive effect of operating parameters on CO				Interactive effect of operating parameters on EGT				
Source	DF	F-Value	P-Value	Remarks	Source	DF	F-Value	P-Value	Remarks	Source	DF	F-Value	P-Value	Remarks
Model	9	11.07	0.008	*	Model	9	16.87	0.003	**	Model	9	164.16	< 0.0001	***
BL	1	0.19	0.683	NS	BL	1	0.00	0.956	NS	BL	1	33.17	0.002	*
LD	1	10.79	0.022	*	LD	1	3.15	0.136	NS	LD	1	1207.90	< 0.0001	***
SP	1	3.48	0.121	NS	SP	1	2.25	0.194	NS	SP	1	129.78	< 0.0001	***
BL*BL	1	9.26	0.029	*	BL*BL	1	18.67	0.008	*	BL*BL	1	0.04	0.846	NS
LD*LD	1	17.24	0.009	*	LD*LD	1	21.73	0.006	*	LD*LD	1	96.17	< 0.0001	***
SP*SP	1	7.34	0.042	*	SP*SP	1	18.96	0.007	*	SP*SP	1	1.51	0.273	NS
BL*LD	1	0.37	0.569	NS	BL*LD	1	0.01	0.910	NS	***BL*LD***	***1***	***8.30***	***0.035***	*
BL*SP	1	0.00	0.979	NS	BL*SP	1	0.00	0.973	NS	BL*SP	1	0.86	0.398	NS
LD*SP	***1***	***49.24***	***0.001***	***	***LD*SP***	***1***	***83.68***	***< 0.0001***	***	LD*SP	1	0.03	0.866	NS
Lack of Fit	3	15.86	0.060	NS	Lack-of-Fit	3				Lack-of-Fit	3	0.99	0.538	NS
Pure Error	2				Pure Error	2				Pure Error	2			
Total	14				Total	14				Total	14			
R^2 = 0.9522			Adj. R^2 = 0.8662		R^2 = 0.9681			Adj. R^2 = 0.9107		R^2 = 0.9966			Adj. R^2 = 0.9906	

Note: NS = Not significant (P > 0.05), * = Significant (P < 0.05), ** = Moderately significant (P < 0.001), *** = Highly significant (P < 0.0001).

3.3.2. Interactive effects of operating parameters on responses

The P-values of the model's ANOVA results are highly significant, as shown in Table 8. The linear effect of LD, quadratic effect of BL^2 and LD^2, and all combined effects except BL*LD are found to be highly significant, whereas BL*LD is found significant. Both BL*LD and LD*SP have the lowest P-value (< 0.0001) and higher F-values of 121.57 and 117.62 respectively. According to quadratic equation (2), LD, SP, BL*LD and LD*SP have positive effects on NO_x. BL*SP has a negative effect on NO_x emissions generation, which indicates that, at lower BL and higher SP, NO_x emissions will be higher. The coefficient of determination (R^2) and adjusted coefficient of determination (adj. R^2) were found to be 98.95% and 97.05% respectively which indicates the moderate accuracy of the model.

Fig. 5 shows the results of ANOVA in Table 8 for BL*LD, BL*SP and LD*SP interaction effects on NO_x. It can be seen from Fig. 5(a) and (b) that NO_x rises with an increase in LD regardless of any biodiesel blends. Fig. 5(c) and (d) show that 1800 rpm SP and B10 blend cause the maximum generation of NO_x emissions. With the increase of SP, the NO_x generation reduces. Fig. 5(e) and (f) show that, at lower SP and lower LD, the NO_x emissions are higher, whereas a higher SP with higher LD can generate higher NO_x as well. The maximum NO_x was found to be 429 ppm at 2400 rpm SP and 100% LD.

The CO_2 model presented in Table 8 shows as highly significant due to lower P-values of ANOVA results indicating an insignificant lack of fit. Only the LD linear parameter and LD^2 quadratic terms are found to be highly significant. There are no significant other parameters and combined effects. LD has the lowest P-value (< 0.0001) and highest F-value (630.36). In accordance with the quadratic equation (3), LD, BL*LD and LD*SP have positive effects on CO_2. BL*SP has a negative effect on CO_2 emissions generation, which indicates that, at lower SP and higher BL, CO_2 emissions will be higher. The R^2 and adj. R^2 were 99.38% and 98.27%, indicate an excellent accuracy of the model. The ANOVA results in Table 8 show that there are no significant effects between the operating parameters on CO_2 emissions generation.

The HC model is found highly significant due to lower P-values of ANOVA results from Table 8. It also shows an insignificant lack of fit. Both the BL and SP of the linear parameters are found to be significant, and the BL^2 and SP^2 quadratic terms are highly significant. Only the LD*SP combined effect is found to be significant in this model. LD*SP has the lowest P-value (0.012) and a high F-value (14.76). According to quadratic equation (4), only LD and BL*SP have very little positive effect on HC emissions. This indicates that, at lower SP and higher LD, HC emissions will be higher. Again, R^2 and adj. R^2 were found to be 97.43% and 92.79% respectively that shows the model's reasonable accuracy.

The LD*SP combined interaction effects on HC from the ANOVA results (Table 8) is graphically presented in Fig. 6. The 3D surface plot of LD and SP impact on HC (Fig. 6(a)) and 2D contour plot (Fig. 6(b)) are shown. For increased LD for limited SP impacts, HC increases. The maximum HC at 1200 rpm and 100% LD was found to be 20 ppm. Nevertheless, it was found that LD*SP's combined effects on HC were found to be minimum at 50% LD at 1800 rpm SP.

Table 9 P-values of the ANOVA results show that the model is highly significant. It is found that only the combined effect of LD and SP is highly significant and all quadratic terms are significant. LD of the linear parameter is found significant in this model. LD*SP has the lowest P-value (0.001) and highest F-value (49.24). According to quadratic equation (5), LD and BL*SP have positive effects on PM. LD*SP has a negative effect on PM emissions generation, which indicates that, at lower SP and higher LD, PM emissions will be higher. The model showed an insignificant lack of fit, whereas R^2 and adj. R^2 were found to be 95.22% and 86.62%, which indicate the reasonable accuracy of the model.

Fig. 7 demonstrates the combined effect of LD*SP on PM from ANOVA results in Table 9. The 3D surface plot (Fig. 7(a)) and 2D contour plot of BL and LD (Fig. 7(b)) present the effects on PM. With the

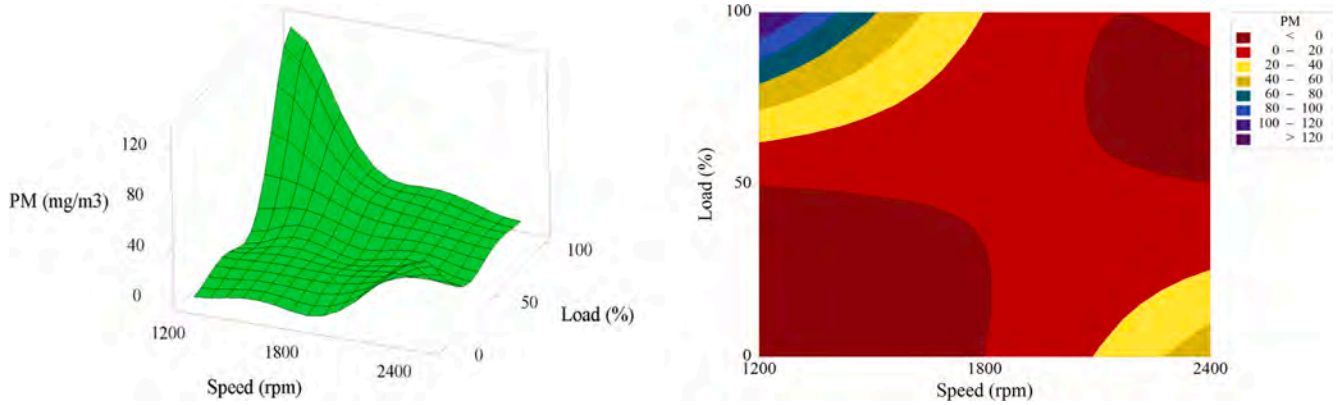

(a) 3D surface plot of load and speed on PM (mg/m^3).

(b) 2D contour plot of load and speed on PM (mg/m^3).

Fig. 7. Interactive effects of biodiesel blends, load, and speed on PM (mg/m^3).

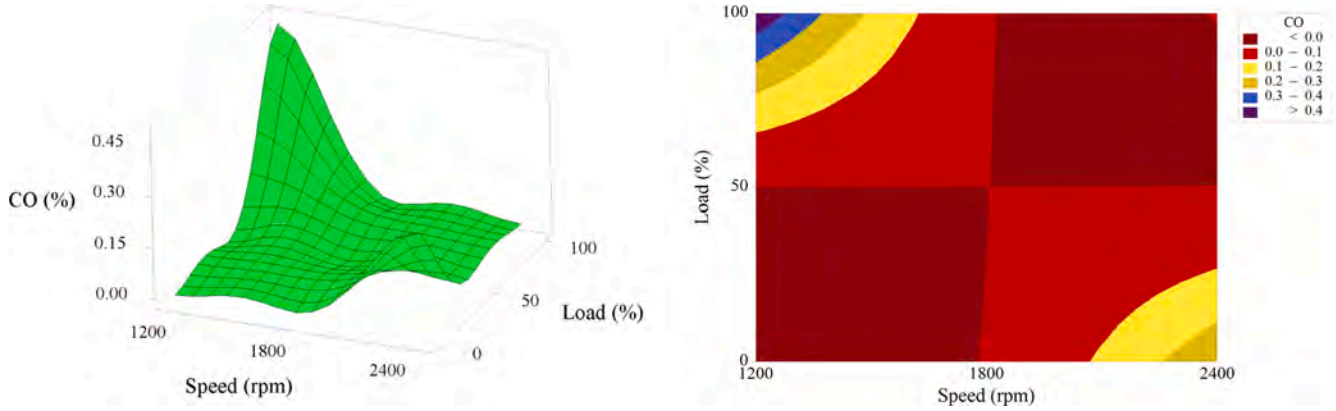

(a) 3D surface plot of speed and loads on CO (vol.%)

(b) 2D contour plot of speed and loads on CO (vol.%)

Fig. 8. Interactive effects of biodiesel blends, load, and speed on CO (vol.%).

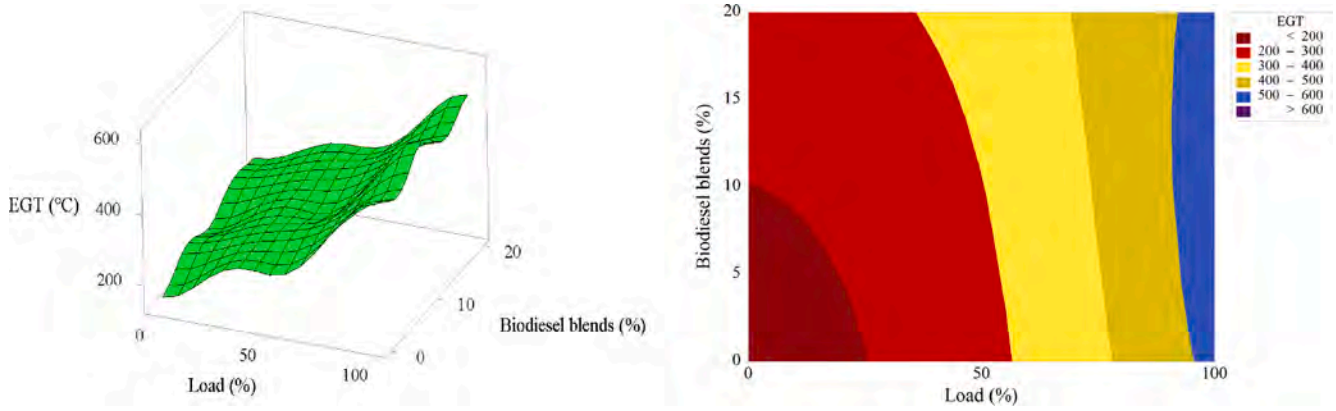

(a) 3D surface plot of biodiesel blends and loads on EGT

(b) 2D contour plot of biodiesel blends and loads on EGT

Fig. 9. Interactive effects of biodiesel blends, load, and speed on EGT (°C).

increase of SP, PM decreases regardless of loading conditions. The maximum PM was found to be 130 mg/m^3 at 1200 rpm SP and 100% LD.

The lower P-values of ANOVA results from Table 9 reveals a very critical model with negligible lack of fit. Only LD and SP of the combined effects is found to be highly significant, and all quadratic terms are highly significant. None of the linear parameters are significant in this model. LD*SP has the lowest P-value (< 0.0001) and highest F-value (83.68). Based on the quadratic equation (6), BL*LD as well as BL*SP have slight positive effects on CO. LD*SP has an adverse

effect on CO emissions generation, which indicates that, at lower SP and higher LD, CO emissions will be higher. The R^2 and adj. R^2 were 96.81% and 91.07% respectively, which shows the model's moderate accuracy.

The ANOVA results in Table 9 for LD*SP interaction effects on CO is shown graphically in Fig. 8. Fig. 8(a) shows the 3D surface plot and Fig. 8(b) shows the 2D contour plot of LD and SP effects on CO. CO decreases with the increase of SP from 1200 rpm to 1800 rpm irrespective of any loading conditions. However, a slight increase in CO was observed at 2400 rpm at 0% LD. The maximum CO was found to be 0.44 vol% at 1200 rpm and 100% LD.

Table 9 reveals that with an insignificant lack of fit the model's P-value is highly significant. All linear parameters and the LD^2 quadratic term are highly significant. Even BL*LD's combined effects are significant, while others are not significant. The findings of ANOVA in Table 9 also indicate that LD and SP both have the lowest P-values (< 0.0001 each) and the highest F-values (1207.9 and 129.78). BL has a low P-value (0.002) and moderate F-value (33.17). All three operating parameters have strong positive effects on EGT as per quadratic equation (7). Other terms in the model such as LD^2, SP^2, BL*SP and LD*SP also have positive effects that can change the EGT value positively. However, the combined effect of BL*LD has a strong negative influence on EGT. The R^2 and adj. R^2 were 99.66% and 99.06% respectively, showing the model's excellent accuracy.

The interaction effects of BL*LD on EGT are shown graphically in Fig. 9. Fig. 9(a) shows the 3D surface plot and Fig. 9(b) shows the 2D contour plot of BL and LD effects on EGT. With any increase in BL and LD, EGT (°C) increases. The average EGT was found to be 600 °C at 100% LD and 20% BL.

4. Conclusions and recommendations

This study evaluated the effects of blending PSO biodiesel, three other non-edible biodiesels and diesel on engine emissions characteristics of a diesel engine. The comparative analysis of emissions characteristics of all tested fuels showed that the minimum and maximum increase in NO_x and CO_2 emissions were 4.1% to 23.6% and 1.7% to 19% for papaya seed biodiesel PB20, and beauty leaf biodiesel BTL20 respectively, compared with diesel at 2400 rpm engine speed with full load condition. The highest and lowest decrease in HC, PM and CO emissions were found to be PB20 (28.2%, 13.7% and 31.6%) and BTL20 (1.3%, 2.7% and 8.8%) respectively. In order to analyse and describe the emission characteristics of this engine, a surface response methodology was introduced. The emissions characteristics of the engine with various loads at 1400 rpm (most rated torque) can be summarized, as follows:

- NO_x values of PB5, PB10 and PB20 were increased in compared with diesel by 1.7%, 3.47% and 6% respectively.
- Compared with diesel, the average increase in CO_2 values for PB5, PB10 and PB20 were 4.5%, 6.3% and 9% respectively.
- The average decrease in HC values for PB5, PB10 and PB20 was 9.3%, 15.6% and 19.3% respectively, compared to diesel.
- PM values of PB5, PB10 and PB20 were reduced by 19.5%, 31.4% and 34.9% respectively in compared with diesel at 100% full load condition.
- A maximum reduction of CO value was observed for P20 at full load condition of 100% compared to diesel. Other biodiesel blends such as PB5 and PB10 11.1% and 22.2% lower than diesel.
- About 3.7% increase in EGT value was observed for PB20 compared with diesel. EGT values of PB5 and PB10 were found to be 1.2% and 2% higher than diesel.

Lastly, ANOVA and a statistical regression model were used to assess interactive effects between three operating parameters (biodiesel blends, load, and speed) and six (NO_x, CO_2, HC, PM, CO and EGT) responses. The engine load and engine speed were found to be the two most significant parameters influencing four of the responses (NO_x, HC, PM and CO). Furthermore, biodiesel blends and load were influential for EGT and NO_x emissions generation. NO_x was continued to be generated irrespective of any variation in biodiesel blends, load and speed. Likewise, CO_2 generation was not influenced by the biodiesel blends at various operating parameters. Hence, PSO could be a probable biodiesel feedstock and its diesel blends along with varying engine speeds, and loads can give optimum engine test characteristics for minimizing emissions concentration. It can, therefore, be inferred that papaya biodiesel blends will substitute diesel fuel in unmodified diesel engines in order to reduce global energy demand and exhaust emissions into the atmosphere. Further investigation of the effects of oxygenated additives on papaya biodiesel blends to control NO_x and CO_2 emissions generation is recommended.

Declaration of Competing Interest

The authors declare that they have no known competing financial interests or personal relationships that could have appeared to influence the work reported in this paper.

Acknowledgement

The authors would like to acknowledge the contribution of Mr. Tim McSweeney, Adjunct Research Fellow, Division of Tertiary Education at Central Queensland University, Australia, to the proof reading of this paper.

References

[1] WHO Department of Public Health. Environmental and Social Determinants of Health, Available from: < https://www.who.int/phe/about_us/en/ > ; 2018 [cited 30 June 2019].
[2] Sims R, Schaeffer R, Creutzig F, Cruz-Núñez X, D'Agosto M, Dimitriu D, Figueroa Meza MJ, Fulton L, Kobayashi S, Lah O, McKinnon A, Newman P, Ouyang M, Schauer JJ, Sperling D, Tiwari G: Transport. In: Edenhofer O, Pichs-Madruga R, Sokona Y, Farahani E, Kadner S, Seyboth K, Adler A, Baum I, Brunner S, Eickemeier P, Kriemann B, Savolainen J, Schlömer S, von Stechow C, Zwickel T, Minx JC, editors. Climate Change 2014: Mitigation of Climate Change. Contribution of Working Group III to the Fifth Assessment Report of the Intergovernmental Panel on Climate Change. Cambridge, United Kingdom and New York, NY, USA: Cambridge University Press; 2014.
[3] Hosseinpoor AR, Forouzanfar MH, Yunesian M, Asghari F, Naieni KH, Farhood D. Air pollution and hospitalization due to angina pectoris in Tehran, Iran: a time-series study. Environ Res 2005;99(1):126–31.
[4] Colvile RN, Hutchinson EJ, Mindell JS, Warren RF. The transport sector as a source of air pollution. Atmos Environ 2001;35(9):1537–65.
[5] Martonen TB, Schroeter JD. Risk assessment dosimetry model for inhaled particulate matter: I. Human subjects. Toxicol Lett 2003;138(1):119–32.
[6] Babu V, MMK, APRG. Butanol and pentanol: the promising biofuels for CI engines – a review. Renew Sustain Energy Rev 2017;78:1068–88.
[7] Mahlia TMI, Syazmi Z, Mofijur M, Abas AEP, Bilad MR, Ong HC, et al. Patent landscape review on biodiesel production: technology updates. Renew Sustain Energy Rev 2020:118.
[8] Silitonga AS, Shamsuddin AH, Mahlia TMI, Milano J, Kusumo F, Siswantoro J, et al. Biodiesel synthesis from Ceiba pentandra oil by microwave irradiation-assisted transesterification: ELM modeling and optimization. Renewable Energy 2020;146:1278–91.
[9] Nabi MN, Zare A, Hossain FM, Rahman MM, Bodisco TA, Ristovski ZD, et al. Influence of fuel-borne oxygen on European stationary cycle: diesel engine performance and emissions with a special emphasis on particulate and NO emissions. Energy Convers Manage 2016;127:187–98.
[10] Sathiyamoorthi R, Sankaranarayanan G, Adhith Kumaar SB, Chiranjeevi T, Dilip Kumar D. Experimental investigation on performance, combustion and emission characteristics of a single cylinder diesel engine fuelled by biodiesel derived from Cymbopogon Martinii. Renewable Energy 2019;132:394–415.
[11] Arunkumar M, Kannan M, Murali G. Experimental studies on engine performance and emission characteristics using castor biodiesel as fuel in CI engine. Renewable Energy 2019;131:737–44.
[12] Patel C, Chandra K, Hwang J, Agarwal RA, Gupta N, Bae C, et al. Comparative compression ignition engine performance, combustion, and emission characteristics, and trace metals in particulates from Waste cooking oil, Jatropha and Karanja oil derived biodiesels. Fuel 2019;236:1366–76.
[13] Roy MM, Wang W, Bujold J. Biodiesel production and comparison of emissions of a DI diesel engine fueled by biodiesel–diesel and canola oil–diesel blends at high

idling operations. Appl Energy 2013;106:198–208.
[14] Uyumaz A. Combustion, performance and emission characteristics of a DI diesel engine fueled with mustard oil biodiesel fuel blends at different engine loads. Fuel 2018;212:256–67.
[15] Kakati J, Gogoi TK. Biodiesel production from Kutkura (Meyna spinosa Roxb. Ex.) fruit seed oil: its characterization and engine performance evaluation with 10% and 20% blends. Energy Convers Manage 2016;121:152–61.
[16] Rashed MM, Kalam MA, Masjuki HH, Mofijur M, Rasul MG, Zulkifli NWM. Performance and emission characteristics of a diesel engine fueled with palm, jatropha, and moringa oil methyl ester. Ind Crops Prod 2016;79:70–6.
[17] Sanjid A, Kalam MA, Masjuki HH, Varman M, Zulkifli NWBM, Abedin MJ. Performance and emission of multi-cylinder diesel engine using biodiesel blends obtained from mixed inedible feedstocks. J Cleaner Prod 2016;112:4114–22.
[18] Asokan MA, Senthur Prabu S, Kamesh S, Khan W. Performance combustion and emission characteristics of diesel engine fuelled with papaya and watermelon seed oil bio-diesel/diesel blends. Energy 2018;145:238–45.
[19] Prabhakaran P, Saravanan CG, Aalam CS. Effects of papaya methyl ester on DI diesel engine combustion, emission and performance characteristics. Int Res J Eng Technol (IRJET) 2016;3(2):319–25.
[20] Raj CS, Karthikayan. Effect of additive on the performance, emission and combustion characteristics of a diesel engine run by diesel-papaya methyl ester blends. Int J Chem Sci 2016;14(4):2823–34.
[21] Anwar M, Rasul MG, Ashwath N. The synergistic effects of oxygenated additives on papaya biodiesel binary and ternary blends. Fuel 2019;256:115980.
[22] Mohan A, Sen S. Emission analysis of the biodiesel from papaya and chicken blends. Int J Inform Futuristic Res 2015;2(7):6.
[23] Anwar M, Rasul M, Ashwath N. A systematic multivariate analysis of carica papaya biodiesel blends and their interactive effect on performance. Energies 2018;11(11):2931.
[24] Anwar M, Rasul MG, Ashwath N. Production optimization and quality assessment of papaya (Carica papaya) biodiesel with response surface methodology. Energy Convers Manage 2018;156:103–12.
[25] Yatish KV, Lalithamba HS, Suresh R, Harsha Hebbar HR. Optimization of bauhinia variegata biodiesel production and its performance, combustion and emission study on diesel engine. Renewable Energy 2018;122:561–75.
[26] Devan PK, Mahalakshmi NV. Performance, emission and combustion characteristics of poon oil and its diesel blends in a DI diesel engine. Fuel 2009;88(5):861–7.
[27] Abed KA, Gad MS, El Morsi AK, Sayed MM, Elyazeed SA. Effect of biodiesel fuels on diesel engine emissions. Egypt J Pet 2019;28(2):183–8.
[28] Godiganur S, Suryanarayana Murthy C, Reddy RP. Performance and emission characteristics of a Kirloskar HA394 diesel engine operated on fish oil methyl esters. Renewable Energy 2010;35(2):355–9.
[29] Yongcheng H, Longbao Z, Shangxue W, Shenghua L. Study on the performance and emissions of a compression ignition engine fuelled with fischer-tropsch diesel fuel. Proc Inst Mech Eng, Part D: J Automob Eng 2006;220(6):827–35.
[30] Wu T, Huang Z, Zhang W-G, Fang J-H, Yin Q. Physical and chemical properties of GTL – diesel fuel blends and their effects on performance and emissions of a multicylinder DI compression ignition engine. Energy Fuels 2007;21(4):1908–14.
[31] Imdadul HK, Masjuki HH, Kalam MA, Zulkifli NWM, Alabdulkarem A, Rashed MM, et al. Higher alcohol–biodiesel–diesel blends: an approach for improving the performance, emission, and combustion of a light-duty diesel engine. Energy Convers Manage 2016;111:174–85.
[32] Mofijur M, Masjuki HH, Kalam MA, Atabani AE, Fattah IMR, Mobarak HM. Comparative evaluation of performance and emission characteristics of Moringa oleifera and Palm oil based biodiesel in a diesel engine. Ind Crops Prod 2014;53:78–84.
[33] Nantha Gopal K, Pal A, Sharma S, Samanchi C, Sathyanarayanan K, Elango T. Investigation of emissions and combustion characteristics of a CI engine fueled with waste cooking oil methyl ester and diesel blends. Alexandria Eng J 2014;53(2):281–7.
[34] Gumus M, Kasifoglu S. Performance and emission evaluation of a compression ignition engine using a biodiesel (apricot seed kernel oil methyl ester) and its blends with diesel fuel. Biomass Bioenergy 2010;34(1):134–9.
[35] Agarwal D, Sinha S, Agarwal AK. Experimental investigation of control of NOx emissions in biodiesel-fueled compression ignition engine. Renewable Energy 2006;31(14):2356–69.
[36] Vallinayagam R, Vedharaj S, Yang WM, Lee PS, Chua KJE, Chou SK. Combustion performance and emission characteristics study of pine oil in a diesel engine. Energy 2013;57:344–51.
[37] Koçak MS, Ileri E, Utlu Z. Experimental study of emission parameters of biodiesel fuels obtained from canola, hazelnut, and waste cooking oils. Energy Fuels 2007;21(6):3622–6.
[38] Ong HC, Milano J, Silitonga AS, Hassan MH, Shamsuddin AH, Wang C-T, et al. Biodiesel production from Calophyllum inophyllum-Ceiba pentandra oil mixture: optimization and characterization. J Cleaner Prod 2019;219:183–98.
[39] Vijay Kumar M, Veeresh Babu A, Ravi Kumar P. The impacts on combustion, performance and emissions of biodiesel by using additives in direct injection diesel engine. Alexandria Eng J 2018;57(1):509–16.
[40] Tse H, Leung CW, Cheung CS. Investigation on the combustion characteristics and particulate emissions from a diesel engine fueled with diesel-biodiesel-ethanol blends. Energy 2015;83:343–50.
[41] Lin C-Y, Li R-J. Engine performance and emission characteristics of marine fish-oil biodiesel produced from the discarded parts of marine fish. Fuel Process Technol 2009;90(7):883–8.
[42] Zhu L, Cheung CS, Zhang WG, Huang Z. Emissions characteristics of a diesel engine operating on biodiesel and biodiesel blended with ethanol and methanol. Sci Total Environ 2010;408(4):914–21.
[43] Ong HC, Masjuki HH, Mahlia TMI, Silitonga AS, Chong WT, Yusaf T. Engine performance and emissions using Jatropha curcas, Ceiba pentandra and Calophyllum inophyllum biodiesel in a CI diesel engine. Energy 2014;69:427–45.
[44] Silitonga AS, Mahlia TMI, Kusumo F, Dharma S, Sebayang AH, Sembiring RW, et al. Intensification of Reutealis trisperma biodiesel production using infrared radiation: simulation, optimisation and validation. Renewable Energy 2019;133:520–7.
[45] Mofijur M, Atabani AE, Masjuki HH, Kalam MA, Masum BM. A study on the effects of promising edible and non-edible biodiesel feedstocks on engine performance and emissions production: a comparative evaluation. Renew Sustain Energy Rev 2013;23:391–404.
[46] Chauhan BS, Kumar N, Cho HM. A study on the performance and emission of a diesel engine fueled with Jatropha biodiesel oil and its blends. Energy 2012;37(1):616–22.
[47] Rahman SMA, Masjuki HH, Kalam MA, Abedin MJ, Sanjid A, Sajjad H. Production of palm and Calophyllum inophyllum based biodiesel and investigation of blend performance and exhaust emission in an unmodified diesel engine at high idling conditions. Energy Convers Manage 2013;76:362–7.
[48] Murillo S, Míguez JL, Porteiro J, Granada E, Morán JC. Performance and exhaust emissions in the use of biodiesel in outboard diesel engines. Fuel 2007;86(12):1765–71.
[49] Ong HC, Masjuki HH, Mahlia TMI, Silitonga AS, Chong WT, Leong KY. Optimization of biodiesel production and engine performance from high free fatty acid Calophyllum inophyllum oil in CI diesel engine. Energy Convers Manage 2014;81:30–40.
[50] Islam MS, Ahmed AS, Islam A, Abdul Aziz S, Xian LC, Mridha M. Study on emission and performance of diesel engine using castor biodiesel. J Chem 2014;2014(8).
[51] Panwar NL, Shrirame HY, Rathore NS, Jindal S, Kurchania AK. Performance evaluation of a diesel engine fueled with methyl ester of castor seed oil. Appl Therm Eng 2010;30(2):245–9.
[52] Sayin C. Engine performance and exhaust gas emissions of methanol and ethanol–diesel blends. Fuel 2010;89(11):3410–5.
[53] Datta A, Mandal BK. Impact of alcohol addition to diesel on the performance combustion and emissions of a compression ignition engine. Appl Therm Eng 2016;98:670–82.
[54] Can Ö. Combustion characteristics, performance and exhaust emissions of a diesel engine fueled with a waste cooking oil biodiesel mixture. Energy Convers Manage 2014;87:676–86.
[55] Gürü M, Koca A, Can Ö, Çınar C, Şahin F. Biodiesel production from waste chicken fat based sources and evaluation with Mg based additive in a diesel engine. Renewable Energy 2010;35(3):637–43.
[56] Kim H, Choi B. The effect of biodiesel and bioethanol blended diesel fuel on nanoparticles and exhaust emissions from CRDI diesel engine. Renewable Energy 2010;35(1):157–63.

{this page is intentionally left blank}

Declaration of Co-authorship and Contribution

Research Division

CHAPTER 7: Part A- Combustion Analysis

Title of the paper	Investigation on the impact of papaya biodiesel-diesel blends on combustion of an agricultural CI engine
Full bibliographic reference	Anwar, M., M. Rasul, and N. Ashwath, Investigation on the impact of papaya biodiesel-diesel blends on combustion of an agricultural CI engine, International Conference on Sustainable Energy and Green Technology 2019, Bangkok, Thailand.
Status	Published

Nature of Candidate's Contribution, including percentage of total
I was responsible for designed the study, performed the experiments, data analysis and wrote the first draft of the manuscript. [80%]

Nature of all Co-Authors' Contributions, including percentage of total
My co-authors, Prof. Mohammad Rasul, and A/Professor Nanjappa Ashwath, were designed the experimentation, reviewed, revised and improved the manuscript. [20%]

Has this paper been submitted for an award by another research degree candidate (Co- Author), either at CQUniversity or elsewhere? (if yes, give full details)
No

Candidate's Declaration

I declare that the publication above meets the requirements to be included in the thesis as outlined in the Research Higher Degree Theses Policy and Procedure.

Mohammad Anwar

Investigation on the impact of papaya biodiesel-diesel blends on combustion of an agricultural CI engine

M Anwar[1], M G Rasul[1] and N Ashwath[2]

1 Central Queensland University, School of Engineering and Technology, Queensland 4702, Australia
2 Central Queensland University, School of Health, Medical and Applied Sciences, Queensland 4702, Australia
E-mail: m.anwar@cqu.edu.au

Abstract. In this study, an overview of combustion characteristics of an agricultural diesel engine fuelled with papaya seed oil (PSO) biodiesel and diesel is presented. A naturally aspirated four-cylinder four-stroke tractor engine was used for all experiments. Various PSO blends (5%, 10%, and 20%) were tested and compared with diesel at speeds of 1400 rpm and 2400 rpm at full load condition. The combustion characteristics such as in-cylinder pressure, heat release rate, ignition delay, mass fraction burned, ignition duration and cylinder temperature were tested. The results show that PSO blends have some excellent attributes as fuel in regard to combustion characteristics. All PSO biodiesel blends have higher in-cylinder pressure; for example, PSO20 has 2.4% more than diesel. Heat release rate values of all PSO biodiesel blends were found to be lower than diesel due to the shorter ignition delay and lower calorific values of biodiesel. PSO20 biodiesel shows faster combustion than diesel by about 11.92% at 1400 rpm and 7.93% at 2400 rpm. The maximum cylinder temperature of all PSO biodiesel blends are also higher than that of diesel, such as PSO20 at 1400 rpm by 3.17% and at 2400 rpm by 3.73%.

1. Introduction

Recently many research studies have been conducted on biodiesels and their amazing environmental attributes over traditional fossil fuel, i.e., diesel. Numerous vegetable oils have been investigated as alternative fuel sources. Some researchers are concerned over the classical debate on “food vs. fuel” due to excessive usage of food/grain based biodiesel as an energy source. However, animal fats and non-edible vegetable based oils have been proved as renewable sources of energy and have largely solved this debate. Among more than 350 biodiesel feedstocks, waste seed based fruits/crops are drawing attention these days. Some of the popular waste seed based non-edible feedstocks are beauty leaf, rubber seed, jatropha, rapeseed, cottonseed, moringa, neem, pongamia seed, stone fruit seed, and papaya seed. This paper examines the potentiality of papaya seed oil (PSO) biodiesel from papaya seed waste.

Over the years, few researchers have investigated the opportunities of PSO biodiesel as a replacement of fossil fuel, i.e., diesel. Most of the researchers have worked on the papaya seed oil extraction techniques [1-3], optimisation of the PSO biodiesel conversion process [4], the effects of PSO biodiesel on diesel engine performance, and analysis of the emission parameters [5-7]. Anwar et al. [8] have optimised the biodiesel production process and obtained a 96.48% biodiesel yield. In another study, Anwar et al. [9] showed that PSO blends caused a slight reduction in brake power (2.88%-5.13%), torque (1.37%-3.85%), and brake thermal efficiency (3.1%-13.1%) and a slight increase in brake specific fuel consumption (3.35%-17.13%). A very few researchers have gone through the complete combustion process using PSO biodiesel over a fully instrumented multi-cylinder diesel engine. Instead,

most have used a single cylinder diesel engine. For example, Prabhakaran et al. [10] investigated a single cylinder engine's combustion characteristics using PSO biodiesel and reported that PSO has peak in-cylinder pressure due to the higher cetane number and oxygen contents of the biodiesel. Again, they found that the HRR of PSO blends were lower than that of diesel. Sundar Raj and Karthikayan [11] reported that PSO biodiesel blends ignited earlier and finished combustion earlier than diesel. However, the above studies and other literatures do not report on analysis of combustion characteristics of a fully instrumented four cylinder 4-stroke diesel engine fuelled with PSO biodiesel. In this study, three blends of PSO biodiesel are compared with diesel and investigated in this type of diesel engine to analyse the overall combustion characteristics.

2. Methodology

The experiment was conducted at the School of Engineering and Technology of Central Queensland University, Rockhampton, Australia. An agricultural tractor four-stroke diesel engine with four-cylinders (Kubota model V3300) was coupled with an eddy current dynamometer. The schematic of the experimental setup of the engine is shown in Figure 1. This tractor engine was used for testing both diesel and PSO biodiesel blends regarding engine performance, exhaust emissions, and combustion characteristics. A piezoelectric pressure transducer and crank angle encoder were used to monitor the combustion characteristics. Heat release rate (HRR) is an important combustion parameter that can be used for measuring ignition delay, start of injection, start of combustion, end of combustion and combustion duration [12]. HRR at different crank angles can be calculated using equation (1) derived from the first law of thermodynamics [13].

$$\dot{Q} = \left(\frac{\gamma}{(\gamma-1)}\right) \times P \times \frac{dV}{d\theta} + \frac{1}{(\gamma-1)} \times V \times \frac{dP}{d\theta} \quad (1)$$

where $\dot{Q}$ is HRR (J/° CA), P is the cylinder gas pressure (kPa), γ is the ratio of specific heat (air), hence $\frac{C_p}{C_v}$ = 1.4, and V is the instantaneous volume of the cylinder (m^3).

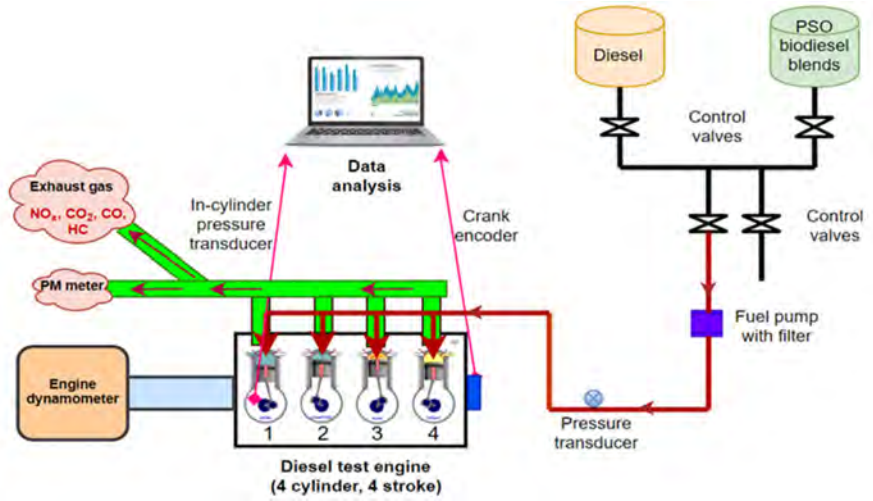

Figure 1. Schematic of the experimental setup of the engine.

The Kubota V3300 used in this experiment is an indirect injection tractor engine with a spherical combustion chamber, i.e., three vortex type combustion system. A detailed engine specification is presented in Table 1. A detailed engine performance analysis was performed in a separate experiment using the same engine and has been well documented in Anwar et al. [9].

Table 1. Specification of the diesel engine.

Items	Unit	Specifications
Model		Kubota V3300, Indirect injection
Type	-	Vertical, 4 cycle liquid cooled diesel

No. of cylinders	-	4
Total displacement	L	3.318
Bore × Stroke	mm	98 × 110
Combustion type	-	Spherical type [E-TVCS (Three vortex combustion system)]
Intake system	-	Naturally aspirated
Rated power output	kW/rpm	53.9/2600
Rated torque	Nm/rpm	230/1400
Compression ratio	-	22.6:1
Fuel injection timing	-	16° before TDC
Injection pressure	MPa	13.73
Emissions certification	-	Tier 2

PSO Biodiesel blends of 5% biodiesel with 95% diesel (denoted as PSO5), 10% biodiesel with 90% diesel (PSO10), and 20% biodiesel with 80% diesel (PSO20) along with pure diesel (B0) were tested in the engine. Before these fuels were tested, a thorough fuel properties characterisation has been conducted, and Table 2 presents the relevant information. Various PSO blends and diesel were tested at full load conditions for an engine speed of 1400 rpm (max. rated torque) and 2400 rpm (near max. rated power output).

Table 2. Basic fuel properties of B0, refined papaya seed oil (PSO), pure PSO biodiesel (PSO100), PSO5, PSO10, and PSO20.

Fuel	Density (kg/m^3)	Viscosity at 40°C, mm^2/s	Acid Value, mg KOH/g	Cetane number (CN)	Calorific value, MJ/kg	Flash Point, °C	Iodine Value (IV) mg.I_2/100g	Oxidation stability (OS), h
B0	827.2	3.23	0.05	48.00	45.30	68.5	38.3	39.0
Refined PSO	885.0	27.3	0.98		40.23		79.95	77.97
PSO100	840.0	3.53	0.42	48.29	38.49	112	115.89	5.61
PSO20	829.76	3.29	0.12	48.06	43.94	77.20	53.82	32.32
PSO10	828.48	3.26	0.09	48.03	44.62	72.85	46.06	35.66
PSO5	827.84	3.25	0.07	48.01	44.96	70.68	42.18	37.33
ASTM D6751-2	870-890.0	1.9-6.0	max 0.5	min. 47	-	min. 93	-	min. 3

3. Results and discussion

3.1. In-cylinder pressure

The variation of in-cylinder pressure (CP) with the crank angle (CA) for diesel and PSO blends at 1400, and 2400 rpm at full engine load conditions are presented in Figure 2(a) and 2(b). At 1400 rpm speed, PSO20 has a peak CP of 66.15 bar at 3° CA, followed by 64.5 bar at 3° CA for PSO10, 64.29 bar at 3° CA for PSO5 and 64.07 bar at 3° CA for diesel. At the higher speed and load, the temperature increases with the increase of pressure that resulted in a higher evaporation rate and better combustion. At 2400 rpm, peak CP was recorded at 0° CA for diesel and all PSO blends. PSO20 was found to be 67.33 bar while PSO10, PSO5, and diesel were 66.29 bar, 65.93 bar, and 65.75 bar respectively. CP of biodiesel blends were found to be higher than diesel due to the higher density of biodiesel being injected for the same injection duration compared with diesel [14, 15]. At full load and 2400 rpm speed, the maximum CPs of PSO5, PSO10, and PSO20 were found to be 0.27%, 0.82%, and 2.4% higher than diesel. All graphs trends are similar and in line with previous researcher Prabhakaran et al.[10].

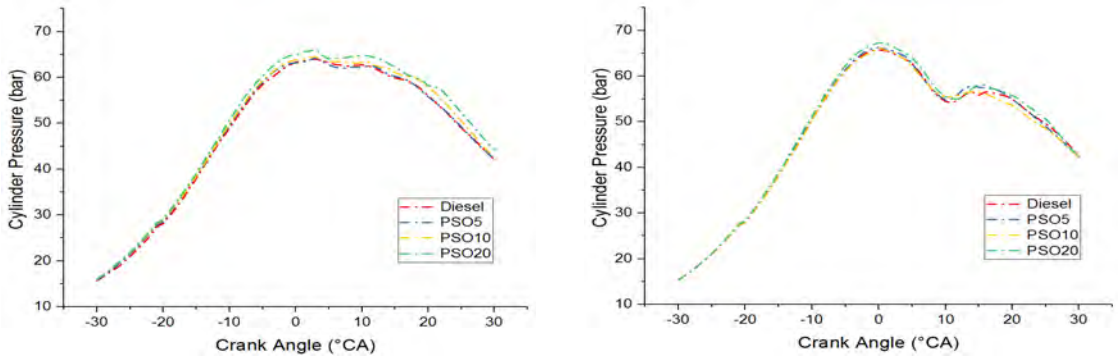

(a) 1400 rpm (b) 2400 rpm

Figure 2. The differences of in-cylinder pressure for PSO blends and diesel under full load at speeds of: (a) 1400 rpm, and (b) 2400 rpm.

3.2. Heat release rate

Heat release rate (HRR) of PSO biodiesel blends and diesel are shown in Figure 3(a) and (b). At 1400 rpm with full load condition, the maximum HRR was recorded as 201.78 J/°CA at 16° CA with diesel, 192.42 J/°CA at 16° CA with PSO20, 186.78 J/°CA at 16° CA with PSO10, and 176.22 J/°CA at 16° CA with PSO5. Several fuel characteristics such as calorific value, cetane number, fuel-air mixing rates, cetane number, ignition number and ignition timings can affect HRR [12, 16]. At 2400 rpm and full load condition, the maximum HRR was found to be 250.59 J/°CA at 15° CA with diesel, 237.15 J/°CA at 15° CA with PSO20, 240.34 J/°CA at 15° CA with PSO10, and 244.56 J/°CA at 15° CA with PSO5. The maximum HRRs at 2400 rpm of PSO20, PSO10, and PSO5 were found to be 5.36%, 4.1%, and 2.40% lower than diesel. PSO biodiesel blends have lower calorific values and lower ignition delay that resulted in lower HRR values than diesel. Again, diesel has longer ignition delay that retarded the start of combustion led to higher HRR [17]. Some researchers also mentioned that diesel has higher HRR values due to its higher calorific value [12, 14, 18].

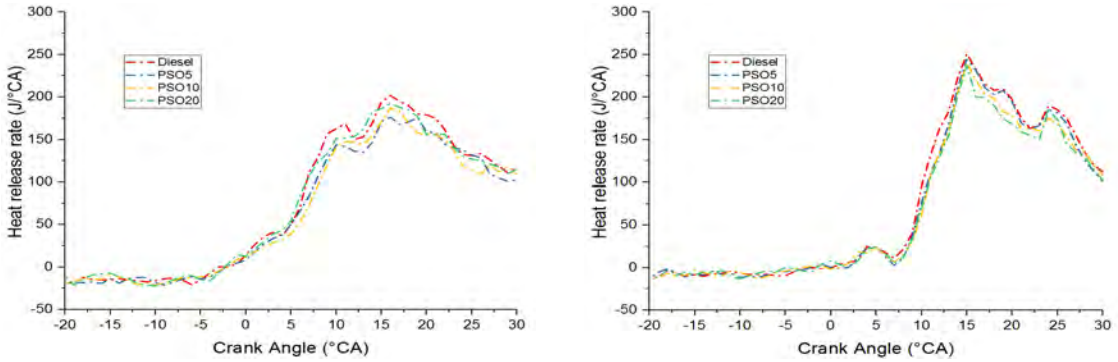

(a) 1400 rpm (b) 2400 rpm

Figure 3. The differences of heat release rate for PSO blends and diesel under full load at speeds of: (a) 1400 rpm, and (b) 2400 rpm.

3.3. Ignition delay

The time difference between the start of injection and combustion of a diesel engine is the Ignition delay (ID). Fuel quality, engine speed, load, air temperature, and fuel-air mixing ratio affect ID [12]. ID also represents the fuel quality as well as being a measure of the ignition quality (cetane number) and knocking tendency of the fuel [19]. The PSO biodiesel blends have higher cetane numbers than diesel, and Figure 4 shows that all blends have a lower ID period compared with diesel. The ID (MS) decreases with the increase of engine speed. Higher oxygen content, i.e., the higher level of biodiesel blends,

PSO20, resulted in lower ID (8.5 °CA at 1400 rpm and 9.5 °CA at 2400 rpm) at full load condition compared with that of diesel (11 °CA at 1400 rpm and 13 °CA at 2400 rpm).

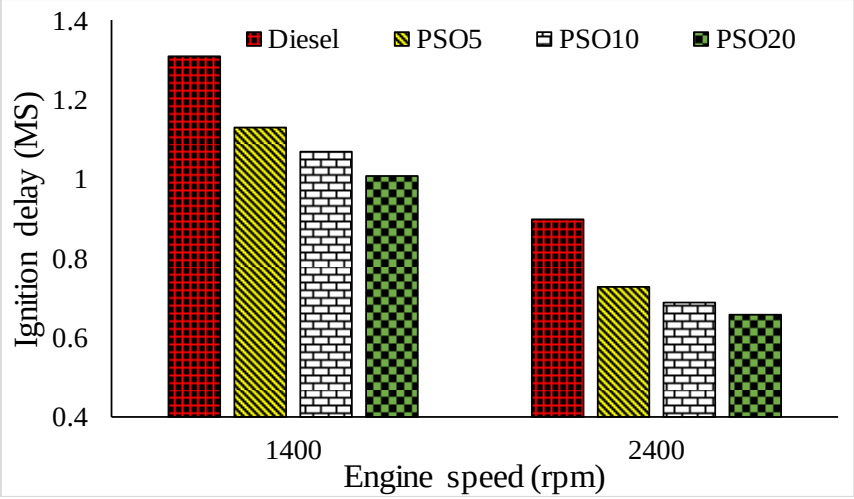

Figure 4. Ignition delay of diesel and PSO biodiesel blends at full load condition.

3.4. Mass fraction burned

The variation of the mass fraction burned (MFB) with the crank angle for PSO biodiesel blends and diesel at 1400 rpm and 2400 rpm engine speed at full loading condition are compared in Figure 5(a) and (b). Biodiesel blends and diesel showed similar trend and the MFB for biodiesel blends were found earlier than that of diesel at full load condition. From Figure 5(a) at 1400 rpm, 90% of the PSO20 biodiesel blend was burnt at 41.5 °CA after TDC, and the same amount of diesel was burnt at 47.2° CA. Again, from Figure 5(b) at 2400 rpm, the same amounts (90%) of PSO20 biodiesel blend and diesel were burnt at 40° CA, and 43° CA respectively.

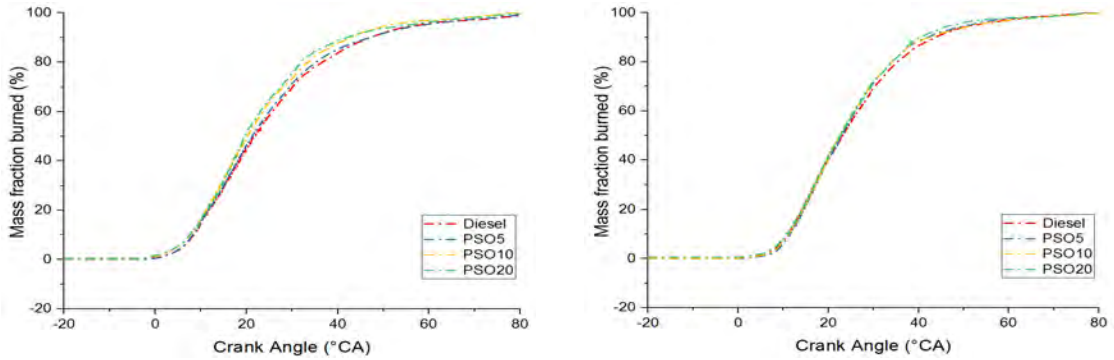

(a) 1400 rpm (b) 2400 rpm

Figure 5. The differences of mass fraction burned (%) for PSO blends and diesel under full load at speeds of: (a) 1400 rpm, and (b) 2400 rpm.

Combustion duration is affected by several factors such as engine speed, load, ignition delay, and fuel characteristics. The higher the engine speed, the lower the combustion duration. Table 3 presents the MFB data for both speeds of 1400 and 2400 rpm at full load condition. PSO20 biodiesel shows faster combustion of about 11.92% at 1400 rpm and 7.93% at 2400 rpm compared to diesel. The fact that biodiesel has a higher content of oxygen than diesel is the primary cause for the shorter combustion duration.

Table 3. Mass fraction burned at full load condition for 1400 rpm and 2400 rpm.

Fuel	Speed	Crank angle (°ATDC) for mass fraction burned (%)			
		10% (°CA)	50% (°CA)	90% (°CA)	Combustion duration (°CA)
Diesel	1400	8.6	21.7	47.2	38.6
PSO5	1400	8.6	21.2	47.1	38.5
PSO10	1400	8	20	42.5	34.5
PSO20	1400	7.5	19.5	41.5	34
Diesel	2400	11.5	23.1	43	31.5
PSO5	2400	11.5	22.5	42.8	31.3
PSO10	2400	11.5	22.5	42.5	31
PSO20	2400	11	22.5	40	29

3.5. In-cylinder temperature

In-cylinder temperature can be derived from HRR, in-cylinder pressure and fuel injection. The variation of in-cylinder temperature with crank angle for PSO biodiesel blends and diesel are shown in Figure 6(a) and (b). At both engine speeds of 1400 rpm and 2400 rpm, PSO biodiesel blends have higher cylinder temperature compared with diesel. It can be seen that, at full load conditions, all cylinder temperature trends of biodiesel blends and diesel are similar. At the start of combustion, the cylinder temperature increases to the maximum temperature corresponding to the peak cylinder pressure during the diffusion combustion phase. As the combustion finished, the cylinder temperature slowly decreased. At 1400 rpm, PSO20 gives the maximum cylinder temperature of 1642 °C at 30 °CA. However, at 2400 rpm, PSO20 gives the maximum cylinder temperature of 1880 °C at 30 °CA. The maximum cylinder temperature of PSO20, PSO10, and PSO5 blends are higher than that of diesel by 3.17%, 2.75% and 0.31% at 1400 rpm; and 3.73%, 1.86% and 0.39% at 2400 rpm. Biodiesel has a higher oxygen content that increases cylinder pressure as well as cylinder temperature during the transition from compression phase to the combustion phase.

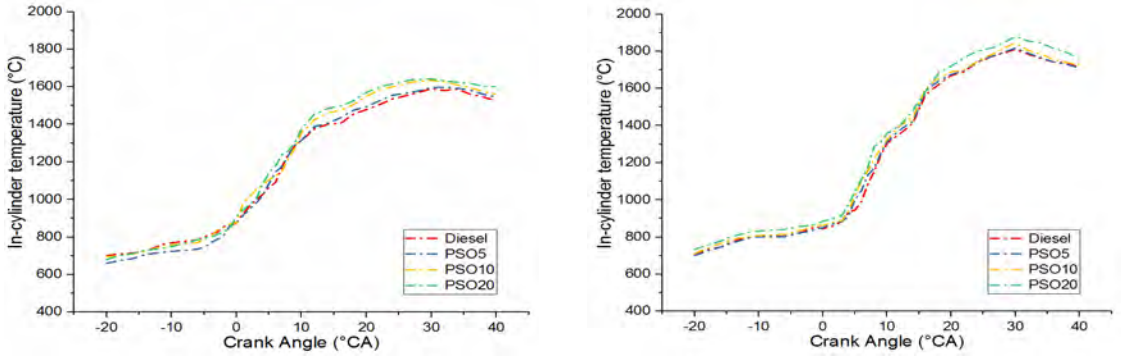

(a) 1400 rpm (b) 2400 rpm

Figure 6. The differences of in-cylinder temperature for PSO blends and diesel under full load at speeds of: (a) 1400 rpm, and (b) 2400 rpm.

4. Conclusion

This study investigated the combustion characteristics of papaya seed oil (PSO) biodiesel in an agricultural diesel engine. Various PSO biodiesel blends and their effects on cylinder pressure, heat release rate, ignition delay, mass fraction burned, combustion duration and cylinder temperature at full load condition at 1400 rpm and 2400 rpm has analysed as well. The results of this investigation can be summarised, as follows:

- In-cylinder peak pressure for PSO biodiesels is higher than that of diesel irrespective of engine speed. At 2400 rpm and full load conditions, the peak cylinder pressure for PSO5, PSO10, and PSO20 were found to be 0.27%, 0.82%, and 2.4% higher than diesel.
- HRR values of PSO biodiesel blends, PSO5, PSO10, and PSO20, were found to be 2.40%, 4.1% and 5.36% lower than diesel due to the lower ignition delay and lower calorific values of biodiesel.
- PSO biodiesel blends have a shorter ignition delay period compared with diesel.
- The mass fraction burned for PSO biodiesel blends is slightly faster than diesel. PSO20 biodiesel shows faster combustion by about 11.92% at 1400 rpm and 7.93% at 2400 rpm than diesel.
- The maximum cylinder temperatures of PSO5, PSO10, and PSO20 blends are higher than that of diesel by 0.31%, 2.75% and 3.17% at 1400 rpm, and by 0.39%, 1.86% and 3.73% at 2400 rpm.

Therefore, it is evident that all PSO biodiesel blends have excellent fuel attributes to be considered as an alternative fuel for agricultural diesel engines. However, a tribology test should be conducted in the future to identify the lubricity behavior of PSO biodiesel blends.

5. References

[1] Malacrida, C.R., M. Kimura, and N. Jorge, *Characterization of a high oleic oil extracted from papaya (Carica papaya L.) seeds.* Food Science and Technology, 2011. **31**: p. 929-934.

[2] Syed H.M, K.S.P., Jadhav B. A and Salve R.V, *Extraction and characterization of papaya seed oil* Elixir Agriculture, 2011. **37A**: p. 4102-4105.

[3] Puangsri T, Abdulkarim SM, Ghazali HM., *Properties of Carica papaya L. (papaya) seed oil following extractions using solvent and aqueous enzymatic methods.* Journal of Food Lipids, 2004. **12**: p. 62-76.

[4] Agunbiade FO, Adewole TA., *Methanolysis of Carica papaya Seed Oil for Production of Biodiesel.* Journal of Fuels, 2014. **2014**: p. 6.

[5] Sivasubramanian, H., *Performance and emission characteristics of papaya seed oil methyl ester–n-butanol–diesel blends on a stationary direct-injection CI engine.* Biofuels, 2017: p. 1-10.

[6] Asokan, M.A., S. Senthur prabu, S. Kamesh, and W. Khan, *Performance, combustion and emission characteristics of diesel engine fuelled with papaya and watermelon seed oil bio-diesel/diesel blends.* Energy, 2018. **145**: p. 238-245.

[7] Mohan, A., and Sen, S.S.S., *Emission Analysis of the Biodiesel from Papaya and Chicken Blends.* International Journal of Informative & Futuristic Research, 2015. **2**(7): p. 6.

[8] Anwar, M., M.G. Rasul, and N. Ashwath, *Production optimization and quality assessment of papaya (Carica papaya) biodiesel with response surface methodology.* Energy Conversion and Management, 2018. **156**: p. 103-112.

[9] Anwar, M., M. Rasul, and N. Ashwath, *A Systematic Multivariate Analysis of Carica papaya Biodiesel Blends and Their Interactive Effect on Performance.* Energies, 2018. **11**(11): p. 2931.

[10] Prabhakaran, P., Saravanan, C.G., Aalam, C.S., *Effects of Papaya Methyl Ester on DI Diesel Engine Combustion, Emission and Performance Characteristics.* International Research Journal of Engineering and Technology (IRJET), 2016. **3**(2).

[11] Sundar Raj, C., and Karthikayan, M., *Effect of additive on the performance, emission and combustion characteristics of a diesel engine run by diesel-papaya methyl ester blends.* Int. J. Chem. Sci, 2016. **14**(4): p. 2823-2834.

[12] Rahman, M.M., M.G. Rasul, N.M.S. Hassan, A.K. Azad, and M.N. Uddin, *Effect of small proportion of butanol additive on the performance, emission, and combustion of Australian native first- and second-generation biodiesel in a diesel engine.* Environmental Science and Pollution Research International, 2017. **24**(28): p. 22402-22413.

[13] Heywood, J.B., *Internal combustion engine fundamentals*. 1988: New York: McGraw-Hill.
[14] Patel, C., K. Chandra, J. Hwang, R.A. Agarwal, N. Gupta, C. Bae, T. Gupta, and A.K. Agarwal, *Comparative compression ignition engine performance, combustion, and emission characteristics, and trace metals in particulates from Waste cooking oil, Jatropha and Karanja oil derived biodiesels.* Fuel, 2019. **236**: p. 1366-1376.
[15] Dhar, A. and A.K. Agarwal, *Performance, emissions and combustion characteristics of Karanja biodiesel in a transportation engine.* Fuel, 2014. **119**: p. 70-80.
[16] Mahmudul, H.M., F.Y. Hagos, R. Mamat, A.A. Abdullah, and O.I. Awad, *Experimental investigation of the impact of using alcohol- biodiesel-diesel blending fuel on combustion of single cylinder CI engine.* IOP Conference Series: Materials Science and Engineering, 2016. **160**: p. 012038.
[17] Datta, A. and B.K. Mandal, *Engine performance, combustion and emission characteristics of a compression ignition engine operating on different biodiesel-alcohol blends.* Energy, 2017. **125**: p. 470-483.
[18] Can, Ö., *Combustion characteristics, performance and exhaust emissions of a diesel engine fueled with a waste cooking oil biodiesel mixture.* Energy Conversion and Management, 2014. **87**: p. 676-686.
[19] Dhinesh, B., J.I.J.R. Lalvani, M. Parthasarathy, and K. Annamalai, *An assessment on performance, emission and combustion characteristics of single cylinder diesel engine powered by Cymbopogon flexuosus biofuel.* Energy Conversion and Management, 2016. **117**: p. 466-474.

Declaration of Co-authorship and Contribution

Research Division

CHAPTER 7: Part B- Combustion Analysis

Title of the paper	Combustion characteristics of an agricultural diesel engine fueled with papaya and stone fruit biodiesel: A comparison
Full bibliographic reference	Anwar, M., M. Rasul, and N. Ashwath, Combustion characteristics of an agricultural diesel engine fueled with papaya and stone fruit biodiesel: A comparison, IEEE 2nd International Conference on Renewable Energy and Power Engineering. 2019. Toronto.
Status	Published

Nature of Candidate's Contribution, including percentage of total
I was responsible for performed the experiments, data analysis and drafted the manuscript. [80%]

Nature of all Co-Authors' Contributions, including percentage of total
My co-authors, Prof. Mohammad Rasul, and A/Professor Nanjappa Ashwath, were designed the experimentation, reviewed, revised and improved the manuscript. [20%]

Has this paper been submitted for an award by another research degree candidate (Co- Author), either at CQUniversity or elsewhere? (if yes, give full details)
No

Candidate's Declaration

I declare that the publication above meets the requirements to be included in the thesis as outlined in the Research Higher Degree Theses Policy and Procedure.

Mohammad Anwar

Combustion characteristics of an agricultural diesel engine fuelled with papaya and stone fruit biodiesel: A comparison

M. Anwar* and M.G. Rasul
School of Engineering and Technology
Central Queensland University
Rockhampton, QLD 4702, Australia
*E-mail: m.anwar@cqu.edu.au
E-mail: m.rasul@cqu.edu.au

N. Ashwath
School of Heath, Medical and Applied Sciences
Central Queensland University
Rockhampton, QLD 4702, Australia
E-mail: n.ashwath@cqu.edu.au

***Abstract*— A comparative study of the combustion characteristics of an agricultural diesel engine fuelled with papaya seed oil (PSO) biodiesel and stone fruit kernel oil (SFO) biodiesel along with diesel was performed. A 3.3 L heavy duty tractor diesel engine with four-cylinder 4-stroke, EURO II standard was used for the comparison. Two binary blends of each of the biodiesels were prepared with 10% and 20% by volume, with the remaining volume made up of petro diesel. All fuel samples were tested at 1400 rpm (rated torque) and 2400 rpm (near rated power output) at full engine load condition. The experimental investigations were conducted to evaluate the effects of binary blends on engine combustion characteristics such as in-cylinder pressure, heat release rate, ignition delay, mass fraction burned, and ignition duration. The results show that all PSO biodiesel blends had higher in-cylinder pressure; for instance, PSO20 had 2.4% and 1.4% higher peak pressure compared to diesel and SFO20. Heat release rate (HRR) values of both PSO and SFO biodiesel blends were found lower than diesel due to shorter ignition delay and lower calorific values of the biodiesel. The maximum HRRs at 2400 rpm of PSO10, PSO20, SFO10, and SFO20 were found to be 4.1%, 5.4%, 11.1%, and 11.8% lower than that of diesel. PSO and SFO blends were found to have lower ignition delay period compared with the diesel. Again, both biodiesel blends show faster combustion than diesel. However, SFO20 showed 7.1% and 6.5% slower than PSO20 at 1400 rpm and 2400 rpm respectively. Overall, PSO blends performed better than SFO blends in all combustions.**

Keywords- Carica papaya, combustion, cylinder pressure, HRR, apricot, stone fruit, diesel.

I. INTRODUCTION

Ongoing concerns of the energy crisis, excessive usage of traditional fossil fuel and its environmental impact pushed the research on clean alternative fuels for internal combustion engines i.e., diesel engine. Biodiesel is an excellent choice for researchers due to its abundant sources, biodegradation and amazing environmental attributes over traditional fossil fuel, i.e. diesel [1]. It is drawing the attention of policymakers of many countries as an alternative for diesel engine as well as its potential to be a part of the sustainable energy mix [2]. Biodiesel can be produced from a renewable plant source or animal fat (tallow) using a chemical reaction called transesterification. Present day's most popular biodiesel feedstock is from non-edible oilseed source. Some of the popular seed based non-edible feedstocks are beauty leaf tree, rubber, jatropha, rapeseed, cottonseed, moringa, neem, pongamia, stone fruit, and papaya. This paper reports the testing of papaya seed oil (PSO) and stone fruit kernel oil (SFO) biodiesel.

Papaya is a tropical fruit that grows well in sub-tropical regions. Papaya fruit contains seeds which constitute up to 15% of fruit weight. These seeds discarded. The dried seeds contain 30-34% oil which can be utilized for biodiesel synthesis [3]. Stone fruit, particularly apricot is cultivated in the cool frost-free region. Apricot fruit contains kernels which make up 22-38% of the fruit weight. These kernels contain up to 54.2% of oil. Since these seeds are discarded due to the presence of hydrocyanic acid, they can be utilized as biodiesel feedstock [4]. A few researchers have explored the use of papaya seed for oil extraction [5-7]; biodiesel production [8]; analysis of diesel engine performance, and their emission characteristics [9-11]. However, no researcher has gone through the complete combustion process using papaya seed oil biodiesel over a fully instrumented diesel engine. The researchers who performed combustion test used a single cylinder engine which is not adequate for evaluating the PSO biodiesel [12, 13]. On the other hand, very few researchers have investigated SFO biodiesel, especially on apricot kernel oil biodiesel [13-17]. While some researchers have performed biodiesel process optimization [18, 19], Gumus et al. [14] and kumar et al. [20] have carried out engine performance and emission analysis using apricot biodiesel. However, the above studies do not report engine combustion characteristics using SFO biodiesel. In the current study, two blends each of PSO and SFO biodiesel blends were evaluated along with diesel using a diesel engine to analyze its overall combustion characteristics. The ultimate aim of the study was to identify a better blend of biodiesel for an agricultural tractor diesel engine.

II. EXPERIMENTAL SETUP AND METHOD

A four-cylinder, 4-stroke and liquid-cooled agricultural tractor diesel engine was used in the evaluation. All experiments were conducted at the thermodynamics laboratory of the School of Engineering at Central

Queensland University, Rockhampton, Australia. Figure 1(a) shows the actual setup of the test engine and Figure 1(b) shows the schematic of the setup. Kubota V3300 model tractor engine with three vortex type combustion system was coupled with an eddy current dynamometer. A detailed list of engine specification and operating conditions, as well as engine performance analysis, has been described in Anwar et al. [21]. Combustion characteristics parameters such as cylinder pressure, heat release rate (HRR), ignition delay (ID), mass fraction burnt (MFB) and ignition duration were measured. A piezoelectric pressure transducer and crank angle encoder were used to measure cylinder pressure. The HRR was calculated based on the cylinder gas pressure data. HRR can be obtained from the first law thermodynamics measured by equation (1), disregarding the cylinder wall heat loss [22]. HRR was also used for calculating ID, beginning of injection, beginning of combustion, end of combustion and combustion duration [23].

$$\frac{dQ}{d\theta} = \left(\frac{\gamma}{(\gamma-1)}\right) \times P \times \frac{dV}{d\theta} + \frac{1}{(\gamma-1)} \times V \times \frac{dP}{d\theta} \qquad (1)$$

Where, $\frac{dQ}{d\theta}$ is HRR per crank angle (J/° CA), θ is the crank angle, P is the cylinder gas pressure (kPa), γ is the ratio of specific heat (air), and V is cylinder volume (m^3).

(a) Engine test bed

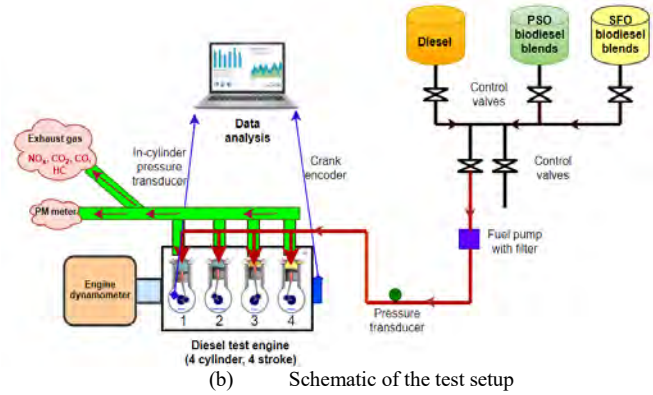

(b) Schematic of the test setup

Figure 1. Experimental setup for engine testing.

III. BIODIESEL-DIESEL BLENDS

Two types of non-edible feedstocks were selected for this study, and they included papaya seed oil and stone fruit oil. Details of the biodiesel production process can be found in Anwar et al. [3, 4]. Biodiesel blends with diesel was prepared at different ratios (10-20% by volume), and the mixture was mixed thoroughly using a magnetic stirrer and a shaker. Biodiesel blends of 10% biodiesel with 90% diesel (PSO10, SFO10) and 20% biodiesel with 80% diesel (PSO20, SFO20) were used in this test. The PSO100 and SFO100 stand for 100% biodiesel content, whereas B0 is denoted as pure diesel. All biodiesel blends and diesel were characterized before they were tested in an engine (Table 1). All fuel samples were tested at full load conditions for an engine speed of 1400 rpm (rated torque) and 2400 rpm (near rated power output).

TABLE I. PROPERTIES OF FUEL SAMPLES USED.

Fuel	Density (kg/m^3)	Viscosity at 40°C, mm^2/s	Acid Value, mg KOH/g	Cetane number (CN)	Calorific value, MJ/kg	Flash Point, °C	Iodine Value (IV) $mg.I_2/100g$	Oxidation stability (OS), h
B0	827.2	3.23	0.05	48.00	45.30	68.5	38.3	39.0
Refined PSO	885.0	27.3	0.98		40.23		79.95	77.97
PSO100	840.0	3.53	0.42	48.29	38.49	112	115.89	5.61
PSO20	829.76	3.29	0.12	48.06	43.94	77.20	53.82	32.32
PSO10	828.48	3.26	0.09	48.03	44.62	72.85	46.06	35.66
Refined SFO	910.0	34.54	1.65		38.4		103	
SFO100	855	4.26	0.25	50.45	39.64	105	104.70	7.15
SFO20	832.76	3.44	0.09	48.49	44.17	75.80	51.58	32.63
SFO10	829.98	3.33	0.07	48.25	44.73	72.15	44.94	35.82
ASTM D6751-2	870-890.0	1.9-6.0	max 0.5	min. 47	-	min. 93	-	min. 3

IV. RESULTS AND DISCUSSION

A. *In-Cylinder pressure*

The variation in in-cylinder pressure (CP) with the crank angle (CA) for diesel and PSO and SFO blends at 1400, and 2400 rpm at full engine load conditions are presented in Figure 2(a) and 2(b). At 1400 rpm speed and 3° CA, PSO20 had a peak CP of 66.2 bar followed by 64.5 bar for PSO10, 64.4 bar for SFO20, 64.2 bar for SFO10, and 64.1 bar for diesel. At 2400 rpm, peak CP was recorded at 0° CA for diesel and all biodiesel blends. PSO20 was found at 67.3 bar where as PSO10, SFO10, SFO20, and diesel were 66.3 bar, 65.9 bar, 66.4 bar and 65.8 bar respectively. Cylinder temperature and pressure increased with the increase of engine speed and load leading to higher evaporation rate i.e., better combustion [10]. CP of biodiesel blends was found to be higher than that of diesel due to higher density of biodiesel being injected for the same injection duration compared with diesel [24, 25]. Other reason for higher CP can be shorter ignition delay and fuel fraction burnt in the premixed combustion phase [26]. Other factors such as cetane number, volatility characteristics, oxygen content, will influence CP variations. The peak CP occurs just at top dead centre (TDC) for biodiesel blends due to their higher cetane number that enabled an earlier beginning of combustion [26]. At the full load and 2400 rpm speed, the

maximum CPs of PSO10, PSO20, SFO10 and SFO20 were found to be 0.82%, 2.4%, 0.17%, and 0.99%, higher than diesel.

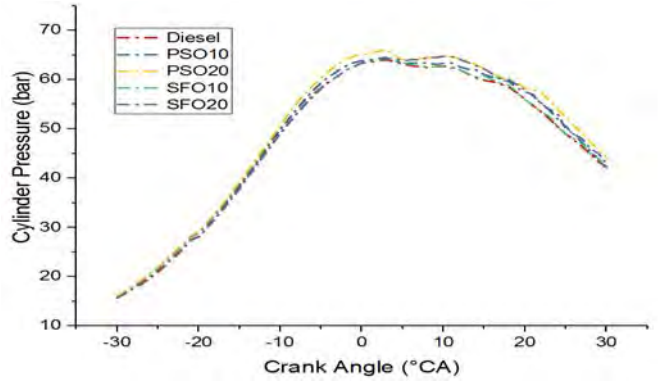

(a) 1400 rpm

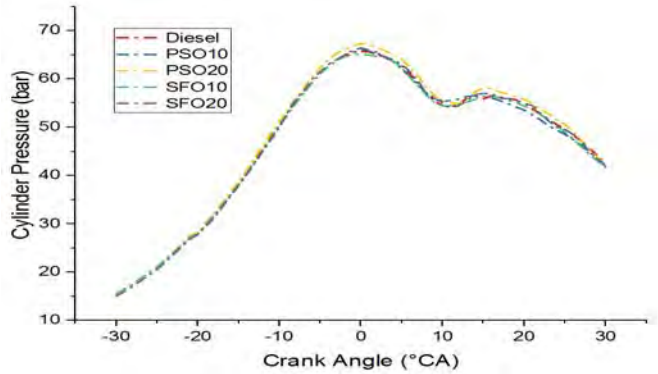

(b) 2400 rpm

Figure 2. In-cylinder pressure comparison between PSO, SFO biodiesel blends and diesel at full load.

B. *Heat release rate*

Heat release rate (HRR) of PSO, SFO biodiesel blends and diesel are shown in Figure 3(a) and (b). It can be seen that at the beginning there is a negtive HRR value and after the combustion was initiated, a positive HRR value is observed due to vaporisation of fuel accumulated during the ignition delay period [26]. At 1400 rpm and 16° CA, maximum HRR of 201.8 J/°CA was recorded for diesel, 186.78 J/°CA for PSO10, 192.42 J/°CA for PSO20, 175.77 J/°CA with SFO10, and 189.82 J/°CA with SFO20. HRR in the diesel engine combustion depends on fuel characteristics such as calorific value, cetane number, fuel-air mixing rates, cetane number, ignition number and ignition timings [23, 27]. At 2400 rpm and 15° CA, the maximum HRR was recorded at 250.6 J/°CA with diesel, 240.34 J/°CA with PSO10, 237.15 J/°CA with PSO20, 222.85 J/°CA with SFO10, and 221.10 J/°CA with SFO20. The maximum HRRs at 2400 rpm of PSO10, PSO20, SFO10 and SFO20 were found to be 4.1%, 5.4%, 11.1 % and 11.8% lower than diesel. The lower the biodiesel content i.e., PSO10 and SFO10, the higher the HRR due to the good mixing rate of fuel-air and Heywood [22] mentioned that is the main affecting parameter of HRR. Again, generally biodiesel has lower calorific values and lower ignition delay that cause lower HRR values. Researchers found longer ignition delay, retardation of start of combustion and higher calorific values effect leading to higher HRR of diesel [23, 24, 28, 29]. Furthermore, the higher viscosities of PSO and SFO biodiesel blends resulted in relatively inferior atomization that led to slower burning, as compared to the diesel.

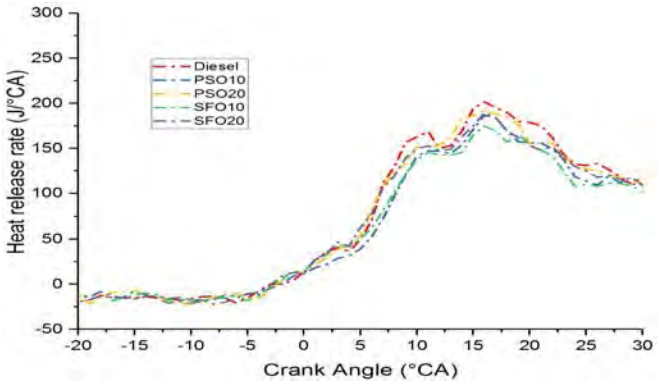

(a) 1400 rpm

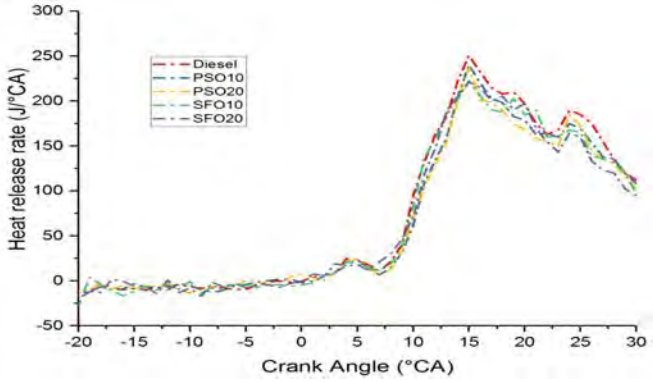

(b) 2400 rpm

Figure 3. Heat release rate comparison between PSO, SFO biodiesel blends and diesel at full load.

C. *Ignition delay*

Ignition delay (ID) shows the time gap between the beginning of injection and the beginning of combustion in a diesel engine. It is the most important parameter used in analyzing combustion performance. Some factors such as fuel quality, engine load and speed, fuel-air mixing ratio and air temperature can influence the ID. Both PSO and SFO biodiesel blends have higher cetane number, and Figure 4 shows that all blends have a lower ID period compared with the diesel. The ID (MS) decreases with an increase of engine speed. Higher oxygen content, i.e., higher biodiesel blends (PSO20) resulted in lower ID (8.5 °CA at 1400 rpm and 9 °CA at 2400 rpm) at full load condition compared to diesel (11 °CA at 1400 rpm and 13 °CA at 2400 rpm). SFO20 biodiesel blends resulted in a bit higher ID than PSO20 and recorded as 10° CA at 1400 rpm and 11° CA at 2400 rpm. Although, SFO biodiesel has higher cetane number than PSO biodiesel and diesel, its higher viscosity and density would have prolonged the ID after PSO biodiesel.

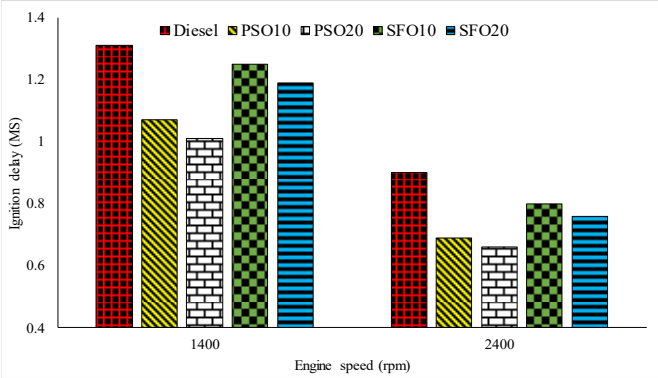

Figure 4. Ignition delay comparison between PSO, SFO biodiesel blends and diesel at full load.

D. *Mass fraction burned*

Mass fraction burned is the fraction (%) of fuel burned in each cycle during the combustion process. Figure 5 shows the differences of mass fraction burned (MFB) with the crank angle for PSO and SFO biodiesels and diesel at full load condition. All biodiesels and diesel show similar trends and start of combustion for biodiesels are earlier than those of diesel irrespective of any loading conditions. As shown in Figure 5(a) at 1400 rpm, 90% of the PSO20 biodiesel blends was burnt at 41.5 °CA after TDC. The SFO20 biodiesel blends were burnt at 49° CA and same amount of diesel was burnt at 47.2° CA. Again, from the Figure 5(b) at 2400 rpm, the same amount (90%) of PSO20, SFO20 biodiesel blends and diesel was burnt at 40° CA, 42.5° CA and 43° CA respectively. A higher rate of fuel burning was observed irrespective of engine speeds for PSO20 as compared to both SFO20 and diesel. The reason could be higher oxygen content and higher cetane number of biodiesel that initiate earlier combustion and enable completing burning of fuel earlier than diesel. SFO biodiesel blends show slower rate of fuel burning due to higher density and higher viscosities in comparison with PSO blends. PSO20 biodiesel shows faster combustion than diesel by 11.9% and 7.9% at 1400 rpm and 2400 rpm respectively. Whereas, SFO20 biodiesel shows a faster combustion than diesel by 5.2 % and 1.6 % at 1400 rpm and 2400 rpm respectively.

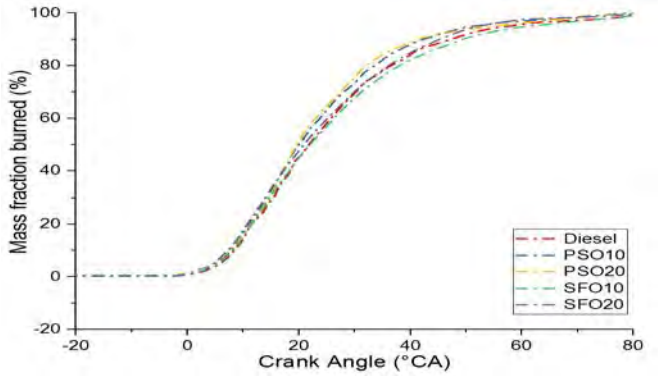

(a) 1400 rpm.

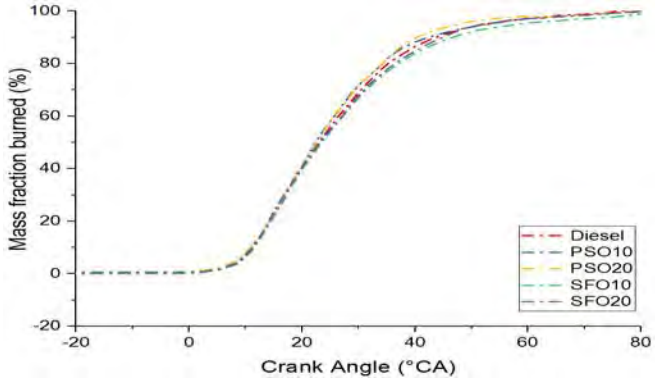

(b) 2400 rpm

Figure 5. Mass fraction burned (%) comparison between PSO, SFO biodiesel blends at full load.

The MFB data for all biodiesel blends and diesel are presented in Table 2. The crank angle duration from 10% mass fraction burned to 90% mass fraction burned has been considered as combustion duration (° CA).

TABLE II. MASS FRACTION BURNED AT FULL LOAD CONDITION FOR 1400 RPM AND 2400 RPM.

Fuel	Speed	Crank angle (°ATDC) for mass fraction burned (%)			
		10% (°CA)	50% (°CA)	90% (°CA)	Combustion duration (°CA)
Diesel	1400	8.6	21.7	47.2	38.6
PSO10	1400	8	20	42.5	34.5
PSO20	1400	7.5	19.5	41.5	34
SFO10	1400	8	22	49	41
SFO20	1400	8.4	21	45	36.6
Diesel	2400	11.5	23.1	43	31.5
PSO10	2400	11.5	22.5	42.5	31
PSO20	2400	11	22.5	40	29
SFO10	2400	11.7	23.2	47	35.3
SFO20	2400	11.5	23.1	42.5	31

Figure 6 compares the ignition duration of all fuel samples, and the patterns of the changes were similar for all samples. The higher the engine speed from 1400 rpm to 2400 rpm, the lower the combustion duration. Combustion duration is affected by several factors such as engine speed, load, ignition delay, and fuel characteristics.

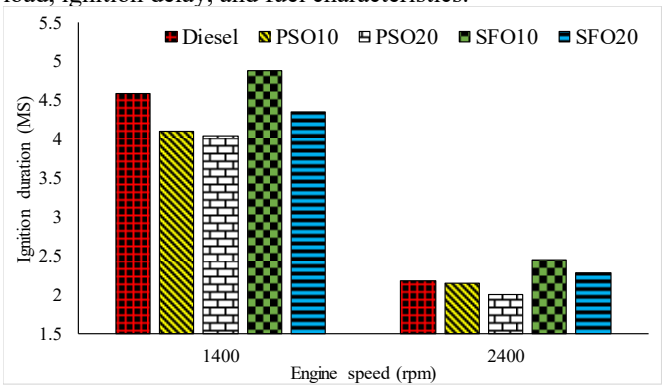

Figure 6. Ignition duration comparison between PSO, SFO biodiesel blends and diesel at full load.

V. CONCLUSION

In this paper, an experimental study of combustion characteristics of an agricultural diesel engine fueled with PSO and SFO biodiesels and diesel was carried out. Based on the combustion parameter measured, the results of this investigation can be summarised, as follows:

- Biodiesel blends show higher in-cylinder peak pressure than diesel, irrespective of the engine speed. At full load and 2400 rpm speed, the maximum CPs of PSO10, PSO20, SFO10 and SFO20 were found to be 0.82%, 2.4%, 0.17%, and 0.99%, higher than diesel.
- The maximum HRRs at 2400 rpm of PSO10, PSO20, SFO10 and SFO20 were found to be 4.1%, 5.7%, 11.1 % and 11.8% lower than diesel due to lower ignition delay and lower calorific values of the biodiesels.
- Biodiesel blends have a shorter ignition delay period compared with diesel.
- Both PSO and SFO biodiesel blends burnt slightly faster than diesel. PSO20 biodiesel shows faster combustion than diesel by 11.2% and 7.9% at 1400 rpm and 2400 rpm respectively. Whereas, SFO20 biodiesel shows a faster combustion than diesel by 5.2% and 1.6 %, at 1400 rpm and 2400 rpm respectively.

Based on this study, it is concluded that both PSO and SFO biodiesel blends can be the potential alternative fuel for agricultural diesel engines. Amongst the two biodiesels tested, the PSO blends performed better than those of SFO blends in all combustion characteristics.

REFERENCES

[1] Anwar, M., M.G. Rasul, and N. Ashwath. Optimization of biodiesel production process from papaya (Carica papaya) seed oil. in 2017 IEEE 7th International Conference on Power and Energy Systems (ICPES). 2017.

[2] Nair, J.N., A.K. Kaviti, and A.K. Daram, Analysis of performance and emission on compression ignition engine fuelled with blends of Neem biodiesel. Egyptian Journal of Petroleum, 2017. 26(4): p. 927-931.

[3] Anwar, M., M.G. Rasul, and N. Ashwath, Production optimization and quality assessment of papaya (Carica papaya) biodiesel with response surface methodology. Energy Conversion and Management, 2018. 156: p. 103-112.

[4] Anwar, M., M. Rasul, N. Ashwath, and M. Rahman, Optimisation of Second-Generation Biodiesel Production from Australian Native Stone Fruit Oil Using Response Surface Method. Energies, 2018. 11(10): p. 2566.

[5] Malacrida, C.R., M. Kimura, and N. Jorge, Characterization of a high oleic oil extracted from papaya (Carica papaya L.) seeds. Food Science and Technology, 2011. 31: p. 929-934.

[6] Syed H.M, K.S.P., Jadhav B. A and Salve R.V, Extraction and characterization of papaya seed oil Elixir Agriculture, 2011. 37A: p. 4102-4105.

[7] Puangsri T, Abdulkarim SM, Ghazali HM., Properties of Carica papaya L. (papaya) seed oil following extractions using solvent and aqueous enzymatic methods. Journal of Food Lipids, 2004. 12: p. 62-76.

[8] Agunbiade FO, Adewole TA., Methanolysis of Carica papaya Seed Oil for Production of Biodiesel. Journal of Fuels, 2014. 2014: p. 6.

[9] Sivasubramanian, H., Performance and emission characteristics of papaya seed oil methyl ester–n-butanol–diesel blends on a stationary direct-injection CI engine. Biofuels, 2017: p. 1-10.

[10] Asokan, M.A., S. Senthur prabu, S. Kamesh, and W. Khan, Performance, combustion and emission characteristics of diesel engine fuelled with papaya and watermelon seed oil bio-diesel/diesel blends. Energy, 2018. 145: p. 238-245.

[11] Mohan, A., and Sen, S.S.S., Emission Analysis Of The Biodiesel From Papaya And Chicken Blends. International Journal of Informative & Futuristic Research, 2015. 2(7): p. 6.

[12] Prabhakaran, P.; Saravanan, C.G.; Aalam, C.S., Effects of Papaya Methyl Ester on DI Diesel Engine Combustion, Emission and Performance Characteristics. International Research Journal of Engineering and Technology (IRJET), 2016. 3(2).

[13] Sundar Raj, C., and Karthikayan, M., Effect of additive on the performance, emission and combustion characteristics of a diesel engine run by diesel-papaya methyl ester blends. Int. J. Chem. Sci, 2016. 14(4): p. 2823-2834.

[14] Gumus, M. and S. Kasifoglu, Performance and emission evaluation of a compression ignition engine using a biodiesel (apricot seed kernel oil methyl ester) and its blends with diesel fuel. Biomass and Bioenergy, 2010. 34(1): p. 134-139.

[15] Fan, S., T. Liang, H. Yu, Q. Bi, G. Li, and L. Wang, Kernel characteristics, oil contents, fatty acid compositions and biodiesel properties in developing Siberian apricot (Prunus sibirica L.) seeds. Industrial Crops and Products, 2016. 89: p. 195-199.

[16] Wang, L., Properties of Manchurian apricot (Prunus mandshurica Skv.) and Siberian apricot (Prunus sibirica L.) seed kernel oils and evaluation as biodiesel feedstocks. Industrial Crops and Products, 2013. 50: p. 838-843.

[17] Ullah, F., A. Nosheen, I. Hussain, and A. Bano, Base catalyzed transesterification of wild apricot kernel oil for biodiesel production. African Journal of Biotechnology, 2009. 8(14): p. 3309-3313.

[18] Yadav, A.K., A. Pal, and A.M. Dubey, Experimental Studies on Utilization of Prunus armeniaca L. (Wild Apricot) Biodiesel as an Alternative Fuel for CI Engine. Waste and Biomass Valorization, 2017.

[19] Fadhil, A.B., Evaluation of apricot (Prunus armeniaca L.) seed kernel as a potential feedstock for the production of liquid bio-fuels and activated carbons. Energy Conversion and Management, 2017. 133: p. 307-317.

[20] Kumar, S., R. Kumar, and M. Kumar, Experimental investigations of oxidation stability of biodiesel produced from Prunus armeniaca oil (apricot oil) and effect of various antioxidants on stability, engine performance and emissions. Fuel, 2018. 216(Supplement C): p. 861-869.

[21] Anwar, M., M. Rasul, and N. Ashwath, A Systematic Multivariate Analysis of Carica papaya Biodiesel Blends and Their Interactive Effect on Performance. Energies, 2018. 11(11): p. 2931.

[22] Heywood, J.B., Internal combustion engine fundamentals. 1988: New York : McGraw-Hill, [1988] ©1988.

[23] Rahman, M.M., M.G. Rasul, N.M.S. Hassan, A.K. Azad, and M.N. Uddin, Effect of small proportion of butanol additive on the performance, emission, and combustion of Australian native first- and second-generation biodiesel in a diesel engine. Environmental science and pollution research international, 2017. 24(28): p. 22402-22413.

[24] Patel, C., K. Chandra, J. Hwang, R.A. Agarwal, N. Gupta, C. Bae, T. Gupta, and A.K. Agarwal, Comparative compression ignition engine performance, combustion, and emission characteristics, and trace metals in particulates from Waste cooking oil, Jatropha and Karanja oil derived biodiesels. Fuel, 2019. 236: p. 1366-1376.

[25] Dhar, A. and A.K. Agarwal, Performance, emissions and combustion characteristics of Karanja biodiesel in a transportation engine. Fuel, 2014. 119: p. 70-80.

[26] Dhar, A., R. Kevin, and A.K. Agarwal, Production of biodiesel from high-FFA neem oil and its performance, emission and combustion characterization in a single cylinder DICI engine. Fuel Processing Technology, 2012. 97: p. 118-129.

[27] Mahmudul, H.M., F.Y. Hagos, R. Mamat, A.A. Abdullah, and O.I. Awad, Experimental investigation of the impact of using alcohol-biodiesel-diesel blending fuel on combustion of single cylinder CI engine. IOP Conference Series: Materials Science and Engineering, 2016. 160: p. 012038.

[28] Datta, A. and B.K. Mandal, Engine performance, combustion and emission characteristics of a compression ignition engine operating on different biodiesel-alcohol blends. Energy, 2017. 125: p. 470-483.

[29] Can, Ö., Combustion characteristics, performance and exhaust emissions of a diesel engine fueled with a waste cooking oil biodiesel mixture. Energy Conversion and Management, 2014. 87: p. 676-686.

{this page is intentionally left blank}

Declaration of Co-authorship and Contribution

Research Division

CHAPTER 8: Synergistic Effects of Binary and Ternary Biodiesel Blends

Title of the paper	The synergistic effects of oxygenated additives on papaya biodiesel binary and ternary blends
Full bibliographic reference	Anwar, M., M.G. Rasul, and N. Ashwath, The synergistic effects of oxygenated additives on papaya biodiesel binary and ternary blends. Fuel, 2019. 256: p. 115980. https://www.sciencedirect.com/science/article/pii/S0016236119313328
Status	Published

Nature of Candidate's Contribution, including percentage of total
I was responsible for designed the study, performed the experiments, data analysis and drafted the manuscript. [80%]

Nature of all Co-Authors' Contributions, including percentage of total
My co-authors, Prof. Mohammad Rasul, and A/Professor Nanjappa Ashwath, were designed the experimentation, reviewed, revised and improved the manuscript. [20%]

Has this paper been submitted for an award by another research degree candidate (Co- Author), either at CQUniversity or elsewhere? (if yes, give full details)
No

Candidate's Declaration

I declare that the publication above meets the requirements to be included in the thesis as outlined in the Research Higher Degree Theses Policy and Procedure.

Mohammad Anwar

Fuel 256 (2019) 115980

Contents lists available at ScienceDirect

Fuel

journal homepage: www.elsevier.com/locate/fuel

Full Length Article

The synergistic effects of oxygenated additives on papaya biodiesel binary and ternary blends

Mohammad Anwar[a,*], Mohammad G. Rasul[a], Nanjappa Ashwath[b]

[a] Central Queensland University, School of Engineering and Technology, North Rockhampton, Queensland 4702, Australia
[b] Central Queensland University, School of Health, Medical and Applied Sciences, North Rockhampton, Queensland 4702, Australia

GRAPHICAL ABSTRACTAT:

Experimental setup for engine testing with PSO binary and ternary blends.

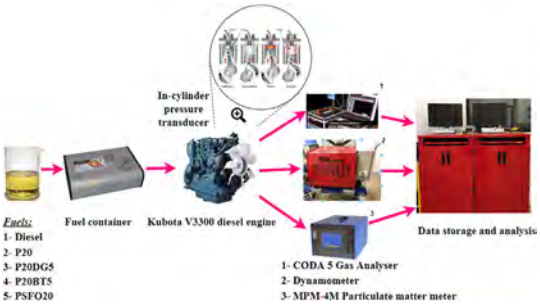

ARTICLE INFO

Keywords:
Papaya carica
Apricot
Binary
Diglyme
Butanol
Ternary
Additive
Biodiesel

ABSTRACT

In this study, engine performance, exhaust emissions and combustion behaviour of a four-cylinder, four stroke indirect injection diesel engine was tested using papaya seed oil (PSO) biodiesel binary and ternary blends. The results were compared with those of diesel fuel under a range of engine speeds from 1200 rpm to 2400 rpm, and for different engine load conditions of 25% to 100%. The PSO biodiesel of 20% v/v with 80% v/v diesel was considered as the binary blend (P20). Two ternary fuel blends of 5% v/v of oxygenated additives (diglyme and n-butanol) with P20 biodiesel and 75% v/v of diesel which are referred to as P20DG5 (diglyme) and P20BT5 (n-butanol). Another ternary blend made of 10% v/v of PSO biodiesel with 80% v/v diesel and 10% v/v stone fruit oil (SFO) biodiesel referred to as PSFO20 is used to compare the overall results. The average brake specific fuel consumption (BSFC) value and brake thermal efficiency (BTE) of P20DG5 was found to be 0.50% lower and 3.30% higher than diesel respectively. The P20DG5 produced about 0.64% less NO_x emissions compared with diesel and had the shortest ignition delay period. As a conclusion, P20DG5 proved to be an excellent choice for mitigating the environmental problems without compromising the engine performance and enhanced better combustion. The P20DG5 ternary blend is recommended to use in diesel engine without any need for physical modification.

1. Introduction

The demand for petroleum-derived fuels (oils, natural gas, and coal) is increasing rapidly due to their extensive dependence, access, and affordability. These petro fuels play a prominent role in the manufacturing, transportation and electricity supply sectors. Oil

* Corresponding author.
E-mail address: m.anwar@cqu.edu.au (M. Anwar).

https://doi.org/10.1016/j.fuel.2019.115980
Received 17 July 2019; Received in revised form 5 August 2019; Accepted 6 August 2019

consumption in 2018 grew by an average of 1.40 million barrels per day or 1.50% that forced the production of a global total of 2.20 million barrels per day, i.e., a 2.40% annual growth in 2018 [1]. A consistent and sustainable supply of petro fuel is essential to any nation's development. However, due to the severe political unrest in the crude oil producing countries and prolonged economic embargoes on certain counties, the world is facing extreme challenges to keep the fuel supply chain economically sustainable. World leaders, politicians and policy-makers are giving emphasis not only to solving these geopolitical situations but also pushing hard for research and development for finding alternative fuel sources that are locally available, cost-effective and sustainable.

Again, the increasing demand for petro fuel not only causes rising prices but its growing exhaust emissions have adverse effects on environmental problems such as glacial melting, loss of biodiversity, climate change, and global warming [2–4]. A study has shown that, by 2030, the greenhouse gas (GHG) emissions would increase by 39% if no actions are taken now [5]. Norhasyima et al. [6] mentioned that the average global temperature would increase by 2 °C by 2050 if the CO_2 emissions are not controlled by 50%. As the transportation and power generation sectors are the major offenders for emitting higher GHG emissions, there is a need for finding alternative fuel sources that can mitigate environmental concerns. Since 2010, research studies on renewable energy sources are growing rapidly with the mission of reducing air pollution as well as dependency on petro fuel [7,8]. Biodiesel is a popular renewable energy source that can be used as an alternative fuel in diesel engines. Researchers show that biodiesel is a much cleaner fuel than diesel and has excellent environmental-friendly attributes [9–14].

Biodiesel is generally produced from vegetable oils, recycled/waste cooking oils and animal fats. Biodiesel is a renewable, non-explosive, biodegradable, non-flammable and non-toxic fuel that has similar combustion characteristics to diesel fuel [15–22]. It can be mixed with diesel as a blend or fed directly into the diesel engine. However, the lower calorific value, higher viscosity, density and pour point, poor cold flow property, lower volatility, higher brake specific fuel consumption (BSFC), lower brake thermal efficiency (BTE), and its generation of higher NO_x, CO_2 emissions and EGT limit the use of biodiesel over diesel fuel [2,23–25]. Research works show that incorporating various additives and alcohols in the biodiesel blend can reduce engine exhaust emissions as well as overcome some of the above-mentioned limitations [26–29]. Table 1 shows the performance parameters and emissions characteristics of a selection of non-edible biodiesel ternary blends with various additives and alcohols.

There have been a few research publications on the binary blends of PSO biodiesel and these reported slight reductions of NO_x and CO emissions [48–50]. However, no literature is available on the engine performance and emissions characteristics of ternary blends of PSO biodiesel using any alcohol or additive. Butan-1-ol, i.e., n-butyl alcohol, which is popularly known as n-butanol has a higher cetane number compared with other alcohols like ethanol and methanol. It is a colourless and clear alcohol that can be better used as an oxygenated additive due to its high miscibility with diesel and less corrosion effect of engine particles [2,51,52]. Butanol has a higher calorific value and lower solubility in water than other alcohols like ethanol and methanol [53]. Butanol has a lower latent heat of vaporisation compared with ethanol and methanol that minimises the percentage of wasted energy. Moreover, the ignition temperature of butanol is lower than both ethanol and methanol. Researchers have shown that butanol can be added to minimise exhaust emissions such as CO, HC and soot emissions compared with other alcohols [54,55].

Bis (2-methoxyethyl) ether, i.e., Diethylene glycol dimethyl ether, commonly known as diglyme, is a clear, colourless oxygenated liquid with an ethereal odour. Diglyme is miscible with water, alcohols, diethyl ether and hydrocarbon solvents. Researchers have shown that diglyme could be effective when used as oxygenated additives due to its combustion performance and soot reduction [56,57]. Diglyme has a higher cetane number that affects the overall engine performance and emissions characteristics. Again, a higher cetane number can improve the ignition quality and reduce the ignition delay, resulting in reducing the fraction of injected fuel that is burnt under premixed conditions [58].

No researchers other than Asokan et al. [59] have made a PSO ternary blend by mixing PSO biodiesel (10% vol) with watermelon biodiesel (10% vol). They reported that the emissions of CO, HC, and smoke were 27.30%, 23.80%, and 8.30% less than for diesel. In another study, Anwar et al. [60] have compared PSO biodiesel blends with SFO biodiesel and found SFO blends have better engine performance while emitting higher exhaust emissions. A 10% biodiesel mix of each PSO and SFO biodiesel with diesel can be an interesting ternary blend to analyse. To the best knowledge of the authors, no other literature has yet been initiated by any researcher to investigate the effects of PSO-SFO-diesel (PSFO20) ternary blends on a diesel engine.

Over the last decade, researchers have been trying tirelessly to improve engine performance, combustion efficiency and exhaust emissions by adding various alcohols and additives in their biodiesel blends. Fig. 1(i) shows that more than 300 journal articles/year based on biodiesel-ethanol ternary blends were published for the last 10 years, noting that biodiesel-butanol ternary blends are comparatively less explored. Biodiesel with additives have also been gaining in popularity over the last few years. Various nanoparticles additives were used in the biodiesel blends, whereas diglyme oxygenated additives are still quite new to explore. Fig. 1(ii) presents the publication status of biodiesel-additive ternary blends. Since there is no literature found on the engine performance, emissions analysis and combustion characteristics of ternary blends of PSO biodiesel using any alcohol or additive. In this present study, the effects of papaya seed oil (PSO) biodiesel with one binary blend (PSO biodiesel-diesel) and three ternary blends (PSO biodiesel-diesel-butanol, PSO biodiesel-diesel-diglyme, PSO biodiesel-diesel-SFO biodiesel) on a diesel engine are critically evaluated experimentally.

2. Materials and methods

2.1. Biodiesel preparation

The waste seed oil of papaya (*Carica papaya*) was purchased from a local supplier in Eumundi, Queensland, Australia. Biodiesel was produced from papaya seed oil (PSO) via a single stage transesterification process over a reflux condenser with a thermocouple fitted on a small-scale three-neck laboratory reactor. Methanol (99.90% purity), potassium hydroxide (KOH pellets, 99% purity), diglyme and n-butanol (99.90% purity) were used in this study. All chemicals were analytical reagent grade (AR) as procured from the School of Engineering and Technology of Central Queensland University, Rockhampton, Australia. Anwar et al. [10] have shown the optimisation of the PSO biodiesel production process (96.50% yield) through a single stage transesterification using KOH catalyst and methanol with an oil molar ratio of 10:1. The reference diesel was purchased from a local Caltex fuel station in Rockhampton.

2.2. Binary and ternary blend preparation for experimental investigation

The experimental investigation was carried out using five fuel samples including the reference diesel and papaya biodiesel blends (binary and ternary). The binary blend was made of 20% vol of PSO biodiesel with 80% vol. of diesel and referred to here as P20. Ternary blends were made with P20 with two oxygenated additives (diglyme and butanol) of 5% vol each and 75% vol of diesel denoted as P20DG5 and P20BT5 respectively. Another ternary blend was prepared using 10% vol of PSO biodiesel with 10% vol of SFO biodiesel and 80% vol diesel, referred to as PSFO20. A magnetic stirrer was used to agitate the

Table 1
Recent research publications on non-edible biodiesel ternary blends with various additives and alcohols.

Biodiesel blends (vol. %)	Additives/Alcohols (vol. %)	Performance parameters	Exhaust emissions	Ref.
Jatropha (10–20%) + Diesel (50–70%)	- Ethanol (20–40%)	BSFC▲,BTE▲	NO_x▲ and CO▼	[30]
Castor (5%) + Diesel (80%)	- Ethanol (15%)	–	NO_x▼ and CO▲	[31]
Calophyllum inophyllum (10–20%) + Diesel (50%)	- Decanol (30–40%) - Hexanol (30–40%)	BSFC▼,BTE▲	NO_x▼ and CO▼	[32]
Calophyllum inophyllum (10–40%) + Diesel (50%)	- Hexanol (10–40%)	BSFC▼,BTE▲	NO_x▲ and CO_2▲	[33]
Calophyllum inophyllum (10–20%) + Diesel (50%)	- Decanol (10–40%)	BSFC▼,BTE▲	NO_x▲ and CO▼	[34]
Calophyllum inophyllum (40–60%)	- 1-pentanol (40–60%) - 1-butanol (40–60%)	BSFC▲,BTE▼	NO_x▼, HC▼ and CO▼	[35]
Calophyllum inophyllum (20%) + Diesel (80%)	- N, N-diphenyl-1, 4-phenylenediamine (1000 ppm) - N-phenyl-a, 4-phenylenediamine (1000 ppm) - 2-ethylhexyl nitrate (1000 ppm)	BP▲, BTE▲, BSFC▼	NO_x▼, HC▲ and CO ▲	[36]
Cottonseed (20%) + Diesel (70%)	- Butanol (10%) - Ethanol (10%) - Methanol (10%)	BSFC▲	NO_x▲ and CO▼	[17]
Cottonseed (5%) + Diesel (95%)	- Ethanol (20%)	BP▼, BSFC▲	NO_x▲ and CO▼	[37]
Safflower biodiesel (40–45%) + Diesel (40–45%)	- Butanol (5–20%)	BTE▲,BSFC▲	NO_x▲ and CO▼	[38]
Jojoba (20–50%) + Diesel (40–70%)	- n-butanol (10%)		NO_x▼, HC▼ and CO▼	[39]
Waste cooking oil (40–45%) + Diesel (40–45%)	- Butanol (10–20%)	No significant difference	NO_x▲	[40]
Waste cooking oil (20–40%) + Diesel (60–80%)	- Butylated hydroxytoluene (BHT) (2000 ppm) - n-butanol (20%)	BTE▼, BSFC▲	- NO_x▲, EGT▼ and CO▼ - NO_x▲, EGT▲ and CO▼	[41]
Waste cooking oil (20–100%) + Diesel	- Titanium dioxide (0.1689 g/2L B20) - n-butanol (10%)	BP▲, T▲, BSFC▼, CP▲, HRR▲	- NO_x▲ and CO_2▲ - NO_x▼ and CO_2▲	[2]
Waste cooking oil (85–100%)	- Ethanol (5–15%) - Butanol (5–15%)	BP▼, BTE▼, BSFC▲, HRR▲	NO_x▼, HC ▲ and CO ▲	[18]
Azadirachta indica (100%)	- Ethanol (5–20%) - Dimethyl carbonate (5–20%) - Diglyme (5–20%)	BTE ▲, CP ▼BTE ▲, CP ▼BTE ▲, CP ▲	- NO_x▼, HC ▲ and CO▲ - NO_x▼, HC ▲ and CO▲ - NO_x▼, HC ▼ and CO▼	[42]
Rubber seed oil (50%) + babassu oil (50%)	- Diglyme (20%)	BTE ▲	NO_x▲, HC▼ and CO▼	[43]
Karanja biodiesel (80–100%)	- n-butanol (5–20%)	BTE▼, CP▼	NO_x▼ and CO▼	[19]
Microalgae biodiesel (20%) + Diesel (60–70%)	- Butanol (10–20%)	BP▼, T▼	NO_x▼ and CO▼	[44]
Alexandrian laurel oil (15–20%) + Diesel (60–70%)	- Pentanol (15–20%) - n-butanol (15–20%)	BP▲, BSFC▼	NO_x▲, HC▼ and CO▼	[45]
Tall oil biodiesel (60%) + Diesel (40%)	- MgO (4, 8, 12 µmol/l) - MoO_2 (4, 8, 12 µmol/l)	No significant difference	NO_x▼, HC▼ and CO▼	[46]
Mango seed oil biodiesel (20–100%) + Diesel (0–80%)	- Pyridoxine Hydro Chloride (100, 250, 500 and 1000 ppm) - Tert-butylhydroquinone (100, 250, 500 and 1000 ppm) - Di-Ethyl Amine (100, 250, 500 and 1000 ppm)	BTE▼, BSFC▲	NO_x▼, HC ▲ and CO▲	[47]

where ▲ represents increase and ▼ decrease.

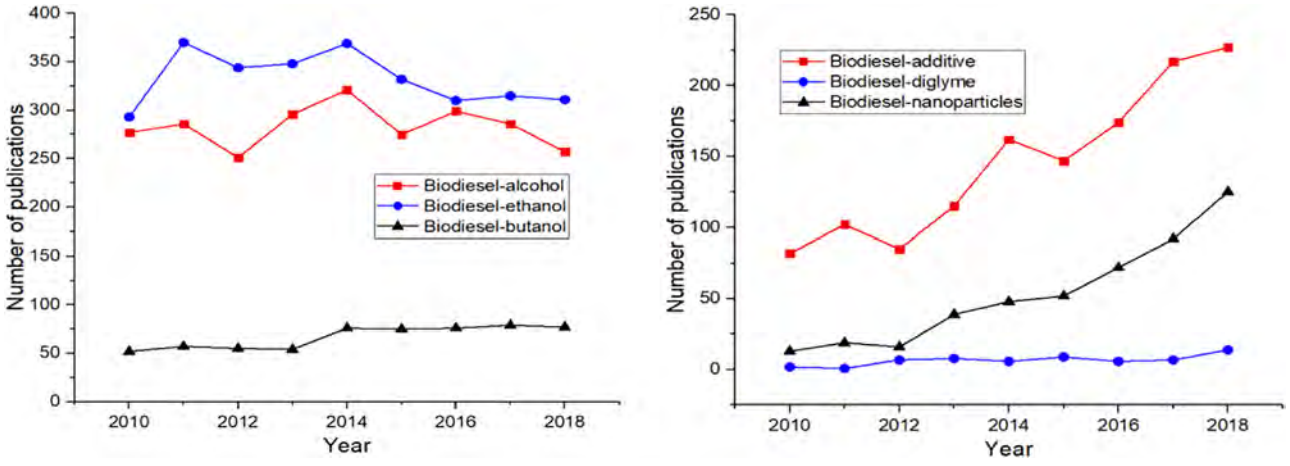

(i) Publications based on biodiesel and alcohols

(ii) Publications based on biodiesel and additives

Fig. 1. Recent publications based on ternary blends of biodiesel using alcohols and additives. (Scopus database using < biodiesel-alcohol, biodiesel-additive, etc. > as keywords).

Table 2
Equipment used for measuring properties of prepared blends in this study.

Fuel Properties	Equipment	Standard applied	Accuracy
Kinematic viscosity	NVB classic (Normalab, France)	ASTM D445	± 0.01 mm^2/s
Density	DM40 LiquiPhysics^{TM} density meter (Mettler Toledo, Switzerland)	ASTM D1298	± 0.1 kg/m^3
Flash point	NPM 440 Pensky-Martens flash point tester (Normalab, France)	ASTM D93	± 0.1 °C
Acid value	Automation titration Rondo 20 (Mettler Toledo, Switzerland)	ASTM D664	± 0.001 mg KOH/g
Calorific value	6100EF semi-auto bomb calorimeter (Perr, USA)	ASTM D240	± 0.001 MJ/kg
Oxidation stability at 110 °C	873 Rancimat (Metrohm, Switzerland)	ASTM D2274	± 0.01 h

binary and ternary blends at 600 rpm for 60 min. No phase change was observed from any blends. Finally, all blends were stored in a dark coloured gas bottle with screw caps for further characterisation.

2.3. Property of the prepared blends

The equipment used in this study to measure the properties of PSO blends and the relevant standard applied are shown in Table 2. The fatty acid composition was determined using a gas chromatograph in accordance with EN14103.

A few literatures mentioned about the physico-chemical properties of PSO biodiesel. The density of PSO biodiesel ranges from 880.20-920.30 kg/m^3, kinematic viscosity 4.52–36.47 mm^2/s, flash point 147–295 °C, calorific value 38.97–42.46 MJ/kg, cetane number 53–63.75 [48,49,59,61]. Table 3 shows the physico-chemical properties of PSO biodiesel and its blends, SFO biodiesel, diesel, diglyme and butanol used in this experiment. Diglyme has the highest cetane number of 126 whereas butanol was found to be only 25. However, the density of diglyme was the highest of 945 kg/m^3 and butanol was recorded as 808 kg/m^3. On the other hand, the viscosities of diglyme and butanol were recorded as 1.09 and 2.63 mm^2/s respectively. The flash point of diglyme (67 °C) was closely matched with diesel (68.50 °C) and nearly double that of butanol (35 °C). The calorific value of the diglyme was recorded as the lowest (24.50 MJ/kg) among all the other additives in this experiment. All the binary and ternary blends were found to be homogenous and no phase separation was observed even after 48 h.

2.4. Experimental setup

All experiments were carried out on a four stroke, four cylinder naturally aspirated diesel engine. Detailed technical specifications and the schematic diagram of the engine are presented in Table 4 and Fig. 2 respectively. Diesel with four alternative PSO biodiesel blends mentioned above, were tested at different engine load (25–100%) conditions by varying engine speeds from 1200 rpm to 2400 rpm, at intervals of 200 rpm. The engine was coupled with an eddy current dynamometer. A control system was available for adjusting the engine speeds and engine loads. The engine exhaust gas emissions of NO_x (ppm), HC (ppm), CO (vol %) and CO_2 (vol %) were measured at the different engine loads with a CODA 5 gas analyser. A non-dispersive infrared (NDIR) sensor in the gas analyser was used for measuring exhaust gas emissions. PM (mg/m^3) emissions were measured with a MPM-4M particulate matter (PM) meter. A piezoelectric pressure transducer and crank angle encoder were used to monitor the combustion characteristics. At the beginning of each experiment, the engine was operated with the tested fuel for sufficient time to ensure total clean out of the remaining tested fuel (from previous experiment) from the engine fuel systems. Every set of data was repeated three times to avoid any possible error. The engine was flushed with diesel soon after each experiment was conducted.

Table 4
Test engine specifications.

Items	Specifications
Model	Kubota V3300, Indirect injection
Type	Vertical, 4 cycle liquid cooled diesel
No. of cylinders	4
Total displacement (L)	3.318
Bore × Stroke (mm)	98 × 110
Combustion type	Spherical type [E-TVCS (Three vortex combustion system)]
Intake system	Naturally aspirated
Rated power output (kW/rpm)	53.90/2600
Rated torque (Nm/rpm)	230/1400
Compression ratio	22.60:1
Fuel injection timing	16° before TDC
Injection pressure (MPa)	13.73
Emissions certification	Tier 2

Experimental error and uncertainty analysis determined the accuracy of the experiment. Errors may occur in several ways such as test planning, reading and observing, instrument selection, condition monitoring, calibration and changes in the experimental environment while the test was conducted. All of the equipment, instruments and sensors were not made and installed by the same manufacturer. Therefore, uncertainty may occur due to random or fixed errors. The technical details of the gas analyser, PM meter and error analysis are shown in Table 5.

3. Performance characteristics

The variations of engine speeds with brake power (BP) for all PSO blends and diesel at full load condition are presented in Fig. 3(i). The BP increased steadily with the increase of engine speeds for all blending conditions. At any given engine speed, diesel had the highest BP value followed by P20DG5, P20BT5, PSFO20 and P20. The average BP values of diesel, P20DG5, P20BT5, PSFO20 and P20 were 39.30, 38.60, 38.10, 38 and 37.30 kW. P20DG5, P20BT5 and PSFO20 had 3.30%, 2.20% and

Table 3
Properties of diesel, diglyme, butanol and blended fuels.

Property	Diesel	Diglyme	Butanol	PSO biodiesel	SFO biodiesel	P20	P20 DG5	P20 BT5	PSFO20
Density (kg/m^3)	827.20	945	808	840	855	829.80	835.70	828.80	831.30
Viscosity at 40 °C (mm^2/s)	3.23	1.09	2.63	3.53	4.26	3.29	3.18	3.26	3.36
Cetane number (CN)	48.00	126	25.00	48.29	50.45	48.06	51.96	46.91	48.27
Calorific value (MJ/kg)	45.30	24.50	33.10	38.49	39.64	43.94	42.90	43.33	44.05
Flash point (°C)	68.50	67.00	35.00	112	105	77.20	77.13	75.53	76.50
Acid value (mg KOH/g)	0.05	–	–	0.42	0.25	0.12	–	–	0.11
Oxidation stability (h)	39.00	–	–	5.61	7.15	32.32	–	–	32.48

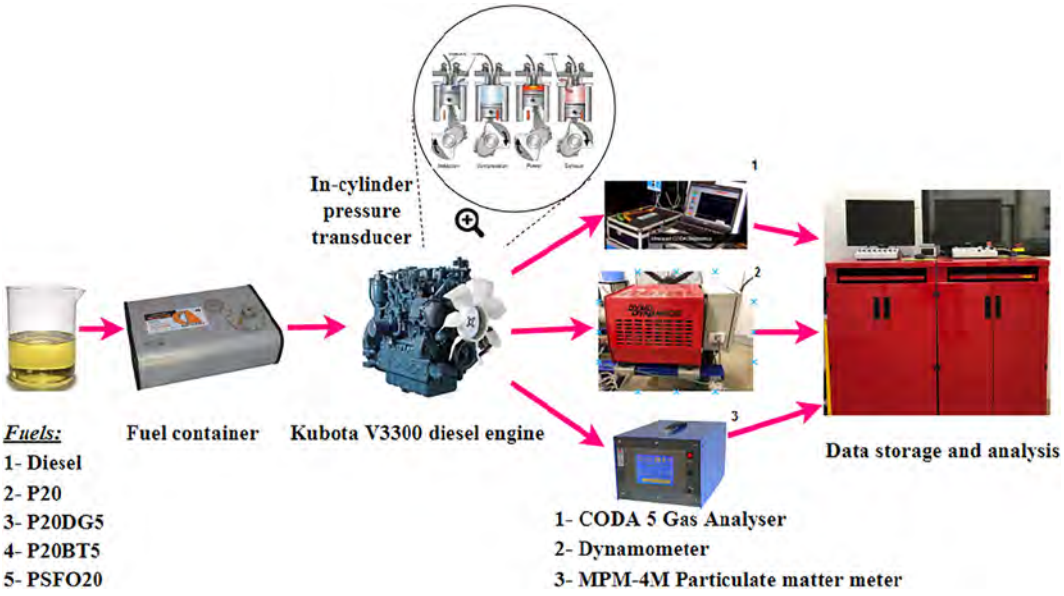

Fig. 2. Experimental setup for engine testing.

Table 5
Uncertainty, range and accuracy of exhaust gas analyser and PM meter.

Exhaust emissions	Measurement		
	Range	Resolution	Accuracy
HC (ppm)	0–30,000	1.00	± 1.00
CO (%)	0–15	0.001	± 0.02
CO_2 (%)	0–20	0.001	± 0.30
NO_x (ppm)	0–5000	1.00	± 1.00
Meter	**Particle size**	**Particle concentration range**	**Resolution**
PM (mg/m^3)	< 100 nm to > 10 μm	0.10 to > 700	± 0.10
Measurements	**Accuracy**	**Relative Uncertainty (%)**	**Average Reading for (diesel)**
BP	± 0.41 kW	0.0105	39.30
BSFC	± 5 g/kWh	0.0195	256.50

1.80% higher BP values than P20. Average BP value reductions for P20DG5, P20BT5, PSFO20 and P20 in comparison with diesel were 1.80%, 2.90%, 3.20%, and 5%. The reduction in BP of P20 biodiesel blend due to its lower calorific values, higher viscosities and higher densities is supported by the literature [55,62,63].

Fig. 3(ii) shows the relationship between the engine torque and variation of engine speeds at full load condition. Torque increased with the increase of engine speed up to 1400 rpm and then decreased continuously until the maximum speed of 2400 rpm for all PSO blends and diesel. The reason behind this is that the Kubota engine has its maximum rated torque recorded at 1400 rpm. A further factor is the mechanical friction loss and lower volumetric efficiency of the engine as supported by researchers [11,62,64]. Torque decreased with the increase of biodiesel content in the blends. As expected, diesel had the highest torque at all engine speeds followed by P20DG5, P20BT5, PSFO20 and P20. The average torque values of P20DG5, P20BT5, PSFO20, P20 and diesel were 205.40, 204.10, 202.50, 199.90 and 207.90 N.m. P20DG5, P20BT5 and PSFO20 had 2.70%, 2.10% and 1.30% higher torque than P20. Average torque value reductions for P20DG5, P20BT5, PSFO20, and P20 in comparison with diesel were 1.20%, 1.80%, 2.60%, and 3.90%. Rahman et al. [55] and Liaquat et al. [64]mentioned that the lower densities and lower viscosities and higher calorific values of the diesel resulted in its higher engine torque.

Fig. 3(iii) shows that BSFC increases with the increase of engine speed. Ong et al. [65] mentioned that friction heat losses occur at higher speeds and combustion deteriorates, resulting in higher BSFC. Other researchers mentioned that the fuel injection system, and fuel density, viscosity and calorific value affect BSFC values [66,67]. Due to the lower calorific value of biodiesel, it was observed to have higher BSFC values as biodiesel needed more fuel for producing the same power as that produced by diesel. Silitonga et al. [68] mentioned that lower kinetic viscosity of biodiesel blend can lead to lower BSFC. Again, both diesel and P20DG5 had the lowest BSFCs at all engine speeds (except for diesel at 2200 rpm) followed by P20BT5, PSFO20 and P20. The average BSFC values of P20DG5, P20BT5, PSFO20, P20 and diesel were 255.30, 264.60, 272.90, 300.50 and 256.50 g/kWh. P20DG5, P20BT5 and PSFO20 had 17.70%, 13.60% and 10.10% lower BSFC values than P20. Again, average BSFC value increases for P20BT5, PSFO20, and P20 in comparison with diesel were 3.10%, 6.40% and 17.10%. However, the average BSFC value of P20DG5 was found to be 0.50% lower than diesel.

The variation in BTE with engine speed for all PSO blends and diesel at full load condition is shown in Fig. 3(iv). BTE decreases with the increase of engine speed over the entire range. Researchers mentioned that, at higher engine speeds, BTE decreases due to lack of sufficient air that caused uneven combustion of fuel [69]. Again, higher BTE depends on higher calorific value, lower density and lower viscosity. Some researchers mentioned that lower viscosity and higher volatility ensures a better air-fuel mixture that resulted in better combustion [65,69]. P20DG5 had the highest BTE at all engine speeds followed by diesel, P20BT5, PSFO20 and P20. The average BTE values of P20DG5, P20BT5, PSFO20, P20 and diesel were 32.4%, 30.60%, 30.20%, 27.20% and 31.30%. P20DG5, P20BT5 and PSFO20 had 15.80%, 11.10% and 9.80% higher BTE values than P20. Again, average BTE value reductions for P20BT5, PSFO20, and P20 in comparison with diesel were 2.30%, 3.60% and 13.10%. However, the average BTE value of P20DG5 was found to be 3.25% higher than diesel.

4. Comparative engine performance analysis of PSO and other ternary biodiesel blends

The comparative analysis of engine performance of diesel and four PSO biodiesel blends on the basis of BP, torque, BSFC and BTE are

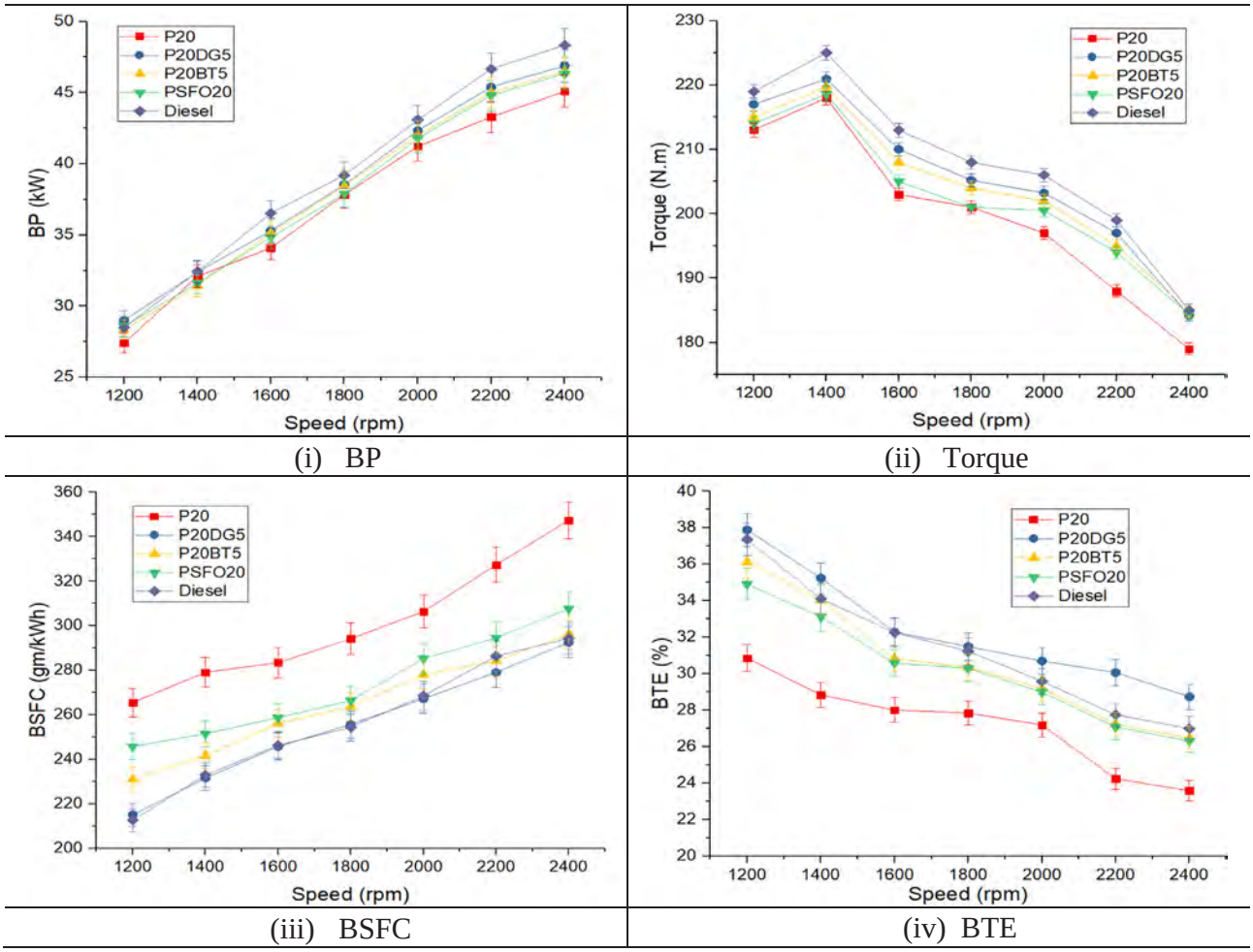

Fig. 3. Variations of engine performance parameters for all PSO biodiesel-diesel-additives blends with respect to engine speed at full load condition.

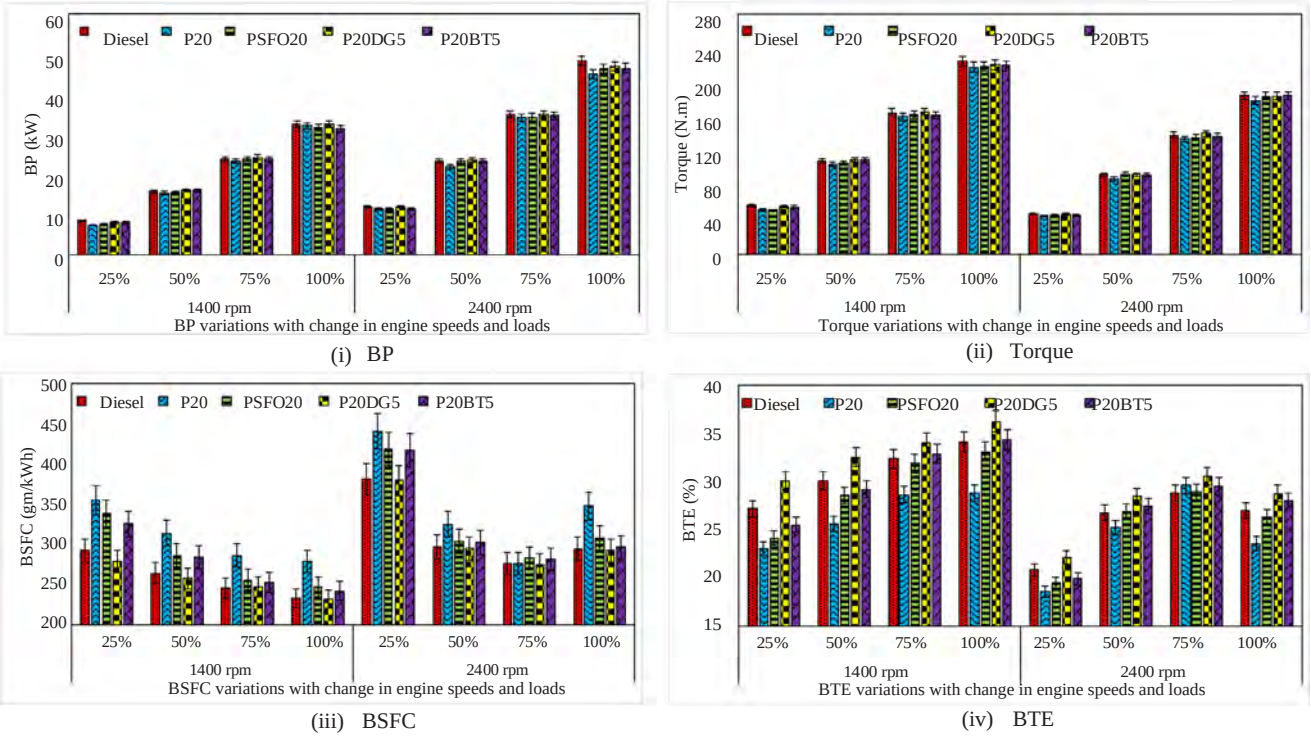

Fig. 4. Variations of engine performance parameters for all PSO biodiesel-diesel-additive blends at different engine loads and speeds.

shown in Fig. 4. Four engine loads (25, 50, 75 and 100%) were varied at two engine speeds (1400 rpm- max. rated torque and 2400 rpm- near max. rated power) to investigate engine performance. Diesel, papaya biodiesel content of 20% vol (P20), papaya biodiesel (P20) with 5% Diglyme additives (P20DG5), papaya biodiesel (P20) with 5% butanol additives (P20BT5), and papaya-stone fruit biodiesel with 20% vol (PSFO20) were used in this analysis.

Fig. 4(i) compares the BP characteristics of PSO biodiesels (P20) with oxygenated additives (DG and BT), PSO-SFO biodiesel blends (PSFO20) and diesel with changing engine loads and speeds. This trend shows an agreement with the results of previous studies about biodiesel brake power [70,71]. For all test samples, BP increased with an increase in engine load. The lower calorific value and higher viscosity of biodiesel can cause uneven combustion which results in lowering the BP value [63,65,72,73]. However, Anwar et al. [11] have found that the viscosity of diesel and PSO biodiesel-diesel blends were close. Thus, it can be concluded that the difference in higher calorific values of PSO blends and diesel would have contributed to the the variations in BP. At all load conditions and speeds, diesel had a higher BP followed by P20DG5, P20BT5, PSFO20 and P20.

The variations in torque with four engine loads for PSO biodiesel blends and diesel at 1400 rpm and 2400 rpm are shown in Fig. 4(ii). As expected, the torque increased with an increase in engine load condition and speed. At all load conditions and speeds, diesel produced higher torque followed by P20DG5, P20BT5, PSFO20 and P20.

Brake specific fuel consumption (BSFC) measures the amount of fuel consumed to generate one unit of power. It is the ratio of fuel flow rate and brake power. Many factors influence BSFC values, such as the fuel injection system, fuel density, calorific value and viscosity [66]. The variations between BSFC and different engine loads at 1400 and 2400 rpm for all PSO biodiesel blends and diesel are shown in Fig. 4(iii). P20DG5 had the lowest BSFC in comparison with P20BT5, PSFO20, P20 and diesel. The BSFC values decreased with an increase in engine load at 1400 rpm for all tested fuels. However, at full load condition and 2400 rpm, a slight increase in BSFC was observed. Since biodiesel has a lower heating value compared to diesel, the engine requires more fuel for producing the same amount of power leading to increased BSFC for PSO biodiesel blends. Asokan et al. [59] and Yatish et al. [74] have also showed an increase in BSFC for biodiesel blends.

BTE indicates how efficiently the combustion heat is converted into mechanical work. A higher BTE is expected from any fuel that depends on some specific fuel properties such as a higher heating value with lower density and viscosity. Fig. 4(iv) shows the variation in BTE with changing engine loads for PSO biodiesel and its blends and diesel at 1400 rpm and 2400 rpm. It can be seen that the BTE increased with engine loads. An et al. [75] mentioned that the fuel injection pressure reached its maximum value at full load condition and caused a negligible effect of viscosity leading to better combustion eventually leading to increased BTE. The lower heating values and higher fuel consumptions of both P20 and PSFO20 resulted in lower BTE values of 6.20% and 1.70% respectively, as compared to diesel. Other researchers have also found reduced BTE when the biodiesel blends were tested against diesel fuel [59,74]. In contrast, using diglyme and butanol additives in the P20 biodiesel, the BTE values of P20DG5 and P20BT5 significantly improved, and were found to be 6.30% and 0.90% higher than those of diesel, respectively.

The overall scenarios of engine performance of PSO biodiesel blends and diesel at full engine loading conditions with different speeds are presented in Table 6. At 100% full load condition and 2400 rpm, the minimum and maximum increases in BP were found to be 0.14% for P20DG5 and 6.70% for P20, and for torque were 1.80% for P20DG5 and 3.20% for P20 respectively, as compared to diesel (D). However, the BSFC of diesel was slightly higher than that of P20DG5 by 0.60% to 0.80%. Again, the P20DG5 had the highest BTE compared to diesel by 3.30% to 6.40%.

Table 6
Overall performance of biodiesel (BD) blends over diesel at full load on different engine speeds.

Performance parameter	Full load (100%)		Comparison between biodiesel (BD) with diesel (D)	
	1400 rpm	2400 rpm	Min. ▲/▼ (%)	Max.▲/▼ (%)
BP	D > BD	D > BD	P20DG5 (▼0.14%)	P20 (▼6.70%)
Torque	D > BD	D > BD	P20DG5 (▼1.80%)	P20 (▼3.20%)
BSFC	P20DG5 < D	P20DG5 < D	D (▲0.60%)	D (▲0.80%)
BTE	P20DG5 > D	P20DG5 > D	D (▼3.30%)	D (▼6.40%)

where ▲ increase and ▼ = decrease.

5. Exhaust emissions parameters

Fig. 5(i) shows variations in hydrocarbon (HC) emissions of the four PSO biodiesel blends and diesel over the entire range of engine speeds ranging from 1200 rpm to 2400 rpm at intervals of 200 rpm. HC emissions decrease with the increase in engine speeds. At low engine speed, HC emissions were found to be higher due to higher fuel density and viscosity that affect fuel atomisation as well as ignition in the combustion chamber [76]. Fuel trapped into the crevice volume of the combustion chamber may also have resulted in higher HC emissions [77]. The average HC values were recorded for P20DG5, P20BT5, PSFO20, P20 and diesel were 15.10, 15.60, 16.70, 15.90 and 22.40 ppm. The average reduction in HC for P20DG5, P20BT5, PSFO20 and P20 as compared to diesel were 32.40%, 30.40%, 25.40% and 28.80%, respectively. With the inclusion of additives in P20 blends, HC emissions reduced noticeably by 5.40% and 2.30% for P20DG5 and P20BT5 respectively. Both oxygenated additives enhanced the fuel atomisation and improved spray formation leading to better combustion and reduced HC emissions [18].

Several factors contribute to an increase in carbon monoxide (CO) emissions. These include incomplete combustion, excessively lean blend of air-fuel ratio, rich blend of air-fuel ratio and insufficient or low air-fuel ratio in rich combustion mixture [78]. Other factors that affect CO emissions are air-fuel ratio, engine speed, injection timing, pressure, and fuel types [72,78,79]. Fig. 5(ii) shows variations in CO emissions by PSO biodiesel blends and diesel. At 100% full load, the CO emissions dropped significantly with an increase in the speed from 1200 rpm. These values were found to be the lowest at 2400 rpm. It is known that the biodiesel contains 12% more oxygen than diesel fuel [80]. Incorporation of oxygenated additives such as diglyme and butanol into biodiesel can increase the oxygen content of the blend significantly. The higher the O_2 content (i.e., biodiesel binary blends-P20, ternary blend-PSFO20 and ternary blends with additives-P20DG5 and P20BT5), the lower the CO emissions. Research shows that higher O_2 content can improve combustion leading to lower CO emission [81–83]. CO emissions from biodiesel blends are lower than those in diesel engines due to their higher oxidation stability as compared with diesel [84]. The average CO recorded for P20DG5, P20BT5, PSFO20, P20 and diesel were 0.08%, 0.10%, 0.11%, 0.14% and 0.20%, respectively. The average reduction in CO emission for P20DG5, P20BT5, PSFO20 and P20, as compared to diesel were 61%, 52%, 46% and 32%. With the inclusion of additives in P20 blends, the CO emissions reduced significantly by 75% and 42% for P20DG5 and P20BT5, respectively.

The variations in nitrogen oxide (NO_x) emissions with changing engine speed for the PSO biodiesels and diesel at full load condition are shown in Fig. 5(iii). The NO_x levels increase with the increase of speeds for all fuels due to higher combustion temperatures and stoichiometry of the fuel mixtures [85]. Factors that affect NO_x emissions are O_2 content, in-cylinder temperature and the residence time [74]. Higher engine loads with a high air-fuel ratio produces higher gas temperatures

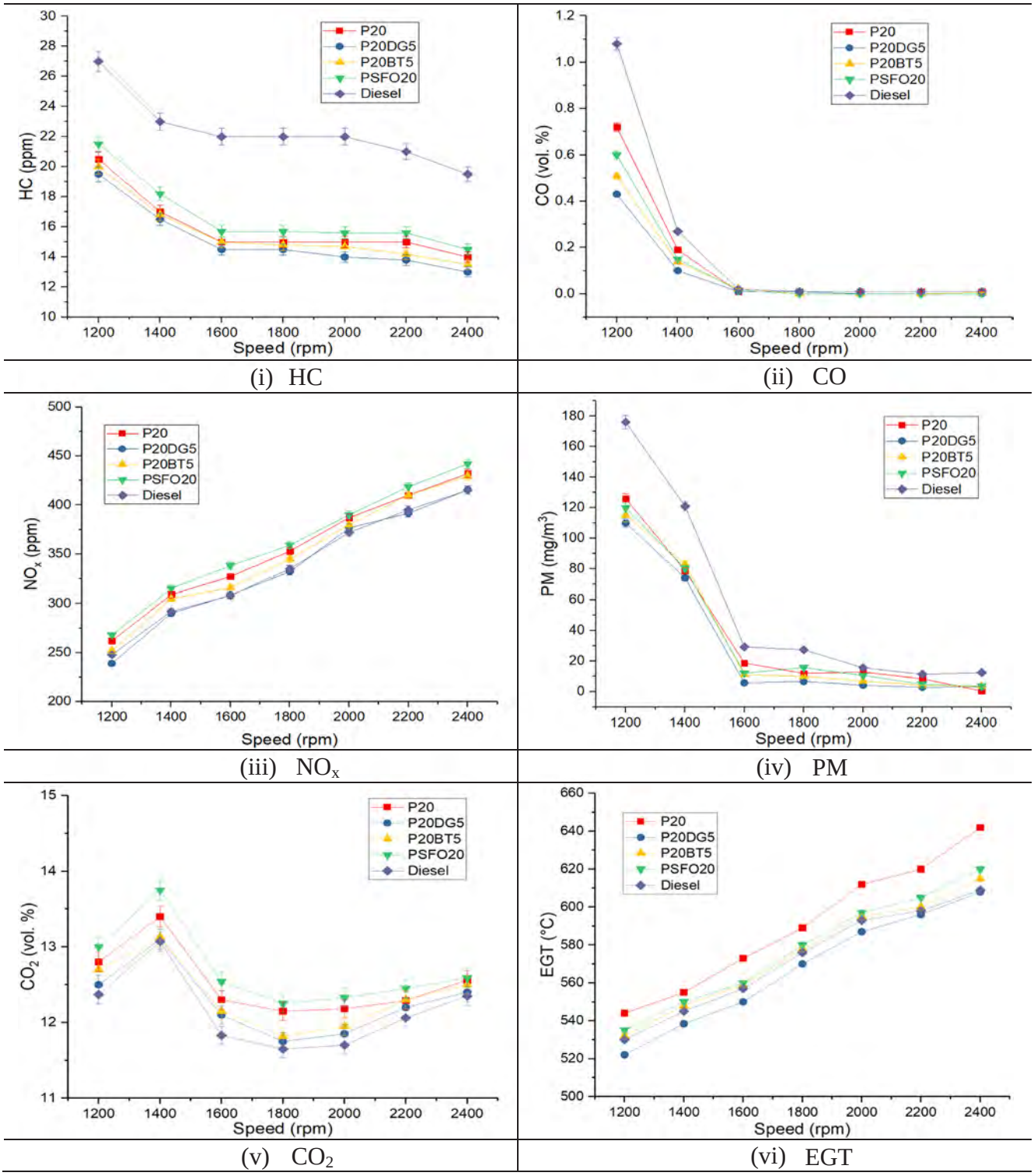

Fig. 5. Variations of exhaust gas emissions for all PSO biodiesel-diesel-additives blends with respect to engine speed at full load condition.

in the combustion chamber and cause higher NO_x emissions [86]. All tested fuels except P20DG5 produced higher NO_x emissions than diesel at any given engine speed. P20DG5 produced about 0.64% less NO_x emissions on average, compared to diesel. The higher cetane number of fuels such as the P20DG5 blend can initiate a shorter ignition delay that results in lower combustion temperatures and pressures that lead to the production of less NO_x [87,88]. The average increase in NO_x for P20BT5, PSFO20, and P20 compared to diesel were 3.50%, 6.50% and 4.10% respectively. With the inclusion of additives in P20 blends, NOx emission reduced by 4.80% and 0.60% for P20DG5 and P20BT5, respectively.

Fig. 5(iv) shows variations in particulate matter (PM) emissions in response to changes in engine speeds for the PSO biodiesels and diesel at full load condition. The PM emissions decreased significantly with an increase in engine speed for both PSO biodiesel blends and diesel. The higher O_2 content and lower volatility of biodiesel causes lower PM emissions than diesel [89]. Again, the higher cetane number of a biodiesel blend such as P20DG5 can cause a shorter ignition delay and

longer combustion which results in low PM emissions [90]. The average PM values for P20DG5, P20BT5, PSFO20, P20 and diesel were recorded as 29.50, 33.40, 35.30, 36.80 and 56.20 mg/m^3. The average reduction in PM values for P20DG5, P20BT5, PSFO20 and P20 compared with diesel were 47.40%, 40.60%, 31.20% and 34.60%. With the inclusion of additives in P20 blends, PM emissions reduced significantly by 24.40% and 10.10% for P20DG5 and P20BT5, respectively.

Emissions of CO_2 increased with an increase in engine speed initially and recorded the highest values at 1400 rpm at which the maximum torque of the engine occurs. The variations in CO_2 emissions with speed are shown in Fig. 5(v). It can be seen that biodiesel blends such as P20 and PSFO20 have generated higher CO_2 emissions at any given speed. Mofijur et al. [72] reported that higher O_2 content and cetane number in the biodiesel blends may result in increased production of CO_2. PSFO20 and P20 have generated slightly higher CO_2 emission at all engine speeds compared with the other biodiesel blends with additives and diesel. The average CO_2 values for P20DG5, P20BT5, PSFO20, P20 and diesel were recorded as 12.30%, 12.30%, 12.70%, 12.50% and 11.97%, respectively. The average increase in CO_2 values for P20DG5, P20BT5, PSFO20 and P20, as compared to diesel were 2.80%, 3.10%, 6.10% and 4.50%. With the inclusion of additives in P20 blends, CO_2 emission was reduced by 1.70% and 1.40% for P20DG5 and P20BT5, respectively.

Fig. 5(vi) shows variations in EGT for the PSO biodiesel blends and diesel over the range of engine speeds. EGT increases with increase in speeds for all tested fuels. Ong et al. [78] found that the EGT of biodiesel increases due to the higher fuel quantity that is needed per unit of time to produce higher heat energy in the combustion chamber at higher engine speeds. In contrast, the lower the biodiesel content in the blend, the lower is the EGT. Again, fuel with a higher cetane number such as the P20DG5 blend produces an oxygenated fuel mixture that assists in improving combustion leading to lower EGT [65]. Again, P20 and PSFO20 have lower heating values and higher viscosity, and this would have caused poor atomisation and incomplete combustion, thus contributing to higher EGTs. Ong et al. [78] reported that diesel has a lower EGT compared to all tested fuels due to its higher heating value and shorter combustion phase. The average EGT values for P20DG5, P20BT5, PSFO20, P20 and diesel were recorded as 567.30, 575.30, 578.10, 590.70 and 572.60 °C. The average increase in EGT values for P20BT5, PSFO20 and P20 compared with diesel were 0.47%, 0.97% and 3.20%. However, a slight reduction in EGT of 0.90% was recorded for P20DG5 compared with diesel. With the inclusion of additives in P20 blends, the EGT values were reduced by 4.10% and 2.70% for P20DG5 and P20BT5 respectively.

6. Comparative engine emissions analysis of PSO and other ternary biodiesel blends

The comparative analyses of engine emission characteristics of PSO biodiesel blends (binary-P20, ternary- PSFO20, P20DG5, and P20BT5) and diesel on the basis of HC, CO, NO_x, PM, CO_2 emissions and EGT are shown in Fig. 6. Four engine loads (25, 50, 75 and 100%) were varied at two engine speeds (1400 rpm- max. rated torque and 2400 rpm- near max. rated power) to investigate emission characteristics.

Fig. 6(i) shows the HC emissions of the biodiesel blends and diesel, with changing engine loads and speeds. At the lower engine speed of 1400 rpm, HC emissions increased with increase in load (25%, 50%, 75% and 100%) for all blends. At 2400 rpm, HC increased with the engine load until 75%, then it declined slightly at full load. This indicates that, at higher speed and full load condition, the increased O_2 content in the air-fuel mixture of the biodiesel blend assisted in improving combustion which resulted in lower HC emissions. Fig. 6(ii) shows the CO emissions of biodiesel blends and diesel with changing engine loads and speeds. At 100% full load condition and 1400 rpm, the highest amounts of CO emissions were recorded for all biodiesel blends and diesel which is due to incomplete combustion. A significant reduction in CO emissions were observed with an increase in engine load and speed. Higher cetane number and O_2 content in the biodiesel blends resulted in complete combustion that led to production of lower CO emissions. These trends are consistent with the published literature [72,91]. In this study, the P20DG5 was found to produce the lowest CO emission followed by P20BT5, PSFO20, P20 and diesel.

Fig. 6(iii) shows comparison between NOx emissions characteristics of the biodiesel blends and diesel in response to changing engine loads and speeds. P20DG5 has higher cetane number that may initiate a shorter ignition delay. This results in lower combustion temperatures and pressures, which contribute to lowest NOx emissions, as compared other biodiesel blends and diesel. Fig. 6(iv) shows that PM emissions decreased as the engine speed increased up to 2400 rpm. The PM emissions were higher at lower speed due to incomplete combustion as well as the burning of heavy lubricating oil. In contrast, the PM reduced significantly at higher engine speed due to better combustion with oxygenated fuels [92–95]. At full load condition and 1400 rpm, P20DG5 was found to produce the lowest PM emissions followed by P20, PSFO20, P20BT5 and diesel. This is due to higher oxygen content in the biodiesel increasing combustion temperature leading to improved combustion [82,85].

CO_2 emissions of biodiesels and diesel at varying engine loads and speeds are presented in Fig. 6(v). Over the entire range of engine speed (1400 and 2400 rpm), CO_2 emissions increased with an increase in load (0%, 50%, 75% and 100%) for all biodiesel blends. At any load condition and engine speed, diesel was found to emit the lowest CO_2 followed by P20DG5, P20BT5, P20 and PSFO20. The exhaust gas temperature (EGT) increased with the increase in load and speed for all biodiesel blends and diesel, as shown in Fig. 6(vi). Higher viscosity and lower heating values of biodiesel blends can cause poor atomisation and incomplete combustion that results higher EGT. After P20DG5, diesel was found to have recorded the lowest EGT followed by P20BT5, PSFO20 and P20. The highest EGT was recorded at 100% full load condition and 2400 rpm.

The overall scenarios of emissions generation of biodiesel blends (P20, P20DG5, P20BT5, and PSFO20) and diesel (D) at full engine loading conditions with two engine speeds (1400 rpm and 2400 rpm) are presented in Table 7. At 100% full load, the maximum decreases in HC and CO emissions were found to be 28.20% and 63% for P20DG5, and the minimum decreases were 20.90% for PSFO20 and 29.60% for P20 respectively, compared with diesel (D). The lowest decrease in NOx (0.60%) was recorded for P20DG5 and the highest (6.50%) was for PSFO20. P20BT5 generated 31.30% lower PM emissions compared with diesel, while P20DG5 emitted 38.80% less than diesel. P20DG5 generated 0.23% more CO_2 while PSFO20 also recorded 5.2% higher PM. The lowest EGT was recorded for P20DG5 at 0.20% below that for diesel, and P20 was found to have the highest at 5.40% above that for diesel.

7. Combustion parameters

The variation of in-cylinder pressures (CP) with the crank angle (CA) for diesel and the PSO biodiesel binary and ternary blends at 1400, and 2400 rpm at full engine load condition are presented in Fig. 7(i) and (ii). At 1400 rpm speed, P20DG5 had a peak cylinder pressure of 67.41 bar at 11° CA, followed by 66.63 bar at 11° CA for P20BT5, 66.02 bar at 11° CA for PSFO20, 66.15 bar at 3° CA for P20 and 64.07 bar at 3° CA for diesel. The cylinder temperature increases with an increase in pressure that contributed to a higher evaporation rate and better combustion at higher speed and engine load. At 2400 rpm, peak cylinder pressure was recorded at 0° CA for diesel and all PSO blends. P20DG5 had 67.51 bar while P20BT5, PSFO20, P20 and diesel were 66.46 bar, 66.81 bar, 67.33 bar, and 65.75 bar respectively. The cylinder pressures of the biodiesel ternary blends were found to be higher than those of diesel due to higher density of biodiesel being injected for the same injection duration compared with diesel [12,96].

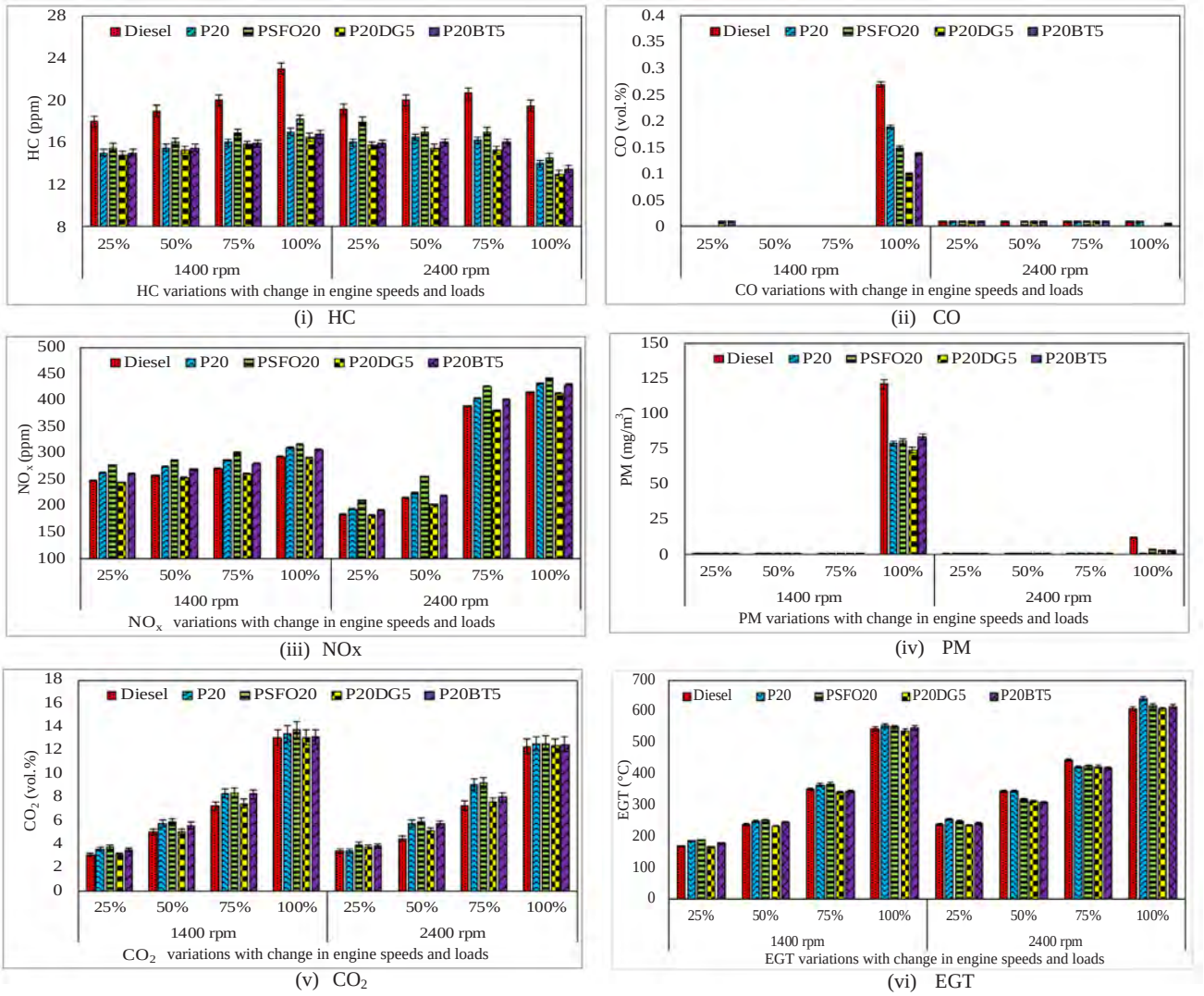

Fig. 6. Variations of emissions of PSO biodiesel-diesel-additives blends with different engine loads and speeds.

CP depends on the fraction of fuel burnt in the premixed combustion phase. Other factors such as cetane number, volatility characteristics and oxygen content also influence CP variations. At full load and 2400 rpm speed, the maximum CPs of P20DG5, P20BT5, PSFO20 and P20 were found to be 2.67%, 1.08%, 1.61% and 2.40% higher than diesel. However, all trends of the graphs are similar and well supported by Prabhakaran et al. [97].

Heat release rates (HRR) of PSO biodiesel binary and ternary blends along with diesel are shown in Fig. 8(i) and 8(ii). At 1400 rpm with full load condition, the maximum HRR was recorded as 201.78 J/°CA at 16° CA with diesel, 192.42 J/°CA at 16° CA with P20, 191.95 J/°CA at 16° CA with P20DG5, 194.25 J/°CA at 16° CA with P20BT5 and 198.25 J/°CA at 16° CA with PSFO20. HRR in the combustion of a diesel engine depends on fuel characteristics such as calorific value, cetane number, fuel-air mixing rates, cetane number, ignition number and ignition timings [55,98]. At 2400 rpm and full load condition, the maximum HRR was found to be 250.6 J/°CA at 15° CA with diesel, 237.15 J/°CA at 15° CA with PSO20, 235.15 J/°CA at 15° CA with P20DG5, 242.50 J/°CA at 15° CA with P20BT5 and 245.85 J/°CA at 15° CA with PSFO20. The maximum HRRs at 2400 rpm of P20, P20DG5, P20BT5 and PSFO20 were found to be 5.36%, 6.16%, 3.23% and 1.90% lower than diesel. HRR values of all biodiesel blends were found to be lower than diesel

Table 7
Overall performance of biodiesel blends (BD) over diesel (D) at full load on different engine speeds.

Emissions generation	Full load (100%)		Comparison between BD with D	
	1400 rpm	2400 rpm	Min. ▲/▼ (%)	Max. ▲/▼ (%)
HC emission	D > BD	D > BD	PSFO20 (▼20.90%)	P20DG5 (▼28.20%)
CO emission	D > BD	D > BD	P20 (▼29.60%)	P20DG5 (▼63.00%)
NO_x emission	P20DG5 < D	P20DG5 < D	P20DG5 (▼0.64%)	PSFO20 (▲6.50%)
PM emission	D > BD	D > BD	P20BT5 (▼31.30%)	P20DG5 (▼38.80%)
CO_2 emission	BD > D	BD > D	P20DG5 (▲0.23%)	PSFO20 (▲5.20%)
EGT value	P20DG5 < D	P20DG5 < D	P20DG5 (▼0.20%)	P20 (▲5.40%)

where ▲ increase and ▼ = decrease.

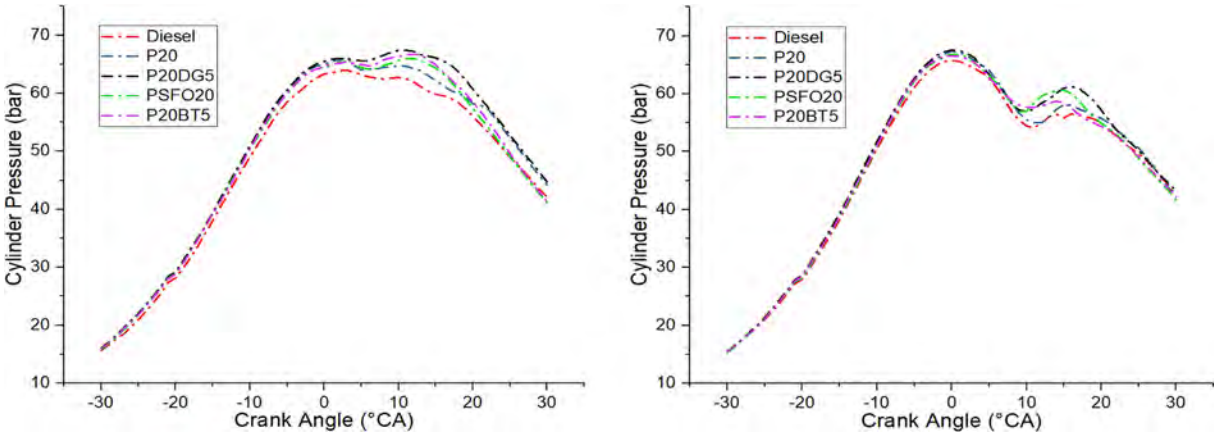

(i) CP vs CA at 1400 rpm (ii) CP vs CA at 2400 rpm

Fig. 7. The differences of in-cylinder pressure for PSO blends and diesel under full load at speeds of: (i) 1400 rpm, and (ii) 2400 rpm.

due to the lower ignition delay and lower calorific values of biodiesel. Further higher viscosities of PSO biodiesel blends resulted in relatively inferior atomisation that led to slower burning compared with diesel. Again, the higher HRR of diesel can be explained due to longer ignition delay, retardation of the start of combustion [99], and higher calorific values as supported by other researchers [12,55,94].

Ignition delay (ID) is the time interval between the start of injection and start of combustion in a diesel engine. ID represents the fuel quality as well as being a measure of the ignition quality (cetane number) and knocking tendency of the fuel [100]. Cetane number has a significant impact on ID as fuels with higher cetane number ignite quickly, resulting in lower ID. The PSO binary and ternary biodiesel blends have higher cetane numbers than diesel, and Fig. 9 shows that all blends have a lower ID period compared with diesel. The ID decreases with the increase of engine speed. Higher oxygen content, i.e., oxygenated additives in the blends (P20DG5 and P20BT5) and the higher level of biodiesel blends (P20 and PSFO20) resulted in lower IDs than for diesel. At full load condition and lower speed of 1400 rpm, the IDs recorded for diesel, P20, P20DG5, P20BT5 and PSFO20 were 11 °CA, 8.50 °CA, 7.70 °CA, 8 °CA, and 7.80 °CA respectively. With the increase of engine speed to 2400 rpm, the ID values changed to 13 °CA, 9.50 °CA, 7.90 °CA, 8.20 °CA, and 8 °CA. Oxygenated fuel blends of P20DG5 showed the lowest ID period compared with the other fuel blends and diesel. Other factors that affect ID are fuel quality, engine speed, load, air temperature, and fuel-air mixing ratio [55]. As discussed in the earlier section, the longer ID leads to delaying fuel-air mixing time, resulting in higher

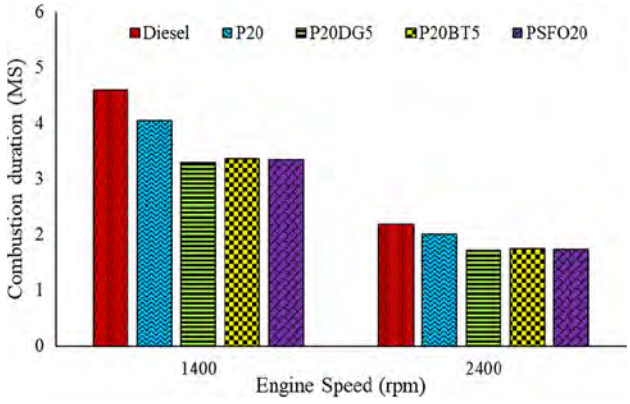

Fig. 9. Ignition delay of diesel and PSO biodiesel blends at full load at speeds of 1400 rpm and 2400 rpm.

HRR.

The variation of the mass fraction burned (MFB) with the crank angle for PSO biodiesel blends and diesel at 1400 rpm and 2400 rpm engine speed at full loading conditions are compared in Fig. 10(i) and (ii). It can be seen from both these figures that the MFB for biodiesel blends were earlier than that of diesel at full load condition. However, all biodiesel blends and diesel show similar trends. From Fig. 10(i) at 1400 rpm, 90% of the P20DG5, PSFO20, P20BT5, and P20 biodiesel

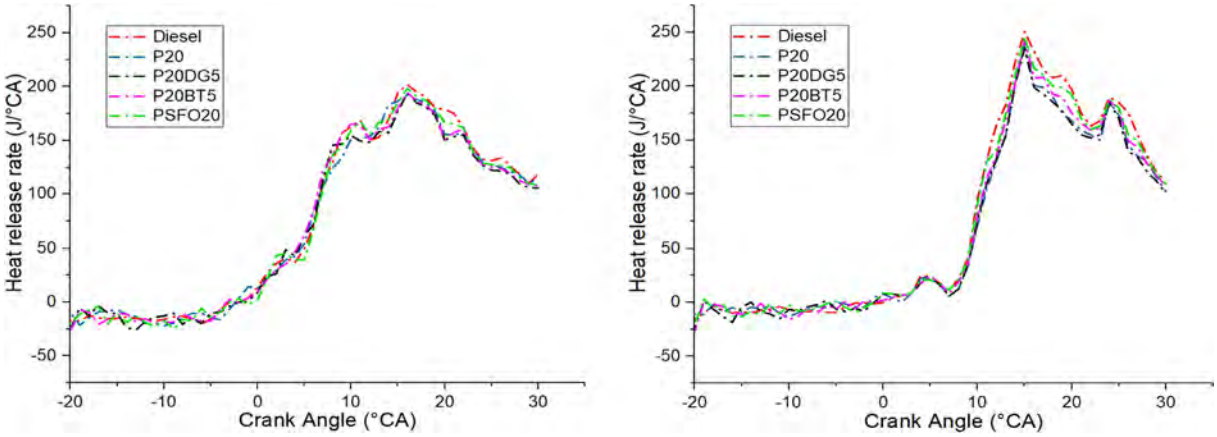

(i) HRR vs CA at 1400 rpm (ii) HRR vs CA at 2400 rpm

Fig. 8. The differences of heat release rate for PSO blends and diesel under full load at speeds of: (i) 1400 rpm, and (ii) 2400 rpm.

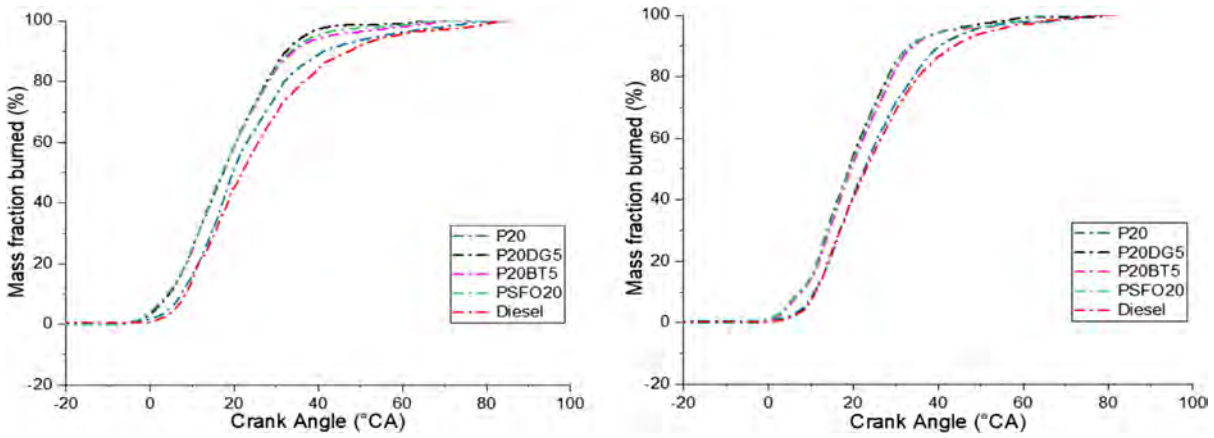

Fig. 10. The differences of mass fraction burned (%) for PSO blends and diesel under full load at speeds of: (i) 1400 rpm, and (ii) 2400 rpm.

blends were burnt at 32.30 °CA, 32.50 °CA, 32.70 °CA and 41.50 °CA respectively after TDC, and the same amount of diesel was burnt at 47.2° CA. Again, from Fig. 10(ii) at 2400 rpm, the same amounts (90%) of P20DG5, PSFO20, P20BT5, P20 biodiesel blend and diesel were burnt at 32.50 °CA, 32.60 °CA, 33 °CA, 40 °CA, and 43° CA respectively.

8. Summary of findings

The effect of papaya seed oil biodiesel blended with diglyme, butanol, and stone fruit biodiesel on engine performance, exhaust emissions and combustion are analysed. Engine performance, exhaust emissions characteristics and combustion analysis were noted at a series of engine speeds from 1200 rpm to 2400 rpm at intervals of 200 rpm along with varying engine loads from 25% to 100%. At 100% full load condition and 2400 rpm, compared to diesel, the minimum and maximum increases in BP were found to be 0.14% for P20DG5 and 6.70% for P20, and for torque were 1.80% for P20DG5 and 3.20% for P20 respectively, whereas the BSFC of diesel was slightly higher than P20DG5 by 0.60–0.80%. Again, P20DG5 had the highest BTE compared with diesel by 3.30–6.40%. The results of the engine performance can be summarised as follows:

- The average BP value reductions for P20DG5, P20BT5, PSFO20 and P20 compared with diesel were 1.80%, 2.90%, 3.20%, and 5% respectively. Adding oxygenated additives such as diglyme (P20DG5) and butanol (P20BT5) increased the BP values by 3.30% and 2.20% compared with P20.
- The average torque value reductions for P20DG5, P20BT5, PSFO20 and P20 compared with diesel were 1.20%, 1.80%, 2.60% and 3.80% respectively. Both P20DG5 and P20BT5 have 2.70% and 2.10% higher torque compared with P20.
- The average BSFC value of P20DG5 was found to be 0.50% lower than diesel. However, BSFC values of the P20BT5, PSFO20, and P20 blends were recorded as 3.10%, 6.40% and 17.10% higher than diesel respectively. Again, both P20DG5 and P20BT5 have 17.70% and 13.60% lower BSFC compared with P20.
- The average BTE value of P20DG5 was found to be 3.30% higher than diesel. The average BTE value reductions of P20BT5, PSFO20 and P20 were measured as 2.3%, 3.60% and 13.10% respectively. Again, both P20DG5 and P20BT5 have 15.80% and 11.10% higher BTE compared with P20.

At 2400 rpm with full load condition, the lowest decrease in NOx was recorded for P20DG5 at 0.64% and the highest was for PSFO20 at 6.50% compared with diesel. P20BT5 generated 31.30% lower PM emissions compared with diesel while P20DG5 emitted 38.80% less than that of diesel. The emission characteristics of the engine at various speeds and loads can be summarised as follows:

- The average reduction in HC values for P20DG5, P20BT5, PSFO20 and P20 compared with diesel were 32.40%, 30.40%, 25.40% and 28.80% respectively. Both P20DG5 and P20BT5 have reduced the HC emissions by 5.4% and 2.3% compared with P20.
- The average reduction in CO values for P20DG5, P20BT5, PSFO20 and P20, compared with diesel were 61%, 52.20%, 45.75% and 31.90% respectively. Both P20DG5 and P20BT5 have reduced CO emissions noticeably by 74.60% and 42.40% compared with P20.
- P20DG5 produced about 0.64% less NOx emissions compared with diesel as an average. The average increase in NO_x values for P20BT5, PSFO20, and P20 compared with diesel were 3.50%, 6.50% and 4.1% respectively. Both P20DG5 and P20BT5 have reduced NOx emissions by 4.80% and 0.60% compared with P20.
- The average reduction in PM values for P20DG5, P20BT5, PSFO20 and P20, compared with diesel were 47.40%, 40.60%, 31.20% and 34.60% respectively. Both P20DG5 and P20BT5 have reduced PM emissions by 24.40% and 10.10% compared with P20.
- The average increase in CO_2 values for P20DG5, P20BT5, PSFO20 and P20, compared with diesel were 2.80%, 3.10%, 6.10% and 4.50% respectively. Both P20DG5 and P20BT5 have reduced CO_2 emissions by 1.70% and 1.40% respectively compared with P20.
- The average EGT values recorded for P20DG5, P20BT5, PSFO20, P20 and diesel were 567.30, 575.30, 578.10, 590.70 and 572.60 °C respectively. The average increase in EGT values for P20BT5, PSFO20 and P20 compared with diesel were 0.50%, 1.00% and 3.20% respectively while a slight reduction of 0.90% was noticed for P20DG5. Both P20DG5 and P20BT5 have reduced their EGT values by 4.10% and 2.70% compared with P20.

Various PSO biodiesel blends and their effects on cylinder pressure, heat release rate, ignition delay, mass fraction burned, and combustion duration at full load condition at 1400 rpm and 2400 rpm have been analysed. The results of this investigation can be summarised as follows:

- In-cylinder peak pressures for all PSO biodiesel blends were higher than that of diesel irrespective of engine speed. At 2400 rpm and full load condition, the peak cylinder pressures for P20DG5, P20BT5, PSFO20 and P20 were found to be 2.67%, 1.08%, 1.61% and 2.40% higher than diesel respectively.
- HRR values of the PSO biodiesel blends P20DG5, P20BT5, PSFO20 and P20, were found to be maximum at 2400 rpm and were recorded as 6.16%, 3.23%, 1.90% and 5.36% lower than diesel

respectively due to the lower ignition delay and lower calorific values of biodiesel.

- P20DG5 had a shorter ignition delay period compared with the other PSO biodiesel blends and diesel.
- The mass fraction burned for all PSO biodiesel blends indicated slightly faster combustion than for diesel. P20DG5, P20BT5, PSFO20 and P20 biodiesel blends showed faster combustion than diesel by about 28.5%, 26.94%, 27.20% and 11.92% at 1400 rpm and 20.95%, 19.68%, 20.32% and 7.93% at 2400 rpm respectively.

9. Conclusion

The above discussions show that the insertion of oxygenated additives in biodiesel binary blend can be a promising technique for using biodiesel blends in a diesel engine efficiently. Adding diglyme additive in PSO20 binary blend performed better in terms of engine performance, emissions and combustion than lone binary blend. Diglyme ternary blend (P20DG5) produced about 0.64% less NO_x emissions compared with diesel as an average. The BTE value of P20DG5 was found to be 3.30% higher than diesel, whereas BSFC was found to be 0.50% lower. P20DG5 had a shorter ignition delay period compared to diesel and other blends. In-cylinder peak pressure was found to be 2.67% higher than diesel. P20DG5 proved to be better than other ternary blends as well. However, further research on tribological performance analysis needs to be conducted to recommend this ternary blend as a future alternative energy source on a commercial scale.

Acknowledgement

The authors would like to acknowledge Mr. Tim McSweeney, Adjunct Research Fellow, Tertiary Education Division at Central Queensland University, Australia for his contribution in proof reading of this article.

References

[1] BP p.l.c., BP Statistical Review of World Energy, London, United Kingdom, Jun. 2019.
[2] Örs I, Sarıkoç S, Atabani AE, Ünalan S, Akansu SO. The effects on performance, combustion and emission characteristics of DICI engine fuelled with TiO2 nanoparticles addition in diesel/biodiesel/n-butanol blends. Fuel 2018;234:177–88.
[3] Silitonga AS, Masjuki HH, Mahlia TMI, Ong HC, Chong WT, Boosroh MH. Overview properties of biodiesel diesel blends from edible and non-edible feedstock. Renew Sustain Energy Rev 2013;22:346–60.
[4] Mofijur M, Masjuki HH, Kalam MA, Hazrat MA, Liaquat AM, Shahabuddin M, et al. Prospects of biodiesel from Jatropha in Malaysia. Renew Sustain Energy Rev 2012;16(7):5007–20.
[5] Sims R, Schaeffer R, Creutzig F, Cruz-Núñez X, D'Agosto M, Dimitriu D, Figueroa Meza MJ, Fulton L, Kobayashi S, Lah O, McKinnon A, Newman P, Ouyang M, Schauer JJ, Sperling D, Tiwari G. Transport. In: Edenhofer O, Pichs-Madruga R, Sokona Y, Farahani E, Kadner S, Seyboth K, Adler A, Baum I, Brunner S, Eickemeier P, Kriemann B, Savolainen J, Schlömer S, von Stechow C, Zwickel T, Minx JC, editors. Climate change 2014: mitigation of climate change. contribution of working group III to the fifth assessment report of the intergovernmental panel on climate change. Cambridge, United Kingdom and New York, NY, USA: Cambridge University Press; 2014.
[6] Norhasyima RS, Mahlia TMI. Advances in CO_2 utilization technology: a patent landscape review. J CO2 Util 2018;26:323–35.
[7] Toivanen H, Novotny M. The emergence of patent races in lignocellulosic biofuels, 2002–2015. Renew Sustain Energy Rev 2017;77:318–26.
[8] Anwar M, Rasul MG, Ashwath N. The efficacy of multiple-criteria design matrix for biodiesel feedstock selection. Energy Convers Manage 2019;198:111790.
[9] Anwar M, Rasul MG, Ashwath N, Nabi MDN. The potential of utilising papaya seed oil and stone fruit kernel oil as non-edible feedstock for biodiesel production in Australia—a review. Energy Rep 2019;5:280–97.
[10] Anwar M, Rasul MG, Ashwath N. Production optimization and quality assessment of papaya (Carica papaya) biodiesel with response surface methodology. Energy Convers Manage 2018;156:103–12.
[11] Anwar M, Rasul M, Ashwath N. A systematic multivariate analysis of carica papaya biodiesel blends and their interactive effect on performance. Energies 2018;11(11):2931.
[12] Patel C, Chandra K, Hwang J, Agarwal RA, Gupta N, Bae C, et al. Comparative compression ignition engine performance, combustion, and emission characteristics, and trace metals in particulates from waste cooking oil, Jatropha and Karanja oil derived biodiesels. Fuel 2019;236:1366–76.
[13] Kusumo F, Silitonga AS, Masjuki HH, Ong HC, Siswantoro J, Mahlia TMI. Optimization of transesterification process for Ceiba pentandra oil: a comparative study between kernel-based extreme learning machine and artificial neural networks. Energy 2017;134:24–34.
[14] Silitonga AS, Atabani AE, Mahlia TMI, Masjuki HH, Badruddin IA, Mekhilef S. A review on prospect of Jatropha curcas for biodiesel in Indonesia. Renew Sustain Energy Rev 2011;15(8):3733–56.
[15] Mofijur M, Rasul MG, Hyde J, Azad AK, Mamat R, Bhuiya MMK. Role of biofuel and their binary (diesel–biodiesel) and ternary (ethanol–biodiesel–diesel) blends on internal combustion engines emission reduction. Renew Sustain Energy Rev 2016;53:265–78.
[16] Gülüm M, Bilgin A. A comprehensive study on measurement and prediction of viscosity of biodiesel-diesel-alcohol ternary blends. Energy 2018;148:341–61.
[17] Emiroğlu AO, Şen M. Combustion, performance and exhaust emission characterizations of a diesel engine operating with a ternary blend (alcohol-biodiesel-diesel fuel). Appl Therm Eng 2018;133:371–80.
[18] Wei L, Cheung CS, Ning Z. Effects of biodiesel-ethanol and biodiesel-butanol blends on the combustion, performance and emissions of a diesel engine. Energy 2018;155:957–70.
[19] Killol A, Reddy N, Paruvada S, Murugan S. Experimental studies of a diesel engine run on biodiesel n-butanol blends. Renew Energy 2019;135:687–700.
[20] Anwar M, Rasul M, Ashwath N, Rahman M. Optimisation of second-generation biodiesel production from Australian native stone fruit oil using response surface method. Energies 2018;11(10):2566.
[21] Dharma S, Masjuki HH, Ong HC, Sebayang AH, Silitonga AS, Kusumo F, et al. Optimization of biodiesel production process for mixed Jatropha curcas–Ceiba pentandra biodiesel using response surface methodology. Energy Convers Manage 2016;115:178–90.
[22] Anwar M, Rasul M, Ashwath N. Optimization of biodiesel production from stone fruit kernel oil. Energy Procedia 2019;160:268–76.
[23] Sivalakshmi S, Balusamy T. Performance and emission characteristics of a diesel engine fuelled by neem oil blended with alcohols. Int J Ambient Energy 2011;32(4):170–8.
[24] Murugesan A, Umarani C, Chinnusamy TR, Krishnan M, Subramanian R, Neduzchezhain N. Production and analysis of bio-diesel from non-edible oils—a review. Renew Sustain Energy Rev 2009;13(4):825–34.
[25] Comin M, de Souza ACD, Roveda AC, Yahagi SS, de Oliveira LH, Amaral MS, et al. Alternatives binary and ternary blends and its effects on stability of soybean biodiesel contaminated with metals. Fuel 2017;191:275–82.
[26] Misra RD, Murthy MS. Blending of additives with biodiesels to improve the cold flow properties, combustion and emission performance in a compression ignition engine—a review. Renew Sustain Energy Rev 2011;15(5):2413–22.
[27] Rashedul HK, Masjuki HH, Kalam MA, Ashraful AM, Ashrafur Rahman SM, Shahir SA. The effect of additives on properties, performance and emission of biodiesel fuelled compression ignition engine. Energy Convers Manage 2014;88:348–64.
[28] Nabi MN. Theoretical investigation of engine thermal efficiency, adiabatic flame temperature, NOx emission and combustion-related parameters for different oxygenated fuels. Appl Therm Eng 2010;30(8):839–44.
[29] Wang X, Cheung CS, Di Y, Huang Z. Diesel engine gaseous and particle emissions fueled with diesel–oxygenate blends. Fuel 2012;94:317–23.
[30] Hulwan DB, Joshi SV. Performance, emission and combustion characteristic of a multicylinder DI diesel engine running on diesel–ethanol–biodiesel blends of high ethanol content. Appl Energy 2011;88(12):5042–55.
[31] Guarieiro LLN, Souza AFd, Torres EA, Andrade JBd. Emission profile of 18 carbonyl compounds, CO, CO2, and NOx emitted by a diesel engine fuelled with diesel and ternary blends containing diesel, ethanol and biodiesel or vegetable oils. Atmos Environ 2009;43(17):2754–61.
[32] Ashok B, Nanthagopal K, Darla S, Chyuan OH, Ramesh A, Jacob A, et al. Comparative assessment of hexanol and decanol as oxygenated additives with calophyllum inophyllum biodiesel. Energy 2019;173:494–510.
[33] Ramesh A, Ashok B, Nanthagopal K, Ramesh Pathy M, Tambare A, Mali P, et al. Influence of hexanol as additive with Calophyllum Inophyllum biodiesel for CI engine applications. Fuel 2019;249:472–85.
[34] Nanthagopal K, Ashok B, Saravanan B, Ramesh Pathy M, Sahil G, Ramesh A, et al. Study on decanol and Calophyllum Inophyllum biodiesel as ternary blends in CI engine. Fuel 2019;239:862–73.
[35] Nanthagopal K, Ashok B, Saravanan B, Patel D, Sudarshan B, Aaditya Ramasamy R. An assessment on the effects of 1-pentanol and 1-butanol as additives with Calophyllum Inophyllum biodiesel. Energy Convers Manage 2018;158:70–80.
[36] Rashed MM, Kalam MA, Masjuki HH, Habibullah M, Imdadul HK, Shahin MM, et al. Improving oxidation stability and NOX reduction of biodiesel blends using aromatic and synthetic antioxidant in a light duty diesel engine. Ind Crops Prod 2016;89:273–84.
[37] Kandasamy SK, Selvaraj AS, Rajagopal TKR. Experimental investigations of ethanol blended biodiesel fuel on automotive diesel engine performance, emission and durability characteristics. Renew Energy 2019;141:411–9.
[38] Çelebi Y, Aydın H. Investigation of the effects of butanol addition on safflower biodiesel usage as fuel in a generator diesel engine. Fuel 2018;222:385–93.
[39] El-Seesy AI, Hassan H, Kosaka H. Improving the performance of a diesel engine operated with jojoba biodiesel-diesel-n-butanol ternary blends. Energy Procedia 2019;156:33–7.
[40] Ibrahim A. Performance and combustion characteristics of a diesel engine fuelled by butanol–biodiesel–diesel blends. Appl Therm Eng 2016;103:651–9.
[41] Senthur Prabu S, Asokan MA, Roy R, Francis S, Sreelekh MK. Performance combustion and emission characteristics of diesel engine fuelled with waste cooking oil bio-diesel/diesel blends with additives. Energy 2017;122:638–48.
[42] Sivalakshmi S, Lenin VR, Hari Prakash C. Investigation on the combustion, performance and emissions of a diesel engine fuelled by biodiesel and its blends with different oxygenated organic compounds. Int J Ambient Energy 2016;37(5):513–9.
[43] Varuvel EG, Subramanian T, Khatri P. Effect of diglyme addition on performance and emission characteristics of hybrid minor vegetable oil blends (rubber seed and babassu oil) in a tractor engine – an experimental study. Biofuels 2018:1–9.

[44] Tüccar G, Özgür T, Aydın K. Effect of diesel–microalgae biodiesel–butanol blends on performance and emissions of diesel engine. Fuel 2014;132:47–52.
[45] Imdadul HK, Masjuki HH, Kalam MA, Zulkifli NWM, Alabdulkarem A, Kamruzzaman M, et al. A comparative study of C4 and C5 alcohol treated diesel–biodiesel blends in terms of diesel engine performance and exhaust emission. Fuel 2016;179:281–8.
[46] Keskin A, Gürü M, Altıparmak D. Influence of tall oil biodiesel with Mg and Mo based fuel additives on diesel engine performance and emission. Bioresour Technol 2008;99(14):6434–8.
[47] Velmurugan K, Sathiyagnanam AP. Impact of antioxidants on NOx emissions from a mango seed biodiesel powered DI diesel engine. Alexandria Eng J 2016;55(1):715–22.
[48] Prabakaran P, Saravanan CG, Yadav SPR, Aalam CS. Experimental investigation of papaya methyl ester on performance, combustion and emission characteristics of DI diesel engine. Int J Innovative Res Creative Technol 2015;1(4).
[49] Raj CS, Karthikayan M. Effect of additive on the performance, emission and combustion characteristics of a diesel engine run by diesel-papaya methyl ester blends. Int. J. Chem. Sci 2016;14(4):2823–34.
[50] Mohan A, Sen S. Emission analysis of the biodiesel from papaya and chicken blends. Int J Inf Futuristic Res 2015;2(7):6.
[51] Işık MZ, Bayındır H, İscan B, Aydın H. The effect of n-butanol additive on low load combustion, performance and emissions of biodiesel-diesel blend in a heavy duty diesel power generator. J Energy Inst 2017;90(2):174–84.
[52] Rajesh Kumar B, Saravanan S. Use of higher alcohol biofuels in diesel engines: a review. Renew Sustain Energy Rev 2016;60:84–115.
[53] Fayyazbakhsh A, Pirouzfar V. Comprehensive overview on diesel additives to reduce emissions, enhance fuel properties and improve engine performance. Renew Sustain Energy Rev 2017;74:891–901.
[54] Kumar M, Gayen K. Developments in biobutanol production: new insights. Appl Energy 2011;88(6):1999–2012.
[55] Rahman MM, Rasul MG, Hassan NMS, Azad AK, Uddin MN. Effect of small proportion of butanol additive on the performance, emission, and combustion of Australian native first- and second-generation biodiesel in a diesel engine. Environ Sci Pollut Res Int 2017;24(28):22402–13.
[56] Ren Y, Huang Z, Miao H, Di Y, Jiang D, Zeng K, et al. Combustion and emissions of a DI diesel engine fuelled with diesel-oxygenate blends. Fuel 2008;87(12):2691–7.
[57] Gill SS, Tsolakis A, Herreros JM, York APE. Diesel emissions improvements through the use of biodiesel or oxygenated blending components. Fuel 2012;95:578–86.
[58] Ying W, Longbao Z, Hewu W. Diesel emission improvements by the use of oxygenated DME/diesel blend fuels. Atmos Environ 2006;40(13):2313–20.
[59] Asokan MA, Senthur prabu S, Kamesh S, Khan W. Performance combustion and emission characteristics of diesel engine fuelled with papaya and watermelon seed oil bio-diesel/diesel blends. Energy 2018;145:238–45.
[60] Anwar M, Rasul MG, Ashwath N. A comparative study of engine performance and emission characteristics of biodiesels produced from the waste seeds of papaya and stone fruit. IEEE 2nd international conference on renewable energy and power engineering. 2019. Toronto (submitted).
[61] Sivasubramanian H. Performance and emission characteristics of papaya seed oil methyl ester–n-butanol–diesel blends on a stationary direct-injection CI engine. Biofuels 2017:1–10.
[62] Bhuiya M, Rasul M, Khan M, Ashwath N. Performance and emission characteristics of binary mixture of poppy and waste cooking biodiesel. Energy Procedia 2017;110:523–8.
[63] Sanjid A, Kalam MA, Masjuki HH, Varman M, Zulkifli NWBM, Abedin MJ. Performance and emission of multi-cylinder diesel engine using biodiesel blends obtained from mixed inedible feedstocks. J Clean Prod 2016;112:4114–22.
[64] Liaquat AM, Masjuki HH, Kalam MA, Varman M, Hazrat MA, Shahabuddin M, et al. Application of blend fuels in a diesel engine. Energy Procedia 2012;14(Supplement C):1124–33.
[65] Ong HC, Masjuki HH, Mahlia TMI, Silitonga AS, Chong WT, Leong KY. Optimization of biodiesel production and engine performance from high free fatty acid Calophyllum inophyllum oil in CI diesel engine. Energy Convers Manage 2014;81:30–40.
[66] Mofijur M, Masjuki HH, Kalam MA, Atabani AE. Evaluation of biodiesel blending, engine performance and emissions characteristics of Jatropha curcas methyl ester: Malaysian perspective. Energy 2013;55:879–87.
[67] Qi DH, Chen H, Geng LM, Bian YZ. Experimental studies on the combustion characteristics and performance of a direct injection engine fueled with biodiesel/diesel blends. Energy Convers Manage 2010;51(12):2985–92.
[68] Silitonga AS, Masjuki HH, Ong HC, Sebayang AH, Dharma S, Kusumo F, et al. Evaluation of the engine performance and exhaust emissions of biodiesel-bioethanol-diesel blends using kernel-based extreme learning machine. Energy 2018;159:1075–87.
[69] Sajjad H, Masjuki HH, Varman M, Kalam MA, Arbab MI, Imtenan S, et al. Influence of gas-to-liquid (GTL) fuel in the blends of Calophyllum inophyllum biodiesel and diesel: an analysis of combustion–performance–emission characteristics. Energy Convers Manage 2015;97:42–52.
[70] Rashed MM, Kalam MA, Masjuki HH, Mofijur M, Rasul MG, Zulkifli NWM. Performance and emission characteristics of a diesel engine fueled with palm, jatropha, and moringa oil methyl ester. Ind Crops Prod 2016;79:70–6.
[71] Altaie MAH, Janius RB, Rashid U, Taufiq-Yap YH, Yunus R, Zakaria R, et al. Performance and exhaust emission characteristics of direct-injection diesel engine fueled with enriched biodiesel. Energy Convers Manage 2015;106:365–72.
[72] Mofijur M, Masjuki HH, Kalam MA, Atabani AE, Fattah IMR, Mobarak HM. Comparative evaluation of performance and emission characteristics of Moringa oleifera and Palm oil based biodiesel in a diesel engine. Ind Crops Prod 2014;53:78–84.
[73] Muralidharan K, Vasudevan D. Performance, emission and combustion characteristics of a variable compression ratio engine using methyl esters of waste cooking oil and diesel blends. Appl Energy 2011;88(11):3959–68.
[74] Yatish KV, Lalithamba HS, Suresh R, Harsha Hebbar HR. Optimization of bauhinia variegata biodiesel production and its performance, combustion and emission study on diesel engine. Renew Energy 2018;122:561–75.
[75] An H, Yang WM, Maghbouli A, Li J, Chou SK, Chua KJ. Performance, combustion and emission characteristics of biodiesel derived from waste cooking oils. Appl Energy 2013;112:493–9.
[76] Koçak MS, Ileri E, Utlu Z. Experimental study of emission parameters of biodiesel fuels obtained from canola, hazelnut, and waste cooking oils. Energy Fuels 2007;21(6):3622–6.
[77] Imdadul HK, Masjuki HH, Kalam MA, Zulkifli NWM, Alabdulkarem A, Rashed MM, et al. Higher alcohol–biodiesel–diesel blends: an approach for improving the performance, emission, and combustion of a light-duty diesel engine. Energy Convers Manage 2016;111:174–85.
[78] Ong HC, Masjuki HH, Mahlia TMI, Silitonga AS, Chong WT, Yusaf T. Engine performance and emissions using Jatropha curcas, Ceiba pentandra and Calophyllum inophyllum biodiesel in a CI diesel engine. Energy 2014;69:427–45.
[79] Gumus M, Kasifoglu S. Performance and emission evaluation of a compression ignition engine using a biodiesel (apricot seed kernel oil methyl ester) and its blends with diesel fuel. Biomass Bioenergy 2010;34(1):134–9.
[80] Mofijur M, Masjuki HH, Kalam MA, Atabani AE, Arbab MI, Cheng SF, et al. Properties and use of Moringa oleifera biodiesel and diesel fuel blends in a multi-cylinder diesel engine. Energy Convers Manage 2014;82:169–76.
[81] Chauhan BS, Kumar N, Cho HM. A study on the performance and emission of a diesel engine fueled with Jatropha biodiesel oil and its blends. Energy 2012;37(1):616–22.
[82] Rahman SMA, Masjuki HH, Kalam MA, Abedin MJ, Sanjid A, Sajjad H. Production of palm and Calophyllum inophyllum based biodiesel and investigation of blend performance and exhaust emission in an unmodified diesel engine at high idling conditions. Energy Convers Manage 2013;76:362–7.
[83] Roy MM, Wang W, Bujold J. Biodiesel production and comparison of emissions of a DI diesel engine fueled by biodiesel–diesel and canola oil–diesel blends at high idling operations. Appl Energy 2013;106:198–208.
[84] Murillo S, Míguez JL, Porteiro J, Granada E, Morán JC. Performance and exhaust emissions in the use of biodiesel in outboard diesel engines. Fuel 2007;86(12):1765–71.
[85] Devan PK, Mahalakshmi NV. Performance, emission and combustion characteristics of poon oil and its diesel blends in a DI diesel engine. Fuel 2009;88(5):861–7.
[86] Godiganur S, Suryanarayana Murthy C, Reddy RP. Performance and emission characteristics of a Kirloskar HA394 diesel engine operated on fish oil methyl esters. Renew Energy 2010;35(2):355–9.
[87] Yongcheng H, Longbao Z, Shangxue W, Shenghua L. Study on the performance and emissions of a compression ignition engine fuelled with fischer-tropsch diesel fuel. Proc Inst Mech Eng, Part D: J Automobile Eng 2006;220(6):827–35.
[88] Wu T, Huang Z, Zhang W-G, Fang J-H, Yin Q. Physical and chemical properties of GTL – diesel fuel blends and their effects on performance and emissions of a multicylinder DI compression ignition engine. Energy Fuels 2007;21(4):1908–14.
[89] Tse H, Leung CW, Cheung CS. Investigation on the combustion characteristics and particulate emissions from a diesel engine fueled with diesel-biodiesel-ethanol blends. Energy 2015;83:343–50.
[90] Lin C-Y, Li R-J. Engine performance and emission characteristics of marine fish-oil biodiesel produced from the discarded parts of marine fish. Fuel Process Technol 2009;90(7):883–8.
[91] Kim H, Choi B. The effect of biodiesel and bioethanol blended diesel fuel on nanoparticles and exhaust emissions from CRDI diesel engine. Renew Energy 2010;35(1):157–63.
[92] Sayin C. Engine performance and exhaust gas emissions of methanol and ethanol–diesel blends. Fuel 2010;89(11):3410–5.
[93] Datta A, Mandal BK. Impact of alcohol addition to diesel on the performance combustion and emissions of a compression ignition engine. Appl Therm Eng 2016;98:670–82.
[94] Can Ö. Combustion characteristics, performance and exhaust emissions of a diesel engine fueled with a waste cooking oil biodiesel mixture. Energy Convers Manage 2014;87:676–86.
[95] Gürü M, Koca A, Can Ö, Çınar C, Şahin F. Biodiesel production from waste chicken fat based sources and evaluation with Mg based additive in a diesel engine. Renew Energy 2010;35(3):637–43.
[96] Dhar A, Agarwal AK. Performance, emissions and combustion characteristics of Karanja biodiesel in a transportation engine. Fuel 2014;119:70–80.
[97] P. Prabhakaran, C.G.S., C. Syed Aalam, Effects of Papaya Methyl Ester on DI Diesel Engine Combustion, Emission and Performance Characteristics. International Research Journal of Engineering and Technology (IRJET), 2016. 3(2).
[98] Mahmudul HM, Hagos FY, Mamat R, Abdullah AA, Awad OI. Experimental investigation of the impact of using alcohol- biodiesel-diesel blending fuel on combustion of single cylinder CI engine. IOP Conf Ser: Mater Sci Eng 2016;160:012038.
[99] Datta A, Mandal BK. Engine performance, combustion and emission characteristics of a compression ignition engine operating on different biodiesel-alcohol blends. Energy 2017;125:470–83.
[100] Dhinesh B, Isaac JoshuaRamesh Lalvani J, Parthasarathy M, Annamalai K. An assessment on performance, emission and combustion characteristics of single cylinder diesel engine powered by Cymbopogon flexuosus biofuel. Energy Convers Manage 2016;117:466–74.

{this page is intentionally left blank}

Chapter 9: Conclusions and Recommendations

9.1 Introduction

The research presented in this thesis investigated the potential of non-edible biodiesel feedstocks as alternative sources of transport fuel in Australia. Multiple-criteria decision matrix was used to initially identify the two most suitable (PSO and SFO) biodiesel feedstocks amongst the six tested feedstocks. These oils of the selected biodiesel feedstocks were analysed and converted into biodiesel by optimising process parameters using the response surface methodology (RSM) statistical tool. The derived biodiesels of the selected feedstocks were tested in a diesel engine for engine performance, emission parameters and combustion characteristics. A four-cylinder, four stroke indirect injection, naturally aspirated water-cooled diesel engine was tested in this test. The biodiesel was blended with the petroleum diesel at 5 to 20% (v/v) biodiesel binary and ternary blends. The biodiesel blends were tested for a range of engine speeds (1200 rpm to 2400 rpm), and for different engine load conditions (25% to 100%). The engine performance parameters of BP, torque, BSFC, and BTE along with the measured emissions such as HC, CO, NO_x, PM, CO_2 emissions and EGT were analysed. A comparative study of the combustion characteristics of the diesel engine fuelled with PSO and SFO blends was performed. All fuel samples were tested at 1400 rpm (rated torque) and 2400 rpm (near rated power output) at full engine load. The experimental investigations were conducted to evaluate the effects of binary and ternary blends on engine combustion characteristics of in-cylinder pressure, heat release rate, ignition delay, mass fraction burned, and ignition duration. The summary of the main findings and recommendation for future studies are presented below.

9.2 Conclusions and summary of findings

The major findings are summarised under 6 sub-heading/groups in this section, as follows.

9.2.1 Biodiesel feedstock selection

Six primarily non-edible biodiesel feedstocks sources were used for screening. Physico-chemical and compositional properties of all the biodiesels produced from these feedstocks met the ASTM, EU and AU standards. Two biodiesel feedstocks were selected using four multiple criteria decision analysis (MCDA) methods, namely PROMETHEE GAIA, WSM, WPM, and TOPSIS. Twelve fuel properties of KV, density, HHV, OS, AV, FP, CFPP, CN, IV, MUFA,

PUFA, and LCSF were selected as criteria, while all six biodiesel feedstocks were the alternatives. Three different weightage (%) determination methods of EQUAL, CRITIC and ENTROPY were used to emphasise the relative importance of each criterion.

The PROMETHEE GAIA MCDA method, when utilised in combination with all three weightage methods, indicated that PSO biodiesel ranked at the top of the list for producing biodiesel, while SFO came as the second. SFO was found to rank first and PSO came second when combining all weightage methods with the WSM MCDA method. Both EQUAL weightage and CRITIC weightage methods showed an exact match of the rankings of all biodiesel feedstocks, whereas ENTROPY weightage showed slightly different lower rankings. WPM indicated PSO as the third-best (all weightage methods), while SFO was second-best under the EQUAL weightage method and first under the CRITIC and ENTROPY methods. However, both CRITIC weightage and ENTROPY weightage methods showed an exact match of all rankings of biodiesel feedstocks, whereas EQUAL weightage showed different first and second rankings. TOPSIS ranked SFO first and PSO second for all different weightage methods. Both EQUAL weightage and CRITIC weightage methods showed an exact match of all biodiesel feedstocks rankings, whereas ENTROPY weightage showed slightly different lower rankings. The average ranking shows that the SFO ranked first and PSO second, followed by BLT, RSB, JBD, and WCB. The mode ranking indicated that SFO was the first choice followed by PSO, RSB, and BLT. Both JBD and WCB were found to be equal lowest in the list as a tie. Finally, the overall results show that SFO was ranked as the best performer amongst the six biodiesel feedstocks examined in this study, PSO came out as the second-best, and the WCB biodiesel feedstock was identified as the worst performer.

The physicochemical and compositional properties of biodiesels produced from all studied feedstocks were analysed and it was found that they met the international standards. Properties of both PSO and SFO biodiesels were found to be better than those produced from the other feedstocks (RSB, BLT, JBD, and WCB) in terms of density, KV, HHV, OS, CFPP, and IV. The total saturated fatty acid content of PSO and SFO biodiesels was found to be lower than that of other feedstocks as well. The lowest LCSFs were recorded for SFO (2.83) and PSO (3.19), whereas the highest was found for BLT biodiesel (10.96). The fuel properties of PSO and SFO biodiesels played a vital role in the feedstock selection process using MCDA methods.

9.2.2 Biodiesel production process optimisation and characterisation

The purpose of this study was to test if papaya seed oil (PSO) and stone fruit kernel oil (SFO) can be used as alternative sources for biodiesel and investigate how to optimise the conditions for producing biodiesel and to identify the optimum reaction conditions for an alkaline transesterification process. A response surface method based Box-Behnken design was employed to understand the relation between the process variables and biodiesel yield. The Box-Behnken design was used to determine the experimental plan/matrix to optimise both PSO and SFO biodiesel conversion processes. In that design matrix, three parameters were each varied within different ranges used to predict biodiesel yield.

A quadratic model was created to predict the biodiesel yield where the R^2 value was found to be 0.99 which indicates the satisfactory accuracy of the model. The optimum process parameters for transesterification of the papaya seed oil mixture at an agitation speed of 600 rpm over a period of 60 min were found to be a methanol:oil molar ratio of 10:1, KOH catalyst concentration of 1wt% and a reaction temperature of 45°C. At these reaction conditions, the predicted and experimental biodiesel yields were 96.12% and 96.48% respectively which shows less than 0.5% variation. Physicochemical properties of the papaya biodiesel meet both ASTM D6751 and EN14214 standards. A quadratic model showed an R^2 of 0.98 indicating the satisfactory performance of the model. Maximum biodiesel yield of 95.8% was obtained at a methanol: oil molar ratio of 6:1, KOH catalyst concentration of 0.5 wt% and a reaction temperature of 55°C. At these reaction conditions, the predicted biodiesel yield was 95.9%. The results also show that the properties of the synthesised SFO biodiesel satisfactorily meet the ASTM D6751 and EN14214 standards. Finally, both PSO and SFO were found to be promising feedstock for second-generation biodiesel production and can be used as alternative fuels in diesel engines.

9.2.3 Comparative analysis of engine performance and emissions behaviour of PSO and SFO biodiesel

Biodiesel produced from papaya seed oil and stone fruit kernel oil, selected as the two most suitable feedstocks for biodiesel production, were evaluated in a diesel engine. The performance of SFO biodiesel blends was slightly better than that of PSO biodiesel blends. The BP and torque produced by these biodiesel blends were almost identical with a deviation of less than 0.5%. However, the BTE of SFO biodiesel blend was 3.2% higher than that of PSO.

In contrast, the BSFC of SFO was 2.4% lower than that of PSO. The SFO biodiesel blends produced higher NO_x emissions than PSO biodiesel blends by a maximum of 2.1%. An increase in NO_x emissions compared with diesel was observed for all PSO and SFO biodiesel blends, and this ranged from 3.4% to 7.1%. The SFO biodiesel blends produced higher PM emissions than PSO biodiesel blends by a maximum of 3%. The highest reduction in PM emissions was recorded for PSO20, and this was found to be 34% lower than diesel fuel. The SFO biodiesel blends produced higher HC emissions compared with PSO blends by a maximum of 10%. The PSO20 can reduce the HC emissions by 33%. A maximum of 5.4% more CO_2 emissions were produced by the SFO biodiesel blends as compared to PSO blends. The average increases in CO_2 for PSO10, PSO20, SFO10, and SFO20, compared with diesel were 1.8%, 3.1%, 6.5% and 8.7%, respectively. SFO biodiesel blends produced a maximum of 13.3% higher CO emissions than PSO biodiesel blends. In comparison with the diesel fuel, the PSO20 produced 31.3% lower CO emissions. Although the SFO biodiesel blends have better engine performance than PSO biodiesel blends, the PSO biodiesel blends prove to be a better overall choice due to their excellent environmentally friendly attributes that can reduce the exhaust emissions to a great extent.

The variation of physicochemical properties of the studied PSO and SFO biodiesels reflected on the engine performance and emission behaviours of the diesel engine. All fuel properties such as density, KV, CN, HHV, FP, and OS of SFO biodiesel were found to be higher than for PSO biodiesel. Higher CN and HHV properties of SFO ensured a better engine performance. However, a significant increase in viscosity (20.7%) and density (1.8%) of SFO biodiesel compared with the PSO biodiesel may result in higher emissions from the SFO product. In conclusion, as indicated earlier, using PSO biodiesel can reduce exhaust emissions significantly while sacrificing the slightly better engine performance of SFO biodiesel.

9.2.4 Interactive effects of operating parameters of PSO biodiesel on engine performance and emissions behaviour

This study investigated the interactive relationships between three operating parameters (papaya seed oil (PSO) biodiesel blends, engine load, and engine speed) and four responses (brake power, BP; torque; brake specific fuel consumption, BSFC; and, brake thermal efficiency, BTE) for engine testing. A response surface methodology (RSM) was introduced to analyse and describe the performance of this engine. PSO biodiesel-diesel blends (B5–B50) meet the European standard EN 590 for having a minimum oxidation stability of 20 h. ANOVA

and a statistical regression model show that load and speed were the two most important parameters that affect all four responses. The biodiesel blends parameter had a significant effect on BSFC.

A comparative analysis of the emission characteristics of four non-edible biodiesel blends and petrodiesel was performed by varying engine loads and speeds. The aim was to optimise operating parameters such as biodiesel blends, engine loads and speed on engine exhaust emissions of nitrogen oxide (NO_x), carbon dioxide (CO_2), hydrocarbon (HC), particulate matter (PM), carbon monoxide (CO) and exhaust gas temperature (EGT). A statistical model and analysis of variance (ANOVA) were used to optimise various parameters. The engine load and engine speed were the two most important parameters that affect four of the responses (NO_x, HC, PM and CO). Furthermore, biodiesel blends and load were influential for EGT and NO_x emissions generation. NO_x continued to be generated irrespective of any variation in biodiesel blends, load and speed. CO_2 generation was not influenced by the biodiesel blends at the various operating parameters.

9.2.5 Combustion characteristics of PSO biodiesel blends

Various PSO biodiesel blends and their effects on cylinder pressure, heat release rate, ignition delay, mass fraction burned, combustion duration and cylinder temperature at full load conditions at 1400 rpm and 2400 rpm has analysed as well.

In-cylinder peak pressure for PSO biodiesels was higher than that of diesel irrespective of engine speed. At 2400 rpm and full load conditions, the peak cylinder pressure for PSO5, PSO10, and PSO20 were found to be 0.27%, 0.82%, and 2.4% higher than diesel. HRR values of PSO biodiesel blends, PSO5, PSO10, and PSO20, were found to be 2.40%, 4.1% and 5.36% lower than diesel due to the lower ignition delay and lower calorific values of biodiesel. PSO biodiesel blends have a shorter ignition delay period compared with diesel. The mass fraction burned for PSO biodiesel blends was slightly faster than diesel. PSO20 biodiesel shows faster combustion by about 11.92% at 1400 rpm and 7.93% at 2400 rpm than diesel. The maximum cylinder temperatures of PSO5, PSO10, and PSO20 blends were higher than that of diesel by 0.31%, 2.75% and 3.17% at 1400 rpm, and by 0.39%, 1.86% and 3.73% at 2400 rpm. Therefore, it is evident that all PSO biodiesel blends have excellent fuel attributes to be considered as the preferred alternative fuel for diesel engines.

9.2.6 Synergistic effects of binary and ternary biodiesel blends

The effect of PSO biodiesel blended with diglyme, butanol, and stone fruit biodiesel on engine performance, exhaust emissions and combustion were analysed. Engine performance, exhaust emissions characteristics and combustion analysis were noted at a series of engine speeds from 1200 rpm to 2400 rpm at intervals of 200 rpm along with varying engine loads from 25% to 100%. Adding oxygenated additives such as diglyme (P20DG5) and butanol (P20BT5) increased the BP values by 3.30% and 2.20% respectively compared with PSO20. Both P20DG5 and P20BT5 have 2.70% and 2.10% higher torque compared with PSO20. The average BSFC value of P20DG5 was found to be 0.50% lower than diesel. The average BTE value of P20DG5 was found to be 3.30% higher than diesel.

Both P20DG5 and P20BT5 have reduced the HC emissions by 5.4% and 2.3% compared with PSO20. The average reduction in HC values for P20DG5, P20BT5, PSFO20 and PSO20 compared with diesel were 32.40%, 30.40%, 25.40% and 28.80% respectively. The average reduction in CO values for P20DG5, P20BT5, PSFO20 and PSO20, compared with diesel were 61%, 52.20%, 45.75% and 31.90% respectively. P20DG5 produced about 0.64% less NOx emissions compared with diesel on average. The average increase in NO_x values for P20BT5, PSFO20, and PSO20 compared with diesel were 3.50%, 6.50% and 4.1% respectively. The average reduction in PM values for P20DG5, P20BT5, PSFO20 and PSO20, compared with diesel were 47.40%, 40.60%, 31.20% and 34.60% respectively. The average increase in CO_2 values for P20DG5, P20BT5, PSFO20 and PSO20, compared with diesel were 2.80%, 3.10%, 6.10% and 4.50% respectively. The average increase in EGT values for P20BT5, PSFO20 and PSO20 compared with diesel were 0.50%, 1.00% and 3.20% respectively while a slight reduction of 0.90% was noticed for P20DG5.

Various PSO biodiesel blends and their effects on cylinder pressure, heat release rate, ignition delay, mass fraction burned, and combustion duration at full load conditions at 1400 rpm and 2400 rpm have been analysed. In-cylinder peak pressures for all PSO biodiesel blends were higher than that of diesel irrespective of engine speed. HRR values of the PSO biodiesel blends P20DG5, P20BT5, PSFO20 and PSO20, were found to be maximum at 2400 rpm and were recorded as 6.16%, 3.23%, 1.90% and 5.36% lower than diesel respectively due to the lower ignition delay and lower calorific values of biodiesel. P20DG5 had a shorter ignition delay period compared with the other PSO biodiesel blends and diesel. P20DG5, P20BT5, PSFO20 and PSO20 biodiesel blends showed faster combustion than diesel by about 28.5%, 26.94%,

27.20% and 11.92% at 1400 rpm and 20.95%, 19.68%, 20.32% and 7.93% at 2400 rpm respectively.

The performance of any fuel can be improved by adding additives that produce better physicochemical properties. The addition of diglyme to PSO biodiesel blends increases the CN and reduced the KV. In some cases, the mixing of two average performing fuel can perform better, for instance, in this study PSFO20 performed better than the individual P20 and SFO20, and some of the properties (CN and HHV) were found to be closely related to diesel. The CN of diglyme was found to be higher (126) than that of both butanol (25) and diesel (48). Again, KV of diglyme was found to be the lowest (1.09 mm^2/s), whereas that of butanol and diesel were 2.63 and 3.23 mm^2/s respectively. The fuel properties of the P20DG5 ternary blend were found to be better than all other ternary blends in this study.

The novelty of this study was to explore how the engine performance can be increased and how the reduction of engine emissions of the engine fuelled with 2^{nd} generation biodiesels, can be maximised. This study achieved that by introducing oxygenated additives in biodiesel binary blends. As articulated earlier, adding diglyme additive in the PSO20 binary blend performed better in terms of engine performance, exhaust emissions and combustion than the binary blend PSO20 itself. Again, P20DG5 proved to be better than other ternary blends such as P20BT5 and PSFO20.

9.3 Recommendations for future study

During this study, several topics were identified that deserve further investigation. Each recommendation is a significant work, which was outside the scope of the thesis. These are listed below:

- Bio-oil extraction by mechanical extraction and chemical extraction to be assessed, although this study used the oil that was purchased from commercial suppliers.
- In this study, all biodiesel blends were prepared up to a maximum of 20% by volume. It would be beneficial to evaluate higher ratio blends by using higher biodiesel percentages (more than 20%) for engine performance, emissions behaviour and combustion characteristics.
- Investigation of the corrosion, tribo-corrosion, long-term engine durability testing and tribological performance analysis of the studied biodiesel blends must be a useful

future study. However, those tests need specialist equipment and involve substantial costs. These analyses will be significant as an extension of the presented work.

- Computational modeling of diesel engine performance, emissions behaviour and combustion characteristics using binary and ternary (with additives) blend warrants further studies. Computational modelling is a big task and that can be a separate PhD topic.
- Effects of several additives (oxygenated and antioxidant and by volume variation) with biodiesel blends on fuel spray formation and combustion duration can be done in the future. Investigation of several additives on fuel spray formation and combustion duration is also a big task and that can be a separate PhD topic.